

**SHORT NYLON-6 FIBRE/RUBBER-TOUGHENED  
POLYSTYRENE COMPOSITES**

*Thesis submitted to*

**Cochin University of Science and Technology**

*in partial fulfilment of the requirements*

*for the award of the degree of*

**Doctor of Philosophy**

*in the*

**Faculty of Technology**

*by*

**JAYALATHA GOPALAKRISHNAN G**



**Department of Polymer Science and Rubber  
Technology**

**Cochin University of Science and Technology**

**Kochi- 682 022, Kerala, India**

**July 2012**

# **Short Nylon-6 Fibre/Rubber-Toughened Polystyrene Composites**

*Ph. D Thesis*

*Author*

**Jayalatha Gopalakrishnan G**

Department of Polymer Science and Rubber Technology

Cochin University of Science and Technology

Cochin- 682 022, Kerala, India

E-mail: jayalatha@cusat.ac.in

*Guide:*

**Dr. Sunil K Narayanankutty**

Professor

Department of Polymer Science and Rubber Technology

Cochin University of Science and Technology

Cochin- 682 022, Kerala, India

E-mail: sunil@cusat.ac.in

July 2012

To

*My Amma and Pappa*



**Department of Polymer Science and Rubber Technology**  
**Cochin University of Science and Technology**

Cochin- 682 022, Kerala, India

---

**Dr. Sunil K Narayanankutty**  
9995300093  
Professor  
mail:sunil@cusat.ac.in

Mob: +91  
E-

---

**Certificate**

This is to certify that the thesis entitled “**Short Nylon-6 Fibre/Rubber-Toughened Polystyrene Composites**” is an authentic report of the original work carried out by Ms. Jayalatha Gopalakrishnan G under my supervision and guidance in the Department of Polymer Science and Rubber Technology, Cochin University of Science and Technology, Kochi – 682 022. No part of the work reported in this thesis has been presented for the award of any degree from any other institution.

**Narayanankutty**

**Dr. Sunil K**

Kochi- 22  
Guide)  
20/07/12

(Supervising

## *Declaration*

I hereby declare that the thesis entitled “**Short Nylon-6 Fibre/Rubber-Toughened Polystyrene Composites**” is the original work carried out by me under the guidance of Dr. Sunil K Narayanankutty, Professor, Department of Polymer Science and Rubber Technology, Cochin University of Science and Technology, Kochi 682 022, and no part of the work reported in this thesis has been presented for the award of any degree from any other institution.

Kochi – 22  
**Gopalakrishnan. G**  
20/07/12

**Jayalatha**

## *Acknowledgements*

---

*First and foremost, I would like to express my sincere gratitude to my research guide, Dr. Sunil K. Narayanankutty, Professor, Department of Polymer Science and Rubber Technology, for the continuous support of my PhD work, for his motivation, suggestions and encouragement. His positive attitude and dedication has inspired me a lot. His guidance helped me in all the time of research and writing of this thesis. I could not have imagined having a better advisor and mentor for my PhD study.*

*I am extremely indebted to Dr. Eby Thomas Thachil, Head of the Department of Polymer Science and Rubber Technology for providing necessary infrastructure and resources to accomplish my research work in the Department.*

*I extend my gratitude to the faculty members of the Department of Polymer Science & Rubber Technology, Dr. K.E George, Dr. Rani Joseph, Dr. Philip Kurian and Dr. Thomas Kurian for their encouragement and whole hearted co-operation. I am indebted to all the faculty members for granting me leave for a period of four months for the completion of my research work.*



*I am thankful to Dr. Mukundan T, Scientist F, Materials Science Lab, NPOL for extending the TGA facilities for my work. I express my thanks to Ms. Kussumakumary, Technical Officer, NPOL for doing the thermal analysis. My heartfelt thanks to Dr. Lakshmikutty Amma, Head, Govt. Engineering College, Thrissur for permitting me to carry out the flexural testing; and to the faculty member, Ms. Anjana, for the assistance provided to me during the testing.*

*I also extend my sincere thanks to the laboratory staffs of Department of Polymer Science & Rubber Technology- Mr. Gopalakrishnan and Mr. Raveendran for their immense help during my research work. Let me thank the members of non-teaching staff of the Department for their support at different stages of my research work.*

*I offer my sincere thanks to Mr. Bipinbal P.K for the fruitful interactions and for being always there with a helping hand. I admire his distinguished helping nature. I wish to thank my fellow research scholars – Ms. Teena, Ms. Renju, Ms. Treasa Sunitha, Ms. Sona, Ms. Nisha, Mr. Jayesh, Mr. Ajilesh, Ms. Jabin, Ms. Pramela and Ms.Preetha for their help throughout my PhD tenure. Besides this, several people have knowingly and unknowingly helped me in the successful completion of this work.*

*I am thankful to Dr. Shibu Eapen, Scientist and Mr. Melby of STIC, CUSAT for patiently helping me to take SEM micrographs of too many samples.*

*I am ever indebted to my mother for the support she provided me through my entire life, without whose love and encouragement, I would not have finished this thesis. The memory of my father still provides a persistent inspiration through the journey of my life. I am grateful to my brother, cousins and aunts for their constant support and motivation.*

*Above all, I thank God Almighty for his blessings for the successful completion of the research work.*

*Jayalatha Gopalakrishnan. G*

## *Preface*

The impact resistance of polystyrene (PS) can be substantially improved by the addition of rubber particles. The rubber forms small inclusions within the matrix of polystyrene. The role of these rubber particles is to act as craze initiators, permitting a large volume of plastic deformation to be formed before individual crazes break down to form cracks leading to fracture. To obtain the highest toughening using the least amount of rubber it is important to keep the rubber particles small. In most applications the rubber particles are between 1-4  $\mu\text{m}$  in diameter.

It is well known that the use of an elastomeric phase for toughening often reduces the modulus and strength, which are important benchmarks for acceptable material performance. In practice, since most polymers are immiscible it is necessary to compatibilise the blends for satisfactory product performance. One method of compatibilisation is the dynamic vulcanisation of the elastomeric phase of the blend. Dynamic vulcanisation prevents the possible coalescence of the rubber phase upon subsequent melt mixing thereby resulting in a fine dispersion of rubber phase in the thermoplastic matrix. This results in improvement of mechanical properties.

An alternative to improve the stiffness and strength of these materials involves the incorporation of reinforcing agents such as short fibres. It will also reduce the cost of the material. In addition, it is well known that the mechanical properties of these systems depend not only on the properties of the components and their proportion in the composite, but also on the morphology of the material, especially on the adhesion at the fibre-matrix interphase.

The present study aims at the preparation of rubber-toughened thermoplastic blends and composites by melt blending polystyrene (PS) with rubbers such as natural rubber (NR), styrene-butadiene-rubber (SBR) and whole tyre reclaim (WTR). The effect of dynamic vulcanisation on the morphology and properties of PS/NR and PS/SBR blends were evaluated. The use of short Nylon-6 fibres as reinforcing agents in these blends opens a new avenue for the utilisation of waste fibres, available in plenty from fibre and textile industries. In this thesis an attempt has been made to investigate systematically the effect of short Nylon-6 fibres- unmodified and resorcinol formaldehyde latex (RFL)-coated and a compatibiliser on the properties of these blends.

The results of the investigations are presented in seven different chapters, as follows:

Chapter 1 presents the fundamentals of blends, composites and fibre reinforced blends. A review of the earlier studies in this field is also presented. Scope and objectives of the present work are also discussed.

Chapter 2 describes the various materials used for the study. The experimental techniques used for preparation of blends and composites, and measurement of various properties are also discussed. The procedure for surface hydrolysis of Nylon-6 fibres and the preparation of the compatibiliser are also described.

Chapter 3 which deals with polystyrene (PS)/natural rubber (NR) blends is divided into three sections. Chapter 3A describes the effect of blend ratio and dynamic vulcanisation using dicumyl peroxide (DCP) on the mechanical properties, morphology and dynamic mechanical properties on these blends. Chapter 3B discusses the effect of short Nylon-6 fibre-

unmodified and RFL-coated on NR-toughened PS. Chapter 3C describes the effect of compatibiliser (MA-g-PS) on untreated and surface hydrolysed Nylon fibres in these composites.

Chapter 4 which focuses on polystyrene (PS) / styrene-butadiene rubber (SBR) blends is divided into three sections. Chapter 4A discusses the effect of blend ratio and dynamic vulcanisation using dicumyl peroxide (DCP) on the mechanical properties, morphology and dynamic mechanical properties of these blends. The effect of short Nylon-6 fibre- unmodified and RFL-coated on SBR-toughened PS is described in Chapter 4B. Chapter 4C discusses the effect of compatibiliser (MA-g-PS) on the composites based on untreated and surface hydrolysed Nylon fibres.

Chapter 5 focuses on blends based on polystyrene (PS)/whole tyre reclaim (WTR). This chapter is divided into three sections. Chapter 5A discusses the effect of blend ratio on the mechanical properties, morphology and dynamic mechanical properties on these blends. Chapter 5B discusses the effect of short Nylon-6 fibre- unmodified and RFL-coated on WTR-toughened PS. Chapter 5C describes the effect of compatibiliser (MA-g-PS) on untreated and surface hydrolysed Nylon fibres in these composites.

Chapter 6 gives an account on thermal degradation studies of the blend, dynamically vulcanised blend, and composites containing Nylon-6 fibres- unmodified and RFL-coated, and the fibres in conjunction with the compatibiliser.

Chapter 7 is the concluding chapter which consolidates the major findings of the present work.

## *Abstract*

The thesis describes studies on development of short Nylon-6 fibre composites based on rubber-toughened polystyrene (PS). Toughening was done using natural rubber (NR), styrene-butadiene rubber (SBR) and whole tyre reclaim (WTR). The composites were prepared by melt mixing in an internal mixer at 170 °C. It was found that the optimum blend ratio was 85/15 for PS/NR, 90/10 for PS/SBR and 90/22 for PS/WTR blends. The effect of dynamic vulcanisation on 85/15 PS/NR and 90/10 PS/SBR blends using dicumyl peroxide (DCP) at various concentrations were also studied. The dynamic crosslinking improved the tensile properties, flexural properties, impact strength and dynamic mechanical properties of both the blends. The effect of unmodified and resorcinol formaldehyde latex (RFL)-coated short Nylon-6 fibres on the mechanical properties, morphology and dynamic mechanical properties of 85/15 PS/NR, 90/10 PS/SBR and 90/22 PS/WTR blends were studied. Fibre loading was varied from 0 to 3 wt.%. For 85/15 PS/NR blend, there was a significant enhancement in tensile properties, flexural properties and impact strength with 1 wt.% of both unmodified and RFL-coated fibres. Dynamic mechanical analysis revealed that the storage modulus at room temperature was maximum at 1 wt.% fiber loading for both composites. The surface functionality of the fiber was improved by giving alkali treatment. Maleic anhydride-grafted-polystyrene (MA-g-PS) was prepared and used as a compatibiliser. The effect of MA-g-PS on the composites was investigated with respect to mechanical properties, morphology and dynamic mechanical properties. The compatibiliser loading was varied from 0 to 2 wt.%. The properties were enhanced significantly in the case of treated and untreated fibre composites at a compatibiliser

loading of 0.75 wt.%. SEM analysis confirmed better bonding between the fibre and the matrix. Dynamic mechanical studies showed that the storage modulus at room temperature improved for treated fibre composites in the presence of compatibiliser. In the case of 90/10 PS/SBR composites, the addition of short Nylon-6 fibres at 1 wt.% loading improved the tensile modulus, flexural properties and impact strength while the tensile strength was marginally reduced. The surface treated fibers along with compatibiliser at 0.5 wt.% improved the tensile properties, flexural properties and impact strength. DMA revealed that the storage modulus at room temperature was better for composites containing untreated fibre and the compatibiliser. In the case of 90/22 PS/WTR blends, 1 wt.% unmodified fibre and 0.5 wt.% RFL-coated fibres improved tensile modulus, flexural properties and impact strength. Tensile strength was improved marginally. The surface treatment of Nylon fibre and the addition of compatibiliser at 0.5 wt.% enhanced the tensile properties, flexural properties and impact strength. The dynamic mechanical analysis showed that the storage modulus at room temperature was better for untreated fibre composites in conjunction with the compatibiliser. The thermal stability of PS/NR was studied by TGA. Thermal stability of the blends improved with dynamic vulcanisation and with the incorporation of RFL-coated Nylon fibres. The untreated and partially hydrolyzed fibre composites in conjunction with the compatibiliser enhanced the thermal stability. Kinetic studies showed that the degradation of the blends and the composites followed first order kinetics.

# CONTENTS

## Chapter 1

### INTRODUCTION-----01 - 50

<b>1.1 Blends-----</b>	<b>01</b>
1.1.1 Thermodynamics of polymer blends-----	02
1.1.2 Classification of polymer blends-----	03
1.1.3 Rubber-toughened thermoplastics-----	04
1.1.3.1 <i>Toughening Mechanism</i> -----	05
1.1.3.1.1 <i>Multiple crazing mechanism</i> -----	06
1.1.3.1.2 <i>Multiple shear yielding mechanism</i> -----	10
1.1.3.1.3 <i>Network yielding mechanism</i> -----	12
1.1.4 Dynamic vulcanisation-----	14
<b>1.2 Composites-----</b>	<b>17</b>
1.2.1 Short fibre polymer composites-----	20
1.2.2 Reinforcing Mechanism of short fibres-----	21
1.2.3 Stress and strain distribution at fibres-----	21
1.2.4 Critical fibre length and average fibre stress-----	23
1.2.5 Parameters influencing the characteristics of short fibre-polymer composites ----- 25	
1.2.5.1 <i>Type and fiber breakage</i> -----	25
1.2.5.2 <i>Critical fiber length and aspect ratio of fiber</i> -----	26
1.2.5.3 <i>Fibre orientation</i> -----	27
1.2.5.4 <i>Fiber dispersion</i> -----	28
1.2.5.5 <i>Fiber concentration</i> -----	29
1.2.5.6 <i>Fiber- matrix adhesion</i> -----	29
<b>1.3 Fiber Reinforced Blends-----</b>	<b>30</b>
1.3.1 Fibre reinforced Rubber-toughened thermoplastics-----	31
1.3.2 Studies on Rubber-toughening of polystyrene-----	33
1.3.3 Composites of Rubber – toughened Polystyrene-----	36
<b>1.4 Scope and objectives of the work-----</b>	<b>37</b>
<b>1.5 References-----</b>	<b>40</b>

## Chapter 2

### MATERIALS AND EXPERIMENTAL TECHNIQUES-----51 - 62

<b>2.1 Materials-----</b>	<b>51</b>
2.1.1 Polymers-----	51



2.1.1.1	<i>Polystyrene (PS)</i>	51
2.1.1.2	<i>Natural Rubber (NR)</i>	51
2.1.1.3	<i>Styrene-butadiene Rubber (SBR)</i>	52
2.1.1.4	<i>Whole Tyre Reclaim (WTR)</i>	53
2.1.2	Nylon-6 fibre	53
2.1.3	Chemicals	53
2.1.3.1	<i>Maleic Anhydride (MA)</i>	53
2.1.3.2	<i>Dicumyl peroxide (DCP)</i>	54
2.1.3.3	<i>Other chemicals</i>	54
<b>2.2</b>	<b>Experimental Procedure</b>	<b>54</b>
2.2.1	Preparation of blends	54
2.2.2	Dynamic vulcanisation	54
2.2.3	Compatibiliser	55
2.2.3.1	<i>Preparation of Maleic anhydride-grafted-polystyrene (MA-g-PS)</i>	55
2.2.3.2	<i>Determination of MA content</i>	55
2.2.4	Treatment of Nylon fibre	55
2.2.5	Preparation of composites	56
<b>2.3</b>	<b>Moulding</b>	<b>56</b>
<b>2.4</b>	<b>Mechanical properties</b>	<b>56</b>
2.4.1	Tensile properties	56
2.4.2	Impact strength	57
2.4.3	Flexural properties	58
<b>2.5</b>	<b>Extraction of composite</b>	<b>59</b>
<b>2.6</b>	<b>Scanning electron microscopy (SEM)</b>	<b>59</b>
<b>2.7</b>	<b>Fourier transform infrared spectroscopy (FTIR)</b>	<b>59</b>
<b>2.8</b>	<b>Dynamic mechanical analysis (DMA)</b>	<b>60</b>
<b>2.9</b>	<b>Thermogravimetric analysis (TGA)</b>	<b>60</b>
<b>2.10</b>	<b>References</b>	<b>61</b>

### Chapter 3

## **POLYSTYRENE / NATURAL RUBBER BLENDS-----63 -**

**120**

### Part A

#### **Toughening of Polystyrene: Effect of Blend ratio & Dynamic vulcanisation**

3A.1	Introduction	63
3A.2	Experimental	66
3A.3	Results and Discussions	67
<b>Part I</b>	<b>Effect of blend ratio</b>	<b>67</b>

3A.3.1 Mechanical Properties-----	67
3A.3.2 Morphology-----	71
3A.3.3 Dynamic mechanical analysis-----	72
<b>Part II Effect of Dynamic vulcanisation-----</b>	<b>76</b>
3A.3.4 Mechanical properties-----	76
3A.3.5 Morphology-----	80
3A.3.6 Dynamic mechanical analysis-----	81
<b>3A.4 Conclusions-----</b>	<b>84</b>
<b>3A.5 References-----</b>	<b>85</b>

### Part B

#### **Effect of short Nylon-6 fibre - unmodified and RFL-coated**

<b>3B.1 Introduction-----</b>	<b>87</b>
<b>3B.2 Experimental-----</b>	<b>89</b>
<b>3B.3 Results and Discussions-----</b>	<b>90</b>
3B.3.1 Mechanical Properties-----	90
3B.3.2 Morphology-----	94
3B.3.3 Dynamic mechanical analysis-----	96
<b>3B.4 Conclusions-----</b>	<b>101</b>
<b>3B.5 References-----</b>	<b>101</b>

### Part C

#### **Effect of surface modification of fibre and use of a compatibiliser.**

<b>3C.1 Introduction-----</b>	<b>105</b>
<b>3C.2 Experimental-----</b>	<b>106</b>
<b>3C.3 Results and Discussions-----</b>	<b>107</b>
3C.3.1 Characterisation of MA-g-PS-----	107
3C.3.2 Mechanical Properties-----	110
3C.3.3 Morphology-----	113
3C.3.4 Dynamic mechanical analysis-----	115
<b>3C.4 Conclusions-----</b>	<b>118</b>
<b>3C.5 References-----</b>	<b>119</b>

#### *Chapter 4*

#### **POLYSTYRENE / STYRENE-BUTADIENE RUBBER BLENDS**

-----**121** -

## Part A

### **Toughening of Polystyrene: Effect of Blend ratio and Dynamic vulcanisation**

<b>4A.1 Introduction</b>	<b>121</b>
<b>4A.2 Experimental</b>	<b>123</b>
<b>4A.3 Results and Discussions</b>	<b>124</b>
<b>Part I Effect of blend ratio</b>	<b>124</b>
4A.3.1 Mechanical Properties	124
4A.3.2 Morphology	127
4A.3.3 Dynamic mechanical analysis	128
<b>Part II Effect of Dynamic vulcanisation</b>	<b>132</b>
4A.3.4 Mechanical properties	132
4A.3.5 Morphology	135
4A.3.6 Dynamic mechanical analysis	136
<b>4A.4 Conclusions</b>	<b>138</b>
<b>4A.5 References</b>	<b>139</b>

## Part B

### **Effect of short Nylon-6 fibre - unmodified and RFL-coated**

<b>4B.1 Introduction</b>	<b>141</b>
<b>4B.2 Experimental</b>	<b>143</b>
<b>4B.3 Results and Discussions</b>	<b>143</b>
4B.3.1 Mechanical Properties	143
4B.3.2 Morphology	147
4B.3.3 Dynamic mechanical analysis	148
<b>4B.4 Conclusions</b>	<b>153</b>
<b>4B.5 References</b>	<b>154</b>

## Part C

### **Effect of surface modification of fibre and use of a compatibiliser**

<b>4C.1 Introduction</b>	<b>157</b>
<b>4C.2 Experimental</b>	<b>158</b>
<b>4C.3 Results and Discussions</b>	<b>159</b>
4C.3.1 Mechanical Properties	159
4C.3.2 Morphology	163
4C.3.3 Dynamic mechanical analysis	164
<b>4C.4 Conclusions</b>	<b>166</b>
<b>4C.5 References</b>	<b>166</b>

**POLYSTYRENE / RECLAIMED RUBBER BLENDS-----169 -  
209**

**Part A**

**Toughening of Polystyrene: Effect of Blend ratio**

<b>5A.1 Introduction</b> -----	<b>169</b>
<b>5A.2 Experimental</b> -----	<b>171</b>
<b>5A.3 Results and Discussions</b> -----	<b>172</b>
5A.3.1 Mechanical Properties-----	172
5A.3.2 Morphology-----	175
5A.3.3 Dynamic mechanical analysis-----	176
<b>5A.4 Conclusions</b> -----	<b>179</b>
<b>5A.5 References</b> -----	<b>180</b>

**Part B**

**Effect of short Nylon-6 fibre - unmodified and RFL-  
coated**

<b>5B.1 Introduction</b> -----	<b>183</b>
<b>5B.2 Experimental</b> -----	<b>186</b>
<b>5B.3 Results and Discussions</b> -----	<b>186</b>
5B.3.1 Mechanical Properties-----	186
5B.3.2 Morphology-----	189
5B.3.3 Dynamic mechanical analysis-----	191
<b>5B.4 Conclusions</b> -----	<b>196</b>
<b>5B.5 References</b> -----	<b>197</b>

**Part C**

**Effect of surface modification of fibre and use of a  
compatibiliser**

<b>5C.1 Introduction</b> -----	<b>199</b>
<b>5C.2 Experimental</b> -----	<b>200</b>
<b>5C.3 Results and Discussions</b> -----	<b>201</b>
5C.3.1 Mechanical Properties-----	201
5C.3.2 Morphology-----	203
5C.3.3 Dynamic mechanical analysis-----	205
<b>5C.4 Conclusions</b> -----	<b>208</b>
<b>5C.5 References</b> -----	<b>208</b>

*Chapter 6*

**THERMAL DEGRADATION OF BLENDS AND COMPOSITES BASED ON POLYSTYRENE/NATURAL RUBBER AND NYLON-6 FIBRE**

**211 - 224**

<b>6.1</b>	<b>Introduction</b> -----	<b>211</b>
<b>6.2</b>	<b>Experimental</b> -----	<b>213</b>
<b>6.3</b>	<b>Results and Discussions</b> -----	<b>214</b>
	6.3.1 Effect of Blend ratio and Dynamic vulcanisation	
	-----	
	214	
	6.3.2 Effect of short Nylon-6 fibres	
	-----	
	218	
	6.3.3 Effect of surface modified fibre and the use of a compatibiliser	
	-----	
	220	
<b>6.4</b>	<b>Conclusions</b> -----	<b>222</b>
<b>6.5</b>	<b>References</b> -----	<b>223</b>

*Chapter 7*

**SUMMARY AND CONCLUSIONS-----225 - 231**

**ABBREVIATIONS**

**PUBLICATIONS**

**CURRICULUM VITAE**

.....❧.....

# INTRODUCTION

## **1.1 Blends**

## **1.2 Composites**

## **1.3 Fibre Reinforced Blends**

## **1.4 Scope and Objective of the work**

## **1.5 References**

### **1.1 Blends**

The field of polymer blends has seen vast growth in both its scientific basis and its technological and commercial development. By definition, a combination of two or more structurally different polymers or copolymers giving rise to materials with a range of properties, not delivered by any of the constituents is a polymer blend.

The rubber industry has used the concept of blending for decades. In recent years, however, there has been a resurgence of interest arising primarily from the demand for engineering plastics and speciality polymers. Development of a new polymer to meet a specific need is a costly enterprise. If the desired properties can be realized simply by mixing two or more existing polymers, there is an obvious economic advantage. The time required to develop a new blend is commercially 3-5 years, compared to 8-10 years required for new materials. Thus, reasons for using blends include attainment of specific article performance, by improving the technical properties of the original polymers, by adjusting the processing

characteristics and reducing the cost [1-6]. The major markets are automotive, electrical and electronic, packaging, building and household.

Polymer blends are either homogeneous or heterogeneous. In homogeneous blends, both blend components lose part of their identity and the final properties usually are the arithmetical average of both blend components. In heterogeneous blends, the properties of all blend components are present. Weaknesses of one polymer can to a certain extent be camouflaged by strengths of the other. In a few exceptional cases, some properties of the either homogeneous or heterogeneous blend can be better than those of the individual components. This synergism is unfortunately hard to predict. Heterogeneous blends appear in a variety of morphologies. The best known and most frequently observed morphologies are: (i) a dispersion of one polymer in the matrix of the other polymer; and (ii) a co-continuous two-phase morphology. Which type of morphology is obtained is dependent on the nature of the blend components, the viscosity and the viscosity ratio of both polymers at the blending temperature, and the blend composition [7].

### 1.1.1 Thermodynamics of polymer blends

Blending of two different kinds of polymers usually results in an immiscible two phase blend, because of thermodynamic reasons. The phase behaviour of polymer mixtures is generally determined by the thermodynamic parameter  $\Delta G_m$ , the Gibbs free energy change of mixing, which is given by the following equation:

$$\Delta G_m = \Delta H_m - T\Delta S_m \dots\dots\dots(1)$$

where,  $\Delta H_m$  = enthalpy change of mixing (J),  
 $\Delta S_m$  = entropy change of mixing (J/K) and

$T$  = absolute temperature (K).

The change in the entropy of mixing,  $\Delta S_m$ , is generally very small in polymer blends due to the high molecular weights of the polymers. This fact, combined with an enthalpy change of mixing,  $\Delta H_m$ , which is generally positive for most non-polar polymer, makes it unlikely to realize the necessary negative Gibbs free energy change for mixing to occur. Because of these thermodynamic aspects, the number of miscible blends is very limited. The miscibility on a molecular scale can be improved, if certain specific interactions are involved, resulting in a negative heat of mixing. Consequently,  $\Delta G_m$  will be negative despite the small entropy change. These interactions may range from strong ionic to weak non-bonding interactions, such as hydrogen bonding, ion-dipole, dipole-dipole and donor-acceptor interactions [5,8].

### **1.1.2 Classification of polymer blends**

Polymer blends may be classified in general into two broad classes: immiscible and miscible blends. Immiscible blends are those which exist in two distinct phases, but are still very useful materials, e.g., toughened plastics. Miscible blends are those, which exist in a single homogeneous phase and may exhibit synergistic properties, different from the pure components. Apart from these two, there exists a third category of blends, often known as technologically compatible blends or alloys. Alloys are those, which exist in two or more different phases on a micro-scale, but exhibit macroscopic properties akin to that of a single-phase material [7,8]. Rubber-thermoplastic blends can be classified broadly into three types:

- (1) Impact resistant rubber-toughened thermoplastics;



- (2) Blends of vulcanisable rubbers, which contain various amounts of resins that can act as reinforcing or stiffening agents and
- (3) Blends showing thermoplastic elastomeric behaviour, commonly known as thermoplastic elastomers (TPEs) [8-12].

### 1.1.3 Rubber-toughened thermoplastics

Impact resistance, a measure of toughness is often a deciding factor in material selection for many engineering applications. Consequently, rubber toughening was discovered to overcome the brittleness of glassy polymers such as polystyrene (PS). This led to the development of rubber modified polystyrenes (containing 5-15% rubber), the so-called *high impact polystyrenes* (HIPS). It is fabricated by dissolving the rubber in styrene monomer and then polymerizing the styrene by conventional means. The final product consists of a polystyrene matrix with inclusions of discrete rubber particles, some of which themselves contain smaller particles of polystyrene [13]. The technology of rubber toughening, which proved to be effective was extended to other commercial glassy polymers such as poly(methyl methacrylate) (PMMA), poly(vinyl chloride) (PVC) and even polycarbonate (PC). Rubber toughening of thermoplastics depends on many factors, including size and morphology of the rubber inclusions, rubber phase volume, interfacial adhesion between the rubber and the matrix, relaxation behaviour of the rubber (modulus and  $T_g$ ) and the composition of the matrix [14,15].

From the morphological perspective, two types of rubber-toughened polymers can be distinguished: “disperse systems” that contain homogeneous, heterogeneous or core-shell particles, and “inclusion systems” or “network systems” that present a network arrangement of the rubber phase. Figure 1.1

shows the phase structures of high-impact PS (HIPS). During the polymerisation of PS in the presence of the dissolved rubber, phase inversion takes place, yielding rubber particles with PS inclusions, and various types of particles can be created depending on the stirring rate, ranging from core-shell particles to so-called “salami particles”.

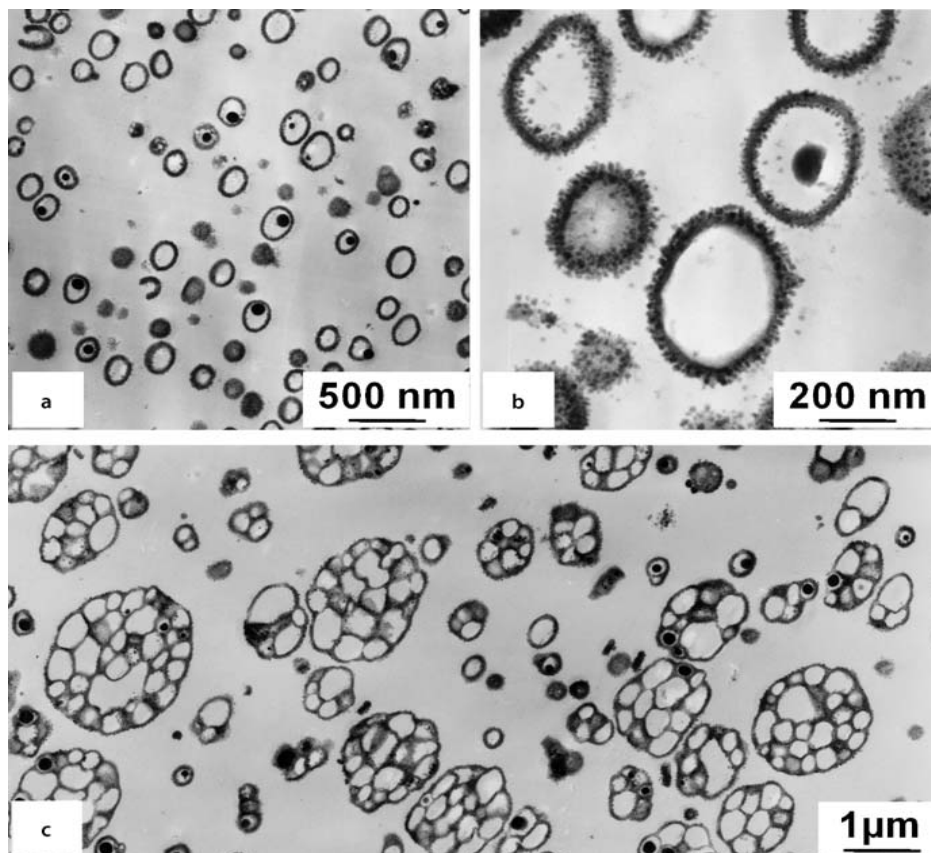


**Figure 1.1:** HIPS with rubber particles in the form of: a),b) rubber shells (core-shell) with SAN-grafted surfaces; c) “salami particles”. (Rubber selectively stained, ultrathin sections, TEM) [reproduced from (17)].

### 1.1.3.1 Toughening Mechanism

Rubber toughening of glassy polymers involve three main micromechanical deformation mechanisms:

- Multiple crazing mechanism (e.g. in HIPS, ABS, ACS),

- Multiple shear yielding mechanism (e.g. in rubber-toughened PMMA, PA, PP) and
- Network (particle) yielding mechanism (e.g. in toughened PVC).

### 1.1.3.1.1 Multiple crazing mechanism

The polymer crazing process can be distinguished by noting that crazes are usually initiated in zones of chain segments that are weakly bonded, loosely packed, and contain structural defects under a dilatational stress field, and that craze growth gives rise to strain-softening of the craze/bulk interface and strain-hardening of craze fibrils. It was observed that the fracture of HIPS is usually preceded by an opaque whitening of the stress area. This whitening is associated with the absorption of a large amount of energy. At low TEM magnification, these stress-whitened areas exhibit many whitening bands perpendicular to the loading direction (Figure 1.2 a). However, when observed at larger magnifications, these small whitening bands, are bridged by many tiny fibrils, revealing the nature of the crazes. The crazes are usually microcracks filled with voids and fibrils.

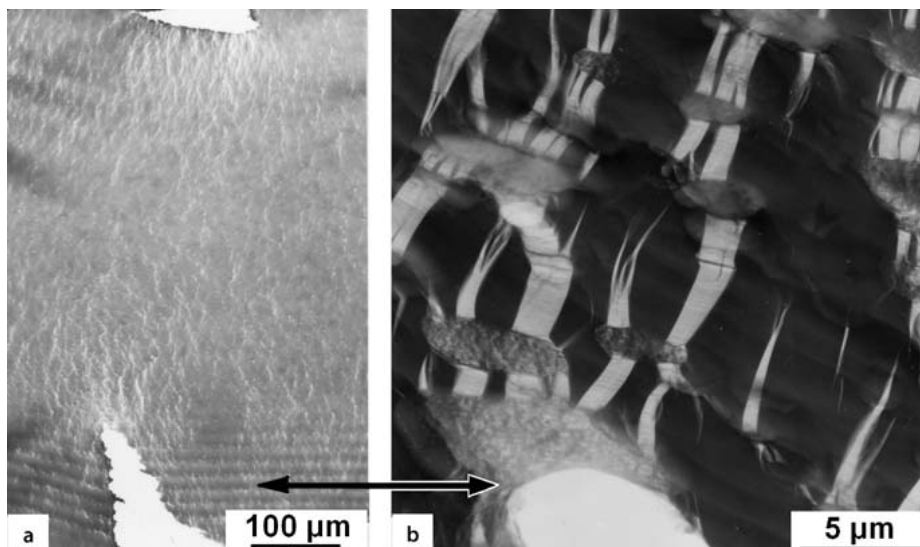


**Figure1.2(a,b): Deformation structures in HIPS: a) overview of deformation area; b) area in front of a crack tip with rubber particles (grey) in a matrix (black) with crazes (bright). (2  $\mu\text{m}$  thick deformed section, for deformation direction see arrow) [reproduced from (16)].**

Crazes are usually initiated at zones of stress concentration at the rubber particles, i.e. in the equatorial zones of the matrix perpendicular to the loading direction; see Figure1.2b. When crazing occurs under well-controlled conditions, as in HIPS or ABS, it improves the material's toughness by the mechanism of inelastic deformation. The energy dissipated by crazing can be divided up into the energy dissipated by yielding during fibril formation and the energy stored as surface energy in the matter in the craze. Figure 1.3 shows a high intensity of crazes with broad bands, propagating from one rubber particle to the next.

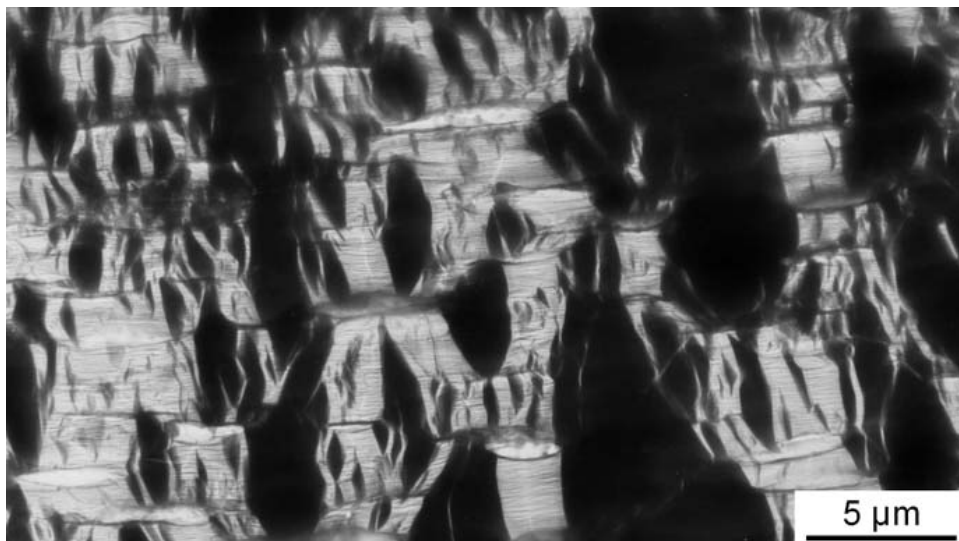


**Figure1.3: Broad crazes and craze bands between rubber particles in HIPS. (Semi-thin section, deformation direction horizontal, HVTEM) [reproduced from (16)].**

Crazes, however, are also the precursors to cracks and, ultimately, failure. Therefore, an important additional process is needed to stop the cracking by rubber particles. The rubber particles retard the rapid propagation of cracks and prevent the premature fracture of the sample. According to the number of rubber particles, many crazes can be created in larger volumes of the sample in order to achieve increased toughness. These individual processes can be summarised in a “three-stage mechanism of toughening”, as shown in Figure 1.4.

- 1) Craze initiation: Each rubber particle generates the stress concentration in the matrix surrounding it. In general, crazes start at points of highly concentrated stress, and then propagate perpendicular to the tensile direction. In many cases, the crazes are accompanied by cavitation inside the particles, but this is not considered to be a precondition for craze initiation.
- 2) Superposition effect: The stress fields around rubber particles overlap when the particle content is more than 15 vol%. As a consequence, plastic strain-softening, which is characterised by a local yielding of matrix, also takes place, and is often followed by multiple crazing such as fibrillated crazes, homogeneous crazes or combinations of them.
- 3) Crack propagation: Once the cracks have formed within the crazes, the crack propagation can be stopped and the crack tip blunted by neighbouring rubber particles. Consequently, the strain hardening of the yield zone, a process caused by stretching the rubber phase to very high strain, also contributes to the enhanced toughness.

Maximum toughening – maximum craze formation due to the three-stage mechanism can be attributed to several parameters, such as:

- rubber particle content by volume
- rubber particle modulus
- particle size and size distribution

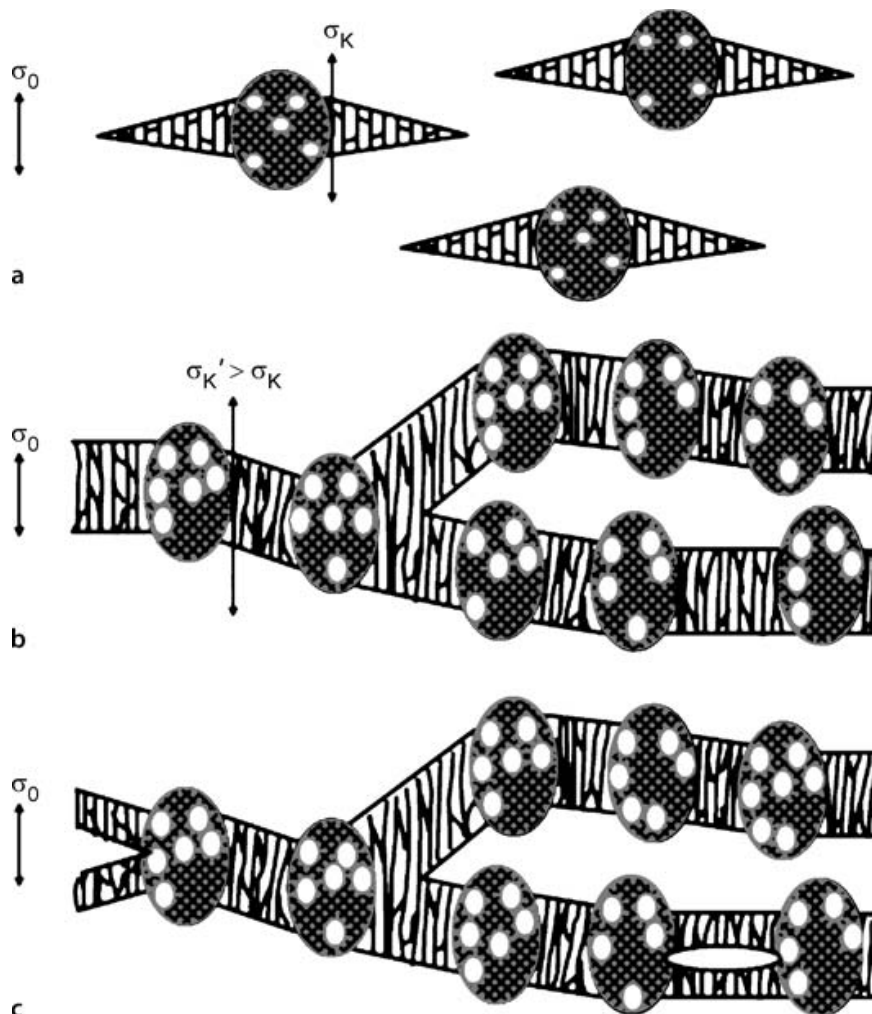


Figure 1.4: Three-stage mechanism of toughening (multiple crazing): a) stress concentration  $\sigma_K$  at individual rubber particles; b) the superposition of stress concentration fields occurs at a larger particle volume content (>15 vol%), and the resulting increased

**stress concentration  $\sigma'_K$  creates thicker crazes and craze bands; c) crack stop at / in rubber particles [reproduced from (17)].**

- shape and internal structure of particles
- degree of grafting at and in particles
- the properties of the matrix itself.

From the morphological point of view, the particle size and the size distribution appear to be the main parameters responsible for enhanced toughness. The optimum rubber particle size is between 0.05 $\mu\text{m}$  and 1  $\mu\text{m}$ , especially between 0.1 and 0.5  $\mu\text{m}$ , with a small size distribution. Very small modifier particles below 200 nm in size (half the wavelength of visible light) are used to prepare transparent toughened polymers such as SAN or PMMA [17].

#### **1.1.3.1.2 Multiple shear yielding mechanism**

The micrographs in Figure 1.5 show deformed and elongated rubber particles as bright particles in the polyamide (PA) matrix. The material between the particles is highly deformed and appears as bright, diffuse zones. All of the material between the particles is involved in plastic deformation in the form of homogeneous yielding without internal structure or cavitation, as seen in the crazes in HIPS. In this material, the plastically deformed areas are spread over a large volume of the sample, which indicates high toughness. For such systems, it was established that a sharp brittle-to-ductile transition occurs when surface-to-surface interparticle distances become lower than a critical value  $ID_{\text{crit}}$ , which depends on the type of polymer matrix. Whereas  $ID_{\text{crit}}$  was found to be independent of particle size and rubber volume fraction [18]. The individual steps of stress concentration, initiation of multiple yielding and crack stopping are very

similar to the three-stage mechanism as shown in Figure 1.4 [19]. A basic difference compared to the “multiple crazing” mechanism is the need for local cavitation in or at the rubber particles to enable yielding of the adjacent matrix strands. Extensive experimental studies have confirmed that microvoids form due to internal cavitation within the modifier particles or interfacial debonding at the interface between the matrix and the modifier particle.

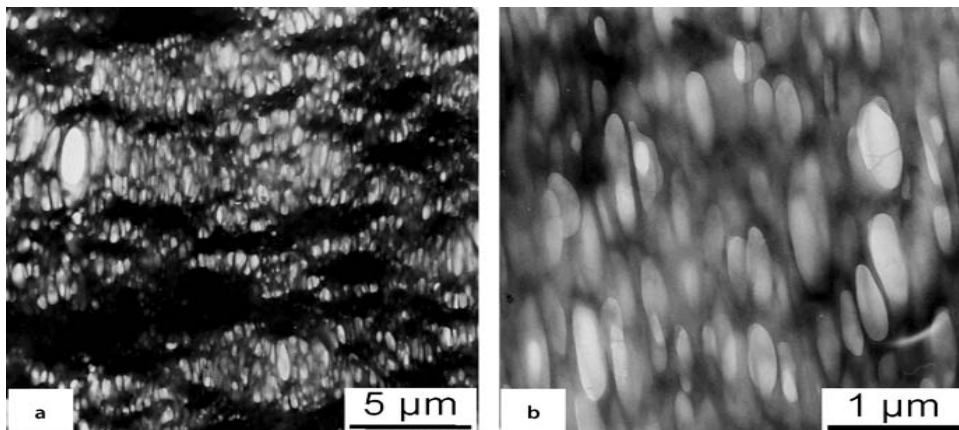


**Figure 1.5: Deformation structures of rubber-modified PA (PA-66, 22 vol% butyl acrylate): a) plastic deformation of the matrix in band-like deformation zones with highly deformed particles; b) microvoid formation inside plastically elongated particles [reproduced from (17)].**

In the case of PP/EPR blends with a low concentration of ethylene in the EPR particles, the modifier particles are of a core-shell type with only one inclusion and are finely dispersed in the matrix. The shell phases consist of an amorphous ethylene-propylene block copolymer, which enhances the interfacial adhesion between the core and the matrix. At the early stage in the deformation, the modifier particles slightly deform in the tensile direction, along with the matrix. When the stress reaches a certain critical value, voids appear in the form of cavitation with or without fibrils



at the interface between the modifier particles and the matrix. This process is strongly dependent upon the inherent properties of the rubbery shell. Along with successive void formation and the continuous growth of the voids, weak shear bands form in the matrix ligaments between particles. When the polymer sample is strained still further, shear yielding is induced in the whole specimen.

In PP/EPR blend with high ethylene content in EPR, the modifier particles possess several inclusions in one rubbery shell. Void formation clearly occurs predominantly in the strongly plastically deformed EPR particles at the interface of the PE inclusions. Shear bands form in the matrix between the modifier particles in the next step. As the strain is increased, the sizes of the voids gradually increase, resulting in an acceleration of the shear flow in the matrix. As demonstrated above, the main energy absorption mechanism that occurs under loading at room temperature is shear deformation of the matrix. When the loading occurs at lower temperatures, two changes must be considered:

- 1) If the temperature is below the glass transition temperature of the modifier particles, the particles can no longer act as rubbery stress concentrators, the initiation of plastic deformation is lost and the materials break in a brittle manner. However, a low-temperature toughness is required for many practical applications.
- 2) Polypropylenes, which are commonly used as matrix materials, possess glass transition temperatures  $T_g$  of about 0 °C, and it is well known that below  $T_g$  the deformation mechanism changes from shear yielding to craze formation [20].

### 1.1.3.1.3 Network yielding mechanism

It has been well established for several decades that there is an alternative and often very effective approach to the rubber toughening of amorphous polymers – the use of “rubber networks”. This method involves embedding small particles of thermoplastic into a rubber network to form a honeycomb structure with thin layers of rubber separating the thermoplastic particles. Figure 1.6 shows a network of a rubbery ethylene vinyl acetate (EVAc) phase containing small particles of PVC. Since there are very thin network layers, the rubber content is usually kept below 10 vol% [21,22]. When this rubbery network is tensile loaded, the PVC particles start to yield and absorb energy. This results in an enhancement in the overall toughness of the system.

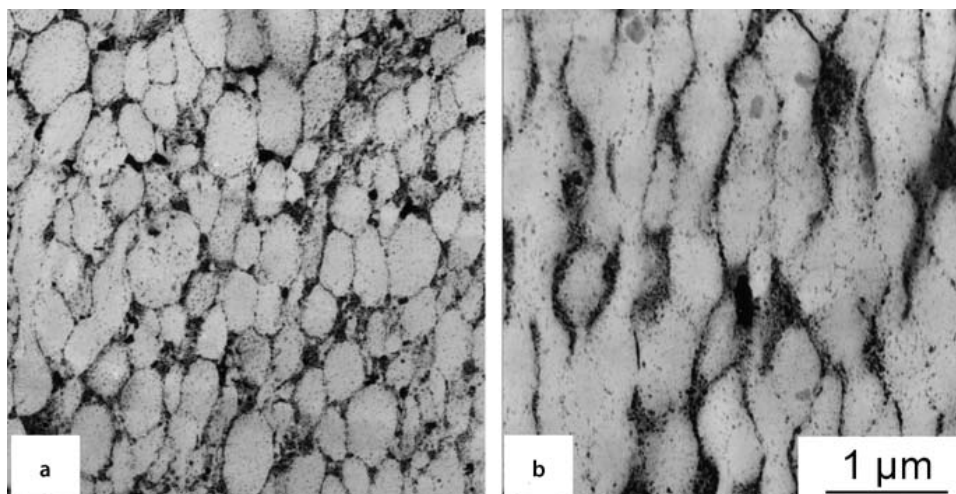


**Figure 1.6: Rubber-toughened PVC with network structure of EVAc:**  
**a) total network morphology;**  
**b) partial network arrangement [reproduced from (16)].**

Under uniaxial tensile load, the following deformation processes occur [21,23]:

- At the start of deformation, the weak rubber phase is stretched, resulting in the growth of a triaxial stress state in the whole network.
- The rubber phase transfers stresses from one PVC particle to another. When the stress transfer is high enough to reach the yield stress of PVC, the particles start to deform plastically; the yielding of numerous PVC particles mainly absorbs the total fracture energy.
- Through the partial rupture of the rubbery network, microvoids are generated in the specimen, yielding intense fibrillation of the network and an additional plastic yielding of the PVC particles.

One critical parameter of this mechanism is the thickness of the rubber network layers, which must be around a few tens of nanometres. Only a thin-walled network like this can generate a triaxial (hydrostatic) stress state that is high enough to reach the yield stress of PVC.

#### **1.1.4 Dynamic vulcanisation**

Dynamic vulcanisation is the procedure in which curing agents are used to crosslink an elastomer in situ during its mixing with molten plastics, which was first described by Gessler [24] in 1962 and further developed by Fisher [25], Coran and Patel [26], and Sabet [27]. The process of dynamic vulcanisation is the route to produce thermoplastic vulcanisate (TPVs), a special case of TPEs. Unlike static vulcanisation, dynamic vulcanisation is performed at a high shear rate, which leads to formation of dispersed phase morphology of the blend components [28,29]. Morphologically, the resulting TPVs are characteristic of finely dispersed,

micrometersized, crosslinked rubber particles distributed in a continuous thermoplastic matrix [31-33]. The morphology change upon dynamic vulcanisation is shown schematically in Figure 1.7. Compared with those blends comprising of uncured or slightly crosslinked components, dynamic vulcanisation possesses significantly improved mechanical properties that can be attributed to the stabilized morphology of rubber particles resulting from crosslinking. Dynamically vulcanised TPEs have been widely used because of their technical advantages in processing as well as their versatile end use properties [34]. The blends have important technical advantages in processing because of the thermoplastic nature of the melt, even though they contain a vulcanised rubber as one component.

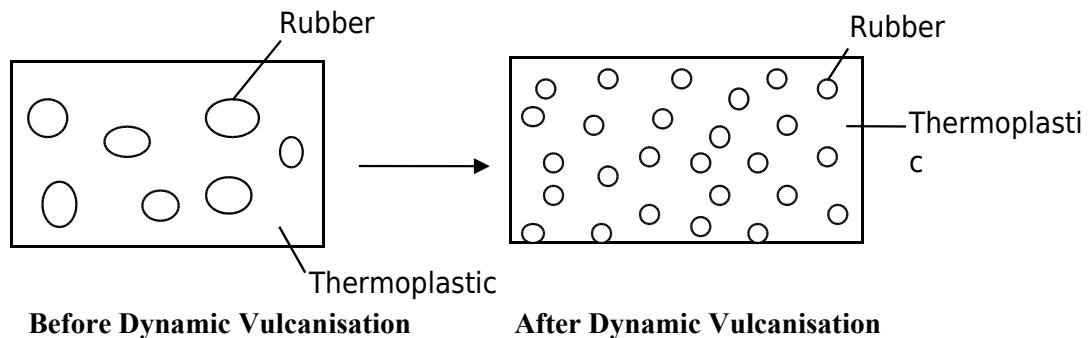


**Figure 1.7: A Schematic model showing the morphology change before and after dynamic vulcanisation of the blend.**

A series of extensive studies on dynamically vulcanised TPEs were carried out by Coran and Patel in the early 1980s [35-39]. Compositions containing all possible combinations of selected types of rubber with selected types of thermoplastics were prepared. The rubbers included butyl rubber (IIR), EPDM, natural rubber (NR), butadiene rubber (BR), styrene-butadiene-rubber (SBR), ethylene vinyl acetate (EVAc), acrylate rubber (ACM), chlorinated polyethylene (CPE), polychloroprene (CR) and nitrile

rubber (NBR). The thermoplastics included polypropylene (PP), polyethylene (PE), polystyrene (PS), acrylonitrile-butadiene-styrene (ABS), styrene-acrylonitrile (SAN), polymethyl methacrylate (PMMA), polybutylene terephthalate (PBT), polyamide (PA) and polycarbonate (PC) [40]. Only a few of them were commercialized, because of the fact that most of these blends were not technologically compatible and hence required one or more steps to make them compatible. Commercialized dynamic vulcanisates are commonly based on blends of unsaturated EPDM rubber and polypropylene, and to a lesser extent on a combination of butyl rubber [41], natural rubber [42-44], or nitrile rubber [9,39] with polypropylene.

Though several crosslinking agents have been employed to crosslink the elastomer phase in TPVs, the phenolic resin, peroxide and silane crosslinking systems have gained considerable commercial importance. Phenolic resin gained considerable commercial importance but still the formation of black specks motivates the development of other potential crosslinking systems [33]. Peroxides can crosslink both saturated and unsaturated polymers without any reversion characteristics. The formation of strong C-C bonds provides substantial heat resistance and good compression set property without any discoloration. However, the activity of peroxide depends on the type of polymer and presence of other ingredients in the system [45,46]. PP/EPDM blend can also be crosslinked by silane grafting in presence of a small amount of catalyst. Grafting, hydrolysis and condensation crosslinking reactions are carried out in a single stage process.

However, only few work has been carried out on the dynamic vulcanisation of rubber-toughened thermoplastics. Crosslinking of rubber raises the shear modulus, making them more difficult to cavitate. In the

more ductile polymers such as PC, this may not present problems. Crosslinking has a similar effect to a reduction in particle size, in that it shifts cavitation of the rubber to higher stresses where dilatational yielding can take place immediately. If the level of crosslinking is excessive, it will delay cavitation so much that the material fails by crazing and fracture from external surfaces before significant yielding has taken place.

Once cavitated, homogeneous rubber particles exercise only a limited influence on the subsequent yielding and fracture of the glassy polymer, because they are unable to form effective orientation-hardened bridges across shear bands, crazes and cracks [47]. The effects of crosslinking in rubber phase are seen most clearly in HIPS and ABS, where multiple crazing is the main mechanism of toughening. Crosslinking of the particles raises tensile yield stresses and depresses impact strength [48-51]. In order to optimize energy absorption in these materials, the rubber should have ideally a low level of crosslinking, allowing early cavitation of the particles and maximum extension of the rubber fibrils, but it should also form a graft or block copolymer with the glassy polymer to provide anchor points for the fibrils.

Excessive crosslinking of the rubber, introduced either deliberately during manufacture or through subsequent oxidation, can lead to a marked reduction in impact strength. Significant levels of crosslinking are also produced simply by prolonged heating at high temperatures. In extreme cases, the  $T_g$  of the rubber is shifted to much higher temperatures. However, studies on both irradiated and vulcanised HIPS have shown that tensile elongation and impact energy absorption are adversely affected even when the upward shift in the rubber  $T_g$  is only a few degree [52]. The rubber

remains rubbery throughout these crosslinking reactions, and the changes in toughness are solely due to its higher shear modulus.

## **1.2 Composites**

Composites are defined as materials consisting of two or more distinct phases with an interface between them. The constituent that is continuous and is often but not always, present in the greater quantity in the composite is termed the matrix. Composites consist of one or more discontinuous phases embedded in the continuous phase. The discontinuous phase, which is harder and stronger than matrix, is called reinforcement or reinforcing material. Properties of the composites are strongly influenced by the properties of their constituent materials, their distribution and the interaction among them. Composite properties may be either the sum of the properties of the distinct phases, or the property resulting from the synergistic action of the constituents. The strengthening mechanism of composites strongly depends on the geometry of the reinforcement. Based on the geometry of the reinforcement, composite materials may be classified as shown in Figure 1.8.

A composite whose reinforcement is a particle, which is non-fibrous and have dimensions approximately equal in all directions is called particulate composite. The shape of the reinforcing particles may be spherical, cubic, platelet or any regular or irregular geometry. Particle fillers are widely used to improve the properties of matrix materials such as to modify the thermal and electrical conductivities, improve performance at elevated temperatures, reduce friction, increase surface hardness and reduce shrinkage. In many cases, they are simply used to reduce cost.

Fibre reinforced composites contain reinforcements which is characterized by its length being much greater than its cross-sectional dimension. However, the ratio of the length to the cross-sectional dimension, known as the aspect ratio, can vary considerably. In fibrous composites, the matrix serves to bind the fibres together, transfer loads to the fibres, and protect them against environmental attack and damage due to handling. Reinforcing fibres in a single-layer composite may be short or long compared to its overall dimensions.



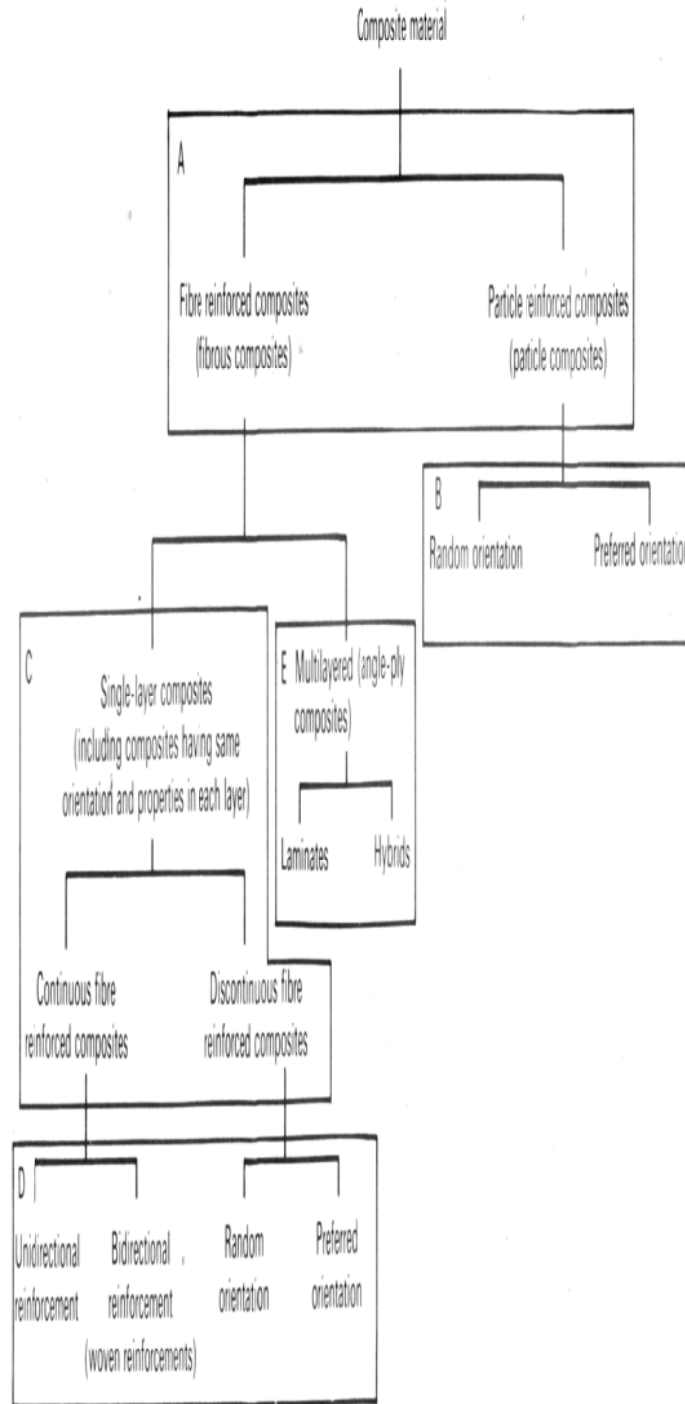


Figure 1.8: Classification of composites.

Composites with long fibres are called continuous-fibre-reinforced composites and those with short fibres, discontinuous-fibre-reinforced composites. Another distinction is that in discontinuous-fibre composites, the fibre length affects the properties of the composites [53].

Natural and man-made fibres are used as reinforcements in fibrous composites. Cellulose [54], jute [55-60], sisal [61,62], coconut fibre [63-66], banana fibre [67,68], hemp [69], flax [70-72], kenaf [73-75], agave [76,77], oil palm fibre [78-81], sugar palm fibre [82-84], etc are examples of natural fibre. All natural fibres except silk are short or staple fibres. Man-made fibres include carbon [85-88], aramid [89-93], polyester [94], Nylon [177-181], glass [95-98] etc. The natural fibres have many attractive characteristics like low density, less abrasiveness, low cost, biodegradability, and renewability over traditional glass and organic fibres. However, the major drawback of the natural fibre-polymer composites is the inherent incompatibility between the hydrophilic fibres and the hydrophobic polymer matrix.

### **1.2.1 Short fibre polymer composites**

In short fibre composites, the length of short fibre is neither too high to allow individual fibres to entangle with each other nor too small for the fibres to lose their fibrous nature. The reinforcement is uniform in the case of composites containing well dispersed short fibres. Short fibre reinforced composites can be processed in a manner similar to the matrix. The properties are strongly dependent on the fibre volume fraction and the fibre orientation distribution [99]. By adding suitable fibres and by controlling factors such as the aspect ratio, the dispersion and orientation of fibres, and the fibre-matrix adhesion, significant improvement in property can be achieved with thermoplastic, thermosetting and rubbery polymers. Typical

advantages of short fibre composites are design flexibility, high low-strain modulus, anisotropy in technical properties and stiffness, good damping, ease in processing and production economy.

### **1.2.2 Reinforcing Mechanism of short fibres**

In composites, loads are not directly applied on the fibres but are applied to the matrix material and transferred to the fibres through the fibre ends and also through the cylindrical surface of the fibre near the ends. In the case of short-fibre composites, the effects associated with fibre ends cannot be neglected and the composite properties are a function of fibre length. The end effects significantly influence the behaviour of and reinforcing effects in short-fibre composites. Early studies concerning variation of stresses along the length of a fibre were performed by Cox [100] and Outwater [101]. Probably the most often quoted theory of stress transfer is the shear-lag analysis applied by Rosen [102], who modified an earlier analysis of Dow [103].

### **1.2.3 Stress and strain distribution at fibres**

On considering a single fibre of length  $l$  embedded in a matrix of lower modulus and aligned with the loading direction, the stress applied to the matrix will be transferred to the fibre across the interface if the fibre is well bonded to the matrix. The matrix and the fibre will experience different tensile strains because of their different moduli; in the region of the fibre ends the strain in the fibre will be less than that in the matrix, as indicated in Figure 1.9. As a result of this strain difference, shear stresses are induced around the fibres in the direction of the fibre axis, and the fibre is stressed in tension. The shear strength of the fibre-matrix interface is relatively low. However, the surface

area of the fibre is large, so that, given sufficient length, the fibre can carry a significant load, even up to the fibre fracture load.

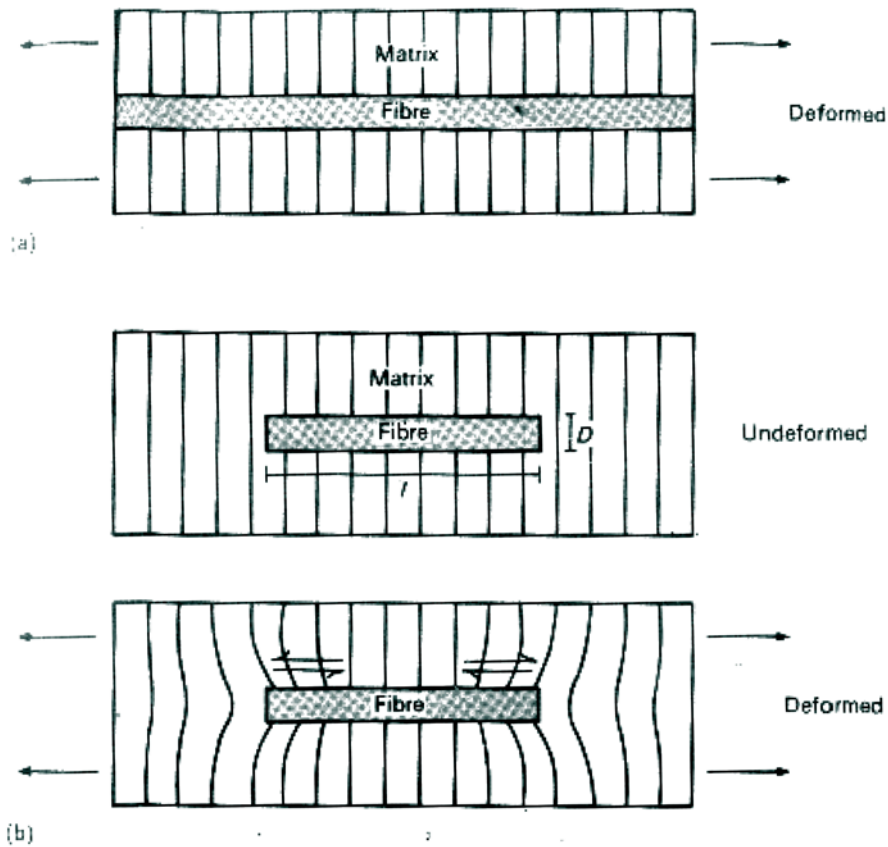


**Figure 1.9: Effect of deformation on the strain around a fibre in a low modulus matrix: a) continuous fibre, b) short fibre.**

The stress distribution along a fibre aligned parallel to the loading direction of the matrix may be represented as in Figure 1.10. The tensile stress is zero at the fibre ends, and a maximum at the centre of the fibre. Conversely, the shear stress around the fibre is a maximum at fibre ends, and for a sufficiently long fibre falls to zero in the centre. It is this variation

of shear stress (shear effect) that causes the build-up of tensile stress in the fibre.

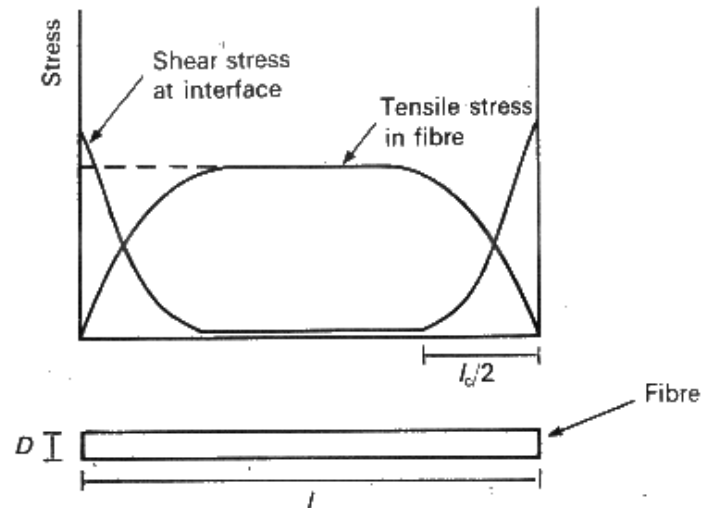


**Figure1.10: Variation of tensile stress in a fibre and shear stress at the interface.**

The reinforcing efficiency of fibres also depends on interface strength since load transfer requires a strong interfacial bond. The large shear stresses at fibre ends can produce undesirable effects such as

- 1) interfacial shear debonding
- 2) cohesive failure of matrix or fibre, and
- 3) matrix yielding

#### **1.2.4 Critical fibre length and average fibre stress**

The maximum strain that can be achieved in a fibre is that applied to the matrix,  $\epsilon_m$ , then the tensile stress in the fibre,  $\sigma_f$ , is given by

$$\sigma_f = \varepsilon_m E_f \dots\dots\dots(2)$$

where  $E_f$  is the Young's modulus of the fibre.

When the applied load is increased then  $\varepsilon_m$  will be larger resulting in a higher stress in the fibre, the maximum stress which can be obtained in the fibre is the fracture stress  $\sigma_{fu}$ . In order to achieve this level of stress in the fibre, the fibre length must be equal to a critical value  $l_c$  known as the critical fibre length.  $l_c$  may be defined as the minimum fibre length for a given diameter which will allow tensile failure of the fibre rather than shear failure of the interface, i.e., the minimum length of fibre required for the stress to reach the fracture stress of the fibre. The critical fibre length may be determined by considering a force balance in the fibre when the fibre stress is  $\sigma_{fu}$ .

$$\text{tensile force in fibre} = \frac{\sigma_{fu} \pi D^2}{4} \dots\dots\dots(3)$$

$$\text{shear force at interface} = \frac{\tau_y \pi D l_c}{2} \dots\dots\dots(4)$$

Equating (3) and (4)

$$\frac{l_c}{D} = \frac{\sigma_{fu}}{2\tau_y} \dots\dots\dots(5)$$

The value of the average stress depends on the stress distribution in the ends of the fibres and upon the fibre length.

a) At  $l < l_c$

The stress never reaches that sufficient to break the fibre and other mechanisms such as matrix failure and fibre pull-out will occur. The peak stress occurs at the centre of the fibre.

The average fibre stress  $\bar{\sigma}_f = \frac{\tau l}{D}$  .....(6)

b) At  $l = l_c$

The peak stress may just reach the fibre stress.

The average fibre stress  $\bar{\sigma}_f = \frac{\tau l_c}{D}$  .....(7)

c) At  $l > l_c$

The peak stress applies over the central portion of the fibre.

The average fibre stress  $\bar{\sigma}_f = \left[1 - \left(\frac{l_c}{2l}\right)\right] \sigma_{fu}$  .....(8)

To obtain an average fibre stress close to the maximum fibre stress, the fibre must be considerably longer than the critical length [104].

### 1.2.5 Parameters influencing the characteristics of short fibre-polymer composites

#### 1.2.5.1 Type and fibre breakage

Several researchers have studied the importance of fibre length and its influence on the properties of the composites [53,105-107]. In a composite material, fibre length is a critical factor which should not be too long so that they entangle with each other causing problems of dispersion. But a very small length of fibre does not offer sufficient stress transfer from the matrix to the fibre and give poor reinforcement. The severity of fibre breakage mainly depends on two factors: i) the type of fibre and its initial

aspect ratio and ii) the magnitude of the shear force generated during mixing. Fibres like glass and carbon are brittle and they possess a low bending strength than Nylon fibre which are more flexible and resistant to bending. There exists a certain aspect ratio for each type of fibre, below which no further breakage can occur depending on its resistance to bending. If the mix viscosity is high, more shear will be generated during mixing thus exceeding the critical bending stress of the fibre which eventually results in severe breakage. The breakage of fibre during mixing has been reported by O'Connor [108]. Murthy and De [109] reported that the breakage of the fibre is due to the buckling effect. Considerable fibre breakage occurred during mixing of fibres with high aspects ratio (as high as 500) resulting in reduction in aspects ratio [110]. Noguchi *et al.* [111] suggested that short PET fibres did not break up during the milling process and they are well dispersed, but carbon fibres did break up during milling, the fibre length being reduced to about 150  $\mu\text{m}$ . Kutty *et al.* [112,113] has reported that significant breakage of short Kevlar fibres occurs during mixing in Brabender plasticorder in TPU matrix.

#### **1.2.5.2 Critical fibre length and aspect ratio of fibre**

The fibre ends in the short fibre reinforced composites plays a major role in the determination of ultimate properties of the composite. The concept of critical fibre length over which the stress transfer allows the fibre to be stressed to its maximum, or at which efficient fibre reinforcement can be achieved has been used to predict the strength of the composites. A theoretical analysis has been done by Broutmann and Agarwal [53] on the mechanism of stress transfer between matrix and fibre of uniform length



and radius and they have given the expression for the critical fibre length ( $l_c$ ) as in eq. (5).

The aspect ratio ( $l/D$ ) of fibres is a major parameter that controls the fibre dispersion and fibre-matrix adhesion that gives the optimum performance of short fibre polymer composites. If the aspect ratio of the fibre is lower than the critical aspect ratio, insufficient stress will be transferred and the reinforcement will be inefficient. An aspect ratio in the range of 100-200, essential for high performance fibre-rubber composites have been suggested by several researchers [114-117]. It was reported that for synthetic fibre like polyester and Nylon aspect ratios of 220 and 170, respectively give good reinforcement in natural rubber vulcanisates [118,119]. Hong Gun Kim [120] have investigated the effects of fibre aspect ratio in short fibre reinforced composites.

### **1.2.5.3 Fibre orientation**

The preferential orientation of fibres in the matrix results in the development of anisotropy in the matrix.

When the composite undergoes shear flow, short fibres get oriented preferentially in a particular direction. The type of flow is determined by the processing techniques adopted, such as milling, extrusion and calendering. Mc Nally [121] has reviewed in detail the orientation of short fibres in polymer matrices. The effect of mill parameters such as number of passes, nip gap and mill roll speed on the fibre orientation was initially studied by Moghe who reported that nearly 60-70% fibres get oriented in the direction of the applied stress [122]. It was observed that the lower the nip gap, higher the anisotropy in tensile properties of the composites

implying greater orientation of fibres. This is represented as anisotropy index, which reduces gradually with increasing nip gap.

During processing and subsequent fabrication of short fibre polymer composites, the fibres orient preferentially in a direction depending upon the nature of flow i.e., convergent and divergent as explained by Goettler [123]. If the flow is convergent the fibres align themselves in the longitudinal direction and if it is divergent they orient in the transverse direction. During shear flow as experienced in a Brabender Plasticorder or a capillary rheometer, the fibre alignment may be random or unidirectional depending on the rate of shear. If the flow is elongational, then the fibre orientation takes place mainly in the direction of applied stress which is experienced during sheeting through the tight nip of a mill or during calendering.

#### **1.2.5.4 Fibre dispersion**

The primary requirement for obtaining a high performance composite is good dispersion of fibres in the matrix. The factors that affect dispersion in polymer matrices are fibre-fibre interaction and fibre length. These factors also account for the tendency to agglomerate during mixing.

Good fibre dispersion is the ultimate objective of any mixing process. Depending on the type of fibre, mixing may be either distributive or dispersive. Distributive mixing increases the randomness of spatial distribution of the minor constituents within the major base without reducing the size of the fibre, whereas dispersive mixing serves to reduce the agglomerate size. However, both phenomena occur simultaneously. Brittle fibres such as glass, jute, Kevlar, carbon and boron break down severely during

mixing on a mixing mill and in an intensive mixer. Therefore, these fibres need more distributive mixing, whereas fibres such as cellulose, Nylon, polyester and silk require more dispersive mixing due to their tendency to agglomerate during the mixing process. Homogeneous dispersion can be made possible by manipulating the mixing technique and controlling mixing parameters. The mixing process is optimised such that the breakage of the short fibres during mixing is minimal and the orientation of fibres is maximized.

#### **1.2.5.5 Fibre concentration**

The concentration of fibres in the matrix plays a crucial role in determining the mechanical properties of the fibre reinforced polymer composites. A lower concentration of fibres gives lower mechanical strength. This has been observed not only in rubbers [124] but also in thermoplastic elastomeric matrices [108, 125-127]. This behaviour has been attributed basically to two factors, (i) dilution of the matrix, which has a significant effect at low fibre loadings, and (ii) reinforcement of the matrix by the fibres which becomes increasingly important as fibre volume fraction increases. The matrix is not restrained by enough fibres at low fibre content and highly localized strains occur in the matrix at low strain levels causing the bond between fibres and the matrix to break, leaving the matrix diluted by non-reinforcing de-bonded fibres. However, at high fibre concentrations, the matrix is sufficiently restrained and stress is more evenly distributed thus the reinforcement effect outweighs the dilution effect [108]. As the concentration of fibres is further increased to a higher level, the tensile properties gradually improve to give strength higher than that of the matrix. The concentration of fibres beyond which the properties of the composite

improve above the original matrix strength is known as optimum fibre concentration. In order to achieve improvement in mechanical properties with short fibres, the matrix is loaded beyond this volume fraction of fibre. Quite often, at very high fibre concentrations, the strength again decreases, because there is insufficient matrix material to adhere the fibres together.

#### **1.2.5.6 Fibre-matrix adhesion**

Fibre-to-matrix adhesion plays a very prominent role in the reinforcement of short fibres in the polymer matrices. The fibre-matrix interfacial adhesion is important in determining the mechanical, dynamic mechanical and rheological characteristics of the composites since the stress transfer occurs at the interface from matrix to fibre. The polymer layer in contact with the fibre surface has different properties from the bulk matrix because of fibre/polymer interactions due to immobilization of the matrix chains, electrostatic forces or chemical bonds in presence of internal stresses, voids or microcracks in the interlayer [128]. The chemical structures of both the fibre and the matrix determine the extent of interfacial adhesion and, therefore, the strength of the composites. Though the mechanism of stress transfer is not clear, it has been postulated that it takes place through shearing at the fibre-matrix interface. In composites with low fibre-matrix adhesion, Derringer [129] observed that a region of yielding occurs extending over a large portion of the strain range which is accompanied by low tensile strength and high permanent set.

### **1.3 Fibre Reinforced Blends**

It is well known that short fibres are extensively used as reinforcing materials for thermosetting as well as thermoplastic and elastomer matrices. Their use in thermoplastic-rubber blends is also increasing.

Anuar *et al.* has reported the development of thermoplastic natural rubber (TPNR)/EPDM and PP/EPDM composites reinforced with kenaf fibre [73]. The mechanical properties and morphology of ternary composites based on PP/EPDM blends reinforced with natural flax fibres was analysed by Biagiotti *et al.* [70]. Gautam *et al.* [130] has investigated the mechanical, thermal and viscoelastic properties of ternary composites based on low density polyethylene (LDPE)/EPDM blend and high density polyethylene (HDPE)/EPDM blend reinforced with short jute fibres. The hybridization of TPNR based on carbon fibre and kenaf fibre was investigated for its mechanical and thermal properties by Anuar *et al.* [74]. Lopez-Manchado *et al.* [131,132] have explored the reinforcing effects of different synthetic fibres on the crystallization kinetics, rheology, dynamic mechanical analysis and mechanical properties of PP/EPDM blends. The results showed that the fibres act as an effective reinforcing agent to PP/EPDM blends, but the reinforcing effect was more pronounced at low EPDM content in the blend (25%). The effect of aramid fibre and maleic anhydride (MA)-g-PE compatibiliser on the mechanical and dynamic mechanical properties of TPNR composites was analysed by Ishak *et al.* [92]. The mechanical properties and morphology of TPNR/ Kenaf fibre composites along with MA-g-PP compatibiliser was investigated by Sameni *et al.* [75].

### 1.3.1 Fibre reinforced rubber-toughened thermoplastics

Appropriate incorporation of rubber particles into a brittle plastic matrix is a well established means of improving fracture toughness [133]. Unfortunately, the addition of an elastomer to a rigid matrix invariably reduces strength and stiffness relative to the unmodified material. On the

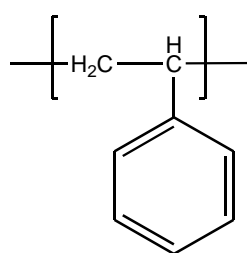
contrary, incorporation of high aspect ratio rigid fillers such as high modulus fibres into a polymer matrix improves stiffness and strength [134].

In principle, combining fibre reinforcement with rubber toughening provides an approach to materials with high stiffness, strength, and toughness. While there is a large body of literature addressing each individual method, the idea of combining the two has received relatively little attention [135,136]. Increasing the fibre loading of rubber toughened blends has shown to increase stiffness and strength, as expected [137,138]. The extent of property enhancement, however, depends on several factors; these include fibre strength and modulus, aspect ratio (fibre length/diameter), effectiveness of coupling between fibre and matrix, fibre orientation, and concentration. So far most investigations on rubber toughened thermoplastic composite systems have been focused on polyamides. Gaymans [138] for instance reported that the incorporation of short glass fibres into polyamide-6/ethylene-propylene rubber (PA-6/EPR) blends has changed the mode of failure of the composites from a relatively clean pull-out for glass-fibre/polyamide composites to a sheathed pull-out for the blend with glass fibres. In the PA-6/EPR/glass fibre, the fibres are coated with a thick layer of matrix material and the thickness has been observed to be related to rubber concentration, temperature and deformation rate. A similar finding has also been reported by Bailey and Bader [139] for short glass fibre-reinforced polyamide 66 blends. More recently, Pacorini *et al.* [140] have reported the fracture behaviour of short glass fibre-reinforced polyamide-66/ethylene-propylene-diene terpolymer rubber (PA-66/EPDM) composites. They have noted that a balance of fracture strength and fracture toughness could be achieved via the combination of glass fibres and EPDM. The fracture behaviour of glass bead incorporated SBS-toughened polypropylene

composites was studied by Mouzakis *et al.* [141]. The effect of glass fibre surface chemistry on the mechanical properties of glass fibre reinforced, EPR-g-MA-toughened Nylon-6 were examined by Laura *et al.* [142]. Ishak *et al.* [143] investigated the fracture behaviour of short glass fibre reinforced rubber-toughened PBT composites. Laura *et al.* [144] studied the effect of glass fibres on the mechanical properties of maleated-EPR/Nylon-6 blend. The impact properties of short glass fibre/rubber/polypropylene composites were examined by Tam *et al.* [145]. The effects of rubber type and particle size on the mechanical properties of glass fibre reinforced blends of Nylon-6 and EPR/EPR-g-MA or SEBS/SEBS-g-MA were investigated by Laura *et al.* [146].

### 1.3.2 Studies on Rubber-toughening of polystyrene

Polystyrene is produced via the free-radical initiated chain polymerization of styrene. It is an odourless, tasteless, rigid thermoplastic. It has the following repeat unit in its molecular structure.



The benzene ring reduces the ability of the polymer chain to bend and interferes substantially with other parts of the molecule. These characteristics prevent crystallization. Therefore, PS is essentially 100% amorphous [147].

Polystyrene is the fourth largest thermoplastic by production volume. Its popularity is due to its transparency, low density, relatively high modulus, excellent electrical insulation properties, low water absorption, dimensional stability, ease of processing and low cost [148]. A major limitation of polystyrene in many applications is its brittleness. This limitation led to the development of rubber modified polystyrenes, the so-called high impact polystyrenes. Packaging and containers are by far the largest outlets. Other applications include housewares, toys, recreational products, housing for appliance parts, disposable food containers etc [149].

Several methods for incorporating rubber into PS matrix are known. Natural rubber (NR) latex was studied for its use as an impact modifier of several polymers [150-152]. Due to its broad particle size distribution, the existence of large size and high molecular weight [153], the NR latex particle might be suitable for the improvement of toughness of glassy polymers including PS. Tangboriboonrat *et al.* [154] reported an attractive method for the preparation of HIPS based on NR. The key steps involved the use of  $\gamma$ -radiation vulcanised natural rubber (RVNR) latex/phase transfer/bulk polymerisation. The phase transfer technique has been successfully used to transfer uncrosslinked,  $\gamma$ -radiation vulcanised and deproteinated NR latex particles from the aqueous phase in to the styrene monomer phase [155-157]. The toughened PS prepared exhibited the HIPS like morphology, and the impact energy was higher than that of the unmodified PS.

Martinez *et al.* [158] has elucidated the connection between morphological structure and mechanical properties of PS/SBR blends using SBR with various structures. Sreenivasan *et al.* [159] has evaluated the



mechanical properties and morphology of nitrile rubber-toughened polystyrene. Some studies on impact modification of PS/EPDM blends by the addition of EPDM-g-styrene, EPDM-g-(styrene-co-methyl methacrylate) and EPDM-g-(styrene-co-maleic anhydride) as compatibilisers were reported [160-162] where improvement in impact strength was achieved because of the better compatibility and the interfacial adhesion of the copolymers with the PS matrix. Various styrene-butadiene copolymers were investigated as compatibilisers in polystyrene/butadiene blends [163]. Mathur *et al.* [164] has reported the effectiveness of PS-PB-PS triblock compatibilisers in improving the impact strength of PS/PB blends. Rubber toughening of syndiotactic polystyrene and poly(styrene/diphenylethylene) with hydrogenated styrene-butadiene-styrene (SBS) block copolymer increased the toughness in terms of notched impact strength and energy release rate [165].

Barbosa *et al.* [166, 167] and Soares *et al.* [168] studied the influence of a non-reactive compatibiliser, EVA-g-PS, on the mechanical and morphological properties of PS and the blends with EVA copolymers, whereas de Almeida *et al.* investigated the possibility of improving the miscibility of EVA in PS by introducing zinc sulphonate and sodium sulphonate groups on to PS. Tang *et al.* [169] has reported the rheological and mechanical properties of polystyrene/ethylene vinyl acetate blends compatibilised with polystyrene-block-polybutadiene. The mechanical properties were comparable to that of HIPS. PS was toughened with EPDM in the presence of styrene-butadiene-styrene (SBS) block copolymer and the incorporation of SBS into the PS/EPDM blends improved the impact properties [170].

The effects of dynamic vulcanisation using sulphur, peroxide, and mixed systems on the morphology and mechanical properties of thermoplastic elastomers based on natural rubber and polystyrene has been reported by Ashaletha *et al.* [171] Dynamic vulcanisation causes a decrease in the size of the dispersed particles and improvement in mechanical properties. The impact strength of blends consisting of PS and EPDM could be increased by adding poly(styrene-ethylene-propylene) (SEP) compatibiliser and an organic peroxide during reactive extrusion [172]. The increased impact strength could be related to an enhanced adhesion between the dispersed EPDM phase and the PS matrix, as a consequence of radical graftlink or co-crosslink reactions between the rubbery part (EP) of the compatibiliser and the dispersed EPDM rubber.

### **1.3.3 Composites of Rubber – Toughened Polystyrene**

Braun *et al.*[173] has investigated that toughness could be improved by the addition of chalk to PS/BR blends with low BR concentrations. The addition of chemically treated rice husk powder (RHP) and maleic anhydride-polypropylene coupling agent improved the mechanical properties of PS/SBR blends [174] The effects of partial replacement of silica by RHP on the processing, mechanical properties, effect of thermo-oxidative aging, water absorption and morphology of PS/SBR blend were investigated by Zurina *et al.* [175].

However, no serious attempt has been made to evaluate the use of short Nylon-6 fibres as a reinforcing fibre for rubber-toughened PS. The main features of Nylon fibres are exceptional strength, high elastic recovery, abrasion resistance, luster, resistance to damage by oil and many chemicals, high resilience and outstanding durability. The reinforcement of

rubbers using Nylon fibres has been reported by various authors [176-178]. Sreeja *et al.* [179-181] studied the effect of short Nylon-6 fibres on the mechanical properties of NR, NBR and SBR composites. Physico-mechanical properties of EPDM/Nylon-6 short fibre composite was studied by Wazzan [182]. Cure characteristic and mechanical properties of short Nylon fibre reinforced composites based on NBR and CR containing epoxy based bonding agent was investigated by Seema *et al.* [183,184]. Mechanical properties of short Nylon fibre reinforced SBR/NR composites were studied in detail by Ma *et al.* [185]. Short Nylon fibre reinforced polypropylene composites [186] and recyclable high density polyethylene composites [187] was studied by Thomas *et al.*

#### **1.4 Scope and objectives of the work**

Polystyrene is a versatile material with very interesting characteristics which makes it a high consumption polymer. However, its major limitation is its poor impact behaviour. In order to improve this deficiency, different elastomers has been used to produce toughened polystyrene. Unfortunately this results in the loss of stiffness and strength, because most rubbers are immiscible with polystyrene. Compatibilisation of the blend may alleviate this problem. The goal of compatibilisation is to obtain a stable dispersion that will lead to the desired morphology and properties. Successful compatibilisation will be able to 1) reduce interfacial energy, (2) permit finer dispersion during mixing, (3) enhance the stability of dispersion against agglomeration or phase separation throughout the processing/ conversion to the final product, and (4) improve the interfacial adhesion. One method of compatibilisation is the dynamic vulcanisation of the elastomeric phase of the blend.

To improve the stiffness-toughness balance of rubber-toughened polystyrene, short fibres may be incorporated in blends. The studies so far reported proved that utilisation of short fibres as reinforcements in single polymer composites offer economical, environmental and qualitative advantages. The use of short Nylon-6 fibres as reinforcing agents opens a new avenue for the utilisation of waste fibres, available in plenty from fibre and textile industries. The properties of short-fibre containing composites depend critically on fibre content, orientation and fibre – matrix interface bond strength. A detailed study of the effect of these parameters on the composite properties will be highly informative. A strong interfacial bond can effectively transfer load from the matrix to the fibre and hence can improve the overall performance of the composite.

The main objectives of the present work are:

- To investigate the effect of blend ratio for toughening polystyrene.

One of the principal weaknesses of polystyrene in many applications is its low impact resistance. To counteract this problem, it is necessary to toughen it with rubbers. The shape, size and distribution of the dispersed phase along with the interfacial characteristics decide the mechanical properties of the blend. The effect of blend ratios of PS/NR, PS/SBR and PS/WTR (whole tyre reclaim) on the mechanical and dynamic mechanical properties has been investigated.

- Evaluation of the effect of dynamic vulcanisation.

The PS/rubber blend systems are incompatible resulting in inferior mechanical properties. Hence it is necessary to

compatibilise it for satisfactory product performance. Dynamic vulcanisation was adopted as a compatibilisation technique. Dicumyl peroxide (DCP) was used as the crosslinking system. The effect of DCP content on the mechanical properties, morphology and dynamic mechanical properties of PS/NR and PS/SBR blends were investigated.

- To study the effect of short Nylon-6 fibres on the blend.

The incorporation of rubber into PS improves the toughness of PS but reduces its strength and elastic modulus. To improve the mechanical properties, an attempt was made to determine the suitability of short Nylon-6 fibres in PS/NR, PS/SBR and PS/WTR blends. The effect of fibre loading on the mechanical and dynamical mechanical properties of the blend were investigated.

- To investigate the effect of RFL-coated Nylon-6 fibre on the blend.

For further improvement of the mechanical properties of the rubber-toughened blends, RFL-coated Nylon fibres were used. The effect of fibre loading on the mechanical and dynamic mechanical properties of PS/NR, PS/SBR and PS/WTR blends were studied.

- To evaluate the influence of surface modification of Nylon fibres and use of compatibiliser on the blends - PS/NR, PS/SBR and PS/WTR.

The interaction between the polar fibre and non-polar blend is poor. Modification of interfacial interaction is carried out by surface hydrolysis of the Nylon fibre and the use of a reactive compatibiliser, maleic anhydride-grafted-polystyrene (MA-g-

PS). The effect of untreated and surface hydrolysed Nylon fibre in conjunction with the compatibiliser on the mechanical and dynamical mechanical properties of PS/NR, PS/SBR and PS/WTR blends were investigated.

- Evaluation of thermal degradation behaviour of the blend and the composites.

Since most of the polymeric materials are manufactured by melt processing, it is essential to study the thermal stability of these materials. One of the most accepted methods for studying the thermal properties of polymeric materials is the thermogravimetry. The thermogravimetric curve and its derivative (DTG) provides information about the nature and extent of degradation of polymeric materials. The effect of blend, dynamic vulcanisation, short Nylon-6 fibres and surface hydrolysed fibres in conjunction with compatibiliser on the thermal stability were evaluated.

## **1.5 References**

- [1] Manson JA, Sperling LH. Polymer Blends and Composites. New York: Plenum Press; 1976.
- [2] Paul DR, Newman S, editors. Polymer Blends Vols. I and II. New York: Academic Press; 1978.
- [3] Shaw MT, Polym Eng Sci 1982; 22:115.
- [4] Robeson LM, Polym Eng Sci 1984; 24:587.
- [5] Utracki LA. Polymer Alloys and Blends - Thermodynamics and Rheology. Munich: Hanser Publishers; 1990.

- [6] Manas Chanda, Salil K Roy. Industrial Polymers, Speciality polymers, and their applications. Boca Raton: CRC press; 2009.
- [7] Cor Koning, Martin Van Duin, Christophe Pagnouille and Robert Jerome. Prog Polym Sci 1998; 23:707.
- [8] Legge NR, Holden G, Schroeder HE, editors. Thermoplastic Elastomer: A Comprehensive Review. Munich: Hanser Publishers; 1987.
- [9] Morris HL. Handbook of Thermoplastic Elastomers. New York: Van Nostrand Reinhold; 1979.
- [10] Walker BM, Rader CP, editors. Handbook of Thermoplastic Elastomers. New York: Van Nostrand Reinhold; 1988.
- [11] Bhowmick AK, Stephens HL, editors. Handbook of Elastomers: New Developments and Technology. New York: Marcel Dekker; 1988.
- [12] De SK, Bhowmick AK, editors. Thermoplastic Elastomers from Rubber Plastic Blends. London: Horwood; 1990.
- [13] Birley A, Scott M. Plastic Materials: Properties and Applications. New York: Leonard Hill; 1982, p.45.
- [14] Bucknall CB, Cote PP, Partridge IK. J Mater Sci 1986; 21:301.
- [15] Bucknall CB, Davies P, Partridge IK. J Mater Sci 1986; 21:307.
- [16] Michler GH. Kunststoff-Mikromechanik: Morphologie, Deformations- und Bruchmechanismen. Munchen: Hanser-Verlag; 1992.
- [17] Goerg H Michler. Electron microscopy of polymers. Berlin: Springer Laboratory; 2008, p.351.
- [18] Wu S. Polymer 1985; 26:1855.
- [19] Kim GM, Michler GH. Polymer 1998; 39:5689.
- [20] Michler GH, Bucknall CB. Plast Rubber Compos 2001; 30:110.

- [21] Menges G, Berndtsen N, Opfermann J. *Kunststoffe* 1979; 69:562.
- [22] Michler GH, Gruber K. *Plaste Kautschuk* 1976; 23:346.
- [23] Michler GH. *J Macromol Sci Phys B* 2001; 40:277.
- [24] Gessler M. U.S. Pat. 3,037,954; 1962.
- [25] Fisher K. U.S. Pat. 3,758,643; 1973.
- [26] Coran AY, Patel RP. *Rubber Chem Technol* 1980; 53:141.
- [27] Sabet AS. U.S. Pat. 4,311,628; 1982.
- [28] Coran AY, Patel RP, William D. *Rubber Chem Technol* 1982; 55:116.
- [29] Abdou-Sabet S, Puydak RC, Rader CP. *Rubber Chem Technol* 1996; 69:76.
- [30] Duin MV, Machado AV. *Polym Degrad Stab* 2008; 90:340.
- [31] Huang H, Liu X, Ikehara T, Nishi T. *J Appl Polym Sci* 2003; 90:824.
- [32] Goharpey F, Katbab AA, Nazockdast H. *J Appl Polym Sci* 2001; 81:2531.
- [33] Duin MV. *Macromol Symp* 2006; 233:11.
- [34] Kim KH, Cho WJ, Ha CS. *J Appl Polym Sci* 1996; 59:407.
- [35] Coran AY, Patel R. *Rubber Chem Technol* 1980; 53:781.
- [36] Coran AY, Patel R. *Rubber Chem Technol* 1981; 54:91.
- [37] Coran AY, Patel R. *Rubber Chem Technol* 1981; 54:892.
- [38] Coran AY, Patel R. *Rubber Chem Technol* 1983; 56:210.
- [39] Coran AY, Patel R. *Rubber Chem Technol* 1983; 56:1045.
- [40] Coran AY. *Rubber Chem Technol* 1995; 68:369.
- [41] Puydak RC, Hazelton DR, Ouhadi T. (to Advanced Elastomer Systems), U.S. 5,073,597; 1991.



- [42] Kuriakose B, De SK. Polym Eng Sci 1985; 25:630.
- [43] Kuriakose B, De SK, Bhagawan SS, Sivaramkrishnan R, Athithan SK. J Appl Polym Sci 1986; 32:5509.
- [44] Tinker AJ. paper presented at the Symposium on Thermoplastic Elastomers, ACS Rubber Division Meeting, October 1988, Cincinnati, OH, USA.
- [45] Naskar K. Rubber Chem Technol 2007; 80:504.
- [46] Naskar K, Noordermeer JWM. Rubber Chem Technol 2003; 76:1001.
- [47] Haward RN, Young RJ, editors. The Physics of Glassy Polymers. London: Chapman and Hall; 1997.
- [48] Birkinshaw C, Buggy M, O’Niell M. J Appl Polym Sci 1990;41:1913.
- [49] Birkinshaw C, Buggy M, Quigley F. J Appl Polym Sci 1993; 48:181.
- [50] Soares VLP. PhD Thesis, Cranfield University.
- [51] Bucknall CB, Soares VLP, Yang HH, Zhang HC. Makromol Chem, Macromol Symp 1996; 101:265.
- [52] Perche N. MSc Thesis, Cranfield University; 1995.
- [53] Broutman LJ, Aggarwal BD. Analysis and performance of fibre composites. Newyork : Soc Plast Ind, John Wiley and Sons; 1980.
- [54] Abdelmouleh M, Boufi S, Belgacem MN, Dufresne A. Comp Sci Technol 2007; 67:1627.
- [55] Rana AK, Mandal A, Mitra BC, Jacobson R, Rowell R, Banerjee AN. J Appl Polym Sci 1998; 69:329.
- [56] Jochen G, Andrzej KB. Polym Comp 1999; 20:604.
- [57] Dash BN, Rana AK, Mishra HK, Nayak SK, Mishra SC, Tripathy SS. Polym Comp 1999; 20:62.

- [58] Rana AK, Mandal A, Bandopadyay S. *Comp Sci Technol* 2003; 63:801.
- [59] Karmakar AC, Youngquist AJ. *J Appl Polym Sci* 1996; 62:1147.
- [60] Rana AK, Mitra BC, Banerjee AN. *J Appl Polym Sci* 1999; 71:531.
- [61] Smita M, Sushi KV, Sanjay KN, Sudhansu ST. *J Appl Polym Sci* 2004; 94:1336.
- [62] Maries A, Malhotra SK, Joseph K, Sabu T. *Comp Sci Technol* 2005; 65:1077.
- [63] Marina HA, Leila LYV, Cristina RGF, Marcia G de O, Jean LL. *Int J Polym Anal Charact* 2008; 13:319.
- [64] Jean LL, Cristina RGF, Marcia CAML, Leila LYV, Ana MF de S. *J Appl Polym Sci* 2007; 106:3653.
- [65] Robson LF, Cristina RGF, Leila LYV, Jean LL. *Int J Polym Mater* 2006; 55: 1055.
- [66] Brahmakumar M, Pavithran C, Pillai RM. *Comp Sci Technol* 2005; 65:563.
- [67] Laly AP, Sabu T, Groeninckx G. *Comp Part A* 2006; 37:1260.
- [68] Laly AP, Zachariah O, Sabu T. *Comp Sci Technol* 2003; 63:283.
- [69] Sharifah HA, Martin PA. *Comp Sci Technol* 2004; 64:1219.
- [70] Biagiotti J, Lopez Manchado MA, Arroyo M, Kenny JM. *Polym Eng Sci* 2003; 43:1031.
- [71] Guillermo C, Aitor A, Rodrigo L, Inaki M. *Comp Sci Technol* 2003; 63:1247.
- [72] Baiardo M, Zini E, Scandola M. *Compos Part A* 2004; 35:703.
- [73] Anuar H, Zuraida A. *Comp Part B* 2011; 42:462.
- [74] Anuar H, Ahmad SH, Rasid R, Ahmad A, Wan Busu WN. *J Appl Polym Sci* 2008; 107:4043.
- [75] Sameni JK, Ahmad SH, Zakaria S. *Polym-Plast Technol Eng* 2003; 42:345.
- [76] Myslamsy K, Rajendran I. *J Mat Des* 2011; 32:4629.

- [77] Mylsamy K, Rajendran I. *J Mat Des* 2011; 32:3076.
- [78] Kalam A, Sahar BB, Khalis YA, Wong SV. *Compos Struct* 2005; 71:34.
- [79] Myrtha K, Holia O, Dawam AAH, Anung SJ. *Bio Sci* 2008; 8:101.
- [80] Rozman HD, Saad MJ, Mohd Ishak ZA. *J Polym Test* 2003; 22:335.
- [81] Rozman HD, Tay GS, Kumar RN, Abusamah A, Ismail H, & Mohd Ishak, Z.A.M. *Euro Polym J* 2001; 37:1283.
- [82] Bachtiar D, Sapuan SM, Hamdan MM. *Polym-Plast Technol Eng* 2009; 48:379.
- [83] Suriani MJ, Hamdan MM, Sastra HY, Sapuan SM. *Multidiscipl Modeling Mater Struct* 2007; 3:213.
- [84] Leman Z, Sastra HY, Sapuan SM, Hamdan MM, Maleque MA. *J Appl Technol* 2005; 3:14.
- [85] Rezaei F, Yunus R, Ibrahim NA. *J Mat Des* 2009; 30:260.
- [86] Fu SY, Lauke B, MaÈder E, Hu X, Yue CY. *Compos Part A* 2000; 31:1117.
- [87] Kuriger RJ, Khairul MA, Anderson PD, Jacobson RL. *Compos Part A* 2002; 33:53.
- [88] Rezaei F, Yunus R, Ibrahim NA, Mahdi ES. *Polym Plast Technol Eng* 2008; 47:351.
- [89] Arroyo M, Zitzumbo R, Avlos F. *Polymer* 2000; 41:6351.
- [90] Sunan S, Taweechai A, Chakrit S, Wiriya M, Bualek-Limcharoen S. *Polymer* 1999; 40:6437.
- [91] Taweechai A, Budsaporn S, Bualek-Limcharoen S, Wiriya M. *Polymer* 1999; 40:2993.
- [92] Ishak A, Wong PY, Ibrahim A. *Poly Comp* 2006; 27:395.

- [93] Anongnuch C, Chakrit S, Taweechai A, Bualek-Limcharoen S, Wiriya M. J Appl Polym Sci 1999; 74:2414.
- [94] Lopez Manchado MA, Arroyo M. Polymer 2000; 41:7761.
- [95] Fares DA, Rakesh KG. Can J Chem Eng 2006; 84:693.
- [96] Nair SV, Wong SC, Goettler LA. J Mater Sci 1997; 32:5335.
- [97] Weizhi W, Longxiang T, Baojun Q. Euro Polym J 2003; 39: 2129.
- [98] Saujanya C, Radhakrishnan S. Poly Comp 2001; 22: 232.
- [99] De SK, White JR editors. Short fibre-polymer composites. England: Woodhead Publishing Limited; 1996
- [100] Cox HL. Br J Appl Phys 1952; 3:72.
- [101] Outwater JO. Mod Plast March 1956; 56.
- [102] Rosen BW. Mechanics of composite strengthening. In: Fibre Composite Materials. Ohio: American Society for metals, Metals Park; 1964 (Chapter 3).
- [103] Dow NF. General Electric Company report No. TISR63SD61 August 1963.
- [104] Mathews FL, Rawlings RD. Composite Materials: Engineering and Science. London: Chapman and Hall; 1994.
- [105] Monette L, Anderson MP, Grest GS. Polym Comp 1993; 14:101.
- [106] Termonia YJ. Mater Sci Lett 1993; 12:732.
- [107] Rosen BW. Fibre Composite Materials. Ohio: American Society for metals, Metal Park; 1965.
- [108] O'Connor JE. Rubber Chem Technol 1977; 50:945.
- [109] Murthy VM, De SK, Bhagavan SS, Sivaramakrishnan R, Athithan SK. J Appl Polym Sci 1983; 28:3485.
- [110] Kutty SKN, Nando GB. Int J Polym Mater 1992; 17:235.

## *Chapter -1*

---

- [111] Noguchi, Ashida M, Mashimo S. Nippon Gomu Kyokaishi 1984; 12:829.
- [112] Kuty SKN, Nando GB. Plast Rub Comp 1993; 19:105.
- [113] Kuty SKN, Nando GB. J Appl Polym Sci 1991; 43:1913.
- [114] Setua DK, De SK. Rubber Chem Technol 1983; 56:808.
- [115] Boustany K, Arnold R L. J Elasto Plast 1976; 8:160.
- [116] O'Connar JE. Rubb Chem Technol 1974; 47:396.
- [117] Boustany K, Coran AY. US Patent No. 3 397 364, to Monsanto Co, 1972.
- [118] Ibarra L, Chamorro AC, J Appl Polym Sci 1991; 43:1805.
- [119] Rueda LI, Chamorro AC, J Appl Polym Sci 1989; 37:1197.
- [120] Hong Gun Kim. J Mech Sci Technol 2008; 22:130.
- [121] McNally DL, Polym Plast Technol Eng 1977; 8:101.
- [122] Moghe SR, Rubber Chem Technol 1976; 49:1160.
- [123] Goettler LA, Lambright AJ, Leib RI. Rubb Chem Technol 1979; 52:838.
- [124] Prasanth Kumar R, Thomas S. J Appl Polym Sci 1995; 58:597.
- [125] Roy D, Bhowmick AK, De SK. Polym Eng Sci 1992; 32:971.
- [126] Senapati AK, Kuty SKN, Nando GB, Pradhan B. Int J Polym Mater 1989; 12:203
- [127] Senapati AK, Nando GB. Int J Polym Mater 1988; 12:73.
- [128] Calleja RD, Ribelles JLG, Pradas MM, Greus AR, Colomer FR. Polym Compos 1991; 12:428.
- [129] Derringer DC. J Elastom Plast 1971; 3:230.
- [130] Gautam S, Arup C. J Appl Polym Sci 2008; 108:3442.

- [131] Lopez Manchado MA, Torre L, Kenny JM. *J Appl Polym Sci* 2001; 81:1063.
- [132] Lopez Manchado MA, Biagiotti J, Kenny JM. *Polym Compos* 2002; 23:779.
- [133] Collyer AA, editor. *Rubber toughened engineering plastics*. London: Chapman and Hall; 1994.
- [134] Krenchel H. *Fibre reinforcement*. Copenhagen: Akademisk Forlag, 1964.
- [135] Wong SC, Mai YW. *Polym Eng Sci* 1999; 39:356.
- [136] Friedrich K, Karger-Kocsis J. *Solid state behaviour of linear polyesters and polyamides*. Schultz JM,
- [137] Fakirov S editors. Englewood Cliffs, NJ: Prentice Hall; 1990.
- [138] Gaymans RJ. Toughened polyamides. In: Collyer AA editor. *Rubber toughened engineering plastics*. London: Chapman and Hall; 1994(Chapter 7),.
- [139] Bailey RS, Bader MG. The effect of toughening on the fracture behaviour of a glass fibre reinforced polyamide. In: Harrington WC, Strife J, Dhingra AK, editors. *5th International Conference on Composite Materials, ICCM-V San Diego, CA*. The Metallographic Society, 1985.
- [140] Pecorini TJ, Hertzberg RW. *Polym Comp* 1994; 15:174.
- [141] Mouzakis DE, Stricker F, Mulhaupt R, Karger-Kocsis J. *J Mater Sci* 1998; 33:2551.
- [142] Laura DM, Keskkula H, Barlow JW, Paul DR. *Polymer* 2002; 43:4673.
- [143] Mohd Ishak ZA, Ishiaku US, Karger-Kocsis J. *Comp Sci Tech* 2000; 60:803.
- [144] Laura DM, Keskkula H, Barlow JW, Paul DR. *Polymer* 2002; 43:4673.
- [145] Tam WY, Cheung TYH, Li RKY. *J Mater Sci* 2000; 35:1525.
- [146] Laura DM, Keskkula H, Barlow JW, Paul DR. *Polymer* 2003; 44:3347.

## *Chapter -1*

---

- [147] Brent Strong A. *Plastics: Materials and Processing* 3<sup>rd</sup> edition. New Jersey: Pearson Prentice Hall; 2006, p. 247.
- [148] Charles Harper A. *Modern Plastics Handbook*. London: Mc Graw-Hill; 2000.
- [149] Manas Chanda, Salil K Roy. *Industrial Polymers, Speciality Polymers and their Applications*. Boca Roton: CRC press; 2009.
- [150] Schneider M, Pith T, Lambla M. *J Appl Polym Sci* 1996; 62:273.
- [151] Schneider M, Pith T, Lambla M. *J Mater Sci* 1997; 32:6331.
- [152] Schneider M, Pith T, Lambla M. *Polym Adv Technol* 1996; 7:577.
- [153] Gazeley KF, Gorton ADT, Pendle TD. *Natural Rubber Science and Technology*. Roberts AD editor. Oxford: Oxford Science Publications; 1988, p.63.
- [154] Tangboriboonrat P, Tiyaipiboonchaiya C. *J Appl Polym Sci* 1999; 71:1333.
- [155] Tangboriboonrat P, Suchiva K, Kuhakarn S. *Polymer* 1994; 35:3144.
- [156] Tangboriboonrat P, Suchiva K, Riess G. *Polymer* 1995; 36:781.
- [157] Tangboriboonrat P, Suchiva K, Kuhakarn S, Thuchinda S. *J Nat Rubb Res* 1996; 11:26.
- [158] Martinez Barrera G, Menchaca C, Pietkiwicz D, Brostow W. *ISSN 1392-1320 Materials Science* 2004; 10:166.
- [159] Sreenivasan PV, Kurian P. *Int J Polym Mat* 2007; 56:1041.
- [160] Shaw S, Singh RP. *J Appl Polym Sci* 1990; 40: 685.
- [161] Shaw S, Singh RP. *J Appl Polym Sci* 1990; 40: 693.
- [162] Shaw S, Singh RP. *J Appl Polym Sci* 1990; 40: 701.
- [163] Cavanaugh TJ, Buttle K, Turner JN, Nauman EB. *Polymer* 1998; 39: 4191.
- [164] Mathur D, Nauman EB. *J Appl Polym Sci* 1999; 72:1151.

- [165] Ramsteiner F, McKee GE, Heckmann W, Oepen S, Geprags M. *Polymer* 2000; 41: 6635.
- [166] Barbosa RV, Soares BJ, Gomes AS. *J Appl Polym Sci* 1993; 47:1411.
- [167] Barbosa RV, Soares BJ, Gomes AS. *Macromol Chem Phy* 1994; 195:3149.
- [168] Soares BJ, Barbosa RV, Covas JC. *J Appl Polym Sci* 1997; 65: 2141.
- [169] Tang LW, Tam KC, Yue CY, Hu X, Lam YC, Li L. *J Appl Polym Sci* 2004; 94: 2071.
- [170] Fang Z, Guo Z, Zha L, *Macromol Mater Eng* 2004; 44: 1295.
- [171] Ashaletha R, Kumaran MG, Sabu Thomas. *Eur Polym J* 1999; 35: 253.
- [172] Crevecoeur JJ, Nellisen L, vander Sanden MCM, Lemstra PJ. *Polymer* 1995; 36:1295.
- [173] Braun D, Klein M, Hellmann GP. *J Appl Polym Sci* 1996; 60: 981.
- [174] Zurina M, Ismail H, Bakar AA. *J Appl Polym Sci* 2004; 92: 3320.
- [175] Zurina M, Ismail H, Bakar AA. *J Reinf Plast Comp* 2004; 23:1397.
- [176] Bipinbal PK, Kutty SKN. *J Appl Polym Sci* 2008;109:1484.
- [177] Seema A, Kutty SKN. *Int J Polymer Mater* 2006; 55: 25.
- [178] Seema A, Kutty SKN. *Int J Polymer Mater* 2005; 54:1031.
- [179] Sreeja TD, Kutty SKN. *J Elastomers Plast* 2001; 33: 225.
- [180] Sreeja TD, Kutty SKN. *J Elastomers Plast* 2002; 34:157
- [181] Sreeja TD, Kutty SKN. *Int J Polym Mater* 2003;52: 239
- [182] Wazzan AA. *Int J Polymer Mater* 2004; 53:59.
- [183] Seema A, Kutty SKN. *J Appl Polym Sci* 2006; 99: 532.
- [184] Seema A, Kutty SKN. *Polym Plast Technol Eng* 2005; 44: 1139.



*Chapter -1*

---

[185] Ma Peiyu, Zhao Jan, Tang J, Dai G. Guofenzi Cailiao Kexue Yu Gongcheng 1994; 10: 55.

[186] Thomas N Abraham, George KE. Polym Plast Technol Eng 2007; 46: 321.

[187] Thomas N Abraham, George KE. Plast Rub Comp 2005; 34:196.

.....

# MATERIALS AND EXPERIMENTAL TECHNIQUES

<b>2.1</b>	<b>Materials</b>
<b>2.3</b>	<b>Moulding</b>
<b>2.4</b>	<b>Mechanical properties</b>
<b>2.5</b>	<b>Extraction of composite</b>
<b>2.6</b>	<b>Scanning electron microscopy (SEM)</b>
<b>2.7</b>	<b>Fourier transform infrared spectroscopy (FTIR)</b>
<b>2.8</b>	<b>Dynamic mechanical analysis (DMA)</b>
<b>2.9</b>	<b>Thermogravimetric analysis (TGA)</b>
<b>2.10</b>	<b>References</b>

This chapter gives a brief description of the materials used for the study, experimental methods, procedures used for blending, sample preparation and measurement of various properties.

## **2.1 Materials**

### **2.1.1 Polymers**

#### **2.1.1.1 Polystyrene (PS)**

Polystyrene (Grade SC 206 GPPS) with specific gravity 1.04 and melt flow index 12 g/ 10 min (at 200 °C and 5 kg load).was obtained from Supreme Petrochemicals Ltd, Maharashtra.

### 2.1.1.2 Natural rubber (NR)

Natural rubber used for the study was ISNR 5 obtained from Rubber Research Institute of India, Kottayam, Kerala. The molecular weight, molecular weight distribution and non-rubber constituents of Natural rubber are affected by clonal variation, season and methods of preparation [1]. Hence rubber obtained from same lot has been used in this study. Its specification is given below.

Parameters	Value
Dirt content, %	0.05
Volatile matter, %	0.5
Nitrogen, %	0.3
Ash content, %	0.4
Initial plasticity number, P <sub>0</sub>	30
Plasticity retention index, PRI	60

### 2.1.1.3 Styrene butadiene rubber (SBR)

Styrene butadiene rubber (SBR) used was Kumho SBR 1502 with a density of 0.94g/cm<sup>3</sup>, supplied by M/s Kumho Petrochemicals, Korea. The specification is given below.

Parameters	Value
Bound styrene content, %	23.3
Volatile matter, %	0.23
Soap content, %	0.01
Ash content, %	0.16
Organic acid content, %	5.46

Mooney viscosity, [ML (1+4)100°C]	51
-----------------------------------	----

#### 2.1.1.4 Whole Tyre Reclaim (WTR)

Whole Tyre Reclaim (WTR) was obtained from Kerala Rubber and Reclaims, Mamala, Kerala, India. The characteristics are given below.

Parameters	Value
Rubber hydrocarbon content, %	45
Acetone extract, %	10
Carbon black content, %	28
Ash content, %	10
Moisture content, %	1
Mooney viscosity, [ML (1+4)100°C]	27

#### 2.1.2 Nylon-6 fibre

Nylon-6 fibre obtained from Apollo Tyres, Chalakudy was chopped to approximately 6 mm. Specifications of Nylon-6 fibre is given below.

Parameters	Undipped	RFL-coated
Breaking strength (N),	278	278
Elongation at break (%),	32	20
Twist (tpm)	335	318
Linear density (tex)	419	415
Dip pick up (%)	-	4.25

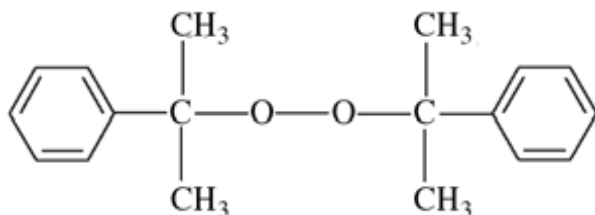
#### 2.1.3 Chemicals

##### 2.1.3.1 Maleic anhydride (MA) [C<sub>4</sub> H<sub>2</sub> O<sub>3</sub>]

Maleic anhydride (MA) was used for grafting on polystyrene. The compound was supplied by Loba Chemie Pvt. Ltd, Mumbai, India.

### 2.1.3.2 Dicumyl peroxide (DCP)

Dicumyl peroxide was commercial grade with 40 % activity. It decomposes on exposure to heat and sunlight with the generation of free radicals.



### 2.1.3.3 Other chemicals

Sodium hydroxide, Tetrahydrofuran (THF), methanol and toluene were also used.

## 2.2 Experimental procedure

### 2.2.1 Preparation of blends

Blends of PS and rubber (NR, SBR and WTR) were prepared by melt mixing in a Thermo Haake PolyLab QC with a mixing chamber volume of 69 cc and roller rotors at a temperature of 170 °C. At first PS was allowed to melt in the chamber at a rotor speed of 30 rpm for 2 min. Then the rubber was incorporated and the rpm was increased to 60 rpm. The mixing was continued for another 5 min to obtain a homogeneous mixture. The resultant blends were then discharged from the internal mixer and while still molten, passed once through a cold two-roll mill to achieve a sheet of about 2 mm thick.

### 2.2.2 Dynamic vulcanisation

Dynamic vulcanisation was carried out by using dicumyl peroxide. The vulcanised blends were prepared under identical conditions. At the on set of 5.5 minutes of the blending cycle, the curing agent was introduced

into the blend. The mixing was then continued for another 1.5 min to accomplish the vulcanisation process.

### **2.2.3 Compatibiliser**

#### **2.2.3.1 Preparation of Maleic anhydride-grafted-polystyrene (MA-g-PS)**

PS was softened by mixing in an internal mixer, Thermo Haake PolyLab QC with roller rolls at 170 °C, 30 rpm for 2 minutes. 4 wt % of maleic anhydride (MA) followed by 1 wt% of DCP was added to the mixer and mixing continued for 1 minute at 60 rpm. The mix was sheeted out on a two roll mill [2]. After MA grafting, the MA-g-PS was dissolved in tetrahydrofuran (THF) and precipitated in methanol in order to remove unreacted MA. The product was subsequently dried in a vacuum oven at 60 °C for 24 h.

#### **2.2.3.2 Determination of MA content**

The amount of MA content grafted on PS was calculated from the acid value [3]. After dissolution of 1g of sample in 100 ml of THF, about 3-4 drops of distilled water was added. The solution was stirred overnight in order to fully hydrolyse the anhydride groups. The acid number was determined by titration with a standardized methanolic potassium hydroxide (KOH) solution (0.025N) using phenolphthalein as indicator. The acid number was converted to the MA content as follows:

$$\text{MA (wt.\%)} = \text{acid number [mg KOH per g]} \times \frac{98}{2 \times 561}$$

#### **2.2.4 Surface treatment of Nylon fibre**

The virgin fibre, as obtained, was dispersed in 5% sodium hydroxide (NaOH) solution for 20 minutes at room temperature. Following the

hydrolysis, the fibre was thoroughly washed with distilled water to remove excess NaOH and dried at 60 °C in vacuum oven for 24 hours. This is referred to as treated fibre.

### **2.2.5 Preparation of composites**

PS/rubber/short Nylon-6 fibre composites were prepared using the same internal mixer under identical conditions. After softening of PS for 2 minutes, the rubber was introduced into the mixer followed by the addition of short Nylon-6 fibres. The mixing was continued for 6 minutes to obtain a homogeneous mixture. In the case of composites with compatibilisers, MA-g-PS was softened along with PS.

## **2.3 Moulding**

The sheet obtained after melt blending was cut and preheated, followed by compression for 2 minutes in a compression moulding hydraulic press at a moulding temperature of 170 °C and 20 MPa pressure to obtain sheets of 0.2 mm and 1mm thickness, respectively. The sheets were cooled to room temperature under pressure for 5 minutes and then ejected out of the mould. The preheating time varied with the blend as shown.

<b>Blend</b>	<b>Preheating time (min)</b>
PS/NR	3
PS/SBR	7
PS/WTR	8

## **2.4 Mechanical properties**

### **2.4.1 Tensile properties**



The tensile strength is defined as the force per unit area of cross-section, required to break the test specimen, the condition being that the stress is substantially uniform over whole of the cross section. Young's modulus is calculated from the slope of the initial part of the stress-strain curve.

For pure blends and dynamically vulcanised blends, tensile testing was done using rectangular specimens  $100 \times 10 \times 0.1 \text{ mm}^3$  on a Universal Testing Machine (UTM) - Shimadzu with a load cell of 10 kN according to ASTM D 882-02 [4]. A cross-head speed of 50 mm/min and a gauge length of 50 mm was used for carrying out the test.

Whereas for composites, dumbbell shaped specimens of 1mm thickness were punched out from the moulded sheets in the two-roll mill direction and tested on the same UTM according to ASTM D 638-03 [5]. The cross-head speed was 50 mm/min. The tests were carried out at  $28 \pm 2^\circ\text{C}$ . In a UTM, one grip is attached to a fixed and the other to a movable (power-driven) member so that they will move freely into alignment as soon as any load is applied.

#### **2.4.2 Impact strength**

Impact strength was measured using unnotched samples (dimensions  $60 \times 12.7 \times 1 \text{ mm}^3$ ) according to ASTM D 4812-99 [6]. Impact strength is the energy absorbed by the specimen during the impact process and is given by the difference between the potential energy of the hammer before and after impact.

The test was done by employing an impact testing machine CEAST Resil Impact Junior with a pendulum capacity of 4 J and striking velocity of

3.46 m/s at room temperature. The sample is clamped vertically in the base of the machine such that 31.5 mm of the specimen project above the top surface of the vise. The pendulum is released. The energy required to fracture the sample was measured from the reading dial. The correction due to air friction was made, and the actual energy was then divided by the thickness of the sample. The measurements were conducted over five specimens for each test and the average was reported.

### **2.4.3 Flexural properties**

The specimens of dimension 60 x 12.7 x 1 mm<sup>3</sup> were taken for flexural test, under three-point bending using the same Universal Testing Machine (UTM), in accordance with ASTM-D 790 [7], at a crosshead speed of 5 mm/min and a span length of 25 mm. Five specimens were tested and the average was calculated. The bar of rectangular cross section rests on two supports and is loaded by means of a loading nose midway between the supports. The loading nose and supports have cylindrical surface. The flexural strength are calculated using the formula

$$\sigma_f = \frac{3PL}{2bd^2}$$

where  $\sigma_f$  = stress in the outer fibres at midspan, MPa,

P = load at a given point on the load-deflection curve, N,

L = support span, mm,

b = width of beam tested, mm,

d = depth of beam tested, mm,

The flexural modulus is calculated from the slope of the initial portion of the stress-strain curve.

## **2.5 Extraction of composite**

The Nylon fibre was extracted from the composites by dissolving in toluene. The extracted fibre was collected, dried in a vacuum oven at 50 °C.

## **2.6 Scanning electron microscopy (SEM)**

Scanning electron microscopy (SEM) is a very useful tool to gather information about topography, morphology, composition and micro structural information of materials. The image is formed by scanning a probe of focused electron beam across the specimen. The electron beam interacts with a thin film surface of the specimen resulting in back scattering of electrons of high energy, generation of secondary electrons of low energy and X-rays. These signals are monitored by detectors and magnified. An image of the investigated microscopic region of the specimen is thus observed in the cathode ray tube and photographed using photographic film. SEM image has characteristic three dimensional appearance and are useful in judging the surface structure of the sample.

In the present study, SEM analysis was carried out using Jeol JSM-6390 LA to analyse the phase morphology of the extracted fibre surface and fractured surface of the sample. Before examination, the surface were sputter-coated with a thin layer of gold in a vacuum chamber.

## **2.7 Fourier transform infrared spectroscopy (FTIR)**

Fourier transform infrared spectra are generated by the absorption of electromagnetic radiation in the frequency range 4000-400  $\text{cm}^{-1}$  by organic molecules. Different functional groups absorb energy at characteristic frequencies. The frequency and intensity of absorption are the indication of the bond strength and structural geometry in the molecule.

The presence of MA grafted on PS was assessed using FTIR spectrometer Thermo Nicolet Avatar 370 with the spectral range of 4000 to 400  $\text{cm}^{-1}$ . Thin films were prepared by compression moulding at 170 °C under 20 MPa for 3 min. One hundred scans at a resolution of 4  $\text{cm}^{-1}$  were signal averaged.

## **2.8 Dynamic mechanical analysis (DMA)**

In DMA, the sample is subjected to a sinusoidal stress at a set frequency and the strain response is monitored as a function of phase angle. The in-phase component of the complex modulus is expressed as the storage modulus ( $E'$ ) and an out of phase component as the loss modulus ( $E''$ ) and the ratio of the loss modulus to the storage modulus as the tan delta ( $\tan \delta$ ).  $E'$  is proportional to the energy stored elastically and is reversible. The loss modulus  $E''$  on the other hand, measures the energy transferred to heat and is irreversibly lost.

The dynamic mechanical properties were measured using a dynamic mechanical analyser, DMA Q800 (TA instrument) in accordance with ASTM D 4065-04 [8]. The temperature of tests ranged from 40 to 120 °C, with a heating rate of 3 °C/min. The frequency was 1 Hz and the oscillation amplitude was 15  $\mu\text{m}$ . The measurement was

carried out using the single cantilever clamp mode on a rectangular sample of size 35 x 12.7 x 1 mm<sup>3</sup>.

## 2.9 Thermogravimetric analysis (TGA)

Thermogravimetric analysis were carried out in a thermogravimetric analyser (TA instrument Q 500). It is a computer-controlled instrument that permits the measurement of the weight changes in the sample material as a function of temperature. The sample placed in a temperature programmed furnace was subjected to a temperature in the range 30 to 800 °C with a heating rate of 10 °C/min and the corresponding weight changes were noted with the help of an ultrasensitive microbalance. Nitrogen was used as purge gas. The data of weight loss verses temperature and time was recorded online in the TA Instrument's Q series Explorer software. The analysis of the thermogravimetric (TG) and derivative thermogravimetric (DTG) curves were done using TA Instrument Universal Analysis 2000 software version 3.3B.

## 2.10 References

- [1] Subramanyam A. Rubber Chem Technol 1972; 45:346.
- [2] Dedecker K, Groeninckx G. Macromolecules 1999; 32:2472.
- [3] Jo WH, Park CD, Lee MS. Polymer 1996; 37:1709.
- [4] ASTM Standards: D 882-02 Test method for tensile properties of thin plastic sheeting. ASTM. Book of Standards, vol. 08.01.
- [5] ASTM Standards: D 638-03 Test method for tensile properties of plastics. ASTM. Book of Standards, vol. 08.01.
- [6] ASTM Standards: D 4812-99 Test method for unnotched cantilever beam impact resistance of plastics. ASTM. Book of Standards, vol. 08.01.

- [7] ASTM Standards: D 790-03 Test method for flexural properties of unreinforced and reinforced plastics and electrical insulating materials. ASTM. Book of Standards, vol. 08.01.
- [8] ASTM Standards: D 4065-06 Standard practice for plastics: dynamic mechanical properties: determination and report of procedures. ASTM. Book of Standards, vol. 08.02.

.....❧.....

# POLYSTYRENE/NATURAL RUBBER BLENDS

## Part A

### TOUGHENING OF POLYSTYRENE: EFFECT OF BLEND RATIO AND DYNAMIC VULCANISATION

#### 3A.1 Introduction

#### 3A.2 Experimental

#### 3A.3 Results and Discussions

#### 3A.4 Conclusions

#### 3A.5 References

### 3A.1 Introduction

Plastic/rubber blends have been commercialized as rubber toughened plastics or as thermoplastic elastomers [1,2]. Generally, if a relatively large portion of the hard plastic is used, the composition is used as an impact resistant plastic; whereas, if a relatively large amount of rubber phase is used, the blend will be soft and have at least some of the properties of an elastomer. Most of the polymer blends are incompatible due to a variety of reasons such as the absence of any specific interaction between the blend constituents; dissimilarity in their structures; and broad differences in their viscosities; surface energy or activation energy of flow, and polarity [3].

Nevertheless, such blends are commercially important because they combine the unique properties of both the constituents of the blend.

Polymer blends vary greatly in morphological complexity. Rubber toughened plastics are typically two phase systems consisting of a rubbery impact modifier dispersed in a thermoplastic matrix. Small changes in the size and arrangement of these dispersed particles can produce large variation in the physical performance and aesthetic qualities of the blend.

Rubber toughening is often used to overcome the brittleness of glassy polymers such as polystyrene (PS). Polystyrene has been toughened by blending with rubbers such as styrene-butadiene (SBR) [4], natural rubber (NR) [5], polybutadiene (BR) [6], ethylene-propylene-diene terpolymer (EPDM) [7], nitrile rubber (NBR) [8] etc. A number of factors, related to the rubber component, have been identified as affecting the toughness of these systems, including the volume fraction of the rubber phase, its chemical composition, degree of crosslinking, particle morphology, level of adhesion to the matrix, type of rubber, and most importantly the rubber particle size and its size distribution [9].

Generally, it is difficult to isolate the effect of changes in rubber particle internal structure from particle size and distribution itself. Many studies supported by microscope techniques have provided enough evidences to support that the rubber particles are responsible for promoting multiple crazing mechanism in the polystyrene matrix by acting as stress concentrators during the craze initiation, thereby proving substantial plastic deformation to occur prior to failure. This is particularly true when considering that no improvement in toughness is achieved in glassy thermoplastics modified with rigid particles [10-12].



However, most polymer blends are immiscible, and often, have poor mechanical properties and unstable morphology. Compatibilisation of such blends is necessary. Dynamic vulcanisation can be considered as a technological compatibilisation technique.

Dynamic vulcanisation is one of the ways to achieve some degree of compatibility between immiscible rubber/plastic blends. It was first described by Gessler [13] 1962 and then developed by Fischer [14] and Coran *et al.* [15]. It is the process of crosslinking the rubber phase during melt mixing with the thermoplastic. The resulting morphology consists of micron sized, finely dispersed crosslinked rubbery particles in a continuous thermoplastic matrix [16-19]. The lightly crosslinked rubber particles can withstand more stress but at the same time the plastic phase retains the flowability. The introduction of crosslinks into one of the phases increases the viscosity of this phase leading to a change in the phase morphology of the blend [20]. For blends of polymers with similar polarities, a fine morphology is frozen in during dynamic vulcanisation and no additional compatibiliser is needed. Dynamic vulcanisation of incompatible blends results in a coarse morphology [21]. Compared with those blends comprising of uncured components, dynamic vulcanisation possesses significantly improved mechanical properties that can be attributed to the stabilized morphology of rubber particles resulting from crosslinking [22-24].

Several studies have been carried out on the dynamically vulcanised TPEs. However, few studies have been done on the dynamic vulcanisation of rubber-toughened thermoplastics. Yoon *et al.* [25] studied the reactive extrusion of polypropylene/natural rubber 90/10 blends in terms of thermal and mechanical properties. The impact strength of reactively extruded

PS/EPDM blends using peroxides and SBS compatibiliser has been investigated by Crevecoeur *et al.* [26].

Part I of this chapter focuses on the preparation of toughened polystyrene by melt blending polystyrene with natural rubber and evaluation of the mechanical properties, morphology and dynamic mechanical properties of the resulting blends.

In Part II the effect of dynamic vulcanisation using dicumyl peroxide (DCP) on the mechanical properties, morphology and dynamic mechanical properties of 85/15 PS/NR blend is discussed.

### 3A.2 Experimental

PS/NR blends were prepared by melt-mixing in a Thermo Haake Polylab QC and the formulations used are given in Table 3A.1.

**Table 3A.1. Blend Formulations**

Ingredients	Composition*				
	100	95	90	85	80
PS	100	95	90	85	80
NR	0	5	10	15	20

\*parts per hundred polymer (php)

The compositions of PS/NR with varying DCP concentrations employed for this study are shown in Table 3A.2.

**Table 3A.2 Composition at fixed PS/NR blend ratio with varying peroxide concentration.**

Components	Mix No.						
	A0	A1	A2	A3	A4	A5	A6
PS	85	85	85	85	85	85	85
NR	15	15	15	15	15	15	15

DCP	0 <sup>a</sup>	0.5 (0.7) <sup>b</sup>	1 (1.4)	1.5 (2.1)	2 (2.8)	2.5 (3.5)	3 (4.2)
-----	----------------	------------------------	---------	-----------	---------	-----------	---------

<sup>a</sup> Concentration of DCP in phr.

<sup>b</sup> Values in parentheses correspond to the milliequivalent concentration of DCP.

The melt-mixed samples were compression moulded to  $\approx 0.1$ mm films and 1mm sheets, conditioned and then tested as discussed in Chapter 2.

### 3A.3 Results and Discussions

#### Part I Effect of blend ratio

##### 3A.3.1 Mechanical Properties

Figures 3A.1 and 3A.2 shows the variation of tensile strength and Young's modulus, respectively, of various PS/NR blends. The tensile strength is found to decrease almost linearly with increasing NR content. Virgin PS has a highly rigid molecular structure arising from the stiffening effect of bulky phenyl group. The segmental motion and molecular mobility is highly restrained and very limited. Hence the PS exhibits very low elongation coupled with high tensile strength. The NR remains as the dispersed phase when combined in low concentrations. This dispersed rubber particles, while enhances the ability of PS to absorb impact energies, renders the matrix weak. This is manifested as lower tensile strength and Young's modulus, and improved impact strength for the PS/NR blends, as discussed in later section of this chapter,

The flexural strength and flexural modulus for various PS/NR blends are shown in Figures 3A.3 and 3A.4, respectively. As the rubber loading increases, the flexural strength and flexural modulus decrease, a trend that is consistent with the variation in the tensile strength and Young's modulus. A negative trend is generally seen in immiscible blends of polyolefins and

is mainly caused by the poor interfacial adhesion [28]. The decrease in flexural strength with increasing NR content in the blends indicates a reduction in rigidity and an increase in the elastomeric nature of the blend.

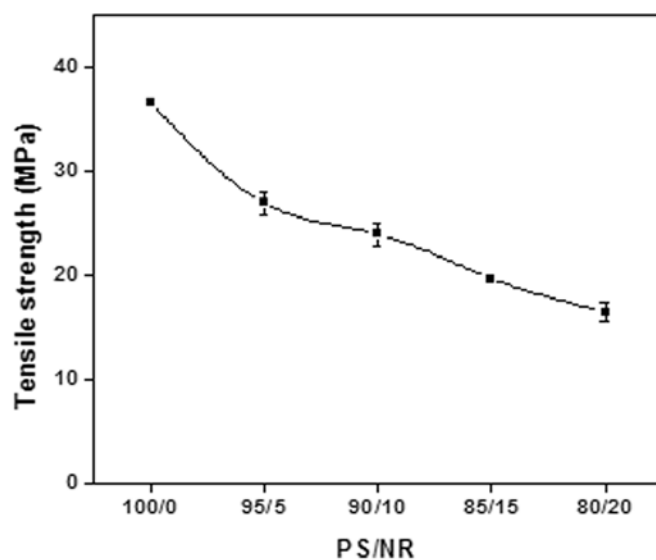


Figure 3A.1: Variation of tensile strength for various PS/NR blends.

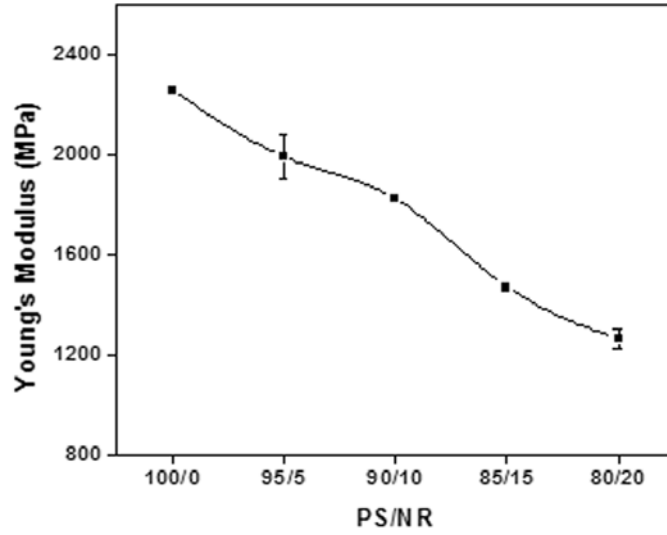


Figure 3A.2: Variation of Young's modulus for various PS/NR blends.

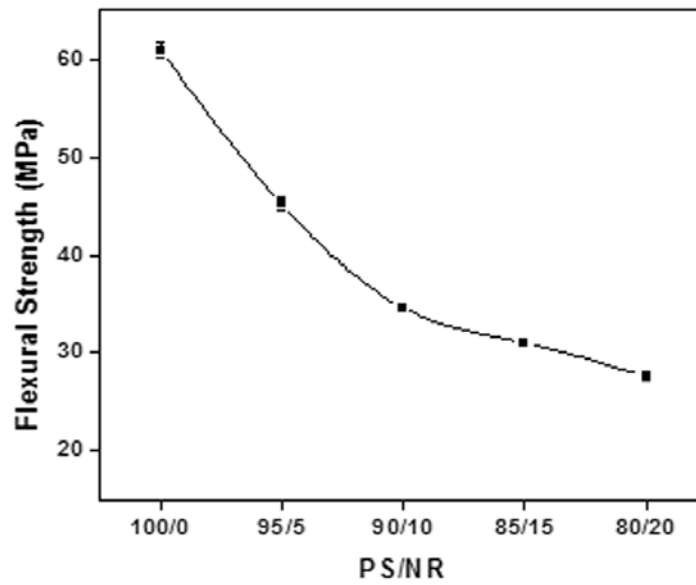
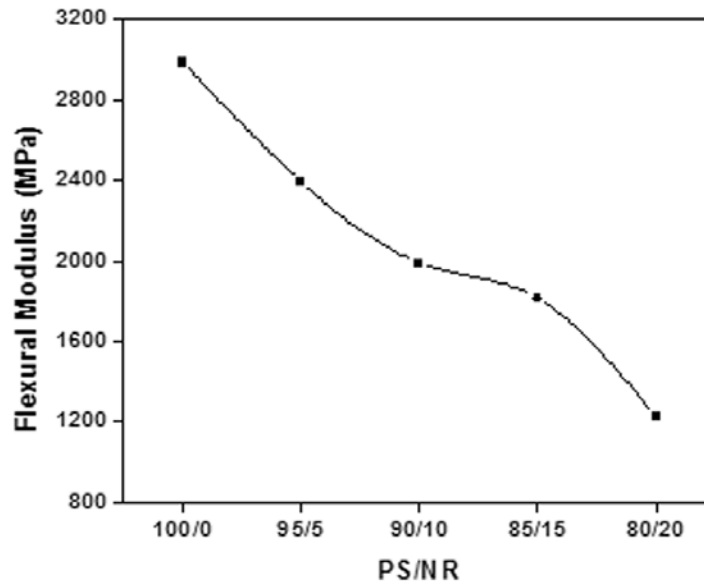
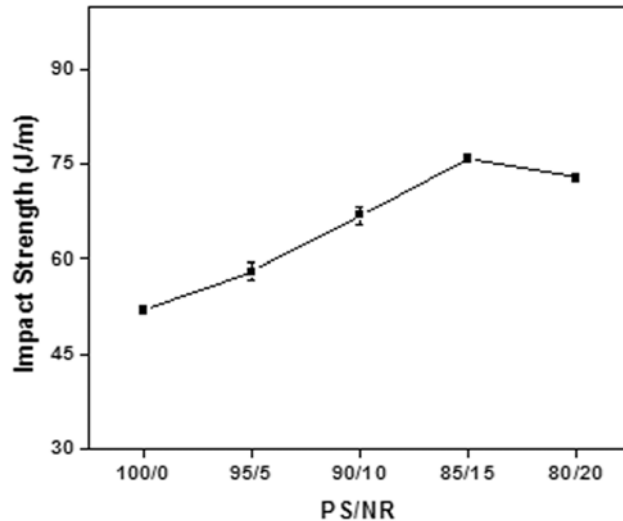


Figure 3A.3: Variation of flexural strength for various PS/NR blends.



**Figure 3A.4: Variation of flexural modulus for various PS/NR blends.**

Figure 3A.5 plots the unnotched Izod impact strength of PS toughened with NR as a function of rubber content. A number of publications propose that polymer blends are only toughened when a critical inter-particle distance is attained. Wu [29,30] has reported that the distance between two rubber particle surfaces is a characteristic property of the matrix polymer for a given mode, rate and temperature of deformation. The toughness of the PS blends determines how much material can be deformed before individual craze breakdown leads to cracks and the fracture of the blend.



**Figure 3A.5: Variation of impact strength for various PS/NR blends.**

An increase in the impact strength of the toughened PS over the unmodified PS is observed in Figure 3A.5. The impact strength of pure PS is very low. The premature failure is due to the brittle fracture initiated by crazes. There exists an optimum rubber content at 15wt. % for which maximum impact resistance of about 46% is attained. More particles permit initiated crazes to be stopped at the next particle before reaching catastrophic craze lengths. When the critical particle concentration is exceeded, no additional crazing is possible and the impact strength cannot be improved further. The plateau obtained beyond 15 wt. % rubber content reflects this reasoning.

### 3A.3.2 Morphology

Figure 3A.6(a) shows the scanning electron micrograph (SEM) of the impact fractured surface of pure PS. It contains large plane areas with sharp, brittle fracture in various planes. The white stress stripes are traces of stress in a propagating process for unmodified PS.

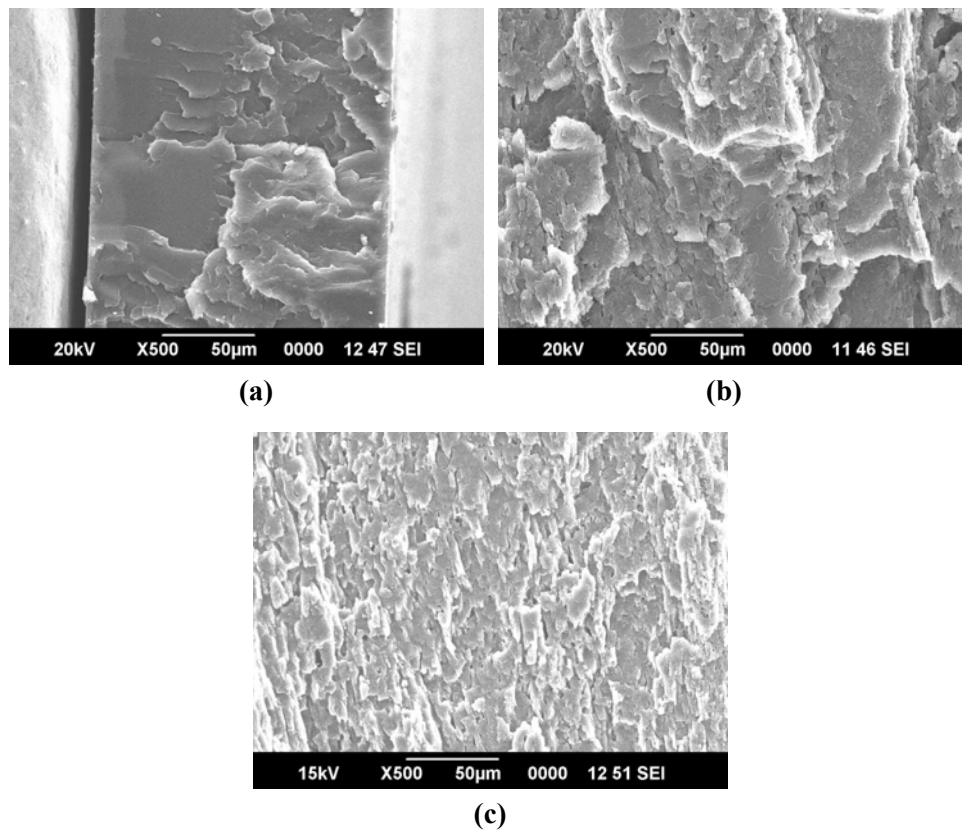


**Figure 3A.6: Scanning electron micrographs of fracture surfaces of PS/NR blends (a) PS, (b) 85/15 PS/NR and (c) 80/20 PS/NR**

The SEM picture of 85/15 PS/NR and 80/20 PS/NR are presented in Figures 3A.6 (b) and (c), respectively. These micrographs have homogeneous craze surfaces. 85/15 PS/NR and 80/20 PS/NR have even and rougher surface compared to unmodified PS. The rougher the surface area indicates that more energy has been absorbed during the impact resistant test. Lower roughness indicates lower impact resistance [31]. According to Jelcic *et al.* [32], when HIPS is blended with SBS, the fracture surface of the blends is rough compared to HIPS. SEM gives the information that SBS as elastomeric impact modifier shows relative phase contrast in the blend due to soft phase induced crazing.



### **3A.3.3 Dynamic mechanical analysis**

Polymers are viscoelastic in nature. Their mechanical properties exhibit a pronounced dependence on the temperature and the rate of deformation. The complex shear modulus could be obtained by subjecting the specimen to a cyclic deformation. The complex modulus  $E^*$  can be represented as

$$E^* = E' + iE'' \dots\dots\dots(1)$$

where  $E'$  is the in-phase modulus (storage modulus) and  $E''$  is the 90° out-of-phase modulus (loss modulus).  $E'$  represents the elastic response and  $E''$  represents the viscose response of a material subjected to deformation. The ratio of the moduli is represented as

$$\tan \delta = E''/ E' \dots\dots\dots(2)$$

Tan  $\delta$  represents the damping and is termed as the loss factor. The mathematical relationships between these parameters and their physical significance is well described in literature [33].

The storage modulus ( $E'$ ) vs. temperature plots of various PS/NR blends are shown in Figure 3A.7. The value of  $E'$  signifies the stiffness of the material. At low temperatures the molecules are frozen in and exhibit very high modulus.

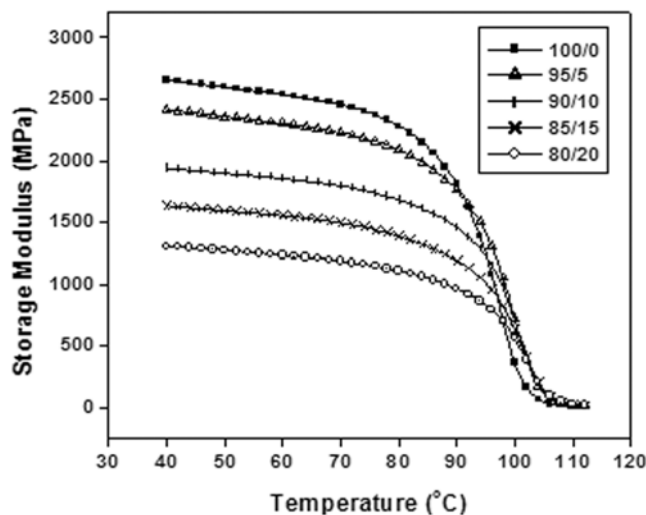


**Figure 3A.7: Effect of temperature on the storage modulus of PS/NR blends.**

At any fixed rate of deformation, the temperature at which  $E'$  starts to decrease rapidly corresponds to the glass transition temperature. At the transition zone there is drastic decrease in modulus with temperature. This is because at the transition zone segmental mobility sets in followed by a corresponding decrease in the  $E'$  values. The storage modulus is dependent on the rubber content. As seen in the figure, pure PS shows the highest modulus and the value of  $E'$  decreases with increase in NR content. The value of modulus of pure PS and the blends are almost the same in the rubbery region.

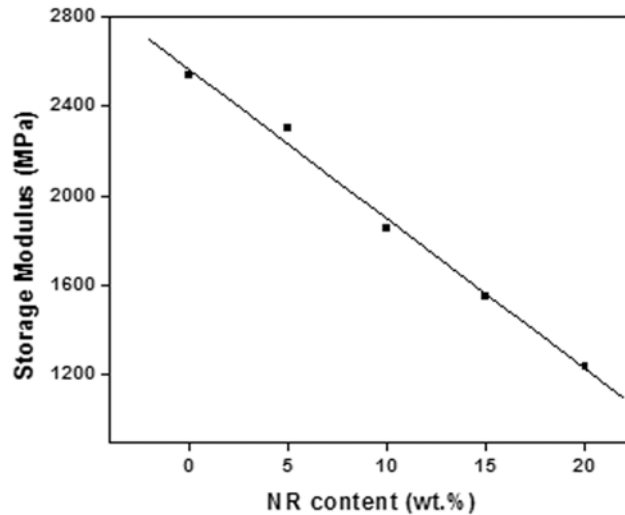


**Figure 3A.8: Variation of storage modulus of PS/NR blends at 60 °C with NR content.**

The effect of NR content on the storage modulus of PS/NR blends is presented in Figure 3A.8. It is clear from the figure that the storage modulus of the blend decreases linearly with the NR content. The following relationship can be fitted for the average storage modulus of the blend as

$$y = 2567 - 67x$$

Where  $y$  = storage modulus (MPa) at 60 °C.

$x$  = NR content (wt.%)

$R^2 = 0.99$ , the coefficient of determination.

The variation of loss modulus ( $E''$ ) and  $\tan \delta$  with temperature of PS/NR blends are shown respectively in Figures 3A.9 and 3A.10. It is clear from Figure 3A.9 that the peak in the range 95-100 °C corresponds to the  $T_g$  of PS. There is a slight outward shift of about 5 °C in the transition peak of PS at 20 wt.% of NR. However, this small increase in the  $T_g$  of PS is insignificant to substantiate any occurrence of partial miscibility.

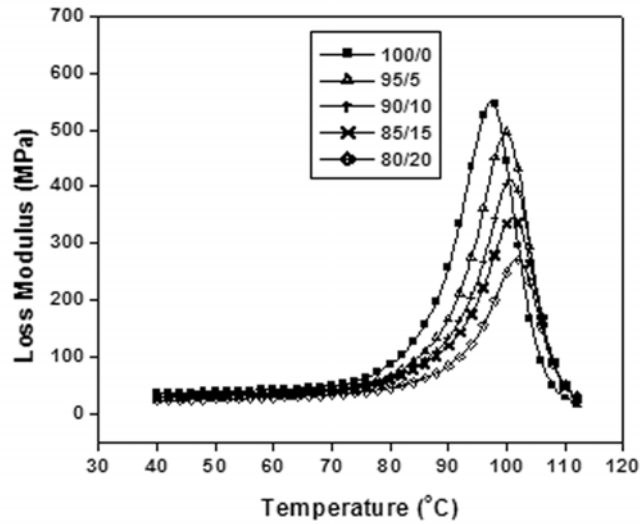


Figure 3A.9: Effect of temperature on the loss modulus of PS/NR blends.

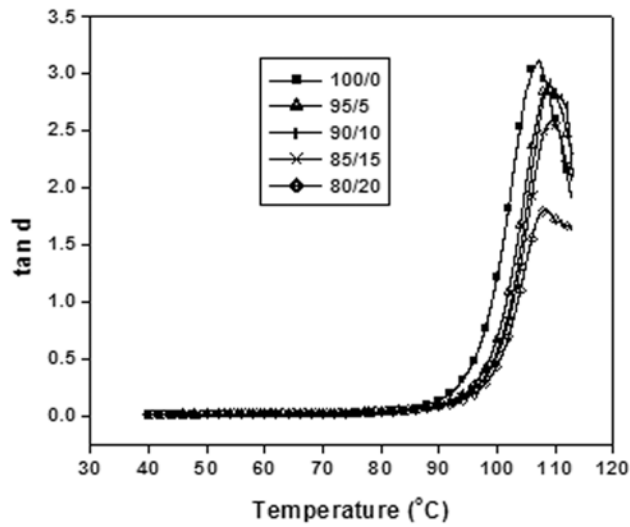


Figure 3A.10: Effect of temperature on  $\tan \delta$  of PS/NR blends.

The main relaxation process in the PS can also be detected in the damping curves presented in Figure 3A.10. As temperature increases, damping goes through a maximum, near  $T_g$ , in the transition region and then a minimum in the rubbery region. This type of behaviour can be partially

explained on a molecular basis. The damping is low below  $T_g$  because the chain segments are frozen in. Below  $T_g$ , the deformations are thus primarily elastic and molecular slip resulting in viscous flow is low. Above  $T_g$ , where rubbery region exists, the damping is also low because molecular segments are very free to move and there is little resistance to flow. So, when the segments are either frozen in or are free to move, damping is low. In the transition region, parts of the segments are free to move about and the rest are not so free. A frozen segment stores energy through deformation and it ultimately releases it as viscous energy when it becomes free to move. The  $\tan \delta$  peak of PS decreases with increase in NR content of the blend.

## **Part II Effect of Dynamic vulcanisation**

### **3A.3.4 Mechanical properties**

The effect of DCP concentration on the tensile strength and Young's modulus of 85/15 PS/NR blend is shown in Figures 3A.11 and 3A.12, respectively. The tensile strength increases slightly with increasing DCP concentration up to 2.8 milliequivalents (meq). The Young's modulus increases significantly by 23% at a DCP concentration of 2.8 meq and then decreases. This increase may be due to the increased crosslink density at higher levels of DCP and better interfacial adhesion. In the case of dynamic vulcanisation, if the rubber particles in a thermoplastic-rubber blend are small enough and if they are sufficiently vulcanised, then the physical and chemical properties of the blend are improved [34]. This again depends on the size of the rubber domains as well as elasticity and strength of the rubber phase.

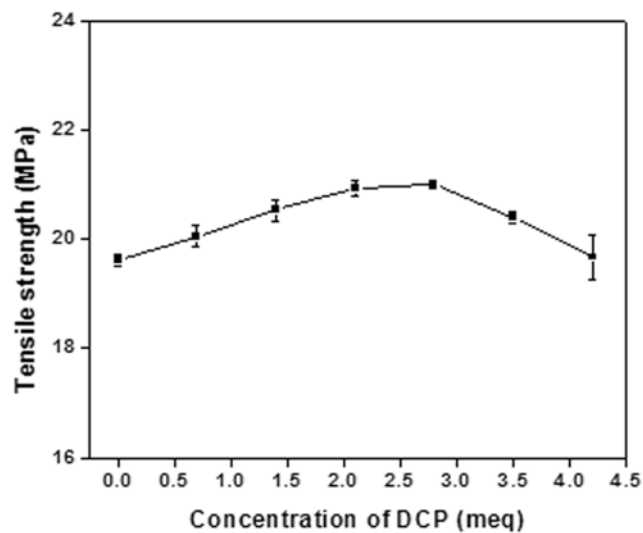


**Figure 3A.11: Variation of tensile strength of 85/15 PS/NR with DCP concentration.**

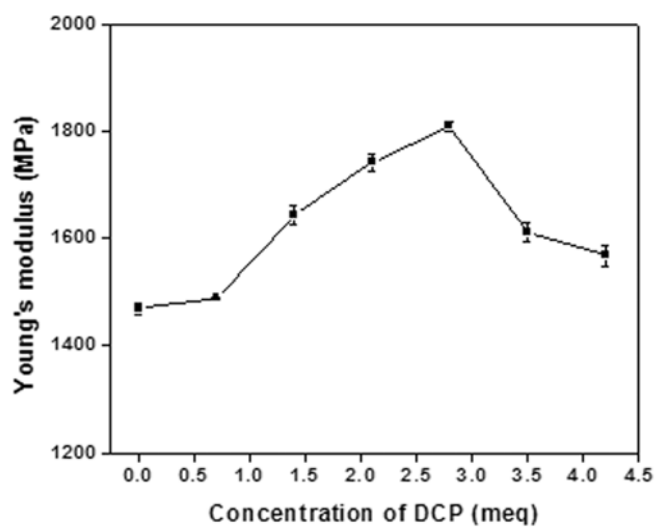


**Figure 3A.12: Variation of Young's modulus of 85/15 PS/NR with DCP concentration.**

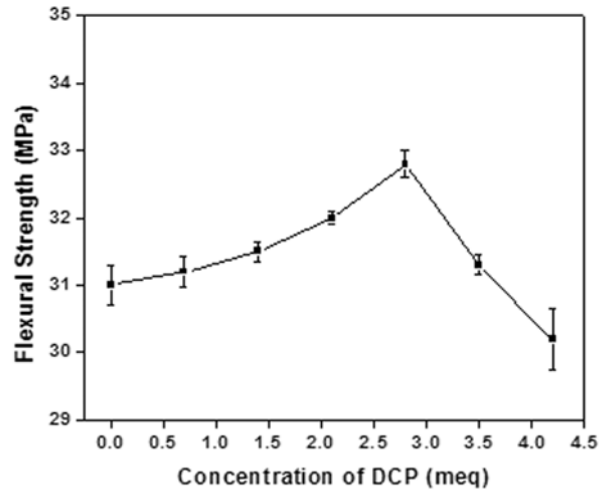


**Figure 3A.13: Variation of flexural strength of 85/15 PS/NR with DCP concentration.**

The effect of DCP concentration on the flexural strength and flexural modulus of 85/15 PS/NR blend is shown in Figures 3A.13 and 3A.14 respectively. The flexural strength increases slightly up to 2.8 meq of DCP loading, a trend similar to that observed for tensile strength. The flexural modulus also increases up to 2.8 meq of DCP and then decreases.

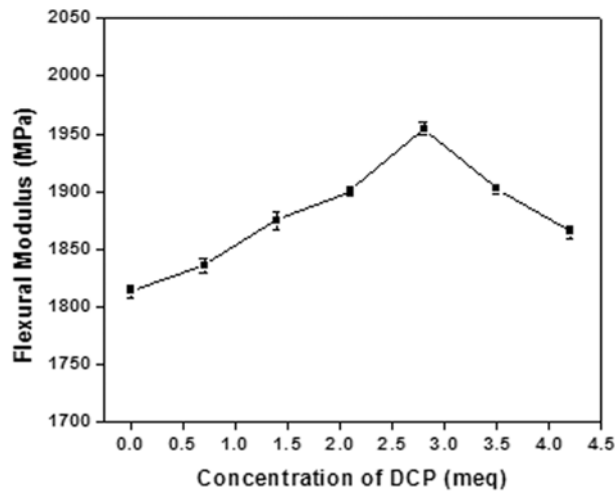


**Figure 3A.14: Variation of flexural modulus of 85/15 PS/NR with DCP concentration.**

The variation of impact strength with DCP content on the 85/15 PS/NR blend is presented in Figure 3A.15. The impact strength increases up to 2.8 meq of DCP loading and then decreases. The low impact value of the unvulcanised blend is attributed to the fact that the rubber droplets formed during blend formation coalesce during static melt cooling, giving rise to irregularly sized rubber domains that are larger than the critical size desired for impact toughening. This size enlargement and shape irregularity also reduce the number density of stress concentration sites and the interfacial adhesion.

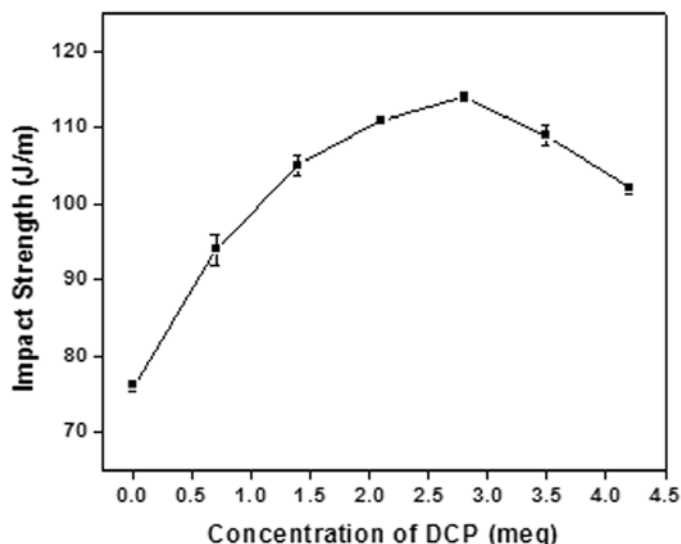


**Figure 3A.15: Variation of impact strength of 85/15 PS/NR with DCP concentration.**

There is a considerable increase of about 50% in impact strength at 2.8 meq. In the vulcanised blend at the optimum DCP concentration, the rubber particles are crosslinked and their size is greatly reduced because of the shear induced size reduction during vulcanisate preparation. The crosslinked structure of these discrete particles greatly inhibits the probability of rubber cohesion during cooling, so the number density of rubber at constant



volume fraction domains are many-fold with good interfacial adhesion promoted by physical interlocking during meltdown. The appearance of the optimum DCP concentration is most likely related to an increasing adhesion between the dispersed NR phase and the PS matrix. Above the optimum DCP concentration, the impact strength decreases. This implies that the crosslinking of NR becomes more pronounced at DCP concentrations higher than the optimum leading to a reduction in the number of craze initiating rubber particles.

### **3A.3.5 Morphology**

The morphology of heterogeneous polymer blends depends on blend composition, viscosity of individual components and processing history. Danesi and Porter [35] have shown that for blends with the same processing history, the morphology is determined by the melt viscosity ratio and composition. In the scanning electron micrographs presented in Figure 3A.15, the morphologies of the impact fracture surfaces of 85/15 PS/NR blends with 1.4, 2.8 and 4.2 meq concentrations of DCP are shown.

The morphological changes accompanying the addition of DCP are evident from the figures. The micrograph of (a) implies that very little crosslinking occurs at low DCP concentration. Morphology coarsening at DCP concentration higher than the optimum (c) results in decreasing impact properties as a consequence of the reduced number of craze initiating rubber particles [7].

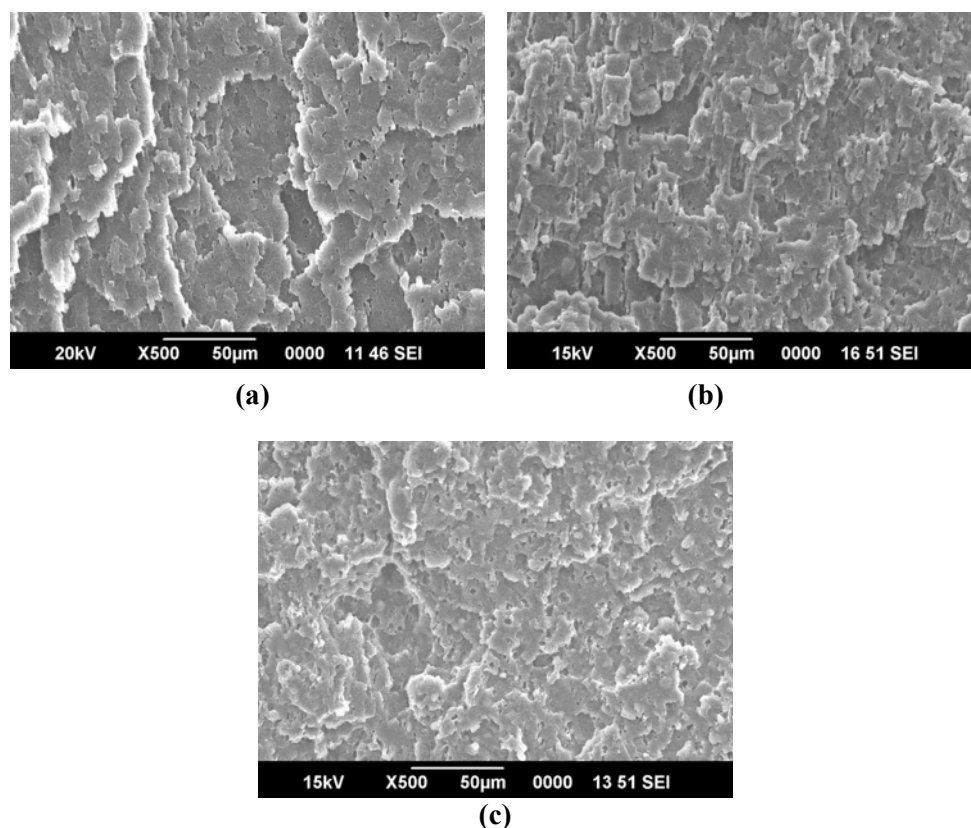
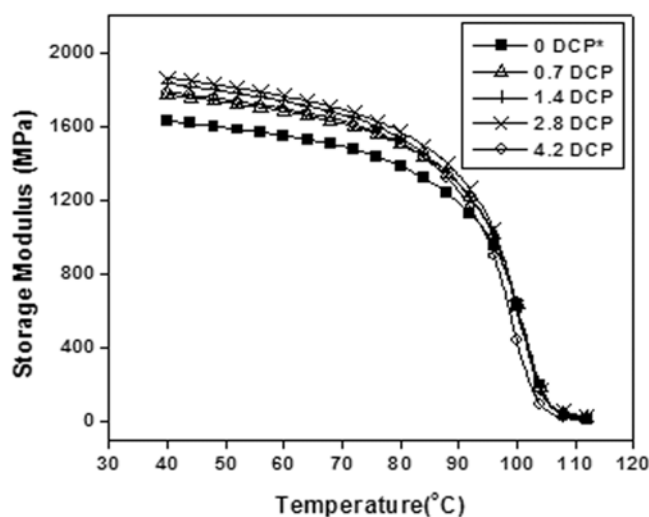


**Figure 3A.16:** Scanning electron micrographs of fractured surface of 85/15 PS/NR blend with (a) 1.4, (b) 2.8 and (c) 4.2 meq of DCP.

### 3A.3.6 Dynamic mechanical analysis

Dynamic mechanical properties of polymers are highly dependent on the material structure. Thus the molecular level changes that occur in a polymer under the application of a sinusoidal stress is reflected in dynamic mechanical measurements. The variation of storage modulus ( $E'$ ) with temperature of dynamically vulcanised blends are shown in Figure 3A.17. Three distinct regions of mechanical behaviour can be observed: (a) a glassy region; (b) a glass–rubber transition region; and (c) a flow region. In the glassy region the chain conformations are frozen into rigid network yielding high  $E'$  values. The glass–rubber transition marks the onset of long

range motions of amorphous polymer chain segments and is characterised by a large drop in modulus and a pronounced loss factor peak. The last region is the flow region, where the amorphous chains undergo net translatory motions relative to each other and a terminal fall off in modulus is accompanied by a continuous decrease in loss factor. The storage modulus at low temperatures increases with increase in DCP concentration showing a maximum at 2.8 meq.



\*Concentration of DCP in milliequivalents (meq)

**Figure 3A.17: Effect of temperature on the storage modulus of dynamically vulcanised 85/15 PS/NR blends.**

The variation of loss modulus of dynamically vulcanised PS/NR blends as a function of temperature is shown in Figure 3A.18. A distinct peak corresponding to the  $T_g$  of PS is observed for all the blends with varying DCP content. Below the  $T_g$  value the polymer chains are intact and stress transfer is possible which is reflected in the more or less constant values of  $E''$ . When the temperature is approaching the  $T_g$ , energy dissipation

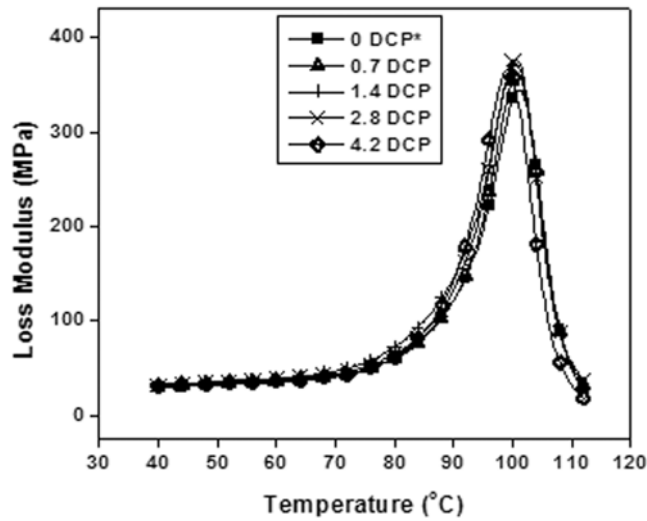


**Figure 3A.18: Effect of temperature on the loss modulus of dynamically vulcanised 85/15 PS/NR blends.**

takes place and a corresponding peak is observed in the values  $E''$ . The blends with a DCP concentration of 2.8 meq registers the maximum loss modulus.

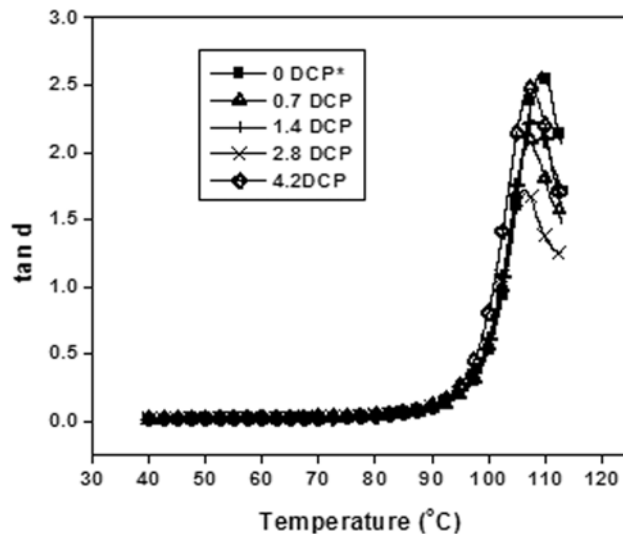


**Figure 3A.19: Effect of temperature on  $\tan \delta$  of dynamically vulcanised 85/15 PS/NR blends.**

The variation of  $\tan \delta$  values of dynamically vulcanised PS/NR blends as a function of temperature is shown in Figure 3A.19. The peak between 170 °C and 110 °C corresponds to the  $T_g$  of PS. It is evident from the figure that the  $T_g$  of PS is shifted to slightly lower temperature for dynamically vulcanised blends. A substantial decrease in the  $\tan \delta$  peak for blend containing 2 meq DCP indicates that crosslinking restricts the chain flexibility.

### **3A.4 Conclusions**

The mechanical properties, morphology and dynamic mechanical properties of natural rubber toughened PS have been studied with reference to the blend ratio. The mechanical properties of the blends are strongly influenced by blend ratio. The tensile strength, Young's modulus, flexural strength and flexural modulus of the blends decrease with increase in rubber content, whereas the impact strength improves by 46% at 85/15 PS/ NR and thereafter there is no considerable change. So 85/15 PS/NR blend was chosen for further studies. The morphology of the blends with rougher surface indicates a two phase structure. The effect of the blend ratio on the dynamic mechanical properties was investigated in the temperature range 40 °C to 120 °C. The storage modulus at room temperature, loss modulus peaks and  $\tan \delta$  peaks decreases with increase in rubber content.

Dynamic vulcanisation of 85/15 blends of PS and NR was carried out using dicumyl peroxide. DCP dosage has a significant effect on the extent of crosslinking. The tensile strength and flexural properties slightly increase up to 2.8 meq of DCP where as the Young's modulus and impact strength increase by 23 % and 50%, respectively at a DCP concentration of 2.8 meq. The optimum value of DCP content is observed at 2.8 meq. The morphology changes drastically as a result of dynamic vulcanisation. Morphology

coarsening occurs above the optimum peroxide content. Dynamical mechanical studies indicate that the storage modulus is the maximum and the  $\tan \delta$  peak, minimum for the optimum DCP content. Although miscibility cannot be brought about by dynamic vulcanisation, the overall improvement in properties suggests that dynamic vulcanisation can be employed as a means of technological compatibilisation of 85/15 PS/NR blends.

### **3A.5 References**

- [1] Bucknall CB. Toughened Plastics. London: Applied Science; 1977.
- [2] Coran AY. In: Thermoplastic Elastomers: A Comprehensive Review. Legge NR, Holden G, Schroeder HE, editors. Munich: Hanser Publishers; 1987.
- [3] Santra RN, Samantaray BT, Bhowmick AK, Nando GB. J Appl Polym Sci 1993; 49:1145.
- [4] Martinez G, Vazquez F, Alvarez-Castillo A, Lopez Castanares R, Castano VM. Int J Poly Mater 2000; 46:27.
- [5] Neoh SB, Hashim AS. J Appl Polym Sci 2004; 93:1660.
- [6] Mathur D, Nauman EB. J Appl Polym Sci 1999; 72:1151.
- [7] Crevecoeur JJ, Nelissen L, vander Sanden MCM, Lemstra PJ, Mencer HJ, Hogt AH. Polymer 1995; 36:753.
- [8] Sreenivasan PV, Kurian P. Intern J Polymeric Mater 2007; 56:1041.
- [9] Echte A. In: Rubber-toughened plastics. Riew CK editor. Washington: American Chemical Society; 1989, p.15.
- [10] Rovere J, Correa CA, Grassi VG, Dal Pizzol MF. J Mater Sci 2008; 43:952.
- [11] Kinloch AJ, Young RJ. In: Polymer reaction engineering. Reichert KH, Giesler W editors. London: Applied Science Publishers; 1983.
- [12] Serpooshan V, Zokaei S, Bagheri R. J Appl Polym Sci 2007; 104:1110.

- [13] Gessler M. U.S. Pat. 3,037,954; 1962.
- [14] Fisher K.U.S. Pat. 3,758,643; 1973.
- [15] Coran AY, Patel R. Rubber Chem Technol 1980; 53:141.
- [16] Duin MV, Machado AV. Polym Degrad Stab 2008; 90:340.
- [17] Huang H, Liu X, Ikehara T, Nishi T. J Appl Polym Sci 2003; 90:824.
- [18] Goharpey F, Katbab AA, Nazockdast H. J Appl Polym Sci 2001; 81:2531.
- [19] Duin MV. Macromol Symp 2006; 11:233.
- [20] Usachav SV, Zakharov, Kuleznev VN, Vetoshkin AB. Int Polym Sci Technol 1980; 7:T48.
- [21] Koning C, Duin MV, Pagnouille C, Jerome R. Prog Polym Sci 1988; 23:707.
- [22] Abdou-Sabet S, Puydak RC, Rader CP. Rubber Chem Technol 1996; 69:476.
- [23] Katbab AA, Nazockdast H, Bazgir S. J Appl Polym Sci 2000; 75:1127.
- [24] Nazockdast H, Goharpey F, Katbab A. Rubber Chem Technol 2003; 76:239.
- [25] Yoon LK, Choi CH, Kim BK. J Appl Polym Sci 1995; 56:239.
- [26] Crevecoeur JJ, Nellisen L, vander Sanden MCM, Lemstra PJ. Polymer 1995; 36:1295.
- [27] Asaletha P, Kumaran MG, Thomas S. Euro Polym J 1999; 35:253.
- [28] Kim KH, Cho WJ, Ha CS. J Appl Polym Sci 1996; 59:407.
- [29] Wu S. Polymer 1985; 26:1855.
- [30] Idem. J Appl Polym Sci 1981; 35:549.
- [31] Lourence E, Felisberti MI. Euro Polym J 2006; 42: 2632.
- [32] Jelcic Z, Holjevac-Grguric T, Rek V. Polym Degrad Stab 2005; 90:295.
- [33] Murayama T. Dynamic mechanical analysis of polymeric materials. New York: Elsevier Scientific; 1978.
- [34] Nazockdast H, Goharpey F, Katbab, A. Rubber Chem Technol 2003; 76:239.

**Part B**

**EFFECT OF SHORT NYLON-6 FIBRE - UNMODIFIED AND  
RFL-COATED**

**3B.1 Introduction**

**3B.2 Experimental**

**3B.3 Results and Discussions**

**3B.4 Conclusions**

**3B.5 References**

### 3B.1 Introduction

Appropriate incorporation of rubber particles into a brittle plastic matrix is a well established means of improving fracture toughness [1,2]. Unfortunately, the addition of an elastomer to a rigid matrix invariably reduces strength and stiffness relative to the unmodified material. On the contrary, incorporation of high aspect ratio rigid fillers such as high modulus fibres into a polymer matrix improves stiffness and strength [3]. While there is a large body of literature addressing each individual method, the idea of combining the two has received relatively little attention [4,5]. Increasing the fibre loading of rubber-toughened blends has been shown to increase stiffness and strength, as expected [6–11].

The effectiveness of short glass fibre reinforcements in maleic anhydride-grafted-styrene-ethylene-butadiene-styrene (MA-g-SEBS)/PET blends has been investigated by Fung *et al.* [12]. Laura *et al.* [13] studied the effect of glass fibre on the impact and tensile properties of Nylon-6



toughened by maleated ethylene-propylene rubber (MA-g-EPR). Weizhi *et al.* have reported the effect of short glass fibres on the mechanical properties and morphology of PP/EPDM [14]. Saujanya *et al.* have examined the mechanical properties of glass fibre reinforced PP/SBS composite [15]. The dynamic mechanical and thermal properties of PE/EPDM based jute fibres composite has been investigated by Gautam *et al.* [16]. The influence of short cellulose fibre on the microstructure, rheological and mechanical properties of EPDM/PP TPVs. was reported by Goharpey *et al.* [17]. Lopez-Manchado *et al.* [18] have investigated the effect of PET fibres on the mechanical properties of PP/EOC blend. Arroyo *et al.* [19] have explored the reinforcing effect of short aramid fibre in PP/EPDM blends. Anuar *et al.* [20] have reported the use of kenaf fibre in improving the mechanical properties of TPNR and PP/EPDM blends.

Nylon short fibre is a waste product of textile industries and hence its utilisation in composites is cost effective and environment friendly. Thomas *et al.* have studied the influence of short Nylon-6 fibre on the mechanical properties of polypropylene [21] and HDPE [22]. Physico-mechanical properties of EPDM/Nylon-6 short fibre composite were studied by Wazzan [23]. Sreeja *et al.* [24,25] studied the effect of short Nylon-6 fibres on the mechanical properties of NR/reclaimed and NBR/reclaimed rubber composites. The mechanical properties of short Nylon fibre reinforced NBR and CR composite containing epoxy based bonding agent was investigated by Seema *et al.* [26,27]. Mechanical properties of short Nylon fibre reinforced SBR/NR composites were studied in detail by Ma *et al.* [28].

The mechanical properties of fibre-reinforced polymers are strongly influenced by the interface characteristics of the fibres and the polymer matrix. To ensure appropriate interfacial interactions, their surface properties must be modified accordingly. The application of chemical treatment to improve surface roughness and to bring various functional groups on the fibre surface is highly required to improve the adhesion between the fibre and the matrix [29-31]. The influence of RFL-treated aramid fibre and MA-g-PE compatibiliser on the mechanical properties of TPNR has been investigated by Ishak *et al.* [32]. The effect of RFL-treated aramid fibre on metallocene catalysed thermoplastic elastomer ethylene-octene copolymer (EOC) has been investigated by Shibulal *et al.* [33]. Ahmad *et al.* [30] have reported the effect of RFL-treatment on aramid fibres in Twaron-ENR composites. However, up to date little work has been reported on the use of Nylon fibres in rubber-toughened PS.

This part explores the effect of short Nylon-6 fibres- unmodified and RFL-coated on the mechanical properties, morphology and dynamic mechanical properties of natural rubber-toughened polystyrene.

### 3B.2 Experimental

Table 3B.1 gives the composition of the composites used for the study. Details of the preparation of the composites and determination of the mechanical properties are given in Chapter 2.

**Table 3B.1 Composition of the composites.**

Composition	Mix No.								
	B0	B1	B2	B3	B4	B5	B6	B7	B8
PS	85	85	85	85	85	85	85	85	85

<b>NR</b>	15	15	15	15	15	15	15	15	15
<b>Unmodified N-6 fibre [F(U)] wt. %</b>	0	0.5	1	2	3	-	-	-	-
<b>RFL-coated N-6 fibre [F(R)] wt. %</b>	-	-	-	-	-	0.5	1	2	3

### **3B.3 Results and Discussion**

#### **3B.3.1 Mechanical properties**

The variation of tensile strength and Young's modulus as a function of fibre loading are shown in Figures 3B.1 and 3B.2, respectively. The fibre content was varied from 0 to 3 wt.%. The tensile strength in the case of unmodified fibre composites, increases up to 24% at 1wt. % of Nylon fibre after which it continuously falls. While with RFL-coated fibre composites, the tensile strength significantly enhances to 45% for 1wt.% Nylon fibre content. Further increase in fibre content leads to a reduction in the strength properties. The increase in tensile strength with the Nylon-6 fibre is expected as the mechanical properties of the composites are determined by several factors, such as nature of the reinforcement fibre, fibre aspect ratio, fibre-matrix interfacial adhesion and also the fibre orientation in the composites. The Nylon fibre coated with RFL promotes the adhesion with natural rubber phase of the blend and therefore, the transfer of stress from matrix to the fibres is improved. This leads to a significant increase in tensile strength. The reduction in tensile strength at higher fibre content could be due to inefficiency of stress transfer from matrix to fibre and vice versa.

A similar trend is observed with Young's modulus as shown in Figure 3B.2. The enhancement in modulus at 1 wt.% fibre loading is 7% and

14 % respectively, for unmodified and RFL-coated fibre composites. Further incorporation of fibre content leads to reduction in the modulus values.

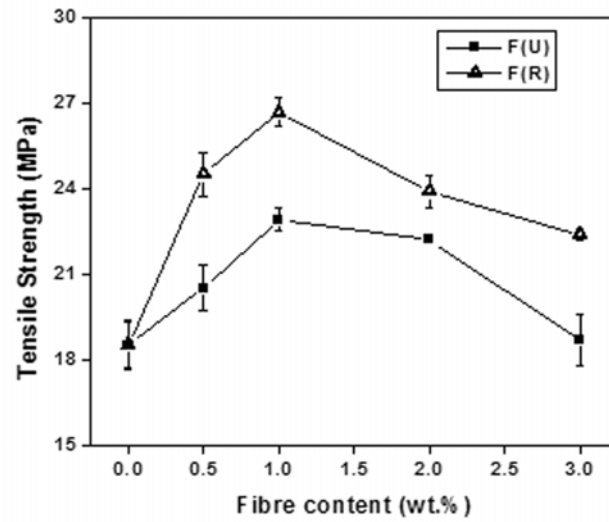


Figure 3B.1: Variation of tensile strength of 85/15 PS/NR with fibre content

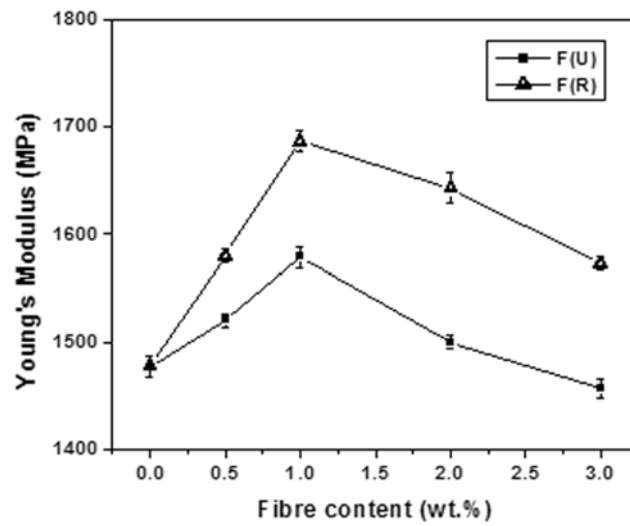


Figure 3B.2: Variation of Young's modulus of 85/15 PS/NR with fibre content.

A flexural test is highly influenced by the properties of the specimen closest to the top and bottom surfaces, whereas a simple tension test reflects the average property through the thickness [34]. Figures 3B.3 and 3B.4

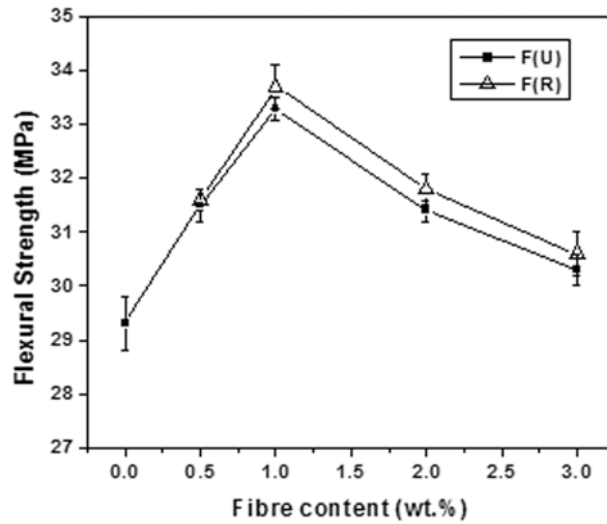


Figure 3B.3: Variation of flexural strength of 85/15 PS/NR with fibre content

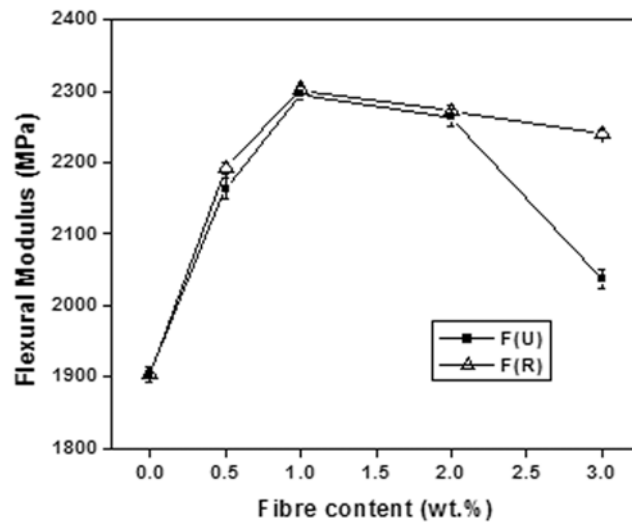
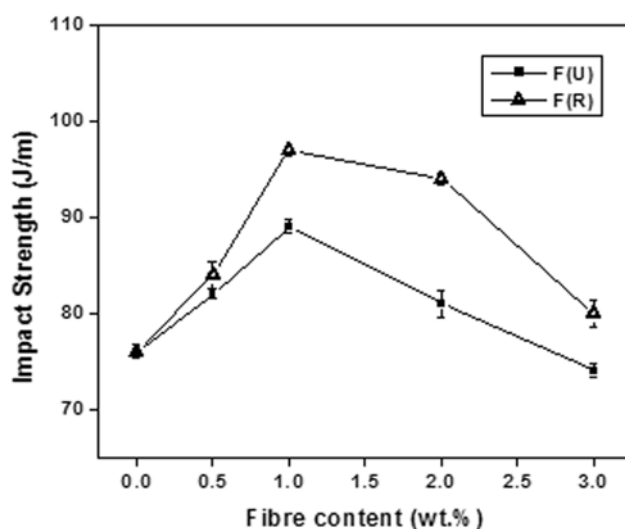


Figure 3B.4: Variation of flexural modulus of 85/15 PS/NR with fibre content.

demonstrates the flexural strength and flexural modulus of PS/NR composites reinforced with unmodified and RFL-coated Nylon-6 fibres. The flexural strength increases by about 13 and 15 % respectively, for unmodified and RFL-coated fibre composites at a fibre loading of 1 wt. %. Whereas the flexural modulus of blends at 1 wt.% fibre loading improved by approximately 20% for both composites in comparison to the unreinforced blend. Previous studies have reported that the flexural properties were affected by fibre–fibre interactions, the alignment of the fibre with the matrix, the presence of voids, dispersion, and the location of resin-rich areas [35,36].



**Figure 3B.5: Variation of impact strength of 85/15 PS/NR with fibre content.**

The effect of unmodified and RFL-coated Nylon-6 fibres on the impact strength of PS/NR composites are illustrated in Figure 3B.5. A considerable increase in impact strength is observed as the fibre content increases up to 1 wt.% beyond which it deteriorates. There is an enhancement of 17% and 27% of impact strength with 1 wt.%, unmodified

and RFL-coated fibres, respectively in comparison to the unreinforced blend. When a material is being broken, during the propagation of fracture, fibres may increase the energy to fracture due to debonding and/or pull-out mechanisms. The debonding and pull-out mechanisms are attributed to the separation and extraction of the fibres from the matrix, both phenomena consume a certain amount of energy giving rise to an increase of the composite impact strength [37]. At higher fibre contents, the stress concentration around the fibre ends tends to reduce the impact strength as it requires less energy to initiate a crack.

### **3B.3.2 Morphology**

Electron microscopy allows one to study the fibres upon fracture. Whether fibres are pulled out from the matrix or are broken, the degree of adhesion with the matrix may be easily visualized. The morphology of the tensile fractured surfaces of 85/15 PS/NR composites containing 1 and 3 wt. % unmodified Nylon-6 fibre, are illustrated in Figures 3B.6 (a), (b), respectively and that of RFL-coated fibre in Figures (c), (c1) and (d). The micrographs of composites with unmodified Nylon fibre show pulled-out fibre and the holes left behind. This indicates poor adhesion between fibre and matrix and inadequate wetting of the unmodified fibres. On the contrary, RFL-coated fibre composites show a rather smooth surface with less amount of fibre pull-out. At higher magnifications in Figure (c1), polymer traces could be seen adhered on the fibre surface. Hence, these composites register improved fibre-matrix adhesion. It is likely that NR is chemically bonded to the fibre surface because of the interaction between NR phase of the blend and RFL-coated fibre [38]. At 3 wt.% fibre content as shown in Figures (b) and (d), the formation of holes generated

### *Chapter -3*

---

by fibre pull-out may be the root cause of decrease in mechanical properties.



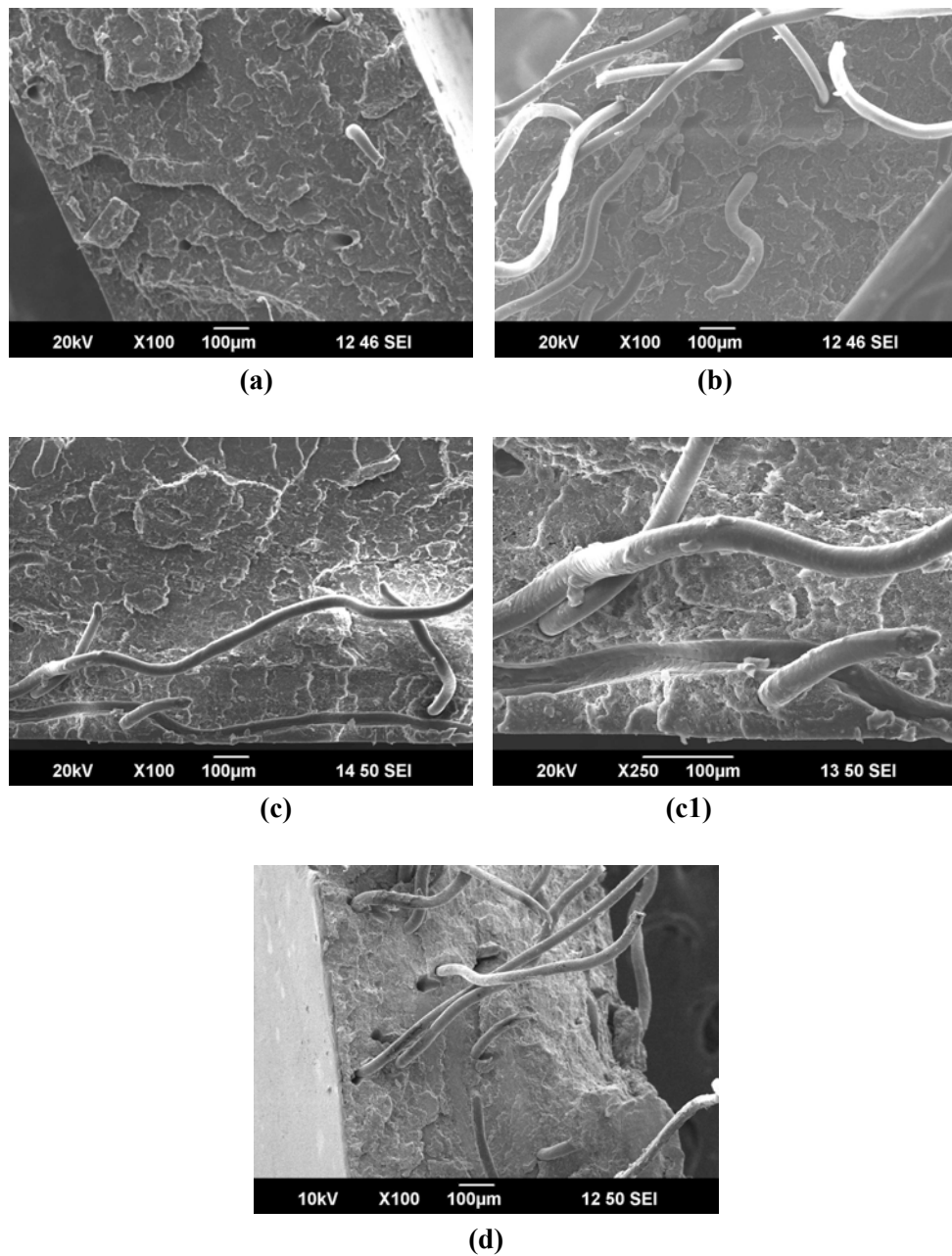


**Figure 3B.6:** Scanning electron micrographs of 85/15 PS/NR composites with (a) 1 (b) 3 wt.% of unmodified Nylon fibres and (c) 1 (x 100 magnification), (c1) 1 (x 250 magnification) and (d) 3 wt.% of RFL-coated Nylon fibres.

### 3B.3.3 Dynamic Mechanical Analysis

The dynamic mechanical properties of composites are significantly dependent upon the amount of fibre [39,40], the presence of additives-like compatibiliser, filler, and impact modifier [41], fibre orientation [42], and mode of testing. The storage modulus is closely related to the load bearing capacity of the material. The variation of storage modulus of composites with different loading of unmodified and RFL-coated fibres as a function of temperature is shown in Figures 3B.7 and 3B.8, respectively. With unmodified fibres, the storage modulus increases from 0 to 1 wt. % fibre content and decreases at higher fibre loadings. The higher storage modulus at 1 wt. % is due to the high stiffness of the composite contributed by the Nylon fibres. A sharp drop at high temperatures corresponds to the  $T_g$  of PS. The storage modulus in the case of RFL-coated fibres follows a trend similar to that of the unmodified fibres as shown in Figure 3B.8.

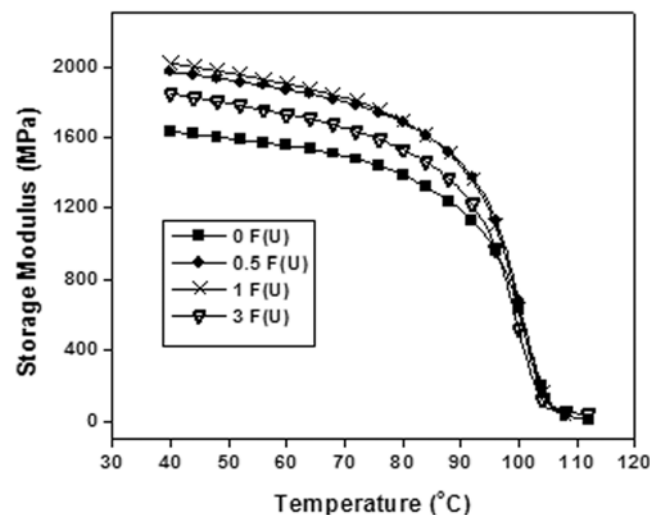


Figure 3B.7: Storage modulus vs. temperature plots of 85/15 PS/NR composites with varying (unmodified) fibre content.

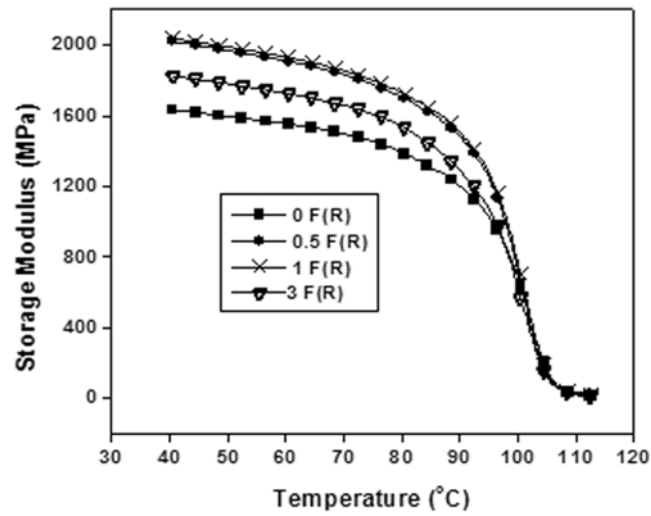


Figure 3C.8: Storage modulus vs. temperature plots of 85/15 PS/NR composites with varying (RFL-coated) fibre content.

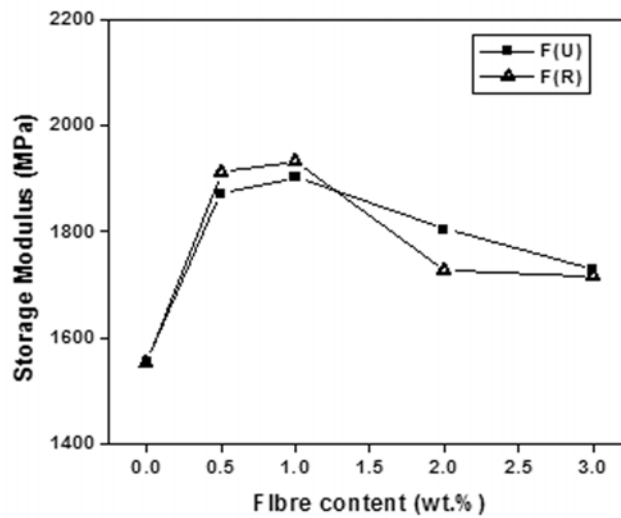


Figure 3B.9: Variation of storage modulus (at 60 °C) of 85/15 PS/NR composites with fibre content.

The storage modulus of the composites at 60 °C as a function of fibre loading is presented in Figures 3B.9. The figure shows that the storage modulus for both the unmodified and RFL-coated fibre composites enhances up to 1 wt.% and then decreases with further increase in fibre

content. The RFL-coated fibre composites shows an increase in storage modulus by 32 MPa than the unmodified one at 1 wt.% fibre loading. This might be due to the better interaction between NR and Nylon fibre in the presence of RFL.

The variation of unmodified and RFL-coated fibre content on the loss modulus of 85/15 PS/NR blends are presented in Figure 3B.10 and 3B.11, respectively. In the case of unmodified fibre composites, the loss modulus curve shows a relaxation peak corresponding to the  $T_g$  of PS. There is no shift in the peak with the incorporation of Nylon fibres. The loss modulus values at this temperature increased with increasing fibre loading up to 1 wt% and then decreases. This increase may be related to the increase in constraints on the segmental mobility of the polymer chains in the presence of Nylon fibres. The broadening of transition peak increased with increase in fibre loading which may due to the increase in energy absorption caused by fibre reinforcement.

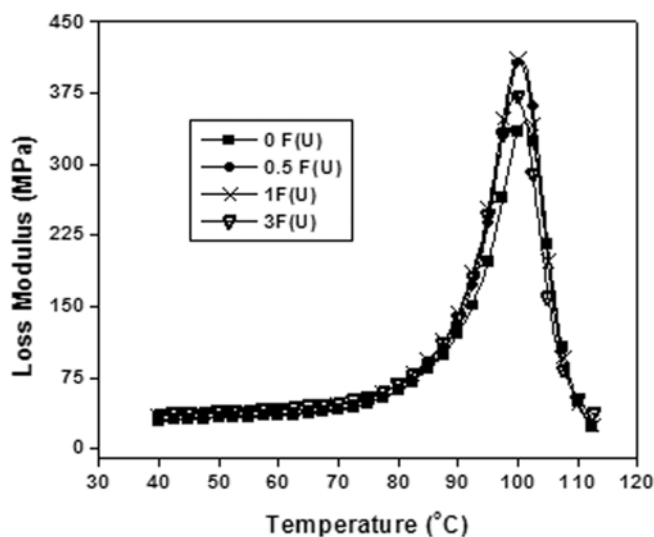
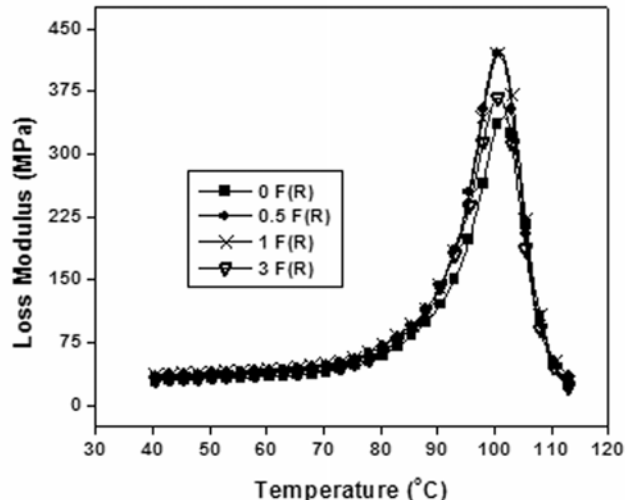


Figure 3B.10: Loss modulus vs. temperature plots of 85/15 PS/NR composites with varying (unmodified) fibre content.

A similar behaviour was observed with RFL-coated fibre composites as shown in Figure 3B.11.



**Figure 3B.11: Loss modulus vs. temperature plots of 85/15 PS/NR composites with varying (RFL-coated) fibre content.**

The ratio of loss modulus to storage modulus ( $E''/E'$ ) is measured as the mechanical loss factor or  $\tan \delta$ . A material will change from rigid to the elastic state with the movement of small groups and the chains of molecules within the polymer structure. In fibre-reinforced composites, damping is affected by the presence of fibres. The variation of  $\tan \delta$  with temperature for unmodified and RFL-coated fibre composites are presented in Figures 3B.12 and 3B.13, respectively. With unmodified fibre composites, the  $\tan \delta$ , which corresponds to the damping properties of the material, is found to decrease with increase in the fibre content. The reason could be attributed to the restriction of the chain mobility by fibre reinforcement. There is a marginal shift of about 4 °C to the glass transition temperature of PS at 3 wt.% fibre loading.

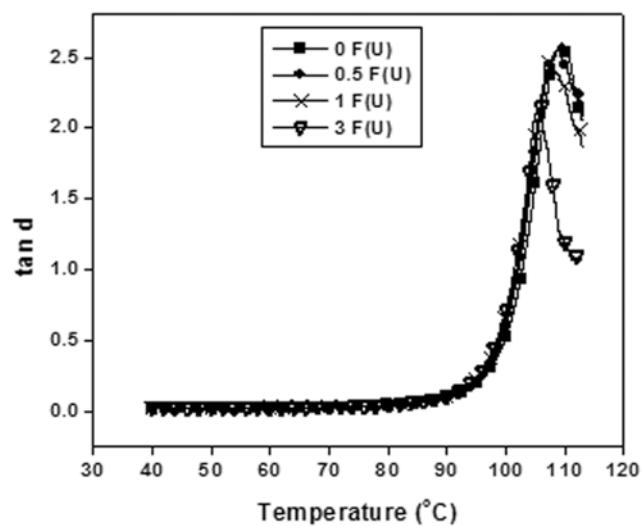


Figure 3B.12: Tan  $\delta$  vs. temperature plots of 85/15 PS/NR composites with varying (unmodified) fibre content.

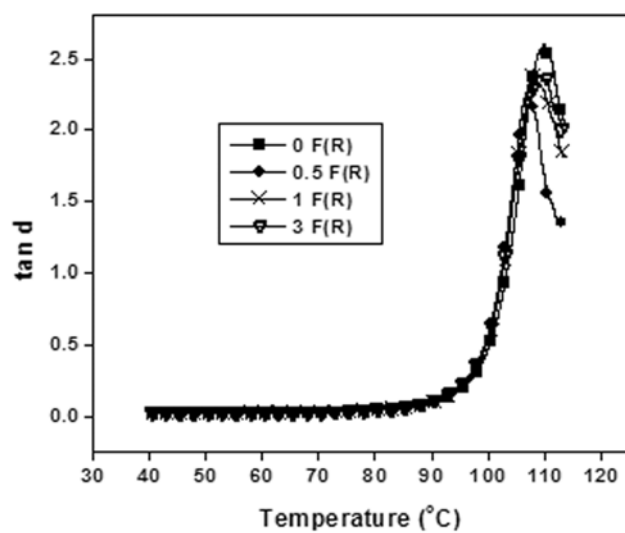


Figure 3B.13: Tan  $\delta$  vs. temperature plots of 85/15 PS/NR composites with varying (RFL-coated) fibre content.

With RFL-coated fibre composites, the  $\tan \delta$  peak is lowest for 0.5 wt.% fibre content and is slightly higher for 1 and 3 wt.% fibre content, which are in turn lower than the unreinforced blend. There is a slight shift of about 3 °C to the location of  $T_g$  for 0.5 wt.% fibre content.

### **3B.4 Conclusions**

Incorporation of short Nylon-6 fibres- unmodified and RFL-coated can significantly improve the mechanical properties of 85/15 PS/NR blend. The tensile strength, Young's modulus, flexural strength, flexural modulus and impact strength shows a maximum for both the composites with 1 wt. % Nylon fibre. The storage modulus vs. temperature plots showed a maximum increase in stiffness of 85/15 PS/NR with 1 wt.% Nylon fibre. On the basis of above studies, it can be concluded that an optimal concentration of 1 wt.% Nylon fibres (unmodified and RFL-coated) can effectively reinforce the 85/15 PS/NR blend.

### **3B.5 References**

- [1] Paul DR, Newman S, editors. Polymer blends. New York: Academic Press; 1978.
- [2] Collyer AA, editor. Rubber toughened engineering plastics. London: Chapman and Hall; 1994.
- [3] Krenchel H. Fibre reinforcement. Copenhagen: Akademisk Forlag, 1964.
- [4] Wong S-C, Mai Y-W. Polym Eng Sci 1999; 39:356.
- [5] Friedrich K, Karger-Kocsis J. In: Schultz JM, Fakirov S, editors. Solid state behaviour of linear polyesters and polyamides. Englewood Cliffs, NJ: Prentice Hall; 1990, p. 249.
- [6] Gaymans RJ. Toughened polyamides. In: Collyer AA, editor. Rubber toughened engineering plastics, London: Chapman and Hall; 1994 (chap. 7).

- [7] Bailey RS, Bader G. The effect of toughening on the fracture behaviour of a glass-fibre reinforced polyamide. In: Harrigan WC, Strife J, Dhingra AK, editors. Fifth International Conference on Composite Materials, San Diego, 1985. Warrendale, PA: Metallurgical Society, Inc. p. 947.
- [8] Karger-Kocsis J. Reinforced polymer blends. In: Paul DR, Bucknall CB, editors. Polymer blends: formulation and performance. New York: Wiley; 1999 (chap. 31).
- [9] Scott JM, Phillips DC. *J Mater Sci* 1975; 10:551.
- [10] Azari A, Boss F. Society of Plastics Engineers 54<sup>th</sup> annual technical conference, Indianapolis, 1996, p. 3022.
- [11] Kinloch AJ, Maxwell DL, Young RJ. *J Mater Sci* 1985; 20:4169.
- [12] Fung KL, Robert Li KY. *Polym Test* 2006; 25:923.
- [13] Laura M, Keskkula H, Barlow JW, Paul DR. *Polymer* 2000; 41:7165.
- [14] Weizhi W, Longxiang T, Qu B. *Euro Polym J* 2003; 39:2129.
- [15] Saujanya C, Radhakrishnan S. *Polym Comp* 2001; 22:232.
- [16] Gautam S, Arup C. *J Appl Polym Sci* 2008; 108:3442.
- [17] Goharpey F, Mirzadeh A, Sheikh A, Nazockdast H, Katbab AA. *Polym Comp* 2009; 30:182.
- [18] Lopez Manchado MA, Arroyo M. *Polymer* 2001; 42:6557.
- [19] Arroyo M, Zitzumbo R, Avalos F. *Polymer* 2000; 41:6351.
- [20] Anuar H, Zuraida A. *Composites: Part B* 2011; 42:462.
- [21] Thomas N Abraham, George KE. *Polym Plast Technol Eng* 2007; 46:321.
- [22] Thomas N Abraham, George KE. *Plast Rub Comp* 2005; 34:196.
- [23] Wazzan AA. *Int J Polymer Mater* 2004; 53:59.
- [24] Sreeja TD, Kutty SKN. *Polym-Plast Technol Eng* 2003; 42:239.
- [25] Sreeja TD, Kutty SKN. *Int J Polym Mater* 2003; 52:175.



- [26] Seema A, Kutty SKN. *J Appl Polym Sci* 2006; 99:532.
- [27] Seema A, Kutty SKN. *Polym Plast Technol Eng* 2005; 44:1139.
- [28] Ma Peiyu, Zhao Jan, Tang J, Dai G. *Guofenzi Cailiao Kexue Yu Gongcheng* 1994; 10:55.
- [29] Chantaratcharoen A, Sirisinha C, Amornsakchai T, Limcharoen SB, Meesiri W. *J Applied Poly Sci* 1999; 74:2414.
- [30] Ahamad I, Chin TS, Cheong CK, Jalar A, Abdullah I. *Am J Appl Sci* 2005; (Special Issue):14.
- [31] Mori M, Uyama Y, Ikada Y. *Polymer* 1994; 34:5336.
- [32] Ishak A, Yong PY, Ibrahim A. *Polym Compos* 2006; 27:395.
- [33] Shibulal GS, Naskar K. *J Polm Res* 2011, 18:2295.
- [34] Folkes MJ. *Short fibre reinforced thermoplastics*. Britain: John Wiley & Sons; 1982. p. 149-151.
- [35] Arbelaiz A, Fernandez G, Cantero R, Llano-Ponte LP, Valea A, Mondragon I. *Compos A* 2005; 36:1637.
- [36] Sastra HY, Siregar JP, Sapuan SM, Leman Z, Hamdan MM. *Am J Appl Sci* 2005; (Special issue):21.
- [37] Arroyo M, Bell M. *J Appl Polym Sci* 2002; 83:2474.
- [38] Begnoche BC, Keefe RL, Causa AG. *Rubber Chem Technol* 1987; 60:689.
- [39] Tasi SW, Halpin HT. *Introduction to Composites Materials*. Westport, CT: Technomic; 1980.
- [40] Adams FD, Short DF. *J Phys D: Appl Phys* 1973; 6:1032.
- [41] Kolarik F, Lednický F, Pukanszky B. In *International Conference on Composite Materials* 1987; Vol. 6, Londo, p. 452.
- [42] Adams FD, Doner DR. *J Compos Mater* 1967; 1:4.

## Part C

### EFFECT OF SURFACE MODIFICATION OF FIBRE AND USE OF A COMPATIBILISER

#### 3C.1 Introduction

#### 3C.2 Experimental

#### 3C.3 Results and Discussions

#### 3C.4 Conclusions

#### 3C.5 References

### 3C.1 Introduction

Nylon fibres are important as reinforcing fibres for plastics and elastomers due to their high strength, sufficient flexibility, abrasion resistance and light weight. However, the main problem due to poor adhesion between the fibre and polymer matrix continues to pose a challenge to researchers. Various methods to modify the Kevlar fibre surface include the incorporation of coupling agents [1], the use of ionomer matrix [2,3], chemical [4,5], and plasma treatments [6-9]. One of the simple chemical treatment techniques reported in the literature is surface hydrolysis [8,10]. This technique has led to an easy preparation of Kevlar with an increased number of active amino groups on its surface thereby providing further reaction with, e.g. reactive or functionalized compatibiliser.

The effect of MAPP as coupling agent in kenaf fibre reinforced TPNR and PP/EPDM composites has been reported by Anuar *et al.* [11]. The influence of MA-g-PB in aramid fibre reinforced ethylene-octene copolymer composites was investigated by Shibulal *et al.* [12]. Paunikallio *et al.* [13] have studied the effect of MAPP in polypropylene-viscose fibre composites. Rana *et al.* [14] have reported the influence of MAPP as

compatibiliser in jute fibre–PP composites. Smitha *et al.* [15] have studied the effectiveness of MA-g-PP as coupling agents in sisal fibre-propylene composites. Amornsakchai *et al.* [16] have investigated the effect of partially hydrolysed Conex short fibre and addition of a reactive compatibiliser, MA-g-SEBS on SEBS thermoplastic elastomer. The influence of compatibiliser on surface treated Kevlar fibre–reinforced Santoprene composites was studied by Saikrasun *et al.* [17]. However, little research has been carried out on the hydrolysis of Nylon fibres and its effect in combination with a compatibiliser on PS/NR blends.

This part describes the effect of modification of Nylon-6 fibre by surface treatment (using alkali) and the use of a compatibiliser on the mechanical properties, morphology and dynamic mechanical properties of 85/15 PS/NR composites. Maleic anhydride-grafted-polystyrene (MA-g-PS) was used as the compatibiliser.

### 3C.2 Experimental

Table 3C.1 gives the formulation of the composites used for the study. Details of the surface treatment of fibre, preparation of the composites and determination of the mechanical properties are given in Chapter 2.

**Table 3C.1 Composition of the composites.**

Composition	Mix No.									
	C0	C1	C2	C3	C4	C5	C6	C7	C8	C9
PS*	85	85	85	85	85	85	85	85	85	85
NR*	15	15	15	15	15	15	15	15	15	15
Untreated N-6 fibre [F(U)] (wt.%)	1	1	1	1	1					
Treated N-6 fibre [F(T)] (wt.%)						1	1	1	1	1
MA-g-PS (wt.%)	0	0.5	0.75	1	2	0	0.5	0.75	1	2

\*parts per hundred polymer (php)

### **3C.3 Results and Discussion**

The preparation of maleic anhydride-grafted-polystyrene (MA-g-PS) and the procedure for determining the degree of grafting are given in Chapter 2.

#### **3C.3.1 Characterization of MA-g-PS**

Schematic representation of the formation of MA-g-PS is shown in Figure 3C.1. Degree of grafting, calculated from acid value was obtained as 0.41 wt.% of MA. The grafting was also confirmed using FTIR spectroscopy. Figure 3C.2 shows the spectrum of PS and MA-g-PS in the range 2000-1000  $\text{cm}^{-1}$ . In the spectrum of MA-g-PS, a broad absorption band at 1780  $\text{cm}^{-1}$  and a weak absorption band at 1840  $\text{cm}^{-1}$ , not observed in the spectrum of PS, are found. These characteristic bands can be assigned to symmetric and asymmetric C=O stretching of five membered cyclic anhydrides, respectively in MA grafted on PS [18].

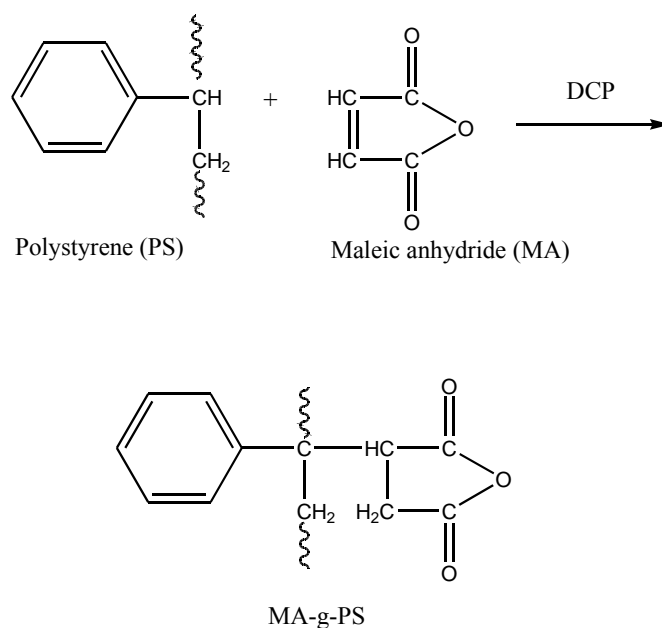


**Figure 3C.1: Schematic representation of formation of maleic anhydride-grafted-polystyrene.**

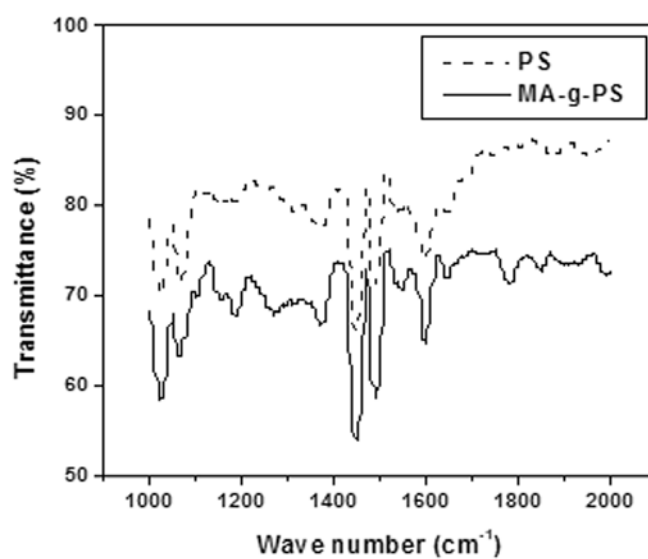


**Figure 3C.2: FTIR spectra of (a) PS and (b) MA-g-PS with MA content-0.41wt.% compression moulded films.**

Modification of interfacial interaction between the fibre and the matrix was carried out by surface hydrolysis (using alkali) of Nylon-6 fibre and the use of a reactive compatibiliser, MA-g-PS. Hydrolysis of the fibre surface introduced more amine groups (Figure 3C.3), which can react with MA groups of the compatibiliser added to form covalent bonds as shown in Figure 3C.4, thus maximizing the compatibiliser efficiency. Furthermore, the non-polar part (PS) of MA-g-PS becomes compatible with the PS phase of the PS/NR blend, lowers the surface energies of the fibres, thereby increasing its wettability and dispersion within the matrix.

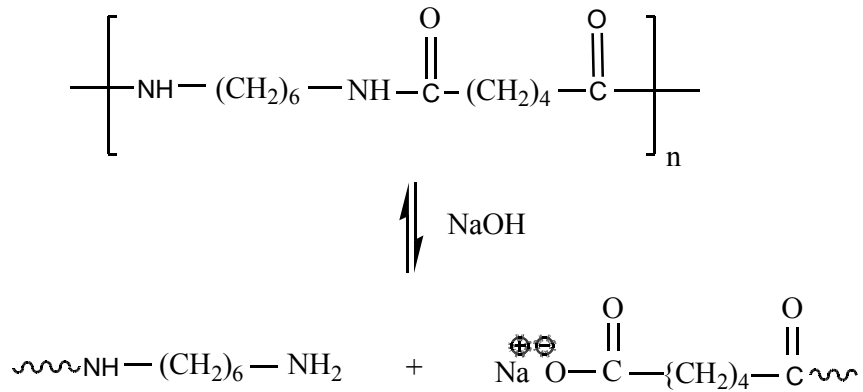


**Figure 3C.3: Hydrolysis of the Nylon-6 fibre**

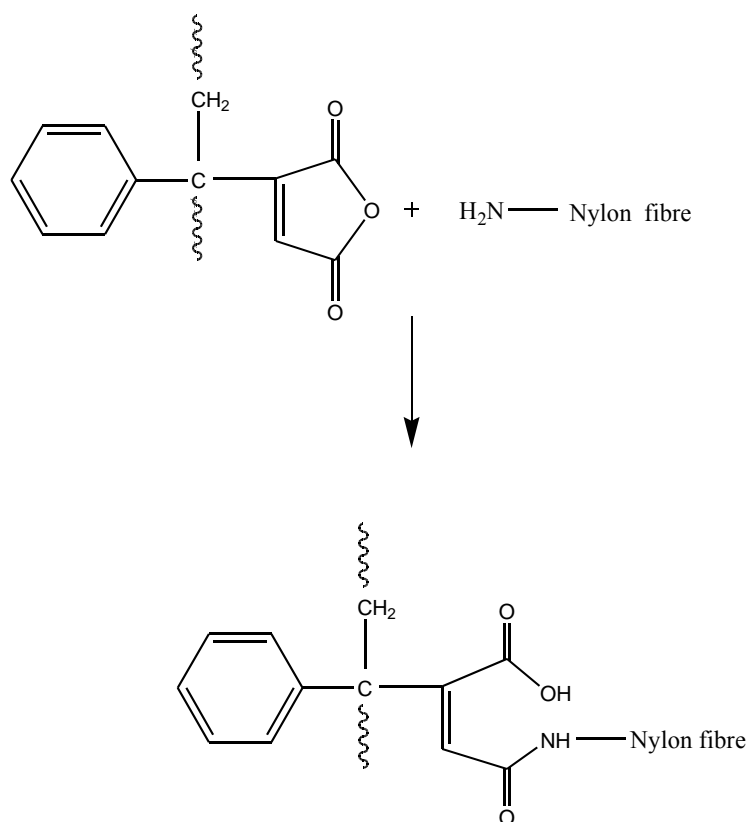


**Figure 3C.4: Reaction between MA-g-PS and the amine group on the Nylon fibre surface.**

### 3C.3.2 Mechanical properties

Effect of MA-g-PS content on tensile properties of the composites containing untreated and treated Nylon-6 fibres are illustrated in Figures 3C.5 and 3C.6. The untreated and treated fibre composites in the presence of compatibiliser significantly enhances the tensile strength to about 9 % and 23 % respectively, at a loading of 0.75 wt.% of MA-g-PS in comparison to the corresponding composites without compatibiliser. The enhancement in tensile properties may be attributed to increase in interfacial adhesion between the fibres and the matrix with the addition of MA-g-PS. The increased polarity of the fibre surface resulting from the hydrolysis is not

productive in the absence of a MA-g-PS; rather it results in polarity segregation leading to lower tensile strength. Beyond 0.75 wt.% of MA-g-PS, the tensile strength deteriorates for both treated and untreated fibre composites. This behaviour may be attributed to the migration of excess MA-g-PS around the fibres, causing self-entanglement among themselves rather than the polymer matrix resulting in slippage [14,15].

The tensile modulus also improved for both composites with 0.75wt. % of compatibiliser as shown in Figure 3C.5. There is an enhancement of 7% and 13%, respectively of tensile modulus for untreated and treated fibre composites in the presence of compatibiliser. However, the treated fibre composites in conjunction with the compatibiliser shows better improvement when compared to the untreated one.

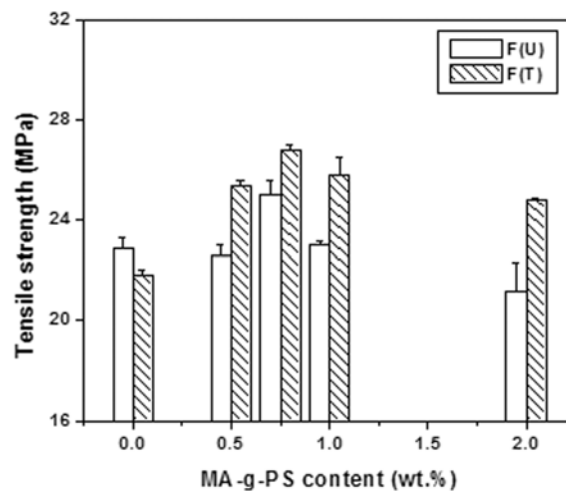
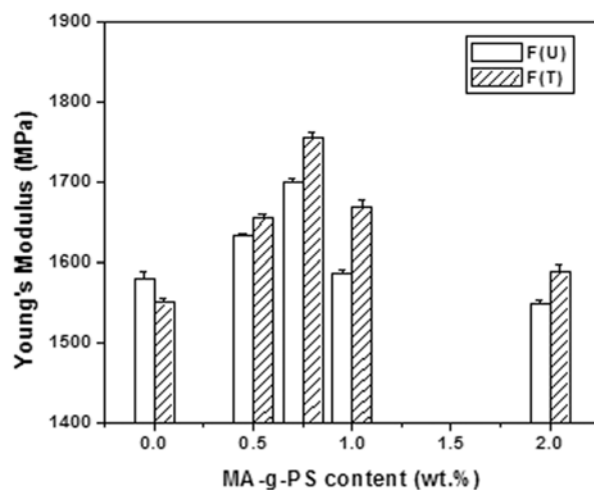


Figure 3C.5: Variation of MA-g-PS on the tensile strength of composites with 1 wt.% fibre.





**Figure 3C.6: Variation of MA-g-PS on the Young's modulus of composites with 1 wt.% fibre.**

The variation of flexural strength and flexural modulus of 85/15/1 PS/NR/Nylon fibre composites with varying MA-g-PS content are shown in Figures 3C.7 and 3C.8, respectively. The flexural strength enhanced with increase in MA-g-PS content to 0.75 wt.% and then decreases. There was an enhancement of about 4% and 10%, respectively of flexural strength for untreated and treated fibre composites with compatibiliser when compared to the corresponding composites in the absence of compatibiliser. A similar behaviour was observed with the flexural modulus for both the composites as shown in Figure 3C.8.

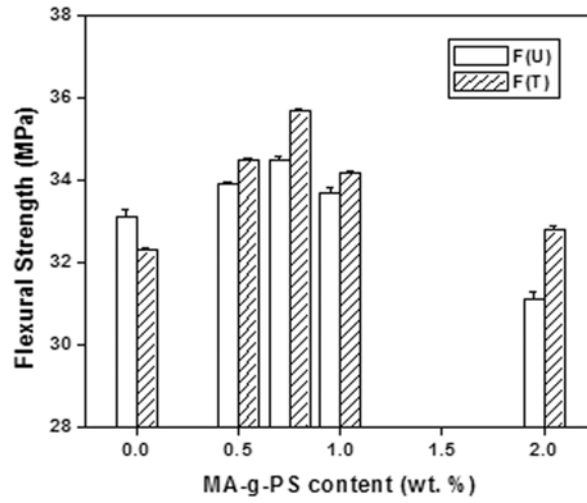


Figure 3C.7: Variation of MA-g-PS on the flexural strength of composites with 1 wt.% fibre.

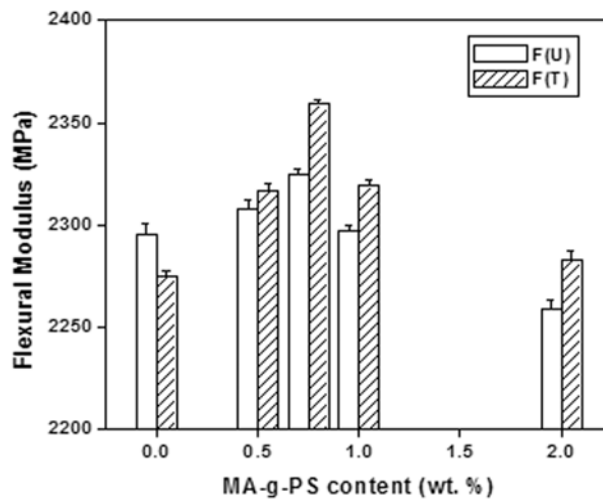
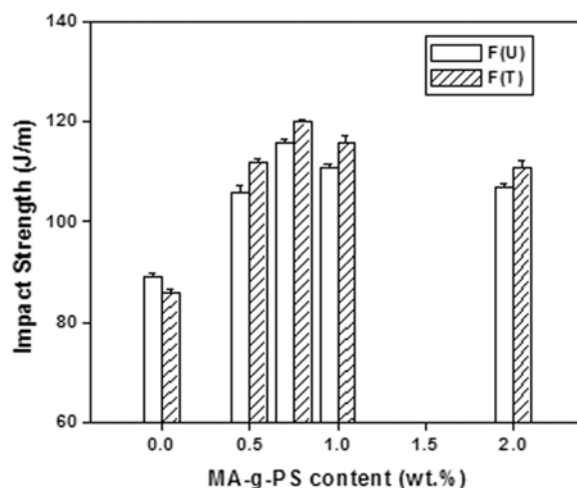


Figure 3C.8: Variation of MA-g-PS on the flexural modulus of composites with 1 wt.% fibre.



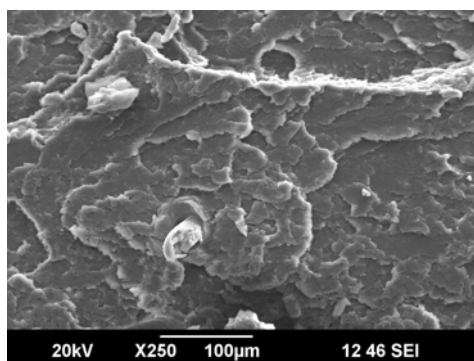
**Figure 3C.9: Variation of MA-g-PS on the impact strength of composites with 1 wt.% fibre.**

The effect of compatibiliser (MA-g-PS) on the impact strength of composites at 1 wt.% untreated and treated Nylon fibres is presented in Figure 3C.9. The treated and untreated fibre composites at a loading of 0.75 wt.% of compatibiliser enhanced the impact strength to 39% and 32%, respectively in comparison to the corresponding composites without compatibiliser. The lower impact strength of treated fibre composites in the absence of compatibiliser may be due to fibre agglomeration resulting from increased polarity of the fibres which creates regions of stress concentration that requires less energy to initiate a crack. At higher concentrations of MA-g-PS, the impact strength decreased. It is likely that the dispersed MA-g-PS domains act as stress concentrators, and that these are not capable of absorbing the impact energy [19].

### 3C.3.3 Morphology

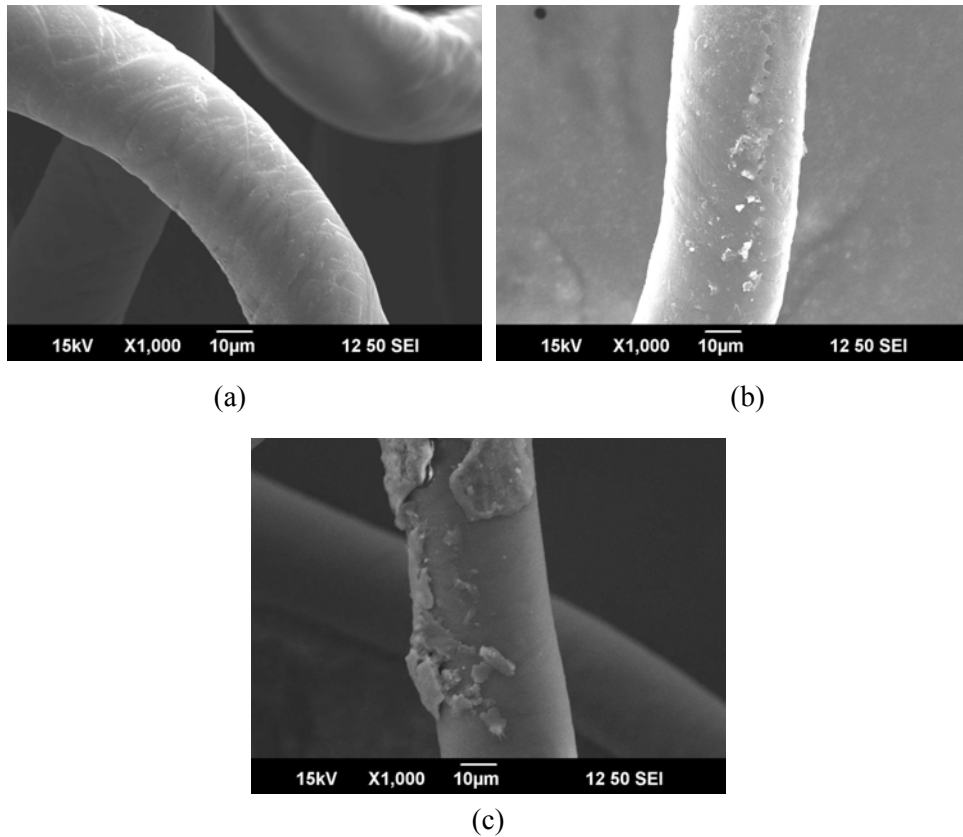
The morphology of the tensile fractured surface of treated fibre composites at 1wt.% fibre loading and 0.75 wt.% MA-g-PS is illustrated in

Figure 3C.10. Fibre breakage is observed with no fibre-pull outs when MA-g-PS is added, which suggests the improvement of interfacial adhesion.



**Figure 3C.10: Scanning electron micrographs of 85/15 PS/NR composites with 1 wt.% treated fibre and 0.75 wt.% MA-g-PS (compatibiliser).**

SEM micrographs of solvent extracted fibres from the composites with (a) untreated fibre, (b) untreated fibre with compatibiliser and (c) treated fibre with compatibiliser (0.75 wt.% MA-g-PS) are shown in Figure 3C.11(a)-(c). In the case of untreated fibre in Figure (a), very clean fibre with smooth surface was obtained after extraction. The extracted fibre from untreated fibre composites containing compatibiliser showed small particles adhered to the fibre surface as shown in Figure (b). On the other hand, for the treated fibre composite with MA-g-PS, the extracted fibre as in Figure (c) showed a rough and irregular surface and also lumps of unextractable MA-g-PS. This would suggest that MA-g-PS reacts with reactive end groups, i.e.  $-\text{NH}_2$ , on the surface of the partially hydrolysed Nylon fibre and hence the tensile properties of the compatibilised composite is improved.



**Figure 3C.11: Scanning electron micrographs of (a) untreated fibre (b) untreated fibre with compatibiliser and (c) treated fibre with compatibiliser.**

### 3C.3.4 Dynamic Mechanical Analysis

Storage modulus is closely related to the load bearing capacity of a material. Storage modulus ( $E'$ ) as a function of temperature is shown in Figure 3C.12. It is observed that composites with treated fibre and compatibiliser shows the highest storage modulus from 40 °C to 95 °C and then shows relatively same values as that of untreated fibre with and without compatibiliser beyond 95 °C up to the end temperature. Thus better stress transfer leads to composites with higher moduli. A similar increase in Young's modulus was also observed in the composites with treated fibre and compatibiliser.

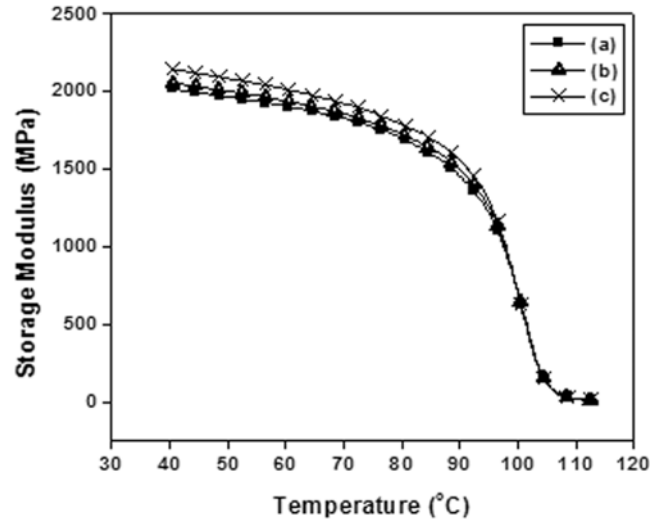


**Figure 3C.12: Storage modulus vs. temperature plots of composites containing (a) untreated fibre (b) untreated fibre with compatibiliser and (c) treated fibre with compatibiliser (0.75wt.%).**

Figure 3C.13 shows the variation of  $E''$  with temperature for various composites. If the applied mechanical energy (work) is not stored elastically, it must be lost—converted to heat through molecular friction, that is, viscous dissipation within the material. This is, precisely, the loss modulus [20]. The relaxation peak corresponds to the glass transition ( $T_g$ ) of PS. The loss modulus value corresponding to the  $T_g$  in the composites with treated fibre and compatibiliser showed the highest value when compared to untreated composites.

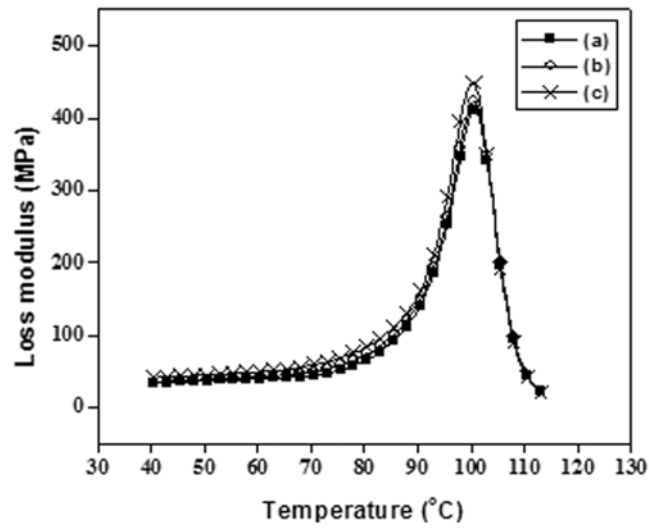


Figure 3C.13: Loss modulus vs. temperature plots of composites containing (a) untreated fibre (b) untreated fibre with compatibiliser and (c) treated fibre with compatibiliser.

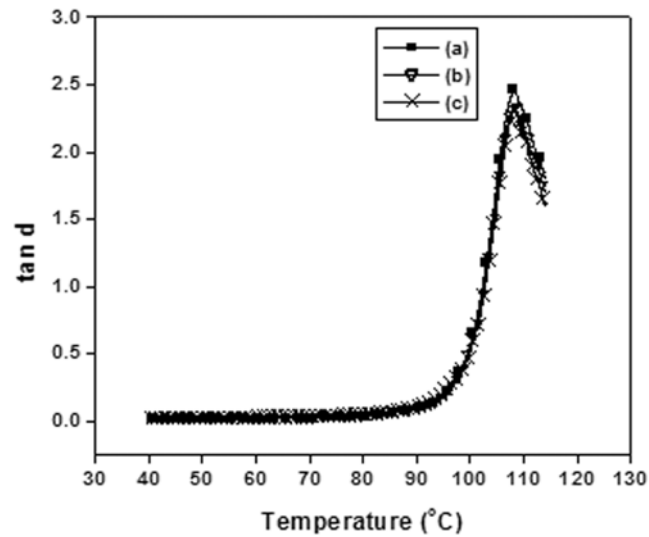


Figure 3C.14: Tan  $\delta$  vs. temperature plots of composites containing (a) untreated fibre (b) untreated fibre with compatibiliser and (c) treated fibre with compatibiliser.

The ratio of loss modulus to storage modulus is measured as the mechanical loss factor or  $\tan \delta$ . The damping properties of the material gives the balance between the elastic phase and viscous phase. Fibre–matrix interface property could be understood to a very good extent based on the damping curves. Figure 3C.14 shows the variation of  $\tan \delta$  as a function of temperature for the composite under study. The peak at about 109 °C is associated with the glass transition of PS. It is seen that there is negligible shift in the  $\tan \delta$  peak, signifying that the treated fibre composites did not influence the glass transition. The  $\tan \delta$  peak of untreated fibre composite exhibited higher magnitude when compared to treated and untreated fibre composites with compatibiliser. This envisages that a composite material with strong interfacial bonding between the fibres and matrix, will tend to dissipate less energy, showing low magnitude of damping peak in comparison to material with poor bonded interface [21].

### **3C.4 Conclusions**

The reinforcement of 85/15 PS/NR blends with short Nylon-6 fibres can be improved by surface treatment of the Nylon fibres and also by using a proper compatibiliser. Alkaline hydrolysis of the Nylon fibre can make the fibre surface more reactive. Maleic anhydride-grafted-polystyrene, prepared by the melt mixing process using DCP at 170 °C, can function as a good compatibiliser. The use of compatibiliser at 0.75 wt.% in conjunction with treated fibre improves the tensile strength and flexural strength by 23 % and 10 %, respectively at a fibre loading of 1 wt %. The impact strength improves by 39% for treated fibre composites in the presence of 0.75 wt.% compatibiliser. The SEM analysis confirms better bonding between the fibre and the matrix. The results from the dynamic mechanical analysis



measurements reveals that the storage modulus of the treated fibre composites in the presence of compatibiliser is better compared to that of the untreated fibre composites, with and without compatibiliser.

### **3C.5 References**

- [1] Vaughan D. *Polym Eng Sci* 1978; 18:167.
- [2] Takayanagi M, Kajiyama T, Katayose T. *J Appl Polym Sci* 1982; 27:3903.
- [3] Takayanagi M, Katayose T. *Polym Eng Sci* 1984; 24:1047.
- [4] Andrepoulos AG. *J Appl Polym Sci* 1989; 38:1053.
- [5] Tarantili PA, Andrepoulos AG. *J Appl Polym Sci* 1997; 65:267.
- [6] Wang Q, Kaliaguine S, Ait-Kadi AJ. *J Appl Polym Sci* 1993; 48:121.
- [7] Yu Z, Ait-Kadi AJ, Brisson J. *Polym Eng Sci* 1991; 31:1222.
- [8] Sheu GS, Shyu SS. *J Adhesion Sci Technol* 1994; 8:1027.
- [9] Brown JR, Mathys Z. *J Mater Sci* 1997; 32:2599.
- [10] Garbassi F, Morra M, Occhiello E. *Polymer surfaces: from physics to technology*. Chichester: Wiley; 1994, p. 251.
- [11] Anuar H, Zuraida A. *Comp Part B* 2011; 42:462.
- [12] Shibulal GS, Naskar K. *J Polym Res* 2011; 18:2295.
- [13] Paunikaloi T, Kasanen J, Suvanto M, Pakkanen TT. *J Appl Polym Sci* 2003; 87:1895.
- [14] Rana AK, Mandal A, Mitra BC, Jacobson R, Rowell R, Banerjee AN. *J Appl Polym Sci* 1998; 69:329.
- [15] Smita M, Sushil KV, Sanjay KN, Sudhansu ST. *J Appl Polym Sci* 2004; 94:1336.
- [16] Amornsakchai T, Sinpatanapan B, Baulek-Limcharoen S, Meesiri W. *Polymer* 1999; 40:2993.

- [17] Saikrasun S, Amornsakchai T, Sirisinha C, Meesiri W, Baulek-Limcharoen S. *Polymer* 1999; 40:6437.
- [18] Li H, Chen H, Shen Z, Lin S. *Polymer* 2002; 43:5455.
- [19] Hristov V, Krumova M, Michler G. *Macromol Mater Eng* 2006; 291:677.
- [20] Rosen SL. *Fundamental Principles of Polymeric Materials*. New York: Wiley; 1982.
- [21] Smita M, Sushil KV, Sanjay KN. *Composites Science and Technology* 2006; 66:538.

.....✍.....

# POLYSTYRENE/STYRENE - BUTADIENE RUBBER BLENDS

## Part A

### TOUGHENING OF POLYSTYRENE: EFFECT OF BLEND RATIO AND DYNAMIC VULCANISATION

#### 4A.1 Introduction

#### 4A.2 Experimental

#### 4A.3 Results and Discussions

#### 4A.4 Conclusions

#### 4A.5 References

### 4A.1 Introduction

Polymer blends and alloys are gaining increasing significance. The large scale acceptance of polymer blends arises from the wide range of properties conferred upon blending. Moreover, they are made from existing polymers and can be processed in conventional processing equipment or machinery, thereby decreasing capital investment. The incorporation of dispersed elastomeric particles in a rigid polymer matrix such as polystyrene has attracted considerable attention because of its industrial importance, among other types of polymer blends [1-5]. The toughening mechanisms involved are influenced by the properties of the matrix material and by the morphology of the blend [6]. The proposed mechanisms for toughening

rely mainly on the dispersion of rubber particles within the glassy matrix that results in energy absorption by the rubber particles, debonding at the rubber-matrix interface and crazing. In the case of a brittle thermoplastic polymer such as polystyrene (PS), toughening particles must initiate a large number of crazes in PS and at the same time control craze break-down in order to avoid premature fracture [7].

Liu and Baker studied the effects of rubber particle size and rubber/matrix adhesion on the impact properties of a brittle polymer. It has been proved that the interfacial adhesion between the rubber phase and PS matrix is improved by reducing the rubber particle size [8]. Most of the polymer pairs are immiscible and incompatible. These incompatible blends often give poor mechanical properties because of the poor interfacial adhesion and the lack of physical and chemical interactions between different phases. Even though most of the polymer blends are incompatible, they can be made compatible by several methods [9,10]. Dynamic vulcanisation can be considered as a technological compatibilisation technique. On dynamic vulcanisation, the lightly crosslinked rubber particles can withstand more stress and at the same time retains the flowability of the plastic phase.

The influence of curing agents and its composition in PP/EPDM blends have been investigated by Nicolini *et al.* [11]. Naskar *et al.* [12] have investigated the effects of different types of peroxides as crosslinking agents for various PP/EPDM blend. Wang *et al.* [13] have reported the dynamic vulcanisation of HIPS/SBR blends using sulphur vulcanising system. Influence of various types of peroxides on the properties of TPVs.. based on NR/PP blends were investigated by Thitithammawong *et al.* [14]. The effects

of dynamic crosslinking on the properties of rice husk powder filled PS/SBR blends were studied by Ismail *et al.* [15].

Part I discusses the preparation of toughened polystyrene by melt blending polystyrene with styrene-butadiene rubber and evaluates the mechanical properties, morphology and dynamic mechanical properties of the resulting blends.

Part II discusses the effect of dynamic vulcanisation using dicumyl peroxide (DCP) on the mechanical properties, morphology and dynamic mechanical properties of 90/10 PS/SBR blend.

#### 4A.2 Experimental

PS/SBR blends were prepared by melt-mixing in a Thermo Haake Polylab QC and the formulations used are given in Table 4A.1.

**Table 4A.1. Blend Formulations**

Ingredients	Composition*				
<b>PS</b>	100	95	90	85	80
<b>SBR</b>	0	5	10	15	20

\*parts per hundred polymer (php)

The compositions of PS/SBR with varying DCP concentrations are shown in Table 4A.2.

**Table 4A.2 Composition at fixed PS/SBR blend ratio with varying peroxide concentration.**

Components	Mix No.					
	A0	A1	A2	A3	A4	A5
<b>PS</b>	90	90	90	90	90	90
<b>SBR</b>	10	10	10	10	10	10
<b>DCP<sup>a</sup></b>	0	0.5 (0.7) <sup>b</sup>	1 (1.4)	1.5 (2.1)	2 (2.8)	2.5 (3.5)

<sup>a</sup> Concentration of DCP in phr.

<sup>b</sup> Values in parentheses correspond to the milliequivalent concentration of DCP.

The melt mixed samples were compression moulded to  $\approx 0.1$ mm films and 1 mm sheets, conditioned and then tested as discussed in Chapter 2.

### 4A.3 Results and Discussions

#### Part I Effect of Blend Ratio

##### 4A.3.1 Mechanical Properties

The tensile strength and Young's modulus as a function of blend composition are shown in Figures 4A.1 and 4A.2, respectively. The tensile strength and Young's modulus decreases linearly with an increase in rubber content. The addition of a low strength and low modulus rubbery phase (SBR) to a high strength and high modulus glassy phase (PS) directly leads to a decrease in tensile strength and tensile modulus. This is an observation reported by many researchers [16-20].

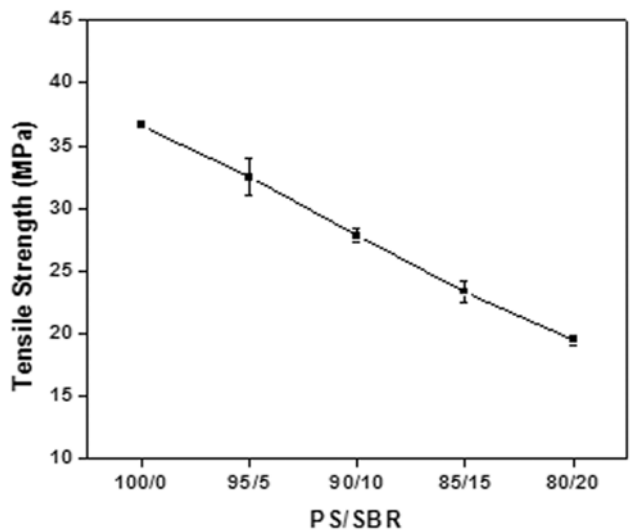
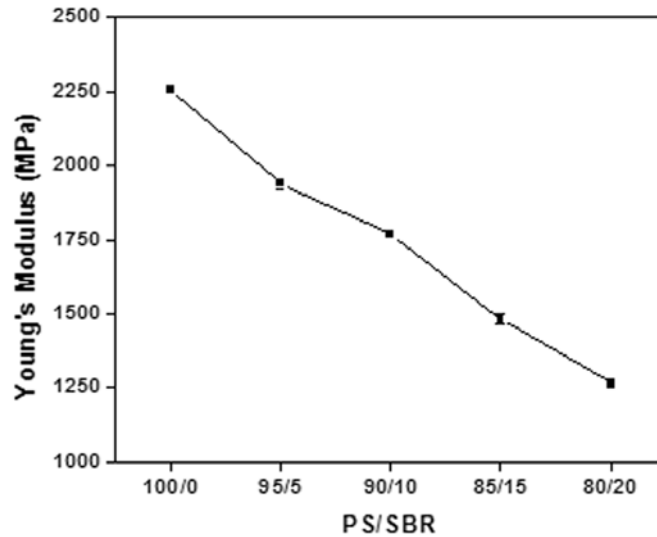
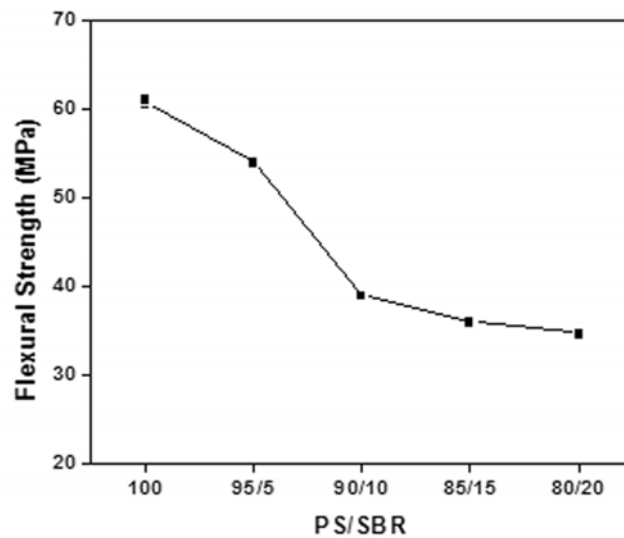


Figure 4A.1: Variation of tensile strength for various PS/SBR blends.



**Figure 4A.2: Variation of Young's modulus for various PS/SBR blends.**



**Figure 4A.3: Variation of flexural strength for various PS/SBR blends.**

Figures 4A.3 and 4A.4 shows the flexural strength and flexural modulus of various blends of PS/SBR. As can be seen in Figure 4A.3, there is an abrupt decrease in flexural strength, as the rubber (SBR) content

increases from 5 to 10 wt.% in the blend and beyond 10wt.% the decrease is gradual. Whereas the flexural modulus decreases almost linearly with increasing SBR content. The decrease in flexural strength with increasing SBR content in the blends indicates a reduction in rigidity and an increase in the elastomeric nature of the blend.

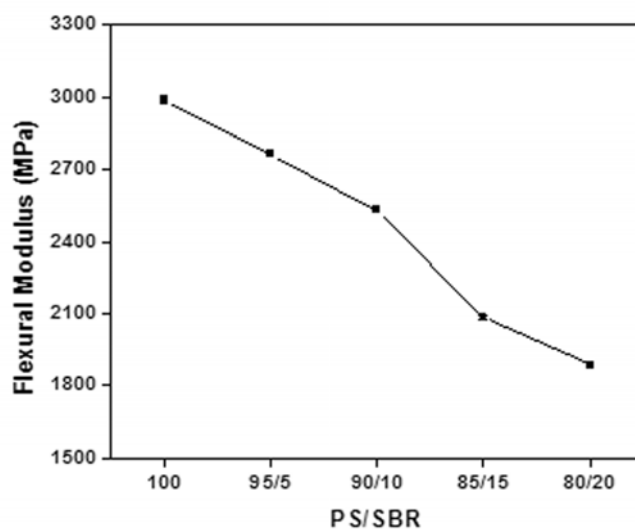


**Figure 4A.4: Variation of flexural modulus for various PS/SBR blends.**

The unnotched Izod impact strength of PS/SBR blend as a function of blend composition is shown in Figure 4A.5. The impact strength increases up to 10 wt.% of rubber (SBR) content and then shows a gradual decrease. The optimum rubber content for attaining maximum impact resistance was found to be 10 wt.%. The impact strength improved by 36 % for the 90/10 blend. Beside this concentration, the unnotched Izod impact resistance is slightly improved over the virgin PS value. A possible reason for this behaviour is that at lower rubber contents, the energy abstracted from the crack during propagation is not sufficient to withstand the complete fracture of the



specimen [6], whereas higher rubber content might affect the interparticle spacing in the matrix with no additional crazing possible [21].

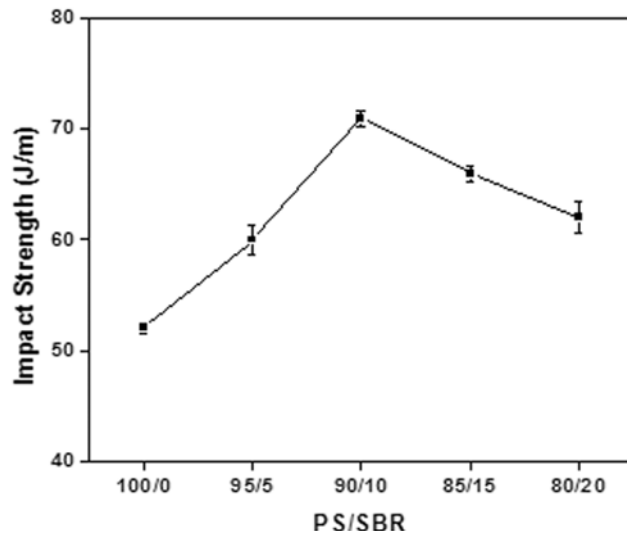


**Figure 4A.5: Variation of impact strength for various PS/SBR blends.**

#### **4A.3.2 Morphology**

The scanning electron micrographs of the impact fractured surface of PS, 90/10 and 85/15 PS/SBR blends are illustrated in Figures 4A.6(a), (b) and (c). With virgin PS, large plane areas with sharp, brittle fracture in various planes could be seen. Whereas homogeneous craze surfaces could be observed in both the blends. Both the blends have rougher surface compared to unmodified PS [Figure (a)]. The rougher the surface area indicates that more energy has been absorbed during the impact test.

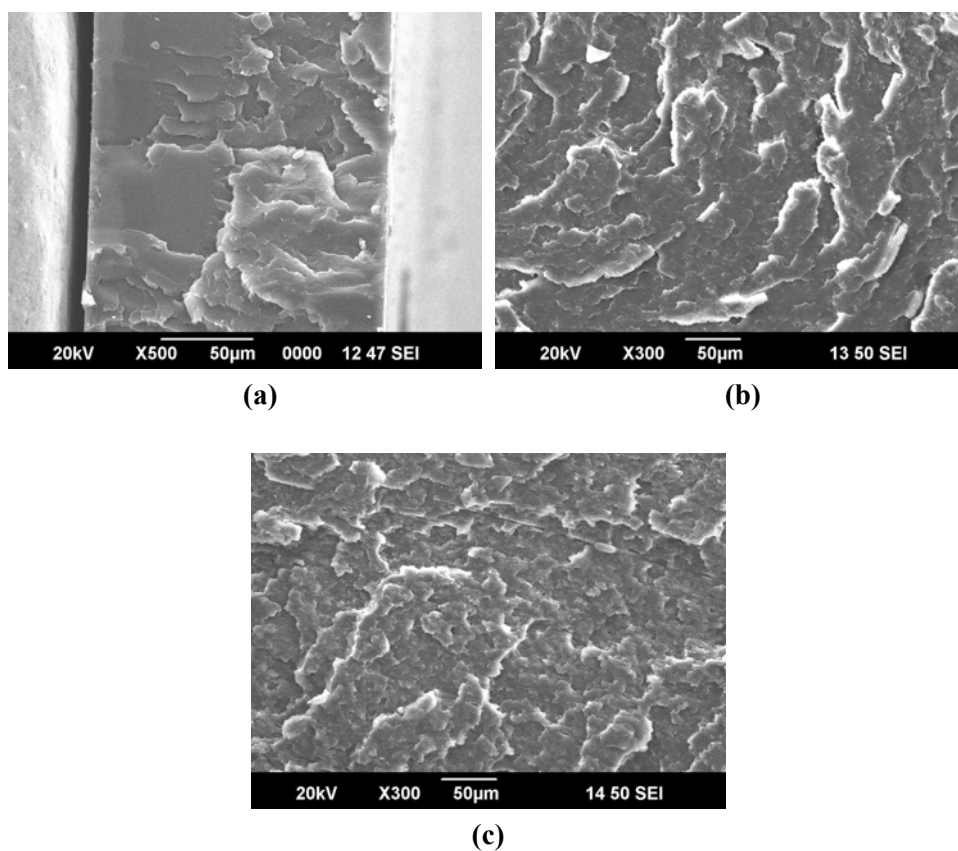


**Figure 4A.6: Scanning electron micrographs of fracture surfaces of PS/SBR blends (a) PS, (b) 90/10 PS/SBR and (c) 85/15 PS/SBR.**

#### **4A.3.3 Dynamic mechanical analysis**

Dynamic mechanical analysis is a technique where a little deformation is applied to the sample in a cyclic manner. This permits the material's response to stress, temperature, frequency and other values. DMA applies a sinusoidal force at a set frequency to the sample and measures changes in stiffness and damping, these are reported as modulus and tan delta.

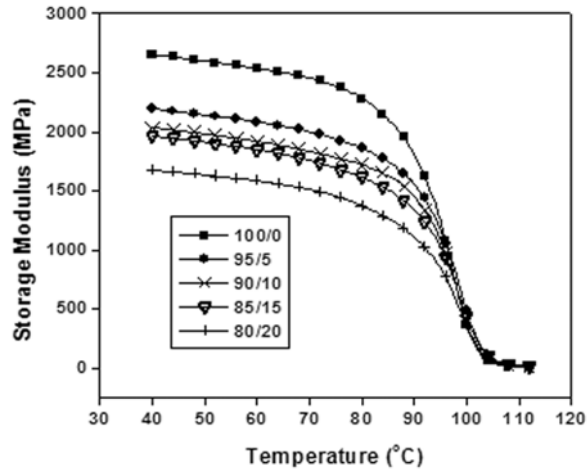


**Figure 4A.7: Effect of temperature on the storage modulus of PS/SBR blends.**

Plots of storage modulus vs. temperature of various PS/SBR blends are shown in Figure 4A.7. PS and all the blends exhibit very high modulus at room temperature as all the molecules are in the frozen condition. As the temperature approaches the glass transition temperature ( $T_g$ ) of PS, segmental mobility sets in and hence there is a drastic decrease in the storage modulus. As observed in the figure, pure PS shows the highest modulus and the value of  $E'$  decreases with increasing SBR content. The value of the modulus above  $T_g$  are almost the same for PS and the blends.

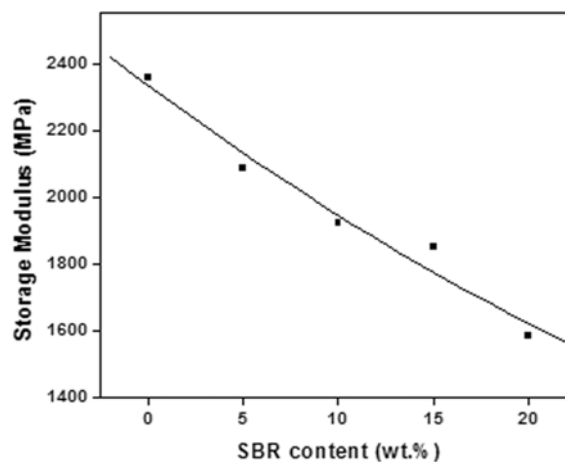


**Figure 4A.8: Variation of storage modulus at 60 °C with SBR content.**

The effect of SBR content on the storage modulus of PS/SBR blends is illustrated in Figure 4A.8. The figure and the regression results show that the SBR content has a significant effect on the storage modulus of PS. The regression equation relating SBR content to storage modulus could be fitted quite well by a polynomial of the second order, with a regression coefficient ( $R^2$ ) of 0.96 as follows:

$$y = 2331 - 41.92x + 0.317x^2$$

where  $y$  = storage modulus (MPa) at 60 °C,

$x$  = SBR content (wt.%)

Figure 4A.9 shows the effect of temperature on the loss modulus values of various PS/SBR blends. The peak for all blend ratios around 100 °C corresponds to the glass transition temperature ( $T_g$ ) of PS. The rapid rise in modulus in all the system indicates the structural mobility of the polymer. The magnitude in loss modulus peak decreases with increasing rubber content.

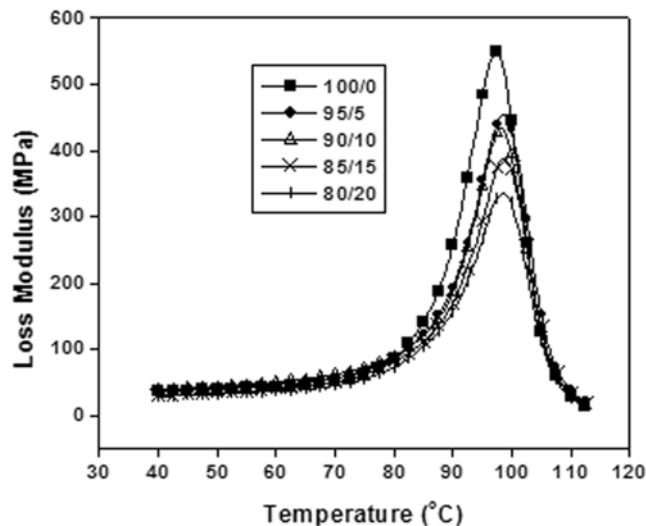
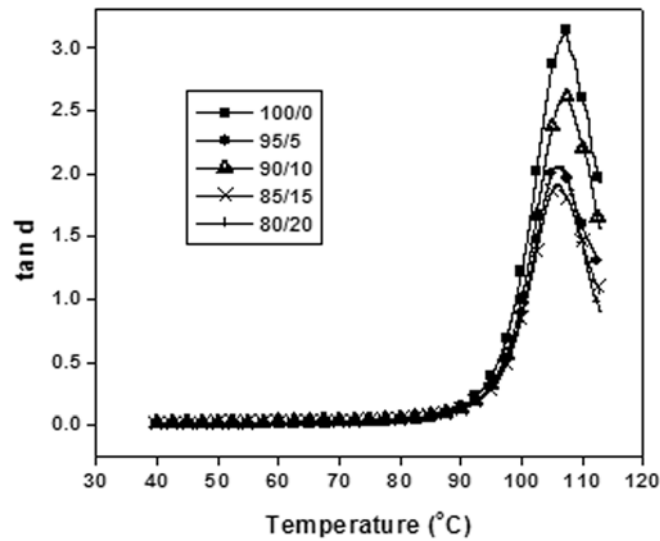


Figure 4A.9: Effect of temperature on the loss modulus of PS/SBR blends.

Damping is a sensitive display of all kinds of molecular motions that are going on in a material. Figure 4A.10 delineates the damping curves of various PS/SBR blends. It can be observed that as the temperature increases, the damping goes through a maximum at  $T_g$  and then decreases in the rubbery region. Below  $T_g$ , the chain segments are frozen in and hence damping is low. Above  $T_g$ , the molecular segments are very free to move which reduced the damping. In the transition region, part of the segment are free to move about and the rest are not so free. A frozen segment stores energy through deformation and it ultimately releases it as viscous energy when it becomes free to move. The  $\tan \delta$  peak is the highest for the unmodified PS and lower for the blends with SBR.



**Figure 4A.10: Effect of temperature on  $\tan \delta$  of PS/SBR blends.**

## Part II Effect of Dynamic Vulcanisation

### 4A.3.4 Mechanical properties

The tensile strength and Young's modulus of 90/10 PS/SBR dynamically vulcanised with different levels of DCP are presented in Figures 4A.11 and 4A.12, respectively. The tensile strength and Young's modulus is increased with increasing content of DCP up to 2.1 meq and then decreases. There is an improvement of 18 % and 17 % in tensile strength and Young's modulus, respectively at 2.1 meq DCP.

As the level of DCP increases, the extent of crosslinking also increases leading to the formation of fine crosslinked rubber particles in the matrix. The crosslinked rubber particles within the matrix can withstand greater stress by undergoing increased extent of deformation before failure, thus resulting in increased tensile strength and Young's modulus. The extensively crosslinked rubber particles beyond 2.1 meq DCP will not effectively transfer the stress to the matrix thereby resulting in substantial reduction in tensile properties.

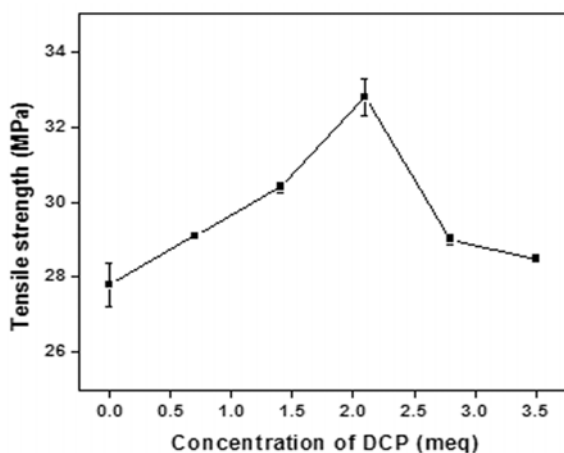
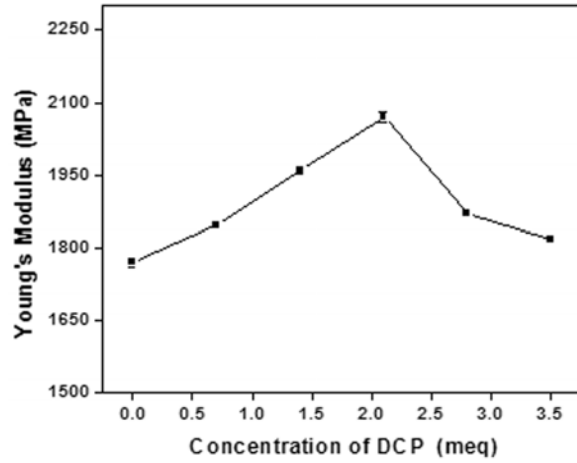
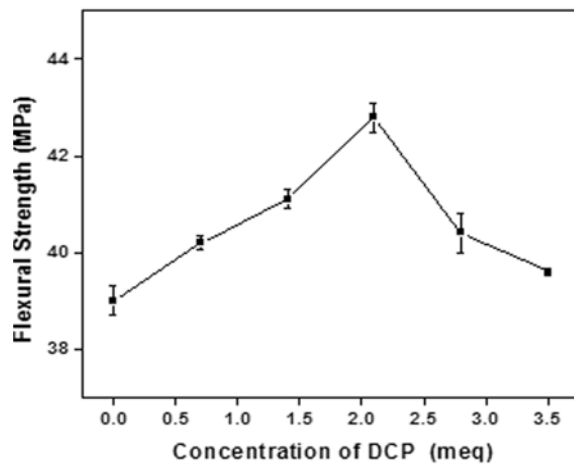


Figure 4A.11: Variation of tensile strength of 90/10PS/SBR with DCP concentration.



**Figure 4A.12: Variation of Young's modulus of 90/10 PS/SBR with DCP concentration.**

The flexural properties such as flexural strength and flexural modulus of dynamically vulcanised 90/10 PS/SBR blend with various levels of DCP are given in Figures 4A.13 and 4A.14. Similar to the tensile properties, the flexural properties also increase up to 2.1 meq of DCP and then decreases. This is attributed to the enhanced crosslinking of the rubbery phase imparted by peroxide cure.



**Figure 4A.13: Variation of flexural strength of 90/10 PS/SBR with DCP concentration.**

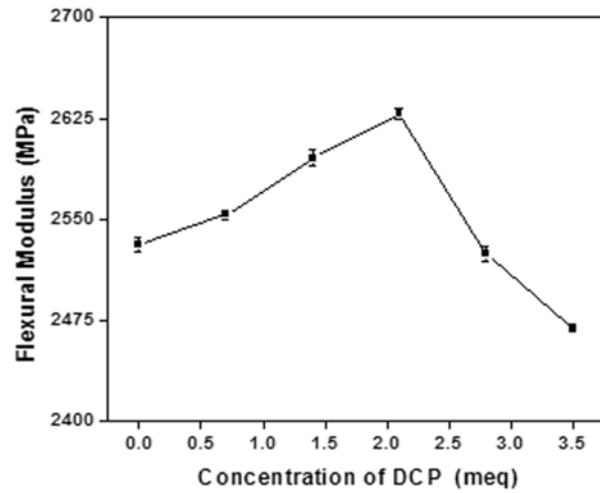


**Figure 4A.14: Variation of flexural modulus of 90/10 PS/SBR with DCP concentration.**

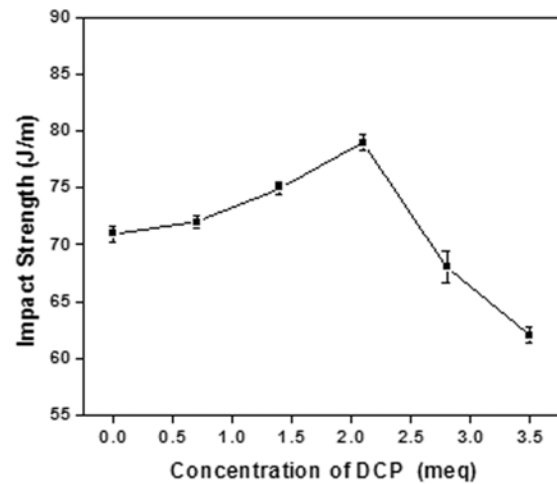


**Figure 4A.15: Variation of impact strength of 90/10 PS/SBR with DCP concentration.**

The impact strength of 90/10 PS/SBR blend dynamically vulcanised with various levels of DCP content is illustrated in Figure 4A.15. The impact strength gradually increases up to 2.1 meq DCP with an enhancement of 11 % beyond which it drastically reduces. At optimum



DCP content, the rubber particles are crosslinked and their size is greatly reduced because of the shear induced size reduction during vulcanisate preparation. The crosslinked structure of these discrete particles greatly inhibits the probability of rubber cohesion during cooling, so the number density of rubber at constant volume fraction domains are many-fold with good interfacial adhesion promoted by physical interlocking during meltdown.

The low impact value of the unvulcanised blend is attributed to the fact that the rubber droplets formed during blend formation coalesce during static melt cooling, giving rise to irregularly sized rubber domains that are larger than the critical size desired for impact toughening. Above the optimum DCP concentration, the impact values decrease. This implies that the crosslinking of SBR becomes more pronounced at DCP concentrations higher than the optimum leading to a reduction in the number of craze initiating rubber particles.

#### **4A.3.5 Morphology**

The morphologies of the tensile fractured surface of 90/10 PS/SBR blends with (a) 2.1 meq and (b) 3.5 meq DCP contents are depicted in Figures 4A.16. The morphology of blend (b) with DCP content higher than the optimum results in a coarse surface when compared to blend (a). Even though the blend (a) with optimum DCP content shows a two-phase morphology, the interfacial adhesion increases due to small concentrations of graft copolymers produced at the interface on crosslinking.

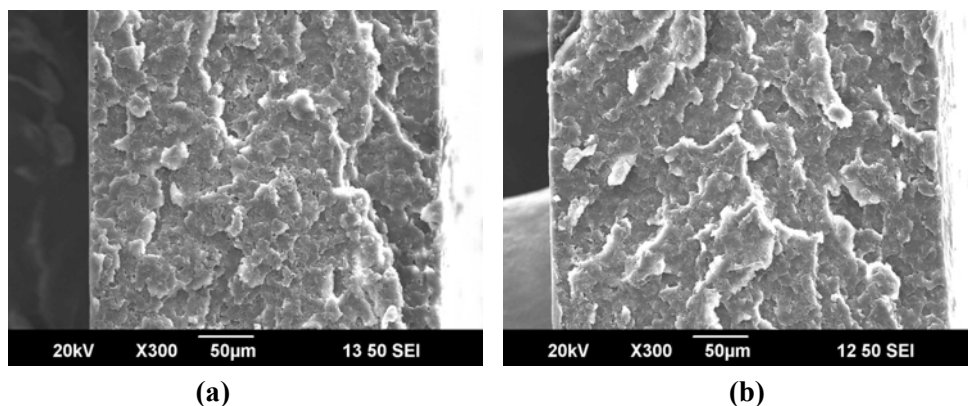


Figure 4A.16: Scanning electron micrographs of fractured surface of 90/10PS/SBR blend with (a) 2.1 meq and (b) 3.5 meq of DCP.

#### 4A.3.6 Dynamic mechanical analysis

The variation of  $E'$  values with temperature of dynamically vulcanised PS/SBR blends is presented in Figure 4A.17. A high modulus glassy region at room temperature can be observed from the figure where the segmental mobility is restricted. The dynamically vulcanised blend with a DCP content of 2.1 meq exhibits the highest  $E'$  value when compared to unvulcanised

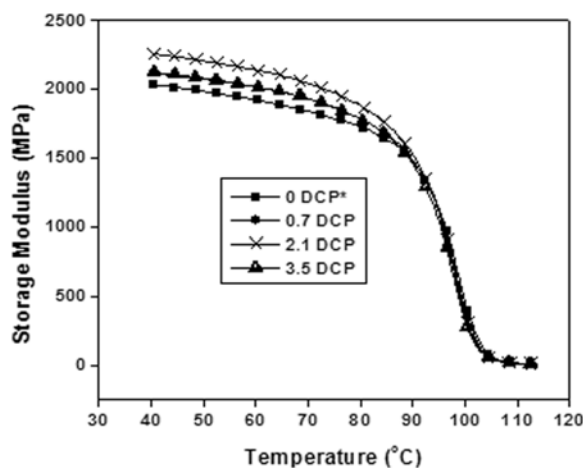
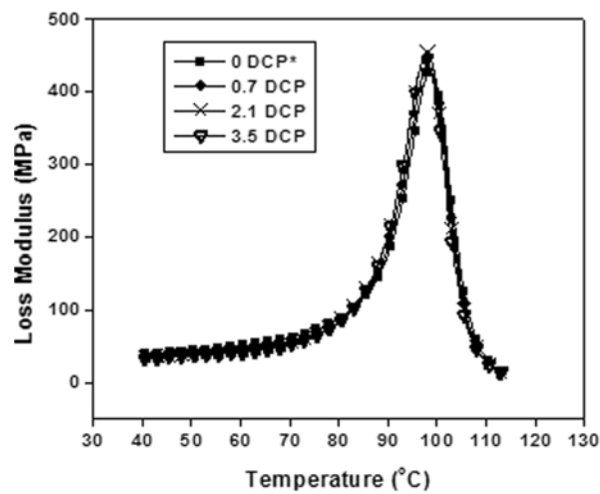


Figure 4A.17: Effect of temperature on the storage modulus of dynamically vulcanised 90/10 PS/SBR blends.

blend and blends with lower and higher levels of DCP. With further increase in temperature approaching the transition region, there is substantial decrease in  $E'$  values for all the blends. In the flow region, a drastic decrease in the modulus with temperature can be observed for all the blends. Here the molecular mobility sets in and the molecules slip past each other.

Loss modulus ( $E''$ ) vs. temperature plots of dynamically vulcanised blends of PS/SBR are given in Figure 4A.18. A distinct peak corresponding to the  $T_g$  of PS is observed for all the blends. As the temperature approaches  $T_g$ , energy dissipation takes place which results in a corresponding peak of  $E''$ . The blend with 2.1 meq DCP shows the higher loss modulus peak when compared to other blends.



**Figure 4A.18:** Effect of temperature on the loss modulus of dynamically vulcanised 90/10 PS/SBR blends.

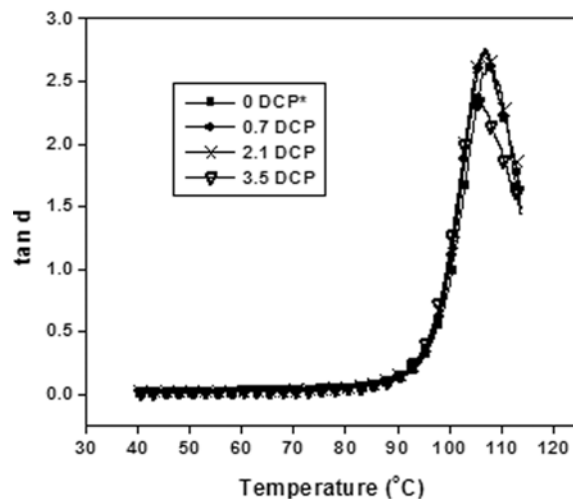


**Figure 4A.19: Effect of temperature on  $\tan \delta$  of dynamically vulcanised 90/10 PS/SBR blends.**

The variation of  $\tan \delta$  values of dynamically vulcanised PS/SBR blends as a function of temperature is shown in Figure 4A.19. The peak around 108 °C corresponds to the  $T_g$  of PS. There is little shift in the  $T_g$  of PS for the dynamically vulcanised blends. Moreover, the  $\tan \delta$  peak for dynamically vulcanised blends is almost identical to that of the unvulcanised blend except for the blend with 3.5 meq DCP content.

#### 4A.4 Conclusions

The mechanical properties, morphology and dynamic mechanical properties of PS/SBR have been studied with reference to the blend ratio. An increase in rubber content of the blend improves impact strength significantly by 36 % at 10 wt.% SBR content, while reducing tensile strength, Young's modulus, flexural strength and flexural modulus. The impact strength shows a maximum for 90/10 PS/SBR blend and therefore chosen for further studies. The rough surface of the SEM micrographs indicates a two phase morphology. The dynamic mechanical analysis reveals

that the storage modulus decreases with increasing rubber content. There is little change to the glass transition temperature of PS with the incorporation of SBR.

Dynamic vulcanisation of 90/10 PS/SBR blend using dicumyl peroxide improves the tensile strength, flexural strength, Young's modulus, flexural modulus and impact strength up to 2.1 meq of DCP content. The tensile strength and Young's modulus increased by 18 % and 17 % respectively, while the impact strength improved by 11 %. Therefore, 2.1 meq of DCP content was considered as the optimum value for dynamically vulcanised PS/SBR blend. Dynamic mechanical studies reveal that the storage modulus is the highest for blends dynamically vulcanised with 2.1 meq of DCP compared to the other blends. The improvement in mechanical properties suggest that dynamic vulcanisation can be considered as a means of technological compatibility.

#### **4A.5 References**

- [1] Bucknall CB. In: Polymer Blends. Paul DR, Newman S editors. New York: Academic Press; 1978, Vol.2.
- [2] Wu S. Polymer 1985; 26:1855.
- [3] Piorkowska E, Argon AS, Cohen RE. Polymer 1993; 34:4435.
- [4] Ohishi H, Ikehara T, Nishi T. J Appl Polym Sci 2001; 80:2347.
- [5] Ramsteiner F, Heckmann W, Mackee GE, Breulmann M. Polymer 2002; 43:5995.
- [6] Bucknall CB. Toughened Plastics. London: Applied Science; 1977.
- [7] Schnedier M, Pith T, Lambla M. J Mater Sci 1997; 32:5191.
- [8] Liu NC, Baker WE. Polym Eng Sci 2004; 32:1695.

- [9] Zhang Q, Yang H, Fu Q. *Polymer* 2004; 45:1913.
- [10] Feng W, Isayeu AI. *Polymer* 2004; 45:1207.
- [11] Nicolini A, De Campos Rocha TLA, Marly AM. *J Elast Plast* 2009; 41:433.
- [12] Naskar K, Noordermeer JWM. *J Elast Plast* 2006; 38:163.
- [13] Wang Z, Zhao H, Zhao J, Wang X. *J Appl Polym Sci* 2010; 117:2523.
- [14] Thitithammawong A, Nakason C, Sahakaro K, Noordermeer J. *Polym Test* 2007; 26:537.
- [15] Ismail H, Mohamad Z, Bakar AA. *Iranian Polymer Journal* 2004; 13:11.
- [16] Sabet A, Patel R. *Rubb Chem Technol* 1997; 64:769.
- [17] Pukanszky B, Tudos F, Kallo A, Badar G. *Polymer* 1989; 30:1407.
- [18] Ismail H, Nasaruddin MN, Ishiaku US. *Polym Test* 1999; 18:287.
- [19] Ismail H, Nizam JM, Abdul Khalil HPS. *Polym Test* 2001, 20:125.
- [20] Ismail H, Mega L. *Polym Plast Technol Eng* 2001, 40:463.
- [21] Tangboriboonrat P, Tiyaipiboonchaiya C. *J Appl Polym Sci* 1999; 71:1333.

## Part B

### EFFECT OF SHORT NYLON-6 FIBRE- UNMODIFIED AND RFL-COATED

**4B.1 Introduction**

**4B.2 Experimental**

**4B.3 Results and Discussions**

**4B.4 Conclusions**

**4B.5 References**

#### 4B.1 Introduction

Rubber-toughening is used to improve the impact properties and low temperature toughness of brittle polymers [1-3]. However, the incorporation of soft rubber particles into a stiffer polymer matrix necessarily results in the loss of stiffness and strength. Incorporation of high aspect ratio rigid fillers such as high modulus fibres into a polymer matrix improves stiffness and strength [4]. By careful selection of fillers/fibres, the material costs can be substantially reduced. The mechanical performance of composites is mainly dependent upon the properties of the matrix and reinforcement and the interaction between the matrix and fibres [5]. Many researchers reported the use of various short fibres on the mechanical, thermal, rheological and morphological characteristics of thermoplastics [6,7] and elastomers [8,9].

The effect of short glass fibres on the mechanical properties and morphology of PP/EPDM have been reported by Weizhi *et al.* [10]. The tensile and impact properties of Nylon-6/MA-g-EPR reinforced by glass fibre were examined by Laura *et al.* [11]. The mechanical properties of glass fibre reinforced PP/SBS composite were studied by Saujanya *et al.* [12].

Arroyo *et al.* [13] have explored the reinforcing effect of short aramid fibre in PP/EPDM blends. Gautam *et al.* [14] have investigated the dynamic mechanical and thermal properties of PE/EPDM based jute fibre composites. The effect of PET fibres on the mechanical properties of PP/EOC blend has been investigated by Lopez-Manchado *et al.* [15]. Goharpey *et al.* [16] have reported the influence of short cellulose fibre on the microstructure, rheological and mechanical properties of EPDM/PP TPVs. Anuar *et al.* [17] have reported the improvement in mechanical properties of TPNR and PP/EPDM blends using kenaf fibre.

Nylon fibres have become important materials due to the fibre's excellent mechanical, physical and chemical properties. Physico-mechanical properties of EPDM/Nylon-6 short fibre composite was studied by Wazzan [18]. Seema *et al.* [19,20] have investigated the mechanical properties of short Nylon fibre reinforced NBR and CR composite containing epoxy based bonding agent. Sreeja *et al.* [21,22] studied the effect of short Nylon-6 fibres on the mechanical properties of NR/reclaimed rubber and NBR/reclaimed rubber blends. Mechanical properties of short Nylon fibre reinforced SBR/NR composites were studied in detail by Ma *et al.* [23]. Short Nylon fibre-reinforced polypropylene composites [24] and recyclable high density polyethylene composites [25] were studied by Thomas *et al.*

Interfacial bond is known to play an important role in short fibre composites since this interface is critical in transferring the load from the matrix to the fibre. RFL-coated Nylon fibres are used as reinforcing items for tyres, where it bonds successfully to the rubber compound. The effect of RFL-treatment on aramid fibres in Twaron-ENR composites has been reported by Ahmad *et al.* [26]. The effect of RFL-treated aramid fibre on



metallocene catalysed thermoplastic elastomer ethylene-octene copolymer (EOC) has been investigated by Shibulal *et al.* [27]. Ishak *et al.* [28] have reported the influence of RFL-treated aramid fibre and MA-g-PE compatibiliser on the mechanical properties of TPNR. Hanafi *et al.* [29] has studied the effect of rice husk powder in unvulcanised and dynamically vulcanised PS/SBR blends. They also compared the effect of filler loading with PS/SBR/silica composites [30].

However, no systematic attempt has been made to evaluate the use of Nylon fibres as a reinforcing fibre for PS/SBR blends. This part explores the effect of short Nylon-6 fibres- unmodified and RFL-coated on the mechanical properties, morphology and dynamic mechanical properties of styrene-butadiene rubber-toughened polystyrene.

## 4B.2 Experimental

Table 4B.1 gives the ingredients of the composites used for the study. Details regarding the preparation of the composites and evaluation of the mechanical properties are given in Chapter 2.

**Table 4B.1 Composition of the composites.**

Composition	Mix No.								
	B0	B1	B2	B3	B4	B5	B6	B7	B8
PS	90	90	90	90	90	90	90	90	90
SBR	10	10	10	10	10	10	10	10	10
Unmodified N 6 fibre [F(U)] wt. %	0	0.5	1	2	3	-	-	-	-
RFL-coated N 6 fibre [F(R)] wt. %	-	-	-	-	-	0.5	1	2	3

## 4B.3 Results and Discussion

### 4B.3.1 Mechanical properties

Plots of tensile strength and Young's modulus of the composites containing unmodified and RFL-coated Nylon fibre as a function of fibre loading are shown in Figures 4B.1 and 4B.2, respectively. The fibre loading is varied from 0 to 3 wt.%. In the case of unmodified fibre composites, there is only a marginal increase of tensile strength at 0.5 wt.% fibre content after which it continuously drops up to 3 wt.%. A similar trend is observed with RFL-coated fibre composites. However, at all fibre loadings the RFL-coated fibre composites show improved tensile strength when compared to the unmodified composites. The reduction in tensile strength at higher fibre loadings for both composites implies that fibres may act as stress raisers. The Young's modulus for RFL-coated fibre composites as shown in Figure 4B.2 shows an enhancement of about 13 % modulus at 1 wt.% fibre content and then decreases. While in the case of unmodified fibre composites, the modulus remains unchanged at 0.5 wt.% and then shows a significant increase of 12% at 1wt.% fibre content. With further increase in fibre loading, the modulus decreases.

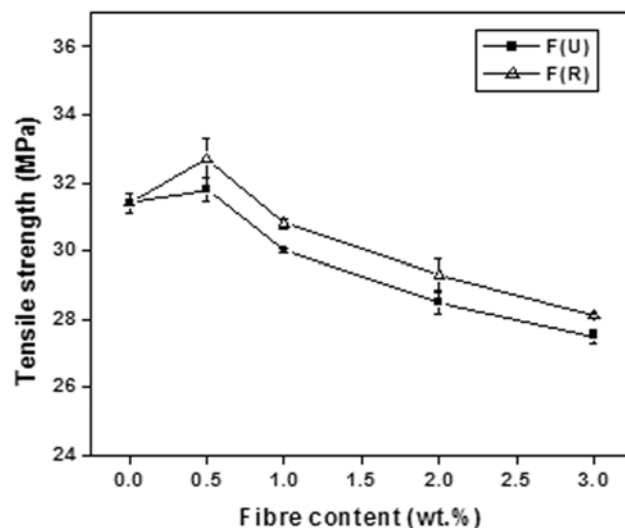


Figure 4B.1: Variation of tensile strength of 90/10 PS/SBR with fibre content.

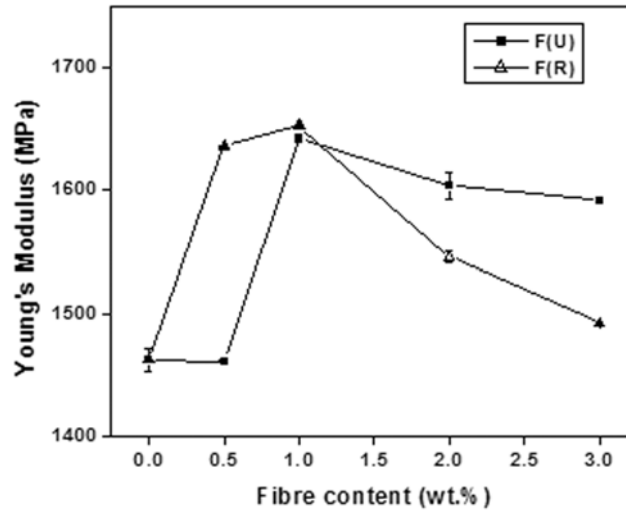


Figure 4B.2: Variation of Young's modulus of 90/10 PS/SBR with fibre content.

The variation of flexural strength of the composites with fibre loading is presented in Figure 4B.3. The flexural strength in the case of both composites increases at 1 wt.% fibre loading with a rise of about 7% and 10% for unmodified and RFL-coated fibre composites, respectively. Further incorporation of fibre reduces the flexural strength. Similar behaviour was observed with the flexural modulus as shown in Figure 4B.4. However, at all fibre loadings the flexural modulus is higher for RFL-coated fibre composites compared to the unmodified one. At 1 wt.% fibre loading, the flexural modulus is enhanced to 4% and 8% respectively, for unmodified and RFL-coated composites.

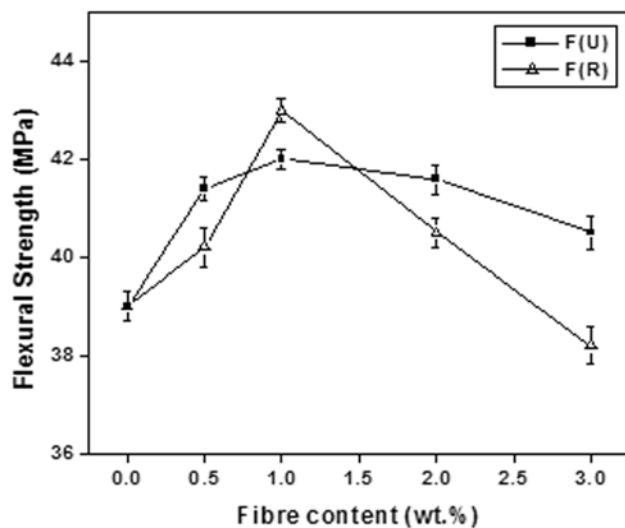


Figure 4B.3: Variation of flexural strength of 90/10 PS/SBR with fibre content.

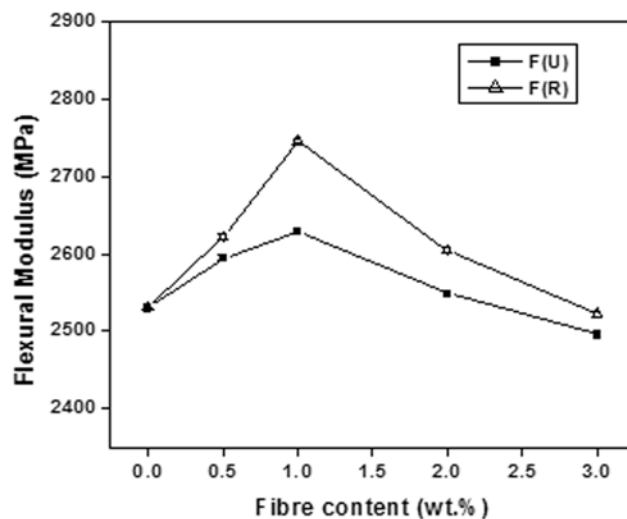
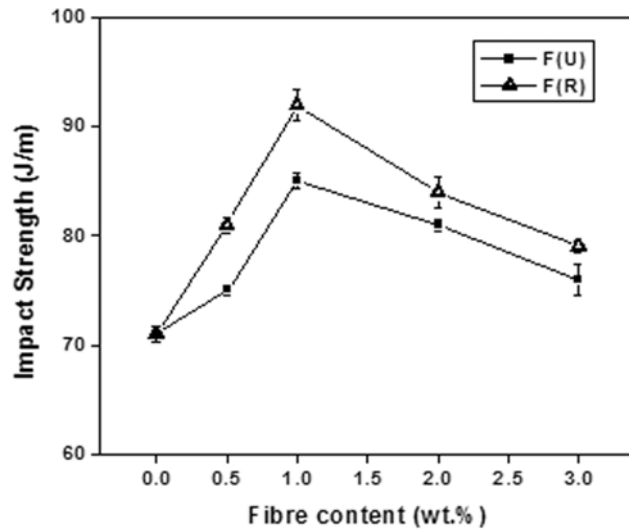


Figure 4B.4: Variation of flexural modulus of 90/10 PS/SBR with fibre content.



**Figure 4B.5: Variation of impact strength of 90/10 PS/SBR with fibre content.**

The effect of fibre loading- unmodified and RFL-coated, on the impact strength of 90/10 PS/SBR composites is presented in Figure 4B.5. The impact strength in the case of both fibres, increases at 1 wt.% fibre loading and then falls. There is an enhancement of 19 % and 29 % with unmodified and RFL-coated fibre composites, respectively in comparison to the unreinforced blend. Major microfailure mechanisms include initiation and propagation of matrix cracking, fibre-matrix debonding, fibre breakage and fibre pull-out. The stress concentration around the fibre ends at higher fibre loading tends to reduce the impact strength.

### 4B.3.2 Morphology

The micrographs of tensile fractured surface of 90/10 PS/SBR composites containing unmodified fibres at a loading of 1 and 3 wt.% are presented in Figures 4B.6(a) and (b) respectively. While Figures (c) and (d) represents the

composites containing RFL-coated fibres at 1 and 3 wt.% fibre content. In both the composites, the matrix surface shows homogeneous crazes. Holes due to fibre pull outs and fibres protruding from the matrix can be seen. At higher fibre loading as shown in Figures (b) and (d), fibre breakage can also be seen in addition to fibre pull out.

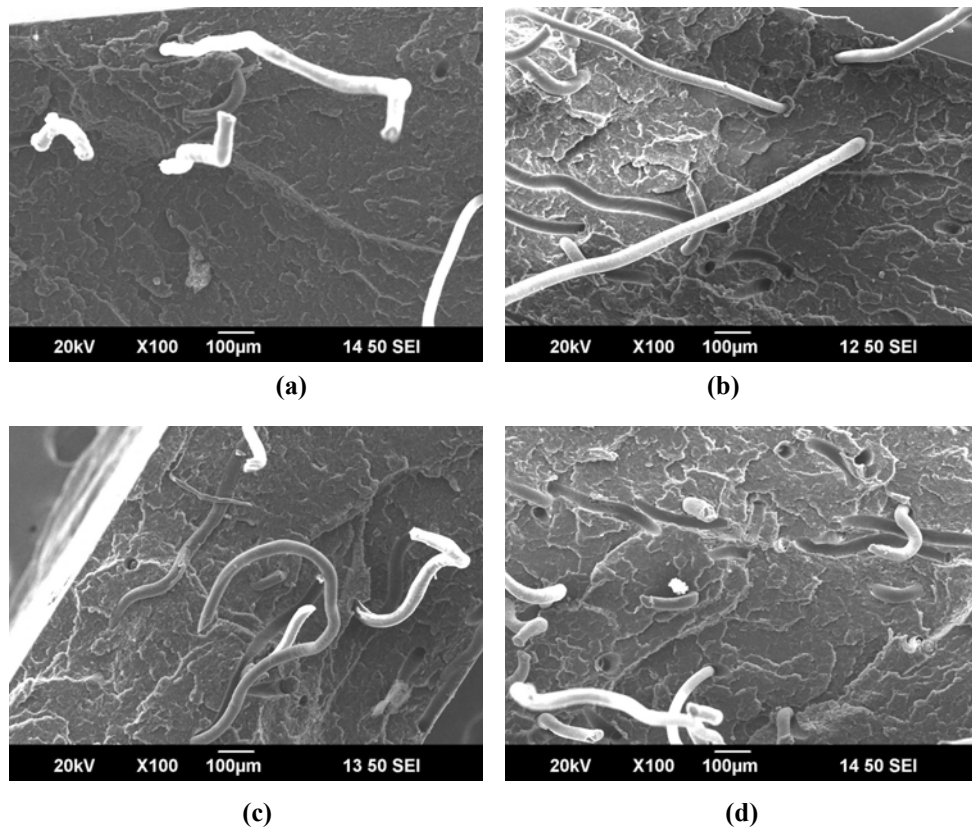


**Figure 4B.6: Scanning electron micrographs of 90/10 PS/SBR composites with unmodified Nylon fibres (a) 1 wt.% (b) 3 wt.% (x 100 magnification) and with RFL-coated Nylon fibres (c) 1 wt.% and (d) 3 wt.% (x 100 magnification).**

### 4B.3.3 Dynamic Mechanical Analysis

The variation of storage modulus of the composites at different loadings of unmodified and RFL-coated fibre as a function of temperature is graphically

represented in Figures 4B.7 and 4B.8, respectively. With unmodified fibres, the storage modulus up to 1 wt.% remains identical to the unreinforced blend throughout the whole temperature range. The storage modulus at 2 and 3 wt.% fibre content gives higher modulus at low temperatures compared to the modulus at low fibre contents.

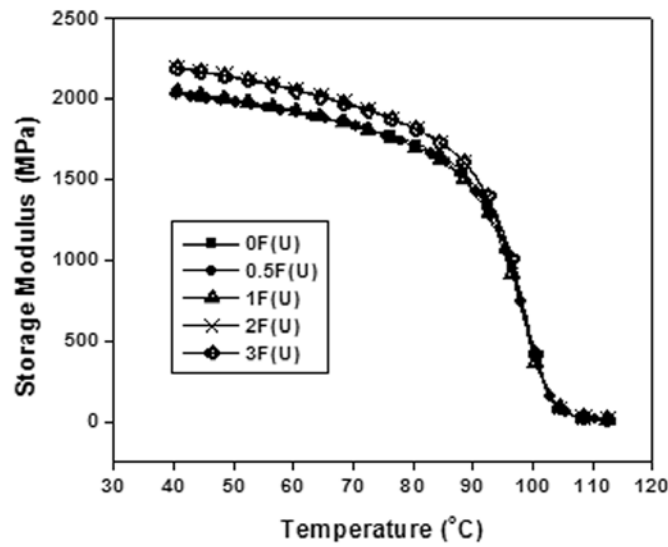


**Figure 4B.7:** Storage modulus vs. temperature plots of 90/10 PS/SBR composites with varying (unmodified) fibre content.

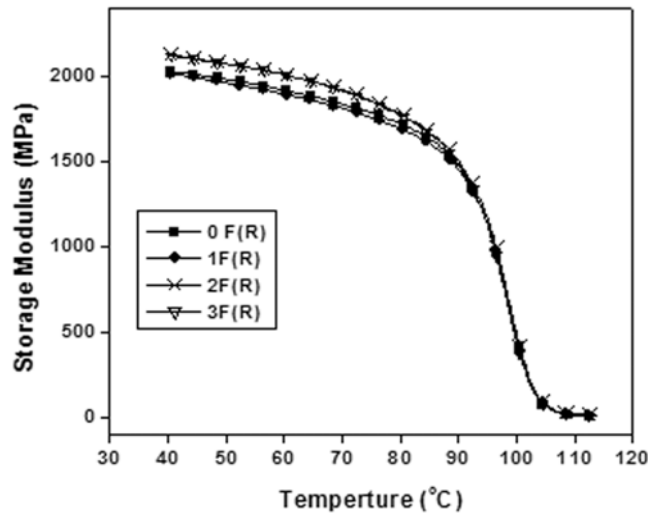


**Figure 4B.8: Storage modulus vs. temperature plots of 90/10 PS/SBR composites with varying (RFL-coated) fibre content.**

Both show identical values throughout the temperature regime. In the case of RFL-coated fibre composites as shown in Figure 4B.8, the trend is similar to that of unmodified composites. As the temperature approaches the glass transition, the storage modulus remains the same for all the composites.

The storage modulus of the composites at 60 °C as a function of fibre loading is presented in Figures 4B.9. It can be seen that in both unmodified fibre and RFL-coated fibre composites, the storage modulus enhances at 2 wt.% fibre content and then remains unchanged with further increase in fibre content. The increase may be due to the increase in stiffness of the matrix imparted by the fibres. However at all fibre loadings, the storage modulus of unmodified fibre composites are higher than the RFL-coated one.

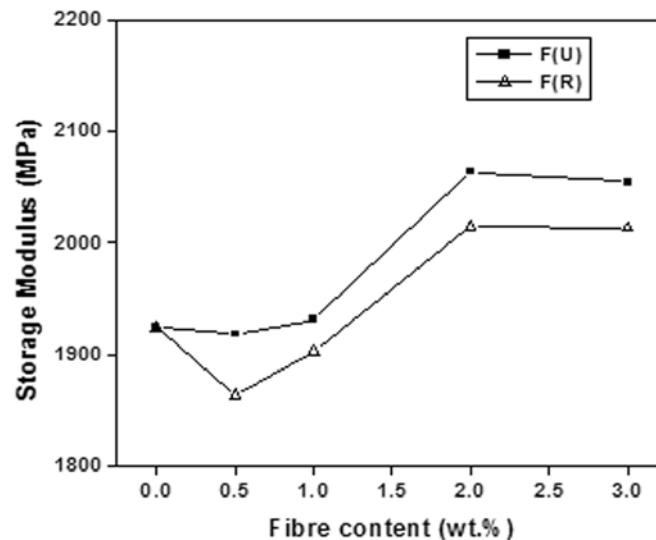


**Figure 4B.9: Variation of storage modulus at 60 °C of 90/10 PS/SBR with fibre content.**



The variation of loss modulus with temperature of unmodified and RFL-coated fibre composites are shown in Figure 4B.10 and 4B.11, respectively. In the case of unmodified fibre composites, the loss modulus peak corresponding to the  $T_g$  increases marginally above 1 wt.% fibre loading.

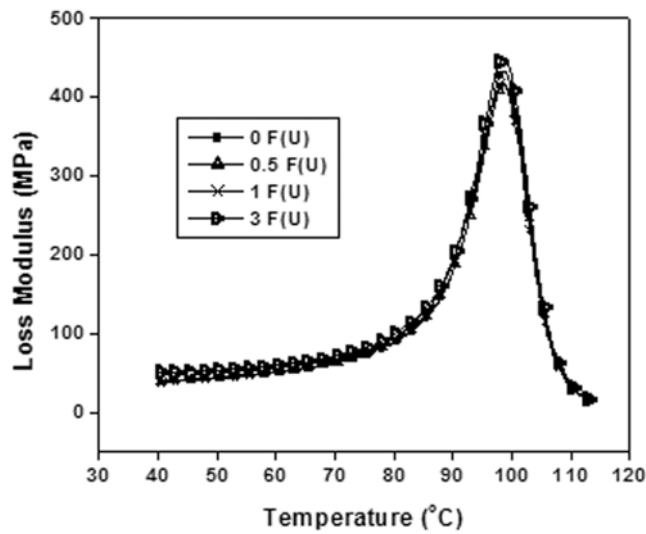


**Figure 4B.10:** Loss modulus vs. temperature plots of 90/10 PS/SBR composites with varying (unmodified) fibre content.

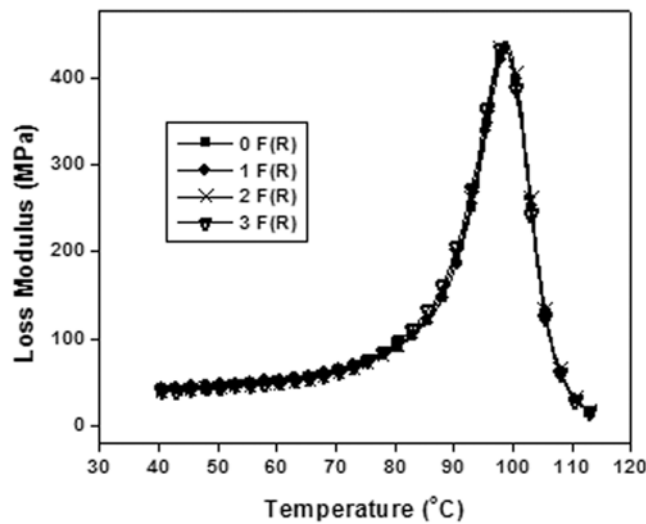


**Figure 4B.11:** Loss modulus vs. temperature plots of 90/10 PS/SBR composites with varying (RFL-coated) fibre content.

The loss modulus values of all the composites above and below  $T_g$  are almost identical to the unreinforced blends. With RFL-coated fibre composites, at all fibre loadings, the loss modulus value remains unchanged in comparison to the unreinforced blend.

The variation of  $\tan \delta$  with temperature of unmodified and RFL-coated fibre composites is presented in Figures 4B.12 and 4B.13, respectively. It is clear from Figure 4B.12 that the  $\tan \delta$  peak decreases at 1 wt.% unmodified fibre content and there is only a marginal shift in the  $T_g$ . With RFL-coated fibre composites, in comparison to the unreinforced blend, the composites show a decreased magnitude in  $\tan \delta$  peak. The lowest magnitude is exhibited by 2 wt.% fibre content.

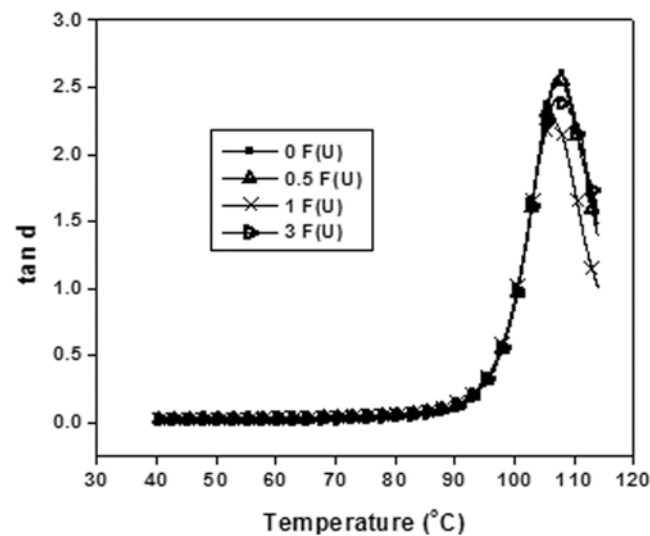


**Figure 4B.12:**  $\tan \delta$  vs. temperature plots of 90/10 PS/SBR composites with varying (unmodified) fibre content.

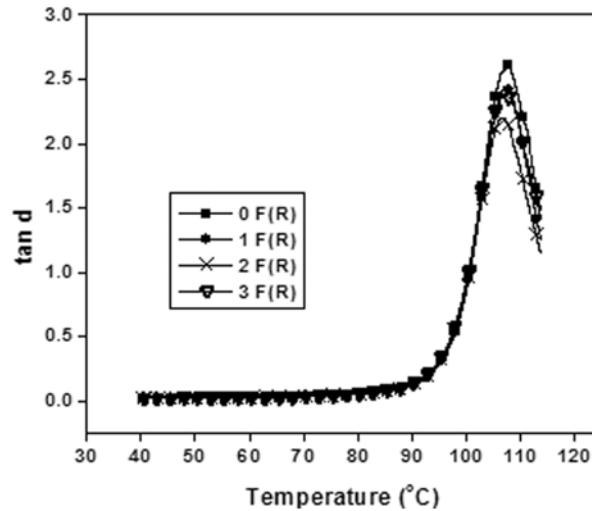


**Figure 4B.13:** Tan  $\delta$  vs. temperature plots of 90/10 PS/SBR composites with varying (RFL-coated) fibre content.

#### 4B.4 Conclusions

Short Nylon-6 fibres and RFL-coated fibres can improve the properties of 90/10 PS/SBR blends. The tensile modulus, flexural strength, flexural modulus and impact strength improve with 1 wt.% fibre loading in both unmodified and RFL-coated fibre composites. The tensile strength is only marginally reduced at 1 wt.% fibre content. The Young's modulus and impact strength improved by 12 % and 19 % for unmodified fibre composites. Further incorporation of fibre content reduces the mechanical properties in both composites.

The dynamic mechanical studies of unmodified Nylon fibre composites show that the storage modulus at 60 °C remains unchanged for 1 wt.% fibre content and increases for higher fibre content. The tan  $\delta$  peak is the lowest for 1 wt.% fibre content. Since the overall mechanical properties are better for 1 wt.% fibre content of unmodified fibre composites, this composition was selected for further studies.

In the case of RFL-coated fibre composites, dynamic mechanical studies reveal that the storage modulus at 60 °C for all fibre loadings are lower than that of unmodified fibre composites. The storage modulus at 1wt.% fibre content marginally decreases in comparison to unreinforced blends. The  $\tan \delta$  peak reduces marginally at 1 wt.% fibre content.

#### 4B.5 References

- [1] Paul DR, Bucknall CB, editors. Polymer blends: formulations and performance. New York: Wiley; 2000.
- [2] Paul DR, Newman S, editors. Polymer blends. New York: Academic Press; 1978.
- [3] Collyer AA, editor. Rubber toughened engineering plastics. London: Chapman & Hall; 1994.
- [4] Krenchel H. Fibre reinforcement. Copenhagen: Akademisk Forlag; 1964.
- [5] Sreekala MS, George J, Kumaran MG, Thomas S. Composites Science and Technology 2002; 62:339.
- [6] Fu SY, Lauke B. Compos Sci Tech 1996; 56:1179.
- [7] Nair KCM, Kumar RP, Thomas S, Schit SC, Ramamurthy K. Composites: Part A 2000; 31:1231.
- [8] Kashani MR. J Appl Poly Sci 2009; 113:1355.
- [9] Rajeev RS, Bhowmick AK, De SK. Polym Compos 2002; 23:574.
- [10] Weizhi W, Longxiang T, Qu B. Euro Polym J 2003; 39:2129.
- [11] Laura DM, Keskkula H, Barlow JW, Paul DR. Polymer 2000; 41:7165.
- [12] Saujanya C, Radhakrishnan S. Polym Comp 2001; 22:232.
- [13] Arroyo M, Zitzumbo R, Avalos F. Polymer 2000; 41:6351.
- [14] Gautam S, Arup C. J Appl Polym Sci 2008; 108:3442.

- [15] Lopez Manchado MA, Arroyo M. *Polymer* 2001; 42:6557.
- [16] Goharpey F, Mirzadeh A, Sheikh A, Nazockdast H, Katbab AA; *Polym Comp* 2009; 30:182.
- [17] Anuar H, Zuraida A. *Composites: Part B* 2011; 42:462.
- [18] Wazzan AA. *Int J Polymer Mater* 2004; 53:59.
- [19] Seema A, Kutty SKN. *J Appl Polym Sci* 2006; 99:532.
- [20] Seema A, Kutty SKN. *Polym Plast Technol Eng* 2005; 44:1139.
- [21] Sreeja TD, Kutty SKN. *Polym Plast Technol Eng* 2003; 42:239.
- [22] Sreeja TD, Kutty SKN. *Int J Polym Mater* 2003; 52:175.
- [23] Ma Peiyu, Zhao Jan, Tang J, Dai G. *Guofenzi Cailiao Kexue Yu Gongcheng* 1994; 10:55.
- [24] Thomas N Abraham, George KE. *Polym Plast Technol Eng* 2007; 46:321.
- [25] Thomas N Abraham, George KE. *Plast Rub Comp* 2005; 34:196.
- [26] Ahamad I, Chin TS, Cheong CK, Jalar A, Abdullah I. *Compos, Am J Appl Sci Special Issue* 2005;14.
- [27] Shibulal GS, Naskar K. *J Polm Res* 2011, 18:2295.
- [28] Ishak A, Yong PY, Ibrahim A. *Polym Compos* 2006; 27:395.
- [29] Hanafi I, Zurina M, Bakar AA. *Iranian Polymer Journal* 2004; 13:11.
- [30] Hanafi I, Zurina M, Bakar AA. *Polym-Plast Technol Eng* 2003; 42:81.

## Part C

# EFFECT OF SURFACE MODIFICATION OF FIBRE AND USE OF A COMPATIBILISER.

### 4C.1 Introduction

### 4C.2 Experimental

### 4C.3 Results and Discussions

### 4C.4 Conclusions

### 4C.5 References

## 4C.1 Introduction

Many reports have been published on the use of various short fibres for improving mechanical, thermal, rheological and morphological characteristics of thermoplastics [1,2] and elastomers [3,4]. It was first proposed by O'Connor and Goettler *et al.* [5] that the reinforcement by short fibres in a polymer matrix depends on the parameters like fibre content, length to diameter ratio of the fibre (aspect ratio), fibre orientation in the matrix and interfacial adhesion between the fibre and the matrix. To improve the interfacial adhesion between polar fibre and non-polar matrix, various methods such as incorporation of coupling agents [6], use of ionomer matrix [7,8], chemical [9,10] and plasma treatments [11-14] of fibre surface has been reported. Hydrolysis was reportedly one of the chemical treatment, allowing simple and easy modification of Kevlar surface [12,15].

The influence of MAPP as compatibiliser in jute fibre–PP composites was reported by Rana *et al.* [16]. Paunikallio *et al.* [17] have studied the effect of MAPP in polypropylene-viscose fibre composites. Smitha *et al.* [18] have studied the effectiveness of MA-g-PP as coupling agents in sisal fibre-propylene composites. Shibulal *et al.* [19] have investigated the influence of

MA-g-PB in aramid fibre reinforced ethylene-octene copolymer composites. The effect of MAPP as coupling agent in kenaf fibre reinforced TPNR and PP/EPDM composites has been reported by Anuar *et al.* [20]. Amornsakchai *et al.* [21] have investigated the influence of partially hydrolysed Conex short fibres and the use of a reactive compatibiliser (MA-g-SEBS) in SEBS thermoplastic elastomer. The effect of partially hydrolysed Kevlar fibre in conjunction with a compatibiliser (MA-g-PP) on Santoprene, a polyolefin based thermoplastic elastomer was studied by Saikrasun *et al.* [22]. However, no serious attempt has been made to modify Nylon fibre surface by hydrolysis and evaluate its use in conjunction with a compatibiliser in PS/SBR blends.

This part evaluates the mechanical properties, morphology and dynamical mechanical properties of PS/SBR composites using surface treated Nylon-6 fibres and MA-g-PS as compatibiliser.

## 4C.2 Experimental

The formulation of the composites used for the study is given in Table 4C.1. Details of the surface treatment of fibre, preparation of the composites and determination of the mechanical properties are given in Chapter 2.

**Table 4C.1 Composition of the composites.**

Composition	Mix No.									
	C0	C1	C2	C3	C4	C5	C6	C7	C8	C9
PS*	90	90	90	90	90	90	90	90	90	90
SBR*	10	10	10	10	10	10	10	10	10	10
Untreated N6 fibre [F(U)] wt.%	1	1	1	1	1					
Treated N6 fibre [F(T)] wt.%						1	1	1	1	1
MA-g-PS wt.(%)	0	0.5	0.75	1	2	0	0.5	0.75	1	2

\*parts per hundred polymer (php)

### **4C.3 Results and Discussion**

Preparation of maleic anhydride grafted polystyrene (MA-g-PS) and its characterisation are given in Chapter 2 and Chapter 3 (Part C), respectively.

It was expected that the hydrolysis of the Nylon fibre surface will release amine groups, which can react with MA groups of the compatibiliser added to form covalent bonds, thus increasing the compatibiliser efficiency.

#### **4C.3.1 Mechanical properties**

Figures 4C.1 and 4C.2 illustrate the effect of MA-g-PS content on the tensile properties of the composites containing 1 wt.% of untreated and surface treated Nylon fibres. It can be found from Figure 4C.1 that the use of MA-g-PS has a positive effect in improving the tensile strength of both untreated and treated fibre composites. The lower tensile strength in the case of treated fibre composite in the absence of compatibiliser is due to the increased polarity of the fibre surface resulting from hydrolysis. The untreated and treated fibre composites gave a slight increase of about 9 % and 12 %, respectively in tensile strength at 0.5 wt.% MA-g-PS when compared to the corresponding composites without compatibiliser. With increasing MA-g-PS from 1 to 2 wt.%, the tensile strength decreases for both treated and untreated fibre composites. This may be attributed to the migration of excess MA-g-PS, causing self-entanglement among themselves rather than with the PS molecules, resulting in slippage [16,18]. However, a fairly higher magnitude of tensile strength is obtained for untreated fibre composites with 0.5 wt.% MA-g-PS in comparison to the treated fibre composites under similar conditions.



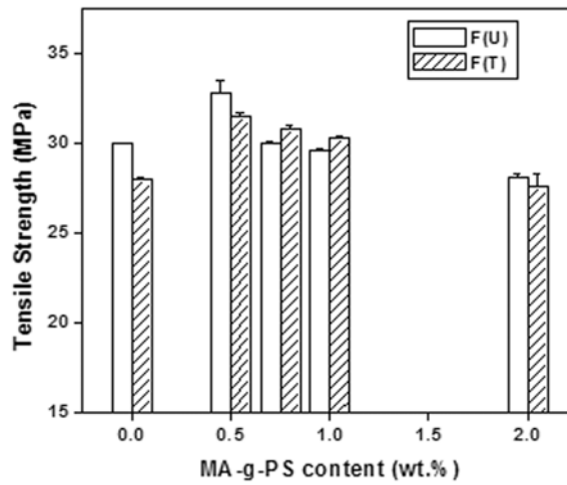


**Figure 4C.1: Variation of MA-g-PS on the tensile strength of composites with 1 wt.% fibre.**

The effect of MA-g-PS on the Young's modulus of both untreated and treated fibre composites as presented in Figure 4C.2 shows a behaviour similar to the tensile strength. The increase in modulus is about 9 % and 12 %, respectively at 0.5 wt.% MA-g-PS for both untreated and treated fibre composite.

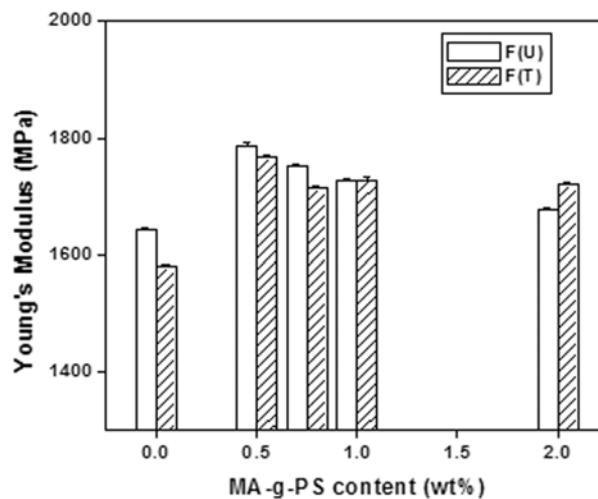


**Figure 4C.2: Variation of MA-g-PS on the Young's modulus of composites with 1 wt.% fibre.**

The effect of MA-g-PS on the flexural strength of composites containing untreated and treated fibres is shown in Figure 4C.3. It is clear from the figure that the flexural strength of the untreated fibre composites remains unchanged with the addition of MA-g-PS. Whereas there is an improvement in flexural strength of about 7 % for treated fibre composites at 0.5 wt.% of compatibiliser in comparison to the treated fibre composites without compatibiliser.

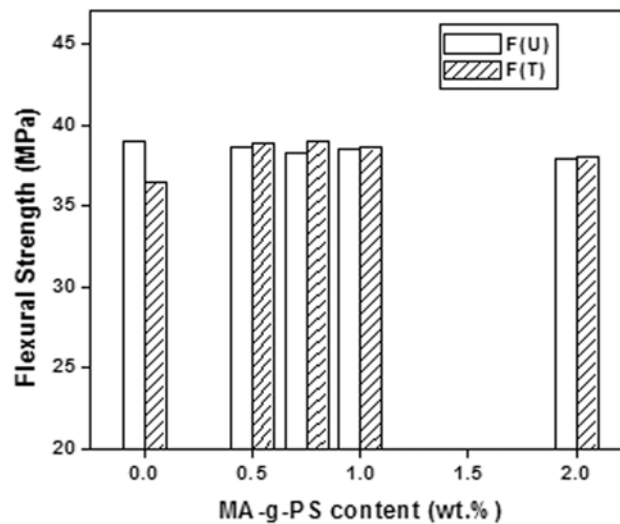


**Figure 4C.3: Variation of MA-g-PS on the flexural strength of composites with 1 wt.% fibre.**

The flexural modulus in Figure 4C.4 shows a marginal increase of 3 % and 4 % respectively, at 0.5 wt.% MA-g-PS for the composites containing untreated and treated fibre. Higher amounts of MA-g-PS in both composites results in deterioration of the flexural modulus.

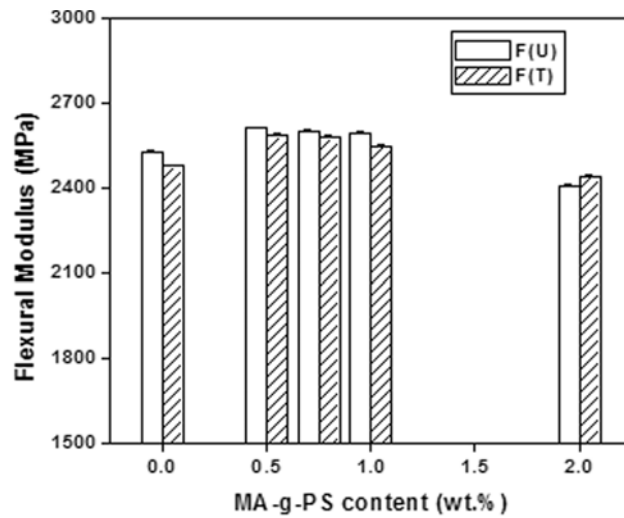


**Figure 4C.4: Variation of MA-g-PS on the flexural modulus of composites with 1 wt.% fibre.**

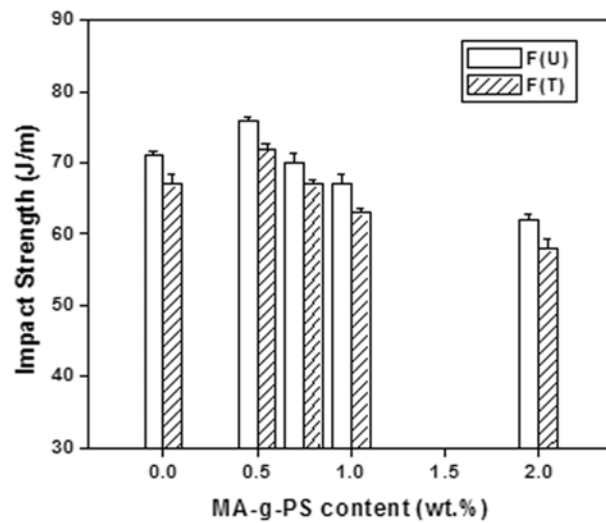


**Figure 4C.5: Variation of MA-g-PS on the impact strength of composites with 1 wt.% fibre.**

The effect of compatibiliser on the impact strength of 90/10/1 PS/SBR/Nylon fibre composites containing untreated and treated fibres is shown in Figure 4C.5. It is clear from the figure that there is only a marginal increase (7 %) in the impact strength at about 0.5 wt.% of compatibiliser

loading for both the composites. The impact strength decreases at higher concentrations of the compatibiliser. It may be due to the fact that the dispersed MA-g-PS domains act as stress concentrators which are not capable of absorbing the impact energy [23].

#### **4C.3.2 Morphology**

The morphology of the tensile fractured surfaces of composites at 1 wt.% fibre loading containing (a) untreated fibre and (b) treated fibre, with 0.5 wt.% MA-g-PS are illustrated in Figure 4C.6. In the case of untreated fibres with 0.5 wt.% MA-g-PS, as shown in Figure (a), fibres protruding from the matrix and holes due to fibres pull-out could be observed. Whereas with treated fibres as given in Figure (b), fibre breakage, fibre pull outs as well as small portions of matrix adhered on the fibres could be seen. This implies that the interfacial adhesion is better in the presence of treated fibres which results in a greater improvement in tensile strength.

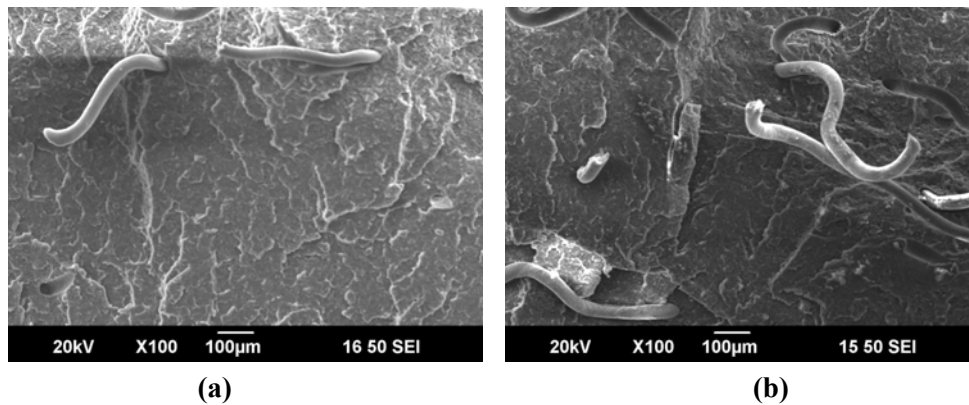


**Figure 4C.6: Scanning electron micrographs of 90/10 PS/SBR composites with 1 wt.% of Nylon fibres (a) untreated and (b) treated at 0.5 wt.% MA-g-PS.**

### 4C.3.3 Dynamic Mechanical Analysis

The variation in storage modulus, loss modulus and  $\tan \delta$  with respect to temperature of PS/SBR/Nylon fibre composites with untreated and treated fibres containing 0.5 wt.% compatibiliser (MA-g-PS) can be seen in Figures 4C.7 to 4C.9. It can be seen from Figure 4C.7 that the storage modulus at room temperature is higher for untreated fibre composites in the presence of compatibiliser in comparison to the treated fibre composites with compatibiliser and untreated fibre composites. The sharp drop in modulus at around 95 °C is in the glass transition region which is almost identical for all the composites.

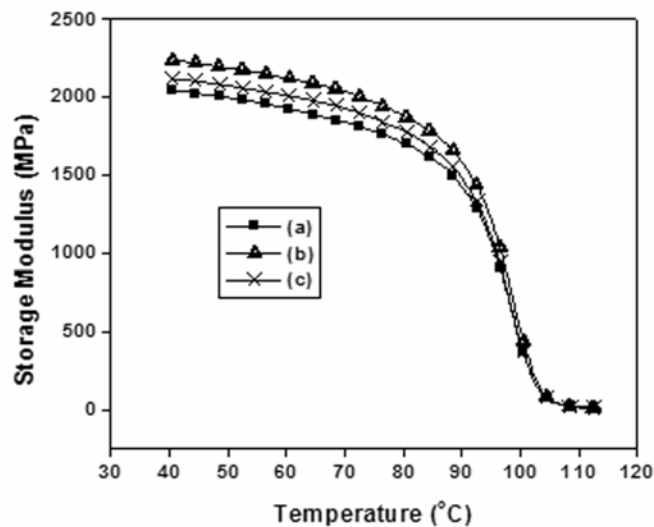


**Figure 4C.7: Storage modulus vs. temperature plots of composites containing (a) untreated fibre (b) untreated fibre with compatibiliser (0.5 wt.%) and (c) treated fibre with compatibiliser (0.5 wt.%).**

Figure 4C.8 shows the loss modulus for the different composites with variation of temperature. The rapid rise in loss modulus indicates an increase in the structural mobility of the polymer, a relaxation process that

permits motions along larger portions of the individual polymer chains than would be possible below the  $T_g$ . The primary transition, that is,  $T_g$  remains unchanged for all the composites. However, the loss modulus peak increases for untreated fibre composites in the presence of compatibiliser in comparison to both the treated fibre composites containing compatibiliser and untreated fibre composites.

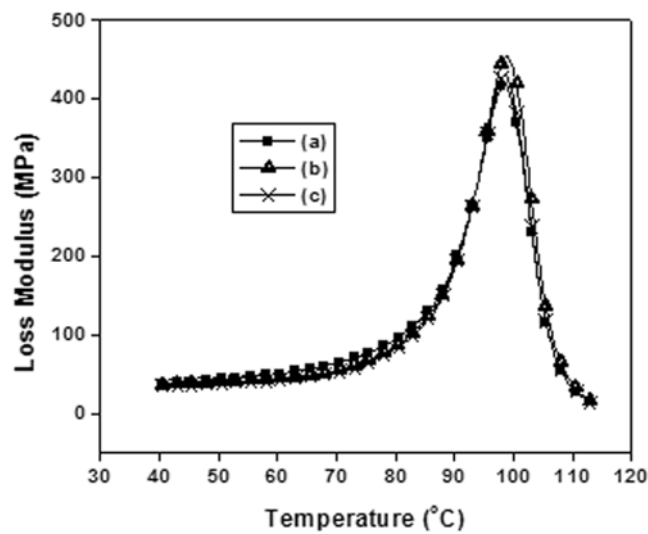


**Figure 4C.8: Loss modulus vs. temperature plots of composites containing (a) untreated fibre (b) untreated fibre with compatibiliser (0.5 wt.%) and (c) treated fibre with compatibiliser (0.5 wt.%).**

The variation of  $\tan \delta$  as a function of temperature is illustrated in Figure 4C.9. The damping peak in the untreated and treated fibre composite with compatibiliser shows an increase in the  $T_g$  region in comparison to the untreated composite. Very little change is observed to the location of glass transition, signifying that the presence of MA-g-PS and treated Nylon fibre does not influence the glass transition temperature of PS.

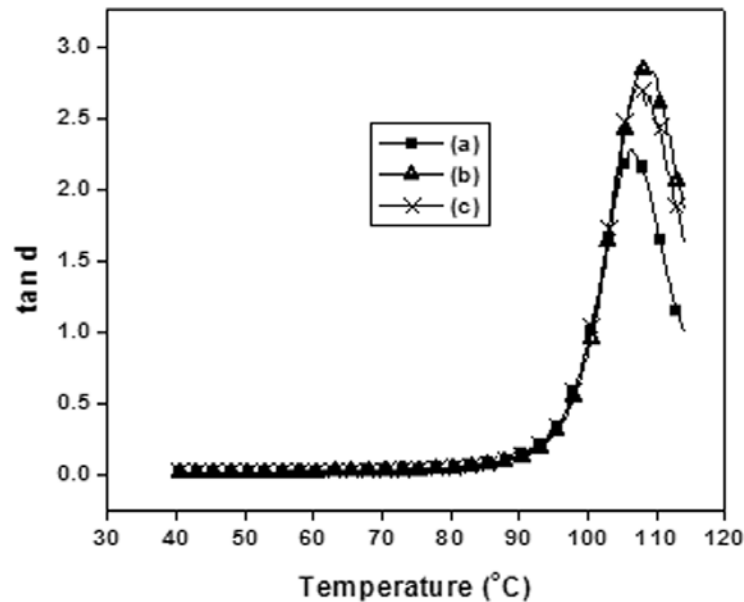


**Figure 4C.9:** Tan  $\delta$  vs. temperature plots of composites containing (a) untreated fibre (b) untreated fibre with compatibiliser (0.5 wt.%) and (c) treated fibre with compatibiliser (0.5 wt.%).

#### 4C.4 Conclusions

The use of 0.5 wt.% compatibiliser can improve the tensile properties, flexural properties and impact strength of untreated and treated fibre PS/SBR composites in comparison to the corresponding composites without compatibiliser. DMA reveals that the storage modulus at room temperature is higher for untreated composites with compatibiliser than the treated composites with compatibiliser and untreated composites.

#### 4C.5 References

- [1] Fu SY, Lauke B. *Compos Sci Tech* 1996; 56:1179.
- [2] Nair KCM, Kumar RP, Thomas S, Schit SC, Ramamurthy K. *Composites: Part A* 2000; 31:1231.

- [3] Kashani MR. *J Appl Poly Sci* 2009; 113:1355.
- [4] Rajeev RS, Bhowmick AK, De SK. *Polym Compos* 2002; 23:574.
- [5] O'Connor JE. *Rubber Chem Technol* 1977; 50:945.
- [6] Vaughan D. *Polym Eng Sci* 1978; 18:167.
- [7] Takayanagi M, Kajiyama T, Katayose T. *J Appl Polym Sci* 1982; 27:3903.
- [8] Takayanagi M, Katayose T. *Polym Eng Sci* 1984; 24:1047.
- [9] Andrepoulos AG. *J Appl Polym Sci* 1989; 38:1053.
- [10] Tarantili PA, Andrepoulos AG. *J Appl Polym Sci* 1997; 65:267.
- [11] Wang Q, Kaliaguine S, Ait-Kadi AJ. *J Appl Polym Sci* 1993; 48:121.
- [12] Yu Z, Ait-Kadi AJ, Brisson J. *Polym Eng Sci* 1991; 31:1222.
- [13] Sheu GS, Shyu SS. *J Adhesion Sci Technol* 1994; 8:1027.
- [14] Brown JR, Mathys Z. *J Mater Sci* 1997; 32:2599.
- [15] Garbassi F, Morra M, Occhiello E. *Polymer surfaces: from physics to technology*. Chichester: Wiley; 1994, p. 251.
- [16] Rana AK, Mandal A, Mitra BC, Jacobson R, Rowell R, Banerjee AN. *J Appl Polym Sci* 1998; 69:329.
- [17] Paunikaloi T, Kasanen J, Suvanto M, Pakkanen TT. *J Appl Polym Sci* 2003; 87:1895.
- [18] Smita M, Sushil KV, Sanjay KN, Sudhansu ST. *J Appl Polym Sci* 2004; 94:1336.
- [19] Shibulal GS, Naskar K. *J Polym Res* 2011; 18:2295.
- [20] Anuar H, Zuraida A. *Comp Part B* 2011; 42:462.
- [21] Amornsakchai T, Sinpatanapan B, Baulek-Limcharoen S, Meesiri W. *Polymer* 1999; 40:2993.
- [22] Saikrasun S, Amornsakchai T, Sirisinha C, Meesiri W, Baulek-Limcharoen S. *Polymer* 1999; 40:6437.



*Chapter -4*

---

[23] Hristov V, Krumova M, Michler G. *Macromol Mater Eng* 2006; 291:677.

.....

# **POLYSTYRENE/RECLAIMED RUBBER BLENDS**

## **Part A**

### **TOUGHENING OF POLYSTYRENE: EFFECT OF BLEND RATIO**

#### **5A.1 Introduction**

#### **5A.2 Experimental**

#### **5A.3 Results and Discussions**

#### **5A.4 Conclusions**

#### **5A.5 References**

#### **5A.1 Introduction**

The waste generated from rubber tyres is becoming a major environmental problem throughout the world. This problem is attributed to the huge volume of used tyres generated each year and the fact that tyres are thermoset. In addition, tyres are virtually resistant to biological degradation [1]. Scrap tyres will be unremittingly available and abundant as long as today's high requirement for the automobiles persist. The drawbacks underlying the disposal of waste rubbers by methods such as landfill, pyrolysis, and incineration encouraged further research on the

recycling technology. Recycle of the waste rubber is thus a great challenge for both environmental and economic reasons [2-7].

Several approaches have been proposed to deal with the problem of used tyres such as converting to tyre-derived fuel in solid-fuel burners, using pyrolysis to recover valuable chemical components [8], incorporation in various rubbers for non-tyre applications, and their use as fillers/tougheners in plastics [9]. Large scale utilisation of rubber waste could be made by incorporating waste rubber into plastics with a view to obtain impact-resistant plastics and thermoplastic elastomers. Generally, waste tyres are ground to small particles known as ground rubber tyre (GRT) [10-14], which are still thermosets. Incorporation of GRT, as a filler into virgin polymer matrices, such as natural rubber (NR) [15], styrene-butadiene rubber (SBR) [16], and low-density polyethylene (LDPE) [17-19], and preparation of thermoplastic elastomer blends based on GRT [7,20,21] are attractive routes for GRT recycling. However, this results usually in low mechanical strength because of the poor adhesion between the rubber particles and the polymer matrix.

Considerable attention has been given to utilising the reclaimed rubber prepared by different methods from scrap rubber from the tyre industry. Reclaiming scrap rubber by mechanical [22,23] and chemical processes [10,11] have received much attention. One process involves thermomechanical degradation of a rubber vulcanisate network [24]. Another process is cryomechanical comminution [25-28]. The chemical process for reclaiming rubber includes devulcanisation or destructive distillation [29]. Practically, reclaimed rubber has been used commercially for cost savings by blending with virgin natural rubber. Al-Malaika and Amir [30] found that

half of the natural rubber (NR) can be replaced by reclaimed rubber in a thermoplastic elastomer blend of NR/PP without adversely affecting the mechanical properties of the blend. Supawan *et al.* [31], have reported the toughening of PP using reclaimed rubber. Zhu *et al.* [32] have prepared thermoplastics elastomers from PP and reclaimed rubber. Nevatia *et al.* developed thermoplastic elastomeric compositions from reclaimed rubber and waste plastics [33]. Punnnarak *et al.* [34] have reported the preparation of reclaimed rubber/HDPE blends. However, the use of reclaimed rubber in a brittle plastic such as polystyrene has not been explored systematically. It is expected that polystyrene (PS) can be made tougher by blending it with reclaimed rubber. This part focuses on the toughening of polystyrene using reclaimed rubber (WTR) and evaluation of the mechanical properties, morphology and dynamical mechanical properties of the blend.

## 5A.2 Experimental

The details of the materials used is given in Chapter 2. PS/WTR blends were prepared by melt mixing in a Thermo Haake PolyLab QC. The rubber content in reclaimed rubber was taken into consideration while calculating total rubber content in the blend formulation. The formulations of the blend used are given in Table 5A.1.

**Table 5A.1. Blend Formulations**

Ingredients	Blend Ratio				
PS	100	95	90	85	80
WTR <sup>a</sup>	0(0)	11(5)	22(10)	33(15)	44(20)

<sup>a</sup> Values in the parentheses refer to the parts of the rubber hydrocarbon in WTR.

The melt mixed samples were compression moulded to 1 mm sheets, conditioned and then tested as discussed in Chapter 2.

## 5A.3 Results and Discussions

### 5A.3.1 Mechanical Properties

Figures 5A.1 and 5A.2 show the tensile strength and Young's modulus of various PS/WTR blends. It is observed that the tensile strength decreases from 36.6 MPa to 9.7 MPa as the WTR content is increased to 44 parts corresponding to a hydrocarbon content of 20 parts. PS is a brittle matrix owing to the bulky phenyl side group which restricts the segmental mobility to a great extent, giving rise to higher ultimate strength. In the blend form, the WTR gets distributed in the matrix with a result that the chain flexibility is increased. However, since the WTR is a recycled material, it has a long heat history and has inherently lower strength. This leads to a net reduction in the tensile strength of the blend with increasing WTR content. This trend is reflected in the case of Young's modulus as well (Figure 5A.2). Any rubbery material that goes between PS phases increases chain flexibility, reducing the overall stiffness of the matrix. The elastic nature of the WTR should, however, compensate for the brittleness of PS, as discussed later in this chapter.

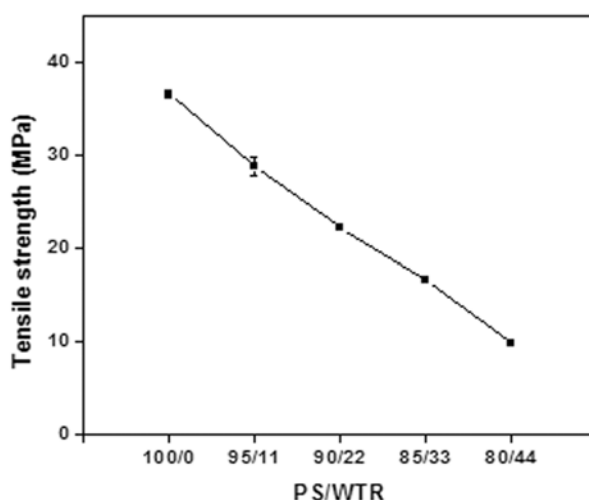


Figure 5A.1: Variation of tensile strength for various PS/WTR blends.

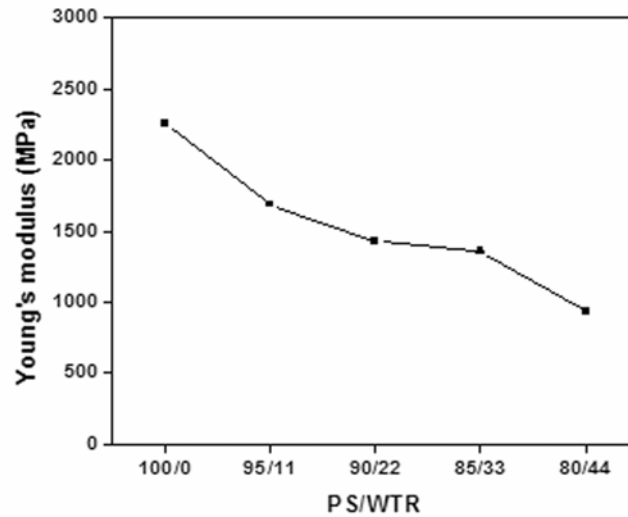


Figure 5A.2: Variation of Young's modulus for various PS/WTR blends.

The flexural properties of various ratios of PS/WTR blends are illustrated in Figures 5A.3 and 5A.4, respectively. As expected, the flexural strength and flexural modulus falls significantly with increase in rubber content, similar to the trend observed in the case of tensile properties.

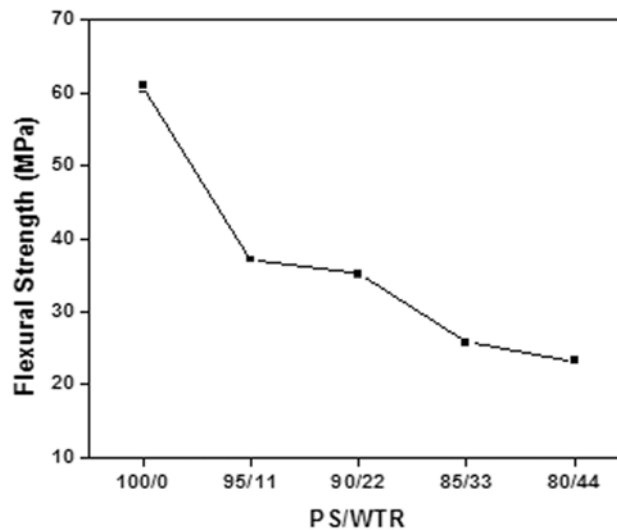
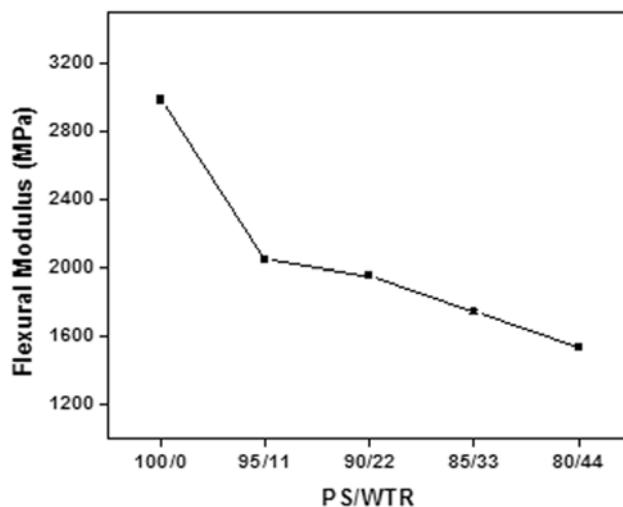


Figure 5A.3: Variation of flexural strength for various PS/WTR blends.



**Figure 5A.4: Variation of flexural modulus for various PS/WTR blends.**

Figure 5A.5 shows the impact strength of PS/WTR blend with various WTR content. The impact strength registers 17 % increase at a WTR loading of 22 wt.%, reaching a value of 61 J/m. The WTR remains as dispersed phase in a continuous PS phase, when the WTR content is lower [36]. Beyond a WTR content of 50 %, however, there can be phase inversion. These dispersed rubber phases can take up and dissipate energy under impact conditions. The yielding of rubber phase under impact loads reduces local stress build up. This helps to improve the toughness of the blends. Beyond an optimum WTR loading, the phase inversion begins to set in and the energy absorbing mechanism becomes less efficient. This is reflected as lower impact strength of the blends beyond 22 wt.% of WTR. Moreover, the presence of large amount of carbon black filler in the WTR also contributes a kind of dilution of the matrix.

It can be reasoned that the incorporation of a more brittle and rigid material, like carbon black in the PS matrix, can form a layer-like structure depending on the amount of carbon black in the blend. Thus at the critical

carbon black concentration, the PS/WTR blend can have a split in the layer structure providing a shorter path for fracture propagation, thereby causing the sudden decrease in impact strength. This phenomenon was previously discovered in some related works [21,31,35].

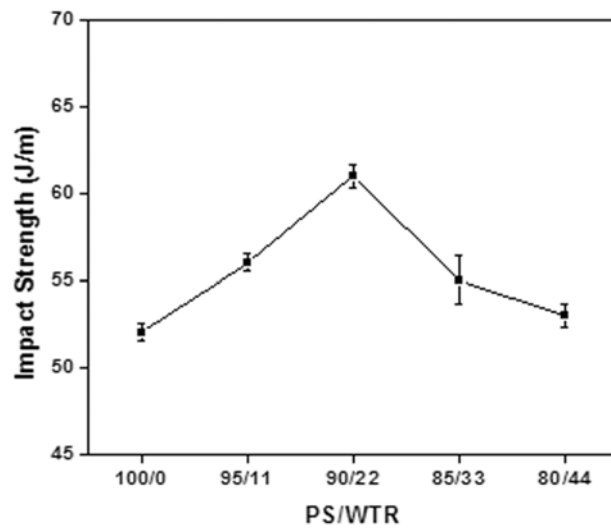


**Figure 5A.5: Variation of impact strength for various PS/WTR blends.**

### **5A.3.2 Morphology**

The SEM micrographs of tensile fractured surface of (a) PS, (b) 95/11, (c) 90/22, and (d) 80/44 of PS/WTR blends are shown in Figure 5A.6. With relatively lower WTR content, Figure (b) shows a fracture surface pattern typical of a brittle failure as in Figure (a). The multiple cracks originated at multiple points are seen spread across the whole surface. Radial propagation of multiple cracks from one origination point is clearly seen in this figure. It also shows a layered structure, indicating a failure occurring at different layers. In Figure 5(c), the failure pattern is similar to that in Figure (b). The crack edges are more elongated- a pattern more akin to a ductile kind of failure. This elongation is one route for dissipation of



energy which can be reflected as improved toughness. In Figure (d), the failure pattern again shows lower elongation of the crack edges.

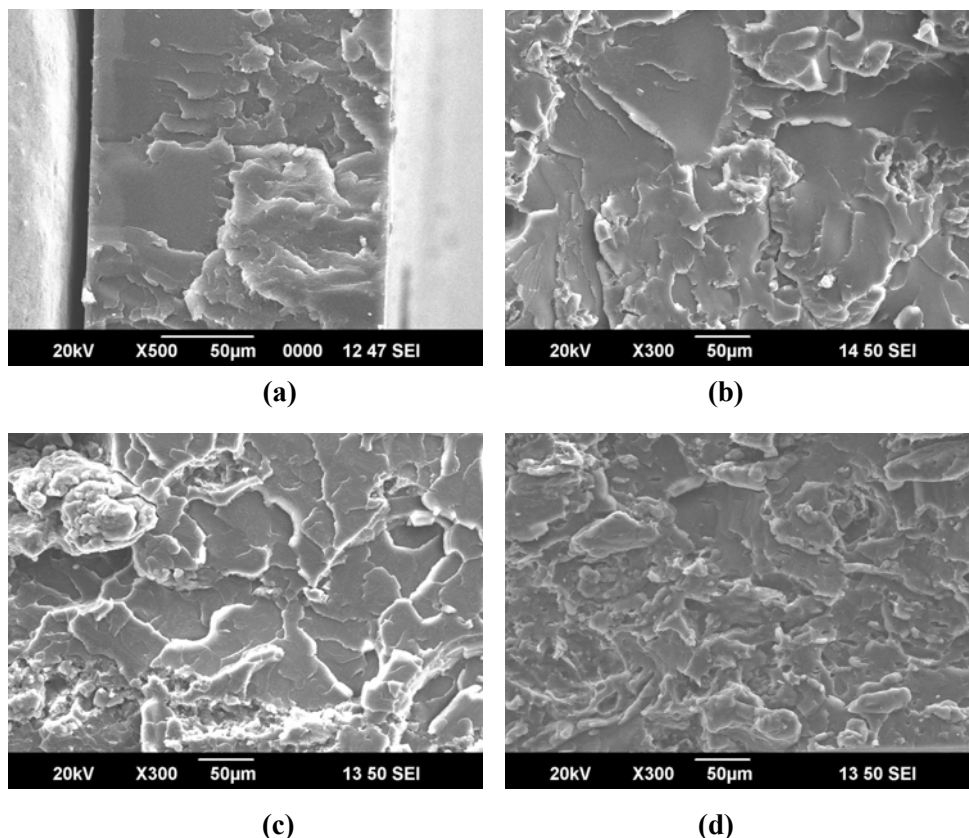


**Figure 5A.6: Scanning electron micrographs of fracture surfaces of PS/WTR blends (a) PS, (b) 95/11 PS/WTR, (c) 90/22 PS/WTR and (d) 80/44 PS/WTR.**

### 5A.3.3 Dynamic mechanical analysis

Figure 5A.7 shows the storage modulus vs. temperature plots of various PS/WTR blends. The value of  $E'$  signifies the modulus of the material. The temperature at which  $E'$  starts to fall drastically corresponds to the glass transition temperature. At low temperatures the molecules are frozen in and exhibit very high modulus. The virgin PS shows the highest modulus at 40 °C. The  $E'$  decreases with increase in WTR content. At the glass

transition zone, there is a drastic decrease in modulus with temperature, which is due to the onset of segmental mobility. Above the glass transition temperature, the storage modulus is identical for all the blends.

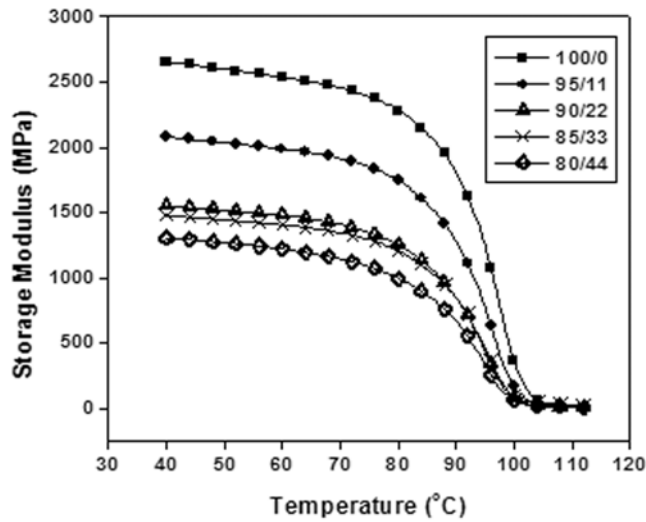


Figure 5A.7: Effect of temperature on the storage modulus of PS/WTR blends.

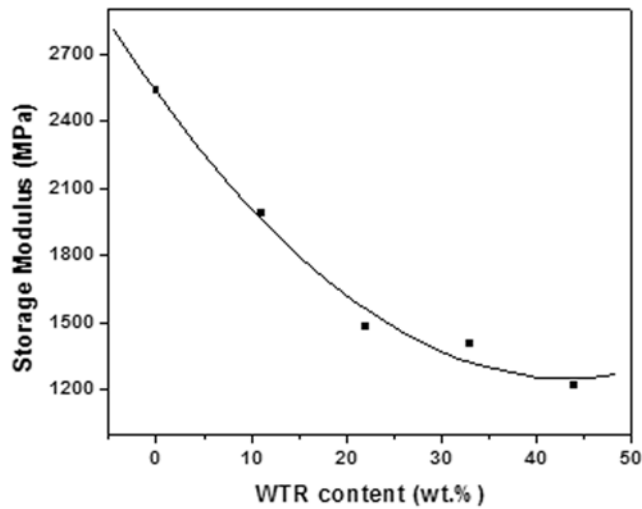


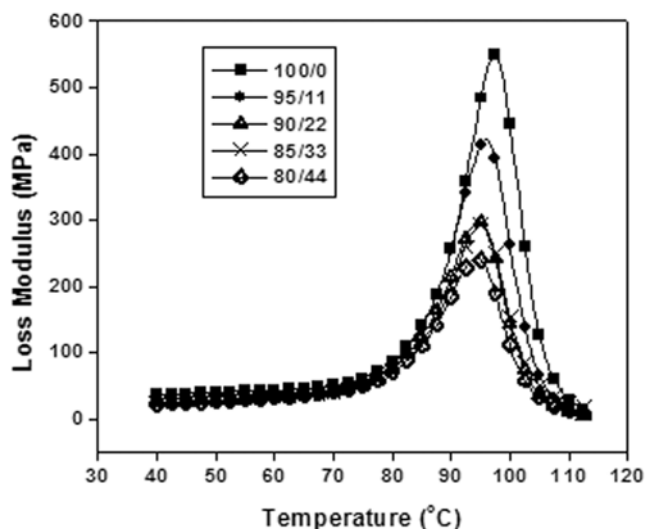
Figure 5A.8: Variation of storage modulus at 60 °C with WTR content.

Figure 5A.8 illustrates the effect of wt.% of WTR on the storage modulus of PS/WTR blends. The figure and the regression results show that the WTR content has a significant effect on storage modulus of the PS. The regression equation relating WTR content to storage modulus, with a regression coefficient ( $R^2$ ) of 0.98 is as follows:

$$y = 2535 - 130x + 3.33x^2$$

where  $y$  = storage modulus (MPa) at 60 °C.

$x$  = WTR content (wt.%)



**Figure 5A.9: Effect of temperature on the loss modulus of PS/WTR blends.**

The variation of loss modulus with temperature of PS/WTR blends is shown in Figure 5A.9. All the blends show a peak around 100 °C corresponding to the  $T_g$  of PS. At the transition region, the value of  $E''$  decreases with increase in rubber content. Moreover, there is a marginal shift in the  $T_g$  towards the lower temperature with increasing rubber content.

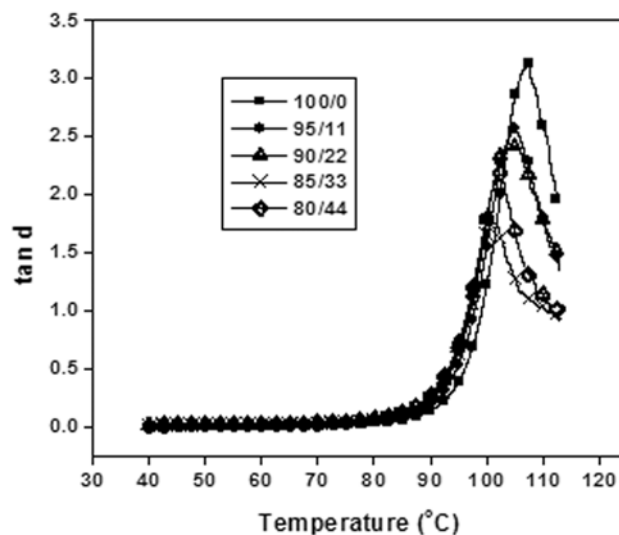


**Figure 5A.10:** Effect of temperature on  $\tan \delta$  of PS/WTR blends.

The damping curves for various PS/WTR blends are presented in Figure 5A.10. As temperature increases, damping goes through a maximum, near  $T_g$ , in the transition region and then a minimum in the rubbery region. It is clear from the figure, that  $\tan \delta$  max decreases with increasing WTR content. The  $T_g$  value also shifts to a lower temperature with increasing rubber content, indicating a better chain flexibility in the case of blends.

#### 5A.4 Conclusions

The whole tyre reclaim (WTR) can be used to prepare blends with polystyrene. The toughness of polystyrene can be improved by blending it with WTR. The optimum PS/WTR blend ratio is 90/22. The impact of PS is improved by 32 % by blending with 22 wt.% WTR. The morphology study shows indications of ductile failure pattern for this optimum blend. The tensile strength and flexural strength of PS/WTR blends decrease with the increase in rubber content. At room temperature, the storage modulus and loss tangent decrease with increase in reclaimed rubber content. The glass transition

temperature of PS is reduced with increasing WTR content. There is a reduction of about 6 °C in the  $T_g$  of PS at a WTR loading of 33 wt %.

### 5A.5 References

- [1] U.S. Environmental Protection Agency Office of Solid Waste, Clark C, Meardon K, Russell B. *Scrap Tire Technology and Markets*. Park Ridge, NJ: Noyes Data Corporation; 1993.
- [2] Tsenoglou C, Kartalis CN, Papaspyrides CD, Pfaendner R. *J Appl Polym Sci* 2001; 80:2207.
- [3] Miller P, Sbarski I, Kosior E, Masood S, Iovenitti P. *J Appl Polym Sci* 2001; 82:3505.
- [4] Zhang JF, Zheng Q, Yang YQ, Yi XS. *J Appl Polym Sci* 2002; 83:3117.
- [5] Thongruand W, Maurice C, Spontak RJ. *J Appl Polym Sci* 2002; 40:1013.
- [6] Lee MG, Nho YC. *J Appl Polym Sci* 2002; 83:2440.
- [7] Naskar AK, Bhowmick AK, De SK. *Polym Eng Sci* 2001; 41:1087.
- [8] Roy C, Unsworth J. *Int Conf Pyrolysis and Gasification* 1989, 180, 9.
- [9] National Rubber Star Tracker, Inc. *Technical Bulletin Canada: National Rubber Company, Inc.*, 1994.
- [10] Ratcliffe A. *Chem Eng* 1972; 79:62.
- [11] Hershaft AA. *Environ Sci Technol* 1972; 6:412.
- [12] Kim JK, Burford RP. *Rubber Chem Technol* 1998; 71:1028.
- [13] Naskar AK, Bhowmick AK, De SK. *J Appl Polym Sci* 2002; 84:370.
- [14] Chang SH, Kim SC. *J Appl Polym Sci* 1987; 35:2211.
- [15] Phadke AA, Chakraborty SK, De SK. *Rubb Chem Technol* 1984; 57:19.
- [16] Gibala D, Thomas D, Hamed GR. *Rubb Chem Technol* 1999; 72:357.
- [17] Rajalingam P, Sharpe J, Baker WE. *Rubb Chem Technol* 1993; 66:664.

- [18] Rajalingam P, Baker WE. *Rubb Chem Technol* 1992; 65:908.
- [19] Pramanik PK, Baker WE. *Plast Rubb Compos Process Appl* 1995; 24:229.
- [20] Mennig G, Michael H, Rzymiski WM, Scholz H. *Int Polym Sci Technol* 1997; 24, T/100.
- [21] Phadke AA, De SK. *Polym Eng Sci* 1986; 26:1079.
- [22] Braton NR. *Waste Age*, 61 (May–June 1972).
- [23] Braton NR, Koutsky JA. *Chem Eng News* 1974; 52:21.
- [24] Lee TCP, Millns W. US Patent 4,046,834; 1977.
- [25] Biddulph MW. *Conserv Recycl* 1977; 1:169.
- [26] Zolin DJ, Frable NB, Gentlecore JF. *Rubber Chem Technol* 1978; 51:385.
- [27] Peterson LE, Moriarty JT, Bryant WC. *Rubber Chem Technol* 1978; 51:386.
- [28] Kazanowicz MC, Osmundson EC, Boyle JF, Savage RW. *Rubber Chem Technol* 1978; 51:386.
- [29] Backman JA, Grane G, Kay EL, Laman JR. *Rubber Age* 1973; 104:43.
- [30] Al-Malaika, S.; Amir, E. J. *Polym Degrad Stab* 1989, 26:31.
- [31] Supawan T, Sukunya J. *J Appl Polym Sci* 2004; 91:510.
- [32] Zhu SH, Tzaoganakis C. *J Appl Polym Sci* 2010; 118:1051.
- [33] Nevatia P, Banerjee TS, Dutta B, Jha A, Naskar AK, Bhowmick AK. *J Appl Polym Sci* 2001; 83:2035.
- [34] Punarak P, Tantayanon S, Tangpasuthadol V. *Polym Degrad Stab* 2006; 91:3456.
- [35] Duhaime, M.; J. R.; Baker, W. E. *Plast Rubb Comp Proc Appl* 1991, 15, 87.

## Part B

# EFFECT OF SHORT NYLON-6 FIBRE- UNMODIFIED AND RFL-COATED

**5B.1 Introduction**

**5B.2 Experimental**

**5B.3 Results and Discussions**

**5B.4 Conclusions**

**5B.5 References**

### 5B.1 Introduction

In the previous section it was found that the PS blends based on WTR exhibit lower strength and modulus. Reinforcing fillers—both particulate and fibrous can be used to improve the performance of polymer systems. Short Nylon-6 fibre is a potential reinforcing material that has found wide acceptance as it can be processed using conventional processing equipments. It also opens up an opportunity to get anisotropic mechanical properties which is an important attribute in many composite applications. Short fibre reinforced polymer composites offer great advantages in a variety of engineering and consumer goods because of their high strength to weight ratio, high low strain modulus together with good mechanical and thermal properties [1]. Many researchers reported the use of various short fibres on the mechanical, thermal, rheological and morphological characteristics of thermoplastics [2,3] and elastomers [4,5]. It was first proposed by O'Connor and Goettler *et al.* [6] that the reinforcement by short fibres in a polymer matrix depends on the parameters like fibre content, length to

diameter ratio of the fibre (aspect ratio), fibre orientation in the matrix and interfacial adhesion between the fibre and the matrix.

Akhtar *et al.*, [7] who studied the use of silk fibre loading on fibre-reinforced TPEs of NR and PE reported that the tensile properties were substantially enhanced with increasing fibre loading. Similar observations were reported by Gupta *et al.*, [8] who studied the glass fibre reinforced PP/EPDM blends. Goharpey *et al.* [9] have reported the influence of short cellulose fibre on the microstructure, rheological and mechanical properties of EPDM/PP TPVs. The mechanical properties and morphology of ternary composites based on PP/EPDM blends reinforced with natural flax fibres were analysed by Biagiotti *et al.* [10]. Anuar *et al.* [11] have reported the improvement in mechanical properties of TPNR and PP/EPDM blends using kenaf fibre. Arroyo *et al.* [12] have explored the reinforcing effect of short aramid fibre in PP/EPDM blends. The dynamic mechanical and thermal properties of PE/EPDM based jute fibre composites were investigated by Gautam *et al.* [13]. The effect of PET fibres on the mechanical properties of PP/EOC blend has been investigated by Lopez-Manchado *et al.* [14]. Weizhi *et al.* [15] have studied the mechanical properties and morphological structures of short glass fibre reinforced PP/EPDM composite. The tensile and impact properties of Nylon-6/MA-g-EPR reinforced by glass fibre were examined by Laura *et al.* [16]. Saujanya *et al.* [17] have reported the mechanical properties of glass fibre reinforced PP/SBS composite.

A few studies have been reported on the utilisation of Nylon-6 fibres as reinforcing agents. Sreeja *et al.* [18,19] studied the effect of short Nylon-6 fibres on the mechanical properties of NR/reclaimed and NBR/reclaimed rubber composites. Physico-mechanical properties of EPDM/Nylon-6 short



fibre composite were studied by Wazzan [20]. The mechanical properties of short Nylon fibre reinforced NBR and CR composite containing epoxy based bonding agent were investigated by Seema *et al.* [21,22]. Mechanical properties of short Nylon fibre reinforced SBR/NR composites were studied in detail by Ma *et al.* [23]. Short Nylon fibre reinforced polypropylene composites [24] and recyclable high density polyethylene composites [25] were studied by Thomas *et al.*

In order to improve the adhesion between the fibre and matrix, either suitable coupling agents [26,27] are added which introduces physical or chemical bonding between the fibre and matrix, or the fibre surface is chemically modified [28-31]. Plasma treatment has also been used to create a functional group on the fibre and hence to provide bonding with the matrix [32-35]. Chantaratcharoen *et al.* [36] have reported the improvement of interfacial adhesion in short Conex fibre-SEBS composites by N-alkylation of the fibre surface. Ahmad *et al.* [37] have studied the effect of RFL-treatment on aramid fibres in Twaron-ENR composites. Ishak *et al.* [38] have reported the effect of RFL-treated aramid fibre and MA-g-PE compatibiliser on the mechanical properties of TPNR. The effect of RFL-treated aramid fibre on metallocene catalysed thermoplastic elastomer ethylene-octene copolymer (EOC) has been investigated by Shibulal *et al.* [39].

Satapaty *et al.* [40] have developed thermoplastic elastomer composites based on waste PE and reclaimed rubber with fly ash. However, little has been reported on the use of short fibres in the blends of a thermoplastic and reclaimed rubber.

This part discusses the effect of short Nylon-6 fibres- unmodified and RFL-coated on the mechanical properties, dynamic mechanical properties and morphology of whole tyre reclaim (WTR)-toughened polystyrene.

## 5B.2 Experimental

Table 5B.1 gives the composition of the composites used for the study. Details of the preparation of the composites and determination of the mechanical properties are given in Chapter 2.

**Table 5B.1 Composition of the composites.**

Composition	Mix No.								
	B0	B1	B2	B3	B4	B5	B6	B7	B8
PS	90	90	90	90	90	90	90	90	90
WTR <sup>a</sup>	22(10)	22(10)	22(10)	22(10)	22(10)	22(10)	22(10)	22(10)	22(10)
Unmodified N 6 fibre [F(U)] wt. %	0	0.5	1	2	3	-	-	-	-
RFL-coated N 6 fibre [F(R)] wt. %	-	-	-	-	-	0.5	1	2	3

<sup>a</sup> Values in the parentheses refer to the parts of the rubber hydrocarbon in WTR.

## 5B.3 Results and Discussion

### 5B.3.1 Mechanical properties

The variation of tensile strength of PS/WTR as a function of fibre loading is illustrated in Figure 5B.1. The fibre loading is varied from 0 to 3 wt.%. In the case of unmodified fibre composites, the tensile strength shows only marginal change up to 1 wt.% after which there is a continuous fall up to 3 wt.%. Nylon-6 fibres with its smooth surface finish fails to anchor polymer matrix chains all through the strain regime. With RFL-coated

fibres also, the tensile strength remains unchanged up to 0.5 wt.% beyond which it continuously decreases. At higher fibre loadings, the fibres act as local stress raisers thereby lowering the tensile strength. The Young's modulus of the composite with varying fibre content is presented in Figure 5B.2. The RFL-coated fibres shows a considerable enhancement of about 8 % in Young's modulus at 0.5 wt.% fibre content and then decreases with increasing fibre content. Whereas the unmodified fibre shows gradual improvement in Young's modulus up to 1wt.% and then decreases. Though there is good amount of interfacial interaction between the fibre surface and polymer matrix, as indicated by the improved Young's modulus (Figure 5B.2), it is not reflected as improved ultimate strength as the interfacial bond is broken at higher elongations. At any fibre loading, the RFL-coated fibre shows improved Young's modulus than the unmodified fibres.

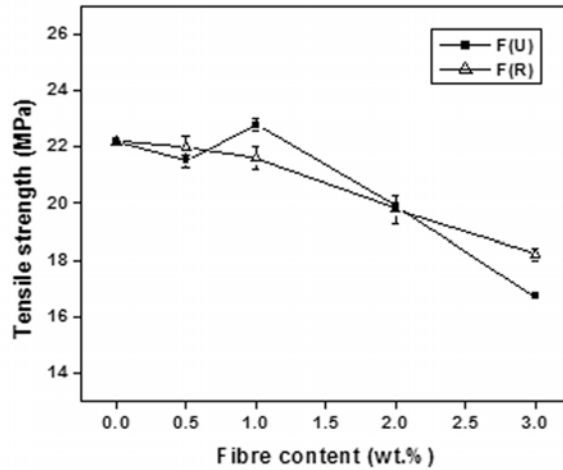


**Figure 5B.1: Variation of tensile strength of 90/22 PS/WTR with fibre content.**

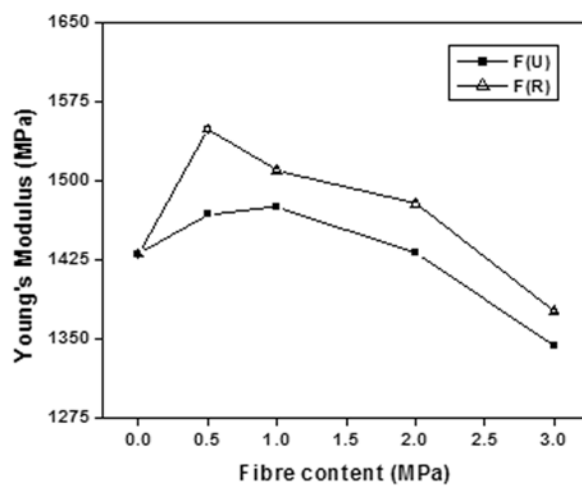


Figure 5B.2: Variation of Young's modulus of 90/22 PS/WTR with fibre content.

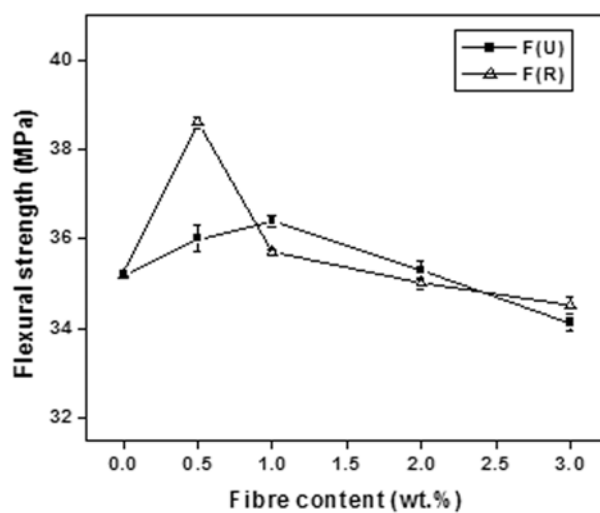
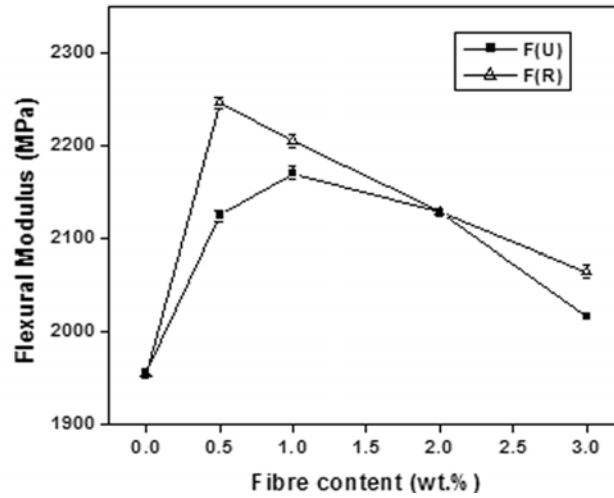
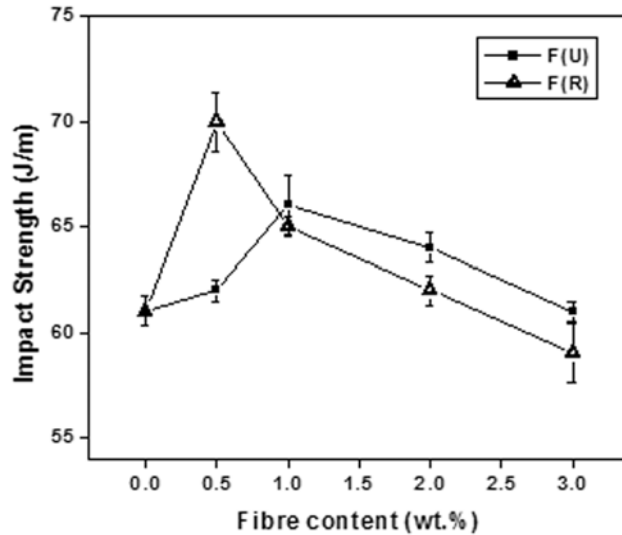


Figure 5B.3: Variation of flexural strength of 90/22 PS/WTR with fibre content.



**Figure 5B.4: Variation of flexural modulus of 90/22 PS/WTR with fibre content.**

The variation of flexural properties with fibre loading are shown in Figures 5B.3 and 5B.4. The flexural strength and flexural modulus shows a trend similar to the Young's modulus. The flexural strength and flexural modulus are higher for composites at 0.5 wt.% of RFL-coated fibres with about 10 % and 15 % enhancement respectively. For unmodified fibres at 1 wt.%, the flexural strength and modulus enhances to about 4 % and 13 %, respectively. However, these properties are lowered with further increase in fibre content. It also suggests that beyond an optimum loading, the fibres function as stress raisers.



**Figure 5B.5:** Variation of impact strength of 90/22 PS/WTR with fibre content.

The influence of fibre loading on the impact strength of PS/WTR composites is presented in Figure 5B.5. The impact strength increases to about 8 % and 14 % for composites at 1 wt.% unmodified fibre and 0.5 wt.% RFL-coated fibres, respectively. Higher fibre content leads to the reduction in impact strength due to stress concentration around fibre ends which requires less energy to initiate a crack.

### 5B.3.2 Morphology

Figures 5B.6(a) and (b) show the scanning electron micrographs of tensile fractured surfaces of 90/22 PS/WTR composites with 1 and 3 wt.% Nylon fibre, respectively. While Figures (c) and (d) show the micrographs of composites with 0.5 and 3 wt.% of RFL-coated fibres. With both unmodified and RFL-coated fibre composites, the matrix surface is rough with multiple crack lines and layered structure. Fibres protruding from the matrix,

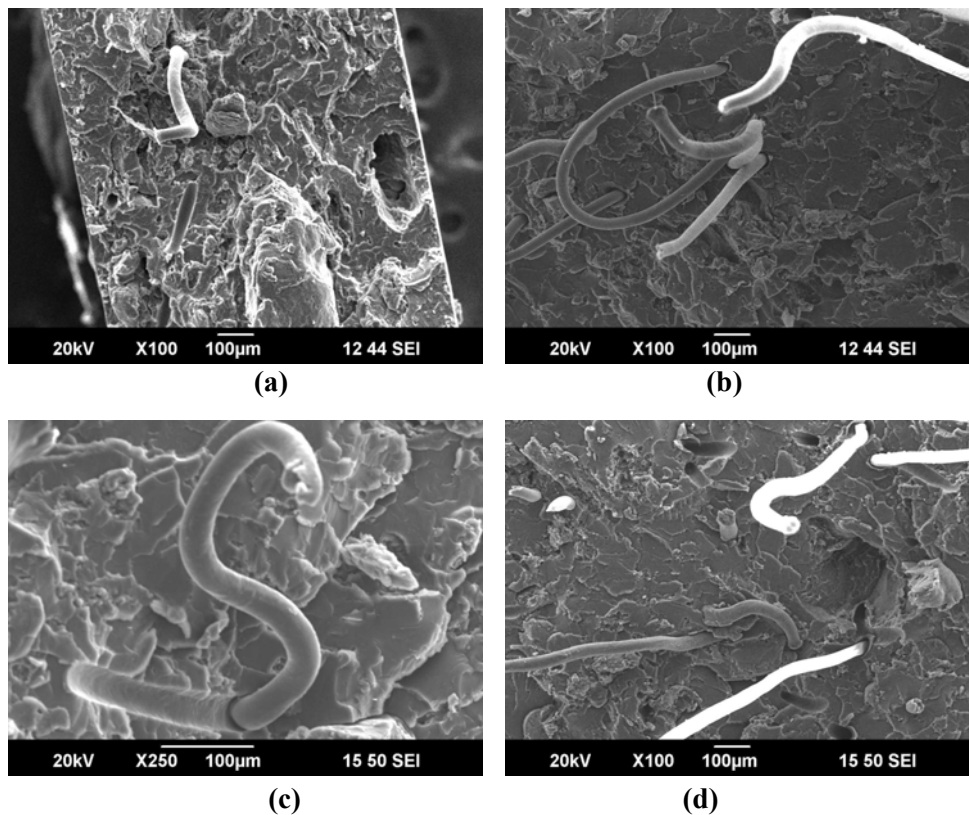


**Figure 5B.6:** Scanning electron micrographs of 90/22 PS/WTR composites with unmodified Nylon fibres (a) 1 wt.% (b) 3 wt.% (x 100 magnification) and with RFL-coated Nylon fibres (c) 0.5 wt.% (x 250 magnification) and (d) 3 wt.% (x 100 magnification).

holes due to fibre pull-out and rubber debonding could be observed in Figures (a)-(d). In Figure (c) with 0.5 wt.% RFL-coated fibres, small gaps could be seen at the fibre-matrix interface which implies that at high stretching, the interfacial bond is broken.

### 5B.3.3 Dynamic Mechanical Analysis

Figure 5B.7 shows the variation of storage modulus as a function of temperature of 90/22 PS/WTR composites with varying (unmodified) fibre content. The  $E'$  value at 40 °C is higher for composites containing 0.5 and 1wt.% of Nylon fibre when compared to the 90/22 PS/WTR blend and composite with higher fibre loading. The  $E'$  values of the composites fall steeply around the glass transition of PS at 95-100 °C. Above the glass transition temperature, all the composites show similar  $E'$  values.

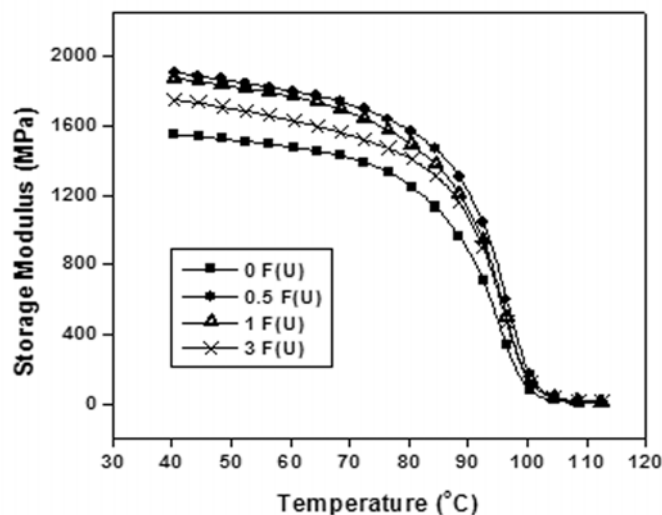


**Figure 5B.7: Storage modulus vs. temperature plots of 90/22 PS/WTR composites with varying (unmodified) fibre content.**

Figure 5B.8 shows the effect of temperature on the storage modulus of composites with varying (RFL-coated) fibre content. It can be seen from the figure that the  $E'$  of the composites are higher than the blend at lower temperatures. With addition of the fibres, the  $E'$  values are increased sharply and gradually. The highest value was obtained for 3 wt.% RFL-coated fibre. However, the studies in mechanical properties are not in agreement with this. The sharp drop in modulus around the glass transition temperature is almost the same for the composites and the unreinforced blend.



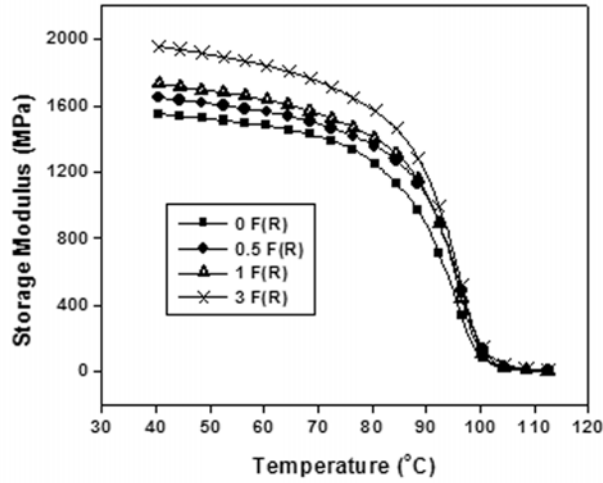


Figure 5B.8: Storage modulus vs. temperature plots of 90/22 PS/WTR composites with varying (RFL-coated) fibre content.

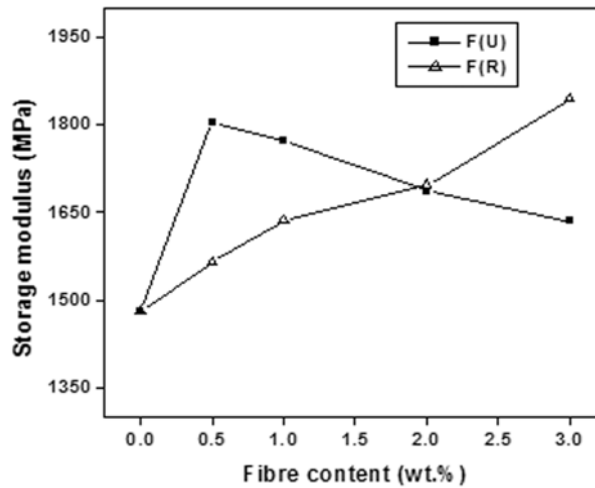
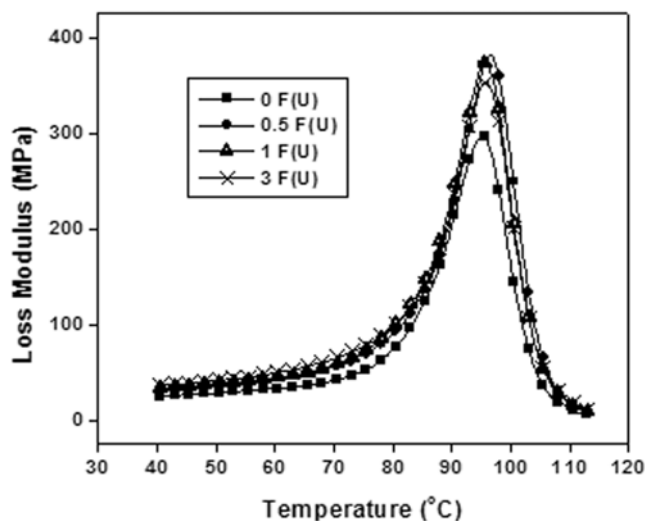


Figure 5B.9: Variation of storage modulus at 60 °C with fibre content.

The variation of storage modulus of 90/22 PS/WTR at 60 °C with varying fibre (unmodified and RFL-coated) content is shown in Figure 5B.9. With unmodified fibres, the storage modulus shows significant enhancement at 0.5 wt.% fibre content and then drops with increasing fibre content whereas the storage modulus increases with increasing fibre content in the case of RFL-coated fibres.

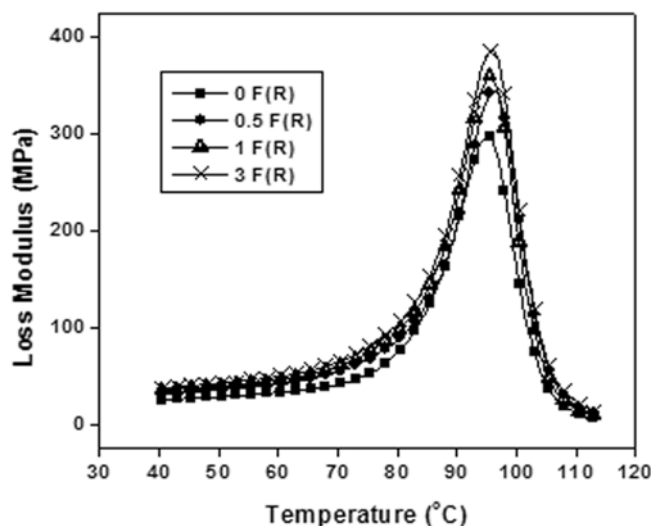
The variation of loss modulus as a function of temperature for varying (unmodified) fibre contents is graphically represented in Figure 5B.10. If the applied mechanical energy (work) is not stored elastically, it must be lost—converted to heat through molecular friction, that is, viscous dissipation within the material. This is, precisely, the loss modulus [41]. The loss modulus peak is again higher for 0.5 and 1 wt.% fibre in comparison to the blend and composite with higher fibre content. The presence of fibre does not alter the glass transition temperature of PS.



**Figure 5B.10: Loss modulus vs. temperature plots of 90/22 PS/WTR composites with varying (unmodified) fibre content.**

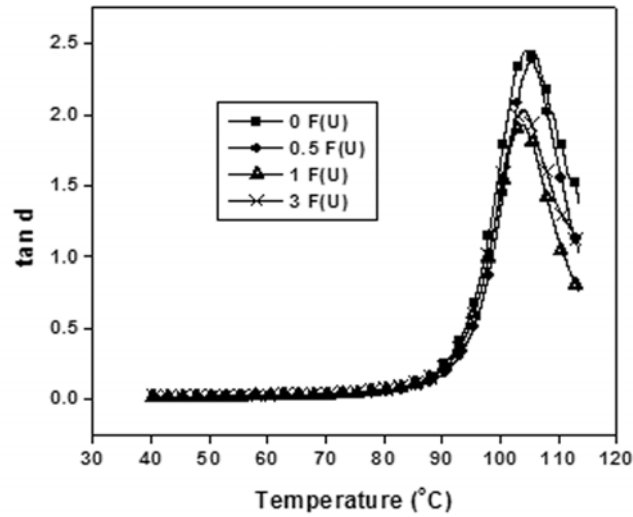
The effect of temperature on the loss modulus of the composites with varying RFL-coated fibres is shown in Figure 5B.11. The peak region at around 95 °C for all the composites corresponds to the glass transition temperature of PS. This implies that the addition of fibre does not cause any shift in the  $T_g$  of PS. The loss modulus peak increases with increasing fibre content. This may be due to the presence of fibres that reduced the

flexibility of the material by introducing constraints on the segmental mobility of polymeric molecules at the relaxation temperature.



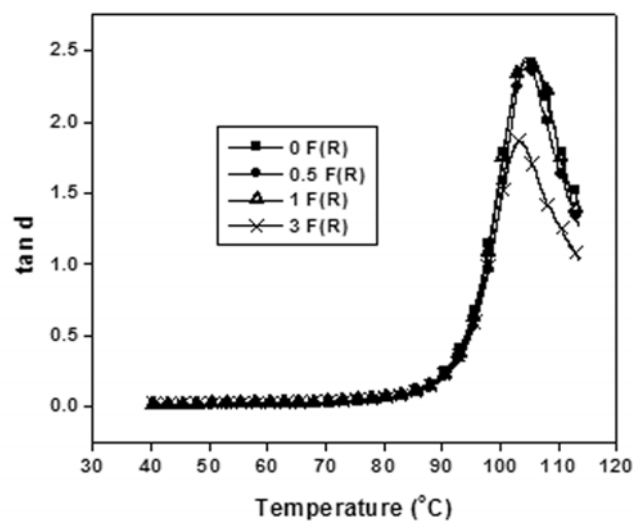
**Figure 5B.11: Loss modulus vs. temperature plots of 90/22 PS/WTR composites with varying (RFL-coated) fibre content.**

Figure 5B.12 shows the variation of  $\tan \delta$  with temperature for different (unmodified) fibre contents. It can be seen that the introduction of fibres has reduced the peak height, that is,  $\tan \delta$  is lowered with increase in fibre content. The reason may be due to the restriction of the mobility of the polymer chains by the fibre. The  $\tan \delta$  peak is the lowest for the composite at 1 wt.% fibre content.



**Figure 5B.12: Tan  $\delta$  vs. temperature plots of 90/22 PS/WTR composites with varying (unmodified) fibre content.**

The effect of temperature on  $\tan \delta$  of the composites with varying RFL-coated fibre content is delineated in Figure 5B.13. It can be observed that the  $\tan \delta$  peaks observed at around 105  $^{\circ}\text{C}$  of the unfilled blend and the composites with low content of fibres are high.



**Figure 5B.13: Tan  $\delta$  vs. temperature plots of 90/22 PS/WTR composites with varying (RFL-coated) fibre content.**

It is associated with the glass transition of polystyrene. The  $\tan \delta$  peak is lowest for the composite with 3 wt.% fibre, which reflects the load bearing property of the system. The storage modulus values obtained are also consistent with the result.

#### **5B.4 Conclusions**

Short Nylon-6 fibre and RFL-coated fibres can be used to improve the properties of PS/WTR blends. The composites containing 1 wt.% unmodified fibre and 0.5 wt.% RFL-coated fibres in 90/22 PS/WTR show improvement in tensile modulus, flexural strength, flexural modulus and impact strength. The tensile strength is only marginally improved. The unmodified fibres at 1 wt.% improves the Young's modulus and impact strength by 3 % and 8 %, respectively. Whereas the RFL-coated fibres enhances the tensile modulus and impact strength by 8 % and 14 % respectively. Incorporation of higher fibre content reduces the mechanical properties in both types of composites. The optimum loading of unmodified Nylon-6 in PS/ WTR blend is 1 wt%. The dynamic mechanical study also reveals that the storage modulus and loss modulus peaks are higher for composites at 0.5 and 1 wt.% (unmodified) fibre content. The  $\tan \delta$  peak is the lowest for composite with 1 wt.% fibre content. Since the overall mechanical properties are better with PS/WTR composite at 1 wt.% fibre content, this composition was selected for further studies .

The dynamic mechanical analysis studies in the case of RFL-coated fibres shows that the storage modulus values at low temperatures is maximum for composites with 3 wt.% fibre. The damping peak is also the lowest for the same composite. However, the results of composites with RFL-coated fibres are not in agreement with the static mechanical properties.

## 5B.5 References

- [1] Peters ST. Handbook of composites. 2nd edn. London: Chapman and Hall; 1998.
- [2] Fu SY, Lauke B. Compos Sci Tech 1996; 56:1179.
- [3] Nair KCM, Kumar RP, Thomas S, Schit SC, Ramamurthy K. Composites: Part A 2000; 31:1231.
- [4] Kashani MR. J Appl Poly Sci 2009; 113:1355.
- [5] Rajeev RS, Bhowmick AK, De SK. Polym Compos 2002; 23:574.
- [6] O' Connor JE. Rubber Chem Technol 1977; 50:945.
- [7] Akhtar S, De PP, De SK. J Appl Polym Sci 1986; 32:5123.
- [8] Gupta AK, Srinivasan KR, Krishna Kumar P. J Appl Polym Sci 1991; 43:451.
- [9] Goharpey F, Mirzadeh A, Sheikh A, Nazockdast H, Katbab AA; Polym Comp 2009; 30:182.
- [10] Biagiotti J, Lopez-Manchado MA, Arroyo M, Kenny JM. Polym Eng Sci 2003; 43:1031.
- [11] Anuar H, Zuraida A. Composites: Part B 2011; 42:462.
- [12] Arroyo M, Zitzumbo R, Avalos F. Polymer 2000; 41:6351.
- [13] Gautam S, Arup C. J Appl Polym Sci 2008; 108:3442.
- [14] Lopez Manchado MA, Arroyo M. Polymer 2001; 42:6557.
- [15] Weizhi W, Longxiang T, Qu B. Euro Polym J 2003; 39:2129.
- [16] Laura DM, Keskkula H, Barlow JW, Paul DR. Polymer 2000; 41:7165.
- [17] Saujanya C, Radhakrishnan S. Polym Comp 2001; 22:232.
- [18] Sreeja TD, Kutty SKN. Polym-Plast Technol Eng 2003; 42:239.
- [19] Sreeja TD, Kutty SKN. Int J Polym Mater 2003; 52:175.
- [20] Wazzan AA. Int J Polymer Mater 2004; 53:59.
- [21] Seema A, Kutty SKN. J Appl Polym Sci 2006; 99:532.

- [22] Seema A, Kutty SKN. *Polym Plast Technol Eng* 2005; 44:1139.
- [23] Ma Peiyu, Zhao Jan, Tang J, Dai G. *Guofenzi Cailiao Kexue Yu Gongcheng* 1994; 10:55.
- [24] Thomas N Abraham, George KE. *Polym Plast Technol Eng* 2007; 46:321.
- [25] Thomas N Abraham, George KE. *Plast Rub Comp* 2005; 34:196.
- [26] Vaughan DJ. *Polym Eng Sci* 1978; 18:168.
- [27] Andreopoulos AG. *J Appl Polym Sci* 1989; 38:1053.
- [28] Breznick M, Banbaji J, Guttman H, Marom G. *Polym Comm* 1987; 28: 55.
- [29] Wu Y, Tesoro GC. *J Appl Polym Sci* 1986; 31:1041.
- [30] Tarantili PA, Andreopoulos AG. *J Appl Polym Sci* 1997; 65:267.
- [31] Sheu GS, Lin TK, Shyu SS, Lai JY. *J Adhesion Sci Technol* 1994; 8:511.
- [32] Wang Q, Kaliaguine S, Ait-Kadi A. *J Appl Polym Sci* 1993; 48:121.
- [33] Mori M, Uyama Y, Ikeda Y. *Polymer* 1994; 35:5336.
- [34] Sheu GS, Shyu SS. *Comp Sci Technol* 1994; 52:489.
- [35] Brown JR, Mathys Z. *J Mater Sci* 1997; 32:2599.
- [36] Chantaratcharoen A, Sirisinha C, Amornsakchai T, Limcharoen SB, Meesiri W. *J Appl Poly Sci* 1999; 74:2414.
- [37] Ahamad I, Chin TS, Cheong CK, Jalar A, Abdullah I. *Compos, Am J Appl Sci Special Issue* 2005;14.
- [38] Ishak A, Yong PY, Ibrahim A. *Polym Compos* 2006; 27:395.
- [39] Shibulal GS, Naskar K. *J Polm Res* 2011, 18:2295.
- [40] Satapaty S, Nag A, Nando GB. *Process Safety and Environmental Protection* 2010; 88:131.
- [41] Rosen SL. *Fundamental Principles of Polymeric Materials*. New York: Wiley; 1982.





## Part C

# EFFECT OF SURFACE MODIFICATION OF FIBRE AND USE OF A COMPATIBILISER.

### 5C.1 Introduction

### 5C.2 Experimental

### 5C.3 Results and Discussions

### 5C.4 Conclusions

### 5C.5 References

## 5C.1 Introduction

In the fibre-reinforced polymer composites, matrix component usually has low strength, fairly good toughness, low density, and higher coefficient of thermal expansion than the reinforcing fibre component. With the discontinuous reinforcing fibres of finite length, the load is transferred from the matrix to the fibre through the effect of shear at the fibre-matrix interface [1]. Nylon fibre is characterized by its high strength, sufficient flexibility, abrasion resistance and light weight. However, the problem of fibre dispersion in the matrix often arises. To overcome the problem of poor dispersion, chemical or physical bonding between the fibre and the matrix is usually introduced through the introduction of a suitable coupling agent [2,3] or chemical modification of the fibre surface [4-7].

Smitha *et al.* [8] have studied the effectiveness of MA-g-PP as coupling agent in sisal fibre/polypropylene composites. The effect of MAPP in polypropylene-viscose fibre composites was studied by Paunikallio *et al.* [9]. Rana *et al.* [10] have reported the influence of MAPP as compatibiliser in jute fibre/PP composites. The effect of MAPP as coupling agent in kenaf

fibre reinforced TPNR and PP/EPDM composites has been reported by Anuar *et al.* [11]. The impact of MA-g-PB in aramid fibre reinforced ethylene-octene copolymer composites was investigated by Shibulal *et al.* [12]. Amornsakchai *et al.* [13] have investigated a system of Conex short-fibre reinforced SEBS thermoplastic elastomer composite where improvement in interfacial adhesion was obtained by partial hydrolysis of the fibre surface and addition of a reactive compatibiliser, MA-g-SEBS. The effect of a reactive compatibiliser (MA-g-PP) and partially hydrolysed Kevlar fibre on Santoprene composites was studied by Saikrasun *et al.* [14].

This part discusses on the effect of modification of Nylon-6 fibre by surface treatment (using alkali) and the use of a compatibiliser, MA-g-PS on the mechanical properties, morphology and dynamic mechanical properties of PS/WTR composites.

## 5C.2 Experimental

The formulation of the composites used for the study are given in Table 5C.1. Details of the surface treatment of fibre, preparation of the composites and determination of the mechanical properties are given in Chapter 2.

**Table 5C.1 Composition of the composites**

Composition	Mix No.									
	C0	C1	C2	C3	C4	C5	C6	C7	C8	C9
PS	90	90	90	90	90	90	90	90	90	90
WTR <sup>a</sup>	22(10 )	22(10 )	22(10 )	22(10 )	22(10 )	22(10 )	22(10 )	22(10 )	22(10 )	22(10 )
Untreated N 6 fibre [F(U)] wt.%	1	1	1	1	1	-	-	-	-	-
Treated N 6 fibre [F(T)] wt.%	-	-	-	-	-	1	1	1	1	1

<b>MA-g-PS wt.(%)</b>	0	0.5	0.75	1	2	0	0.5	0.75	1	2
---------------------------	---	-----	------	---	---	---	-----	------	---	---

<sup>a</sup> Values in the parentheses refer to the parts of the rubber hydrocarbon in WTR.

### **5C.3 Results and Discussion**

Preparation of maleic anhydride grafted polystyrene (MA-g-PS) and its characterisation are given in Chapter 2 and Chapter 3 (Part C), respectively.

#### **5C.3.1 Mechanical properties**

The tensile strength and Young's modulus of composites having 1 wt.% untreated and treated Nylon fibre with varying MA-g-PS content are presented in Figures 5C.1 and 5C.2, respectively. It is clear that the use of MA-g-PS has a positive effect on the tensile strength in the case of composites containing alkali treated fibres. The maximum improvement of 14 % is observed at a MA-g-PS loading of 0.5 wt.% for treated fibres. For the untreated fibres, however, there is marginal reduction in tensile strength with increasing MA-g-PS. At any MA-g-PS loading, the treated fibre composites show higher tensile strength. The increased polarity of the fibre surface resulting from the hydrolysis is not productive in the absence of a MA-g-PS; rather it results in polarity segregation leading to lower tensile strength.

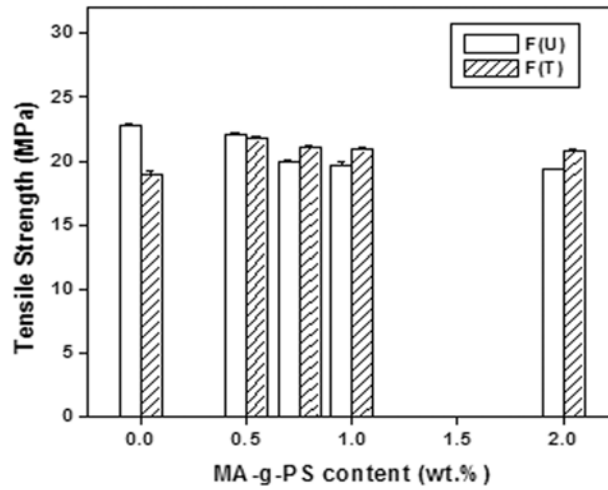


**Figure 5C.1: Effect of MA-g-PS on the tensile strength of composites with 1 wt.% untreated and treated fibre.**

A similar trend is also observed in the case of Young's modulus shown in Figure 5C.2. The Young's modulus enhances by 8 % for treated fibre composites at a compatibiliser loading of 0.5 wt.%.

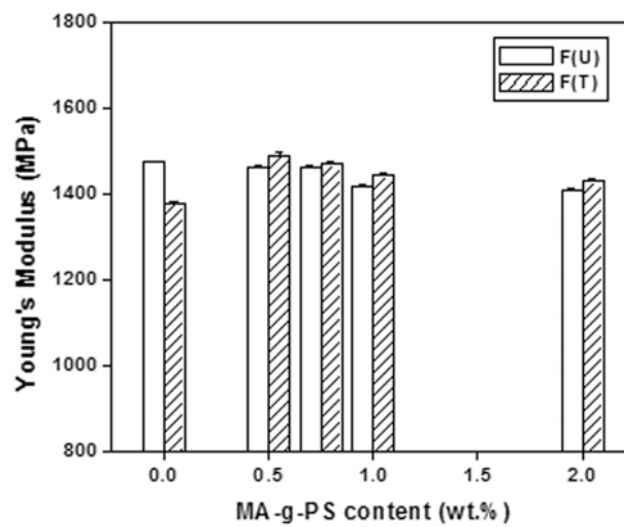


**Figure 5C.2: Effect of MA-g-PS on the Young's modulus of composites with 1 wt.% untreated and treated fibre.**

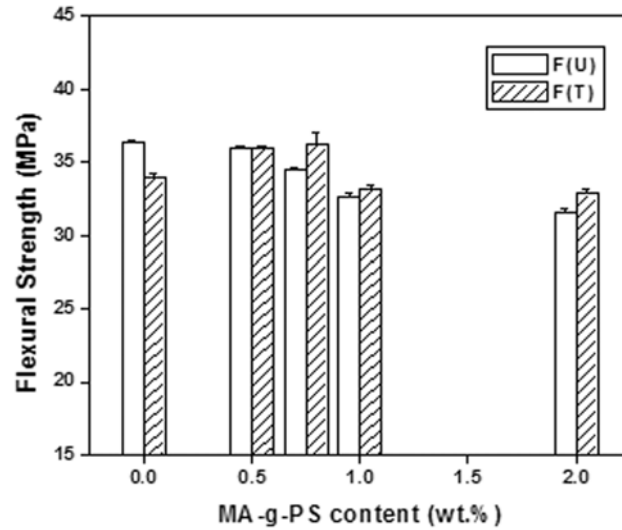


**Figure 5C.3: Effect of MA-g-PS on the flexural strength of composites with 1 wt.% untreated and treated fibre.**

The flexural properties of composites containing 1 wt.% untreated and treated fibre with varying MA-g-PS content is presented in Figures 5C.3 and 5C.4, respectively. The flexural strength and flexural modulus shows a behaviour similar to that of tensile strength and Young's modulus. The use of MA-g-PS enhances the flexural properties in the case of treated fibre composites. The enhancement is higher with 0.5 wt.% MA-g-PS. Increasing MA-g-PS in untreated fibres causes a marginal reduction in flexural strength and modulus.

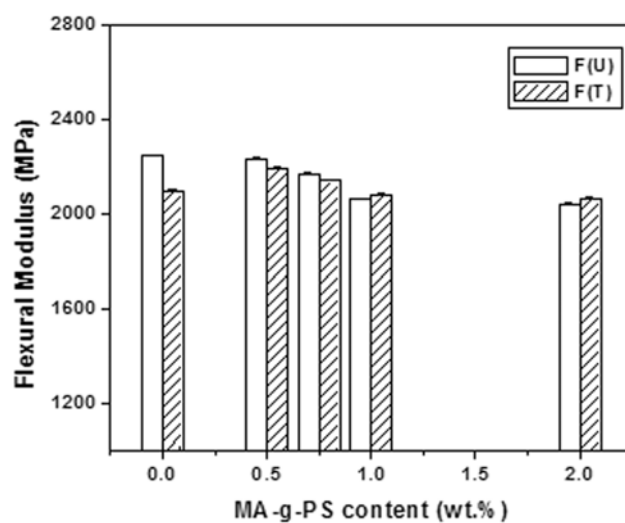


**Figure 5C.4: Effect of MA-g-PS on the flexural modulus of composites with 1 wt.% untreated and treated fibre.**

The effect of varying compatibiliser (MA-g-PS) content on the impact strength of composites with 1 wt.% untreated and treated fibre is illustrated in Figure 5C.5. In the presence of compatibiliser at 0.5 wt.%, there is 9 % and 17 % enhancement, respectively, in impact strength of untreated and treated fibre composites. The treated fibre composites, in the absence of compatibiliser, shows lower impact strength. This may be due to the fibre agglomeration

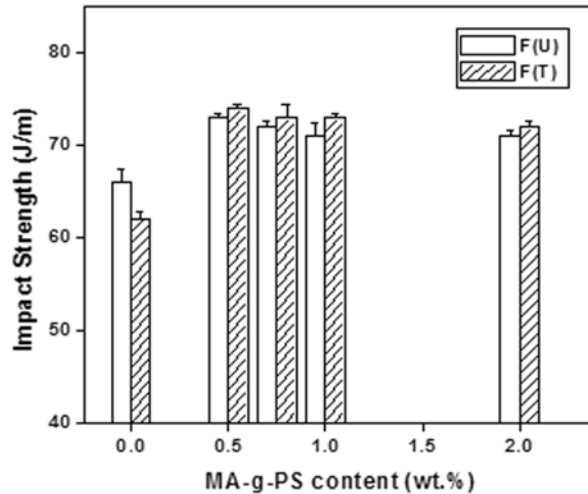


**Figure 5C.5:** Effect of MA-g-PS on the impact strength of composites with 1 wt.% untreated and treated fibre.

resulting from increased polarity which creates regions of stress concentration that requires less energy for crack initiation. Little deterioration in impact strength was observed at higher concentrations of MA-g-PS in both the composites. In this case, the compatibiliser migration around the fibres acted as a damper to the shock wave imparted during the impact that was transmitted onto the fibres evenly [10].

### 5C.3.2 Morphology

The micrographs of tensile fractured surfaces of 90/22 PS/WTR composites containing 1 wt.% untreated fibre with (a) 0.5wt.% (b) 2 wt.% of MA-g-PS and 1 wt.% treated fibre with (c) 0.5 wt.% (b) 2 wt.% of MA-g-PS content are shown in Figure 5C.6. It is seen from all the micrographs that the matrix has a rough surface indicating brittle failure of the composites. The gaps between the fibre and the matrix in Figure (a) and (b) reveal the poor adhesion between them indicating that the use of compatibiliser, MA-g-PS, has little effect in improving the interfacial adhesion in the case of untreated

fibres. In the case of treated fibre composites with 0.5 wt.% MA-g-PS content as shown in Figure (c), the fibre-matrix interaction is better. However, at higher content of MA-g-PS the gaps are found to be wider [Figures (b) and (d)].

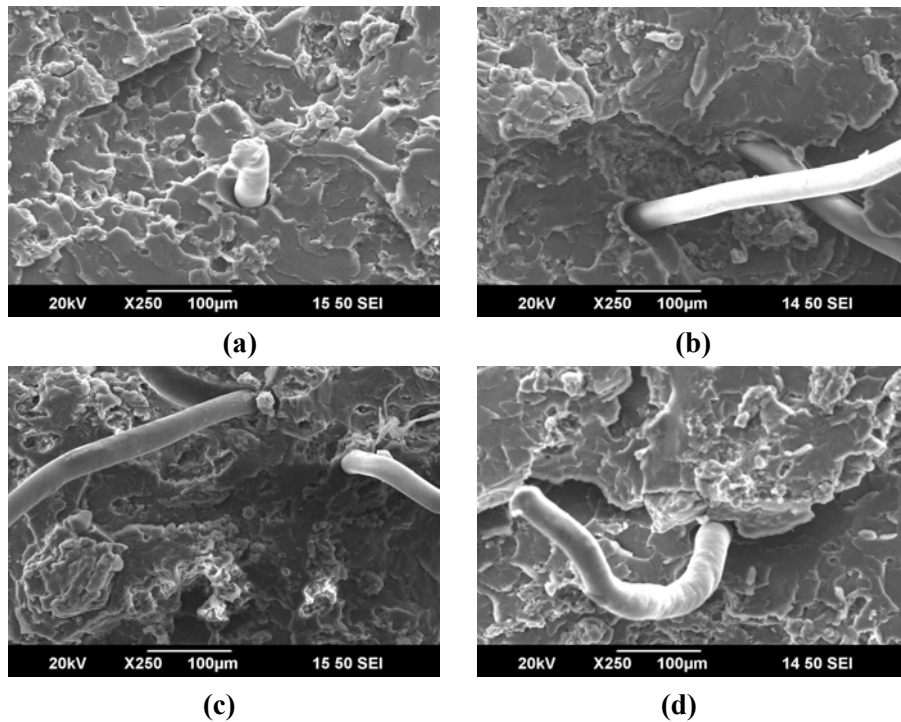


**Figure 5C.6:** Scanning electron micrographs of 90/22/1 PS/WTR/Fibre composites with (a) 0.5 wt.%, (b) 2 wt.% MA-g-PS in untreated fibres, and (c) 0.5 wt.% and (d) 2 wt.% MA-g-PS in treated fibres.

### 5C.3.3 Dynamic Mechanical Analysis

The composites containing 0.5 wt.% MA-g-PS was selected for evaluating the dynamic mechanical properties. The variation in storage modulus with respect to temperature of Nylon fibre-PS/WTR composites with untreated and treated fibres containing 0.5 wt.% compatibiliser (MA-g-PS) is shown in Figures 5C.7. The storage modulus at low temperatures is maximum for the untreated fibre composites with compatibiliser in comparison to the treated fibre composites with compatibiliser and to the



one without compatibiliser. Around the glass transition temperature, there is a drastic fall in modulus for all the composites. Above the glass transition temperature ( $T_g$ ) all the composites show identical  $E'$  values. This is due to the increased molecular mobility of the polymer chains above  $T_g$ .

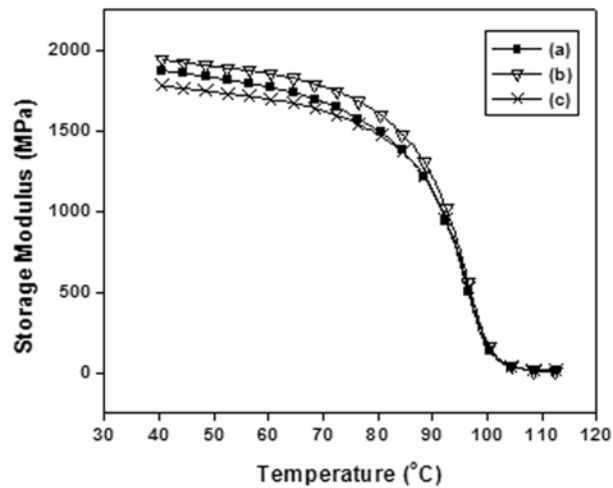


Figure 5C.7: Storage modulus vs. temperature plots of composites containing (a) untreated fibre (b) untreated fibre with compatibiliser and (c) treated fibre with compatibiliser (0.5wt.%).

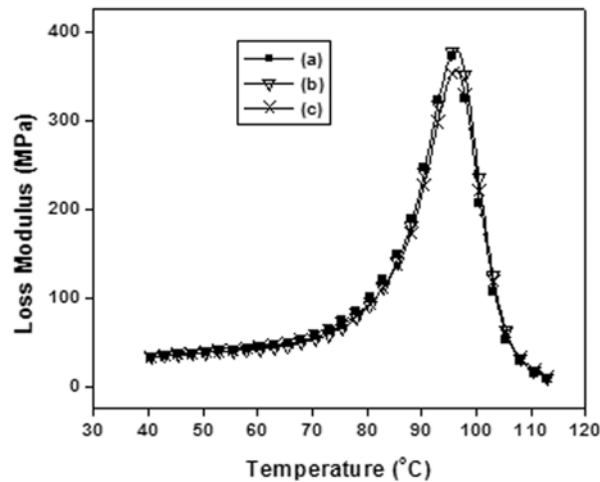
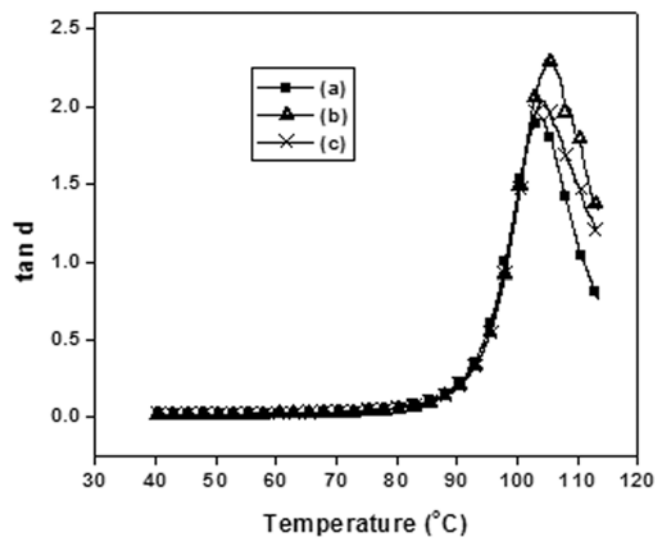


Figure 5C.8: Loss modulus vs temperature plots of composites containing (a) untreated fibre (b) untreated fibre with compatibiliser and (c) treated fibre with compatibiliser.

Figure 5C.8 depicts the variation of loss modulus with respect to temperature of PS/WTR/fibre composites with the addition of the compatibiliser. The loss modulus peak corresponding to the glass transition temperature is the same for the untreated fibre composites with and without compatibiliser and is higher when compared to treated fibre composites with compatibiliser. There is no change in  $T_g$ .



**Figure 5C.9: Tan  $\delta$  vs. temperature plots of composites containing (a) untreated fibre (b) untreated fibre with compatibiliser and (c) treated fibre with compatibiliser.**

The variation of  $\tan \delta$  as a function of temperature for the different composites is represented in Figure 5D.9. The damping peak of untreated composites in the presence of compatibiliser shows the highest magnitude in comparison to treated composites with compatibiliser and the untreated composites. This implies that a composite material with strong interfacial bonding between the fibres and the matrix, tends to dissipate less energy, thus showing a low magnitude of damping peak.

#### **5C.4 Conclusions**

The addition of a compatibiliser, MA-g-PS to treated fibre composites enhances the tensile properties, flexural properties and impact strength compared to the one without compatibiliser. The maximum improvement is obtained for 0.5 wt.% MA-g-PS loading with an enhancement of 14 %, 8 % and 17 % in tensile strength, Young's modulus and impact strength, respectively. The untreated fibre composite show little improvement in mechanical properties with the addition of the compatibiliser. The dynamic mechanical analysis reveals that the storage modulus at low temperatures is better for untreated fibre composites in conjunction with the compatibiliser.

#### **5C.5 References**

- [1] Fu SY, Lauke B, Mader E, Yue CY, Hu X. *Compos Part A: Appl Sci Manuf* 2000; 31:1117.
- [2] Vaughan DJ. *Polym Eng Sci* 1978; 18:168.
- [3] Andreopoulos AG. *J Appl Polym Sci* 1989; 38:1053.
- [4] Breznick M, Banbaji J, Guttman H, Marom G. *Polym Comm* 1987; 28:55.
- [5] Wu Y, Tesoro GC. *J Appl Polym Sci* 1986; 31:1041.
- [6] Tarantili PA, Andreopoulos AG. *J Appl Polym Sci* 1997; 65:267.
- [7] Sheu GS, Lin TK, Shyu SS, Lai JY. *J Adhesion Sci Technol* 1994; 8:511.
- [8] Smita M, Sushil KV, Sanjay KN, Sudhansu ST. *J Appl Polym Sci* 2004; 94:1336.
- [9] Paunikaloi T, Kasanen J, Suvanto M, Pakkanen TT. *J Appl Polym Sci* 2003; 87:1895.
- [10] Rana AK, Mandal A, Mitra BC, Jacobson R, Rowell R, Banerjee AN. *J Appl Polym Sci* 1998; 69:329.

*Chapter -5*

---

- [11] Anuar H, Zuraida A. *Comp Part B* 2011; 42:462.
- [12] Shibulal GS, Naskar K. *J.Polym Res* 2011; 18:2295.
- [13] Amornsakchai T, Sinpatanapan B, Baulek-Limcharoen S, Meesiri W. *Polymer* 1999; 40:2993.
- [14] Saikrasun S, Amornsakchai T, Sirisinha C, Meesiri W, Baulek-Limcharoen S. *Polymer* 1999; 40:6437.

.....❧.....

## **THERMAL DEGRADATION OF BLENDS AND COMPOSITES BASED ON POLYSTYRENE/NATURAL RUBBER AND NYLON-6 FIBRE**

### **6.1 Introduction**

### **6.2 Experimental**

### **6.3 Results and Discussions**

### **6.4 Conclusions**

### **6.5 References**

## **6.1 Introduction**

Thermal degradation of polymers can be considered to be the effect of different concurrent chemical reactions, which are often accompanied by other physical phenomena such as evaporation and ablation [1], that introduce further complications in the modelling of the degradation kinetics. The development of affordable models able to describe the degradation kinetics of polymers has been the concern of many authors [2-6]. The macroscopic phenomenon observed during thermal degradation of polymers is the loss of weight caused by elimination of low molecular weight substances produced by chain unzipping and free radical reactions and by other physical phenomena, such as plasticiser and solvent evaporation [7-11]. Thermal analysis of polymers is an important method in

the characterisation of polymers and in establishing service conditions. The threshold temperature for breakdown determines the upper limit of temperature in fabrication [12,13].

Thermogravimetric analysis (TGA) can help in understanding the degradation mechanism and thus assist any effort to enhance the thermal stability of a polymeric material. This analysis needs only a small quantity of the sample. Thermogravimetric data provide the different stages of thermal breakdown, weight of the material in each stage, threshold decomposition temperature etc. Both TG and differential thermogravimetry (DTG) curves provide information about the nature and conditions of degradation of materials. Thus, thermogravimetric analyser, which measures weight loss as a function of time (isothermal test) and temperature (dynamic test at constant heating rate) [14] is the most suitable instrument for these studies. For a system that loses material while it is reacting, weight loss can be related to the degree of reaction. In this case, it is possible to correlate the TGA measurements directly with the extent of degradation reaction, the values of which are the sum of all the possible reactions that give rise to weight loss during the degradation process. This fact precludes the use of TGA for kinetic studies where many different modes of degradation occur simultaneously. The kinetic parameters such as activation energy and the reaction order can be calculated using both dynamic and isothermal tests [15].

The thermal stability of individual polymers can be enhanced to a greater extent by blending them with other polymers or by reinforcing with fibres [16-21]. Navarro *et al.* has reported the thermal degradation of recycled polypropylene toughened with elastomers [22]. Agung *et al.* [23]

has evaluated the thermal characteristic of abaca fibre reinforced high impact polystyrene (HIPS) composites. The thermal stability of polypropylene composites reinforced with short carbon fibres were studied by Rezaei *et al.* [24]. Smita *et al.* [25,26] have evaluated the thermal behaviour of MAPE treated jute/HDPE and MAPP treated sisal/PP composites. The influence of short glass fibre on the thermal stability of PP/EPDM was evaluated by Weizhi *et al.* [27].

This chapter attempts to analyse the thermal degradation of PS/NR blend with respect to the blend ratio, dynamic vulcanisation, effect of short Nylon-6 fibre, RFL-coated Nylon-6 fibre; and untreated and surface treated Nylon fibre in conjunction with a compatibiliser.

## 6.2 Experimental

The formulation of the blends and composites are given in Table 6.1. PS/NR blends and its composites based on short Nylon-6 fibres were prepared by melt-mixing in a Thermo Haake Polylab QC, followed by compression moulding as described in Chapter 2.

**Table 6.1 Formulation of the mixes.**

Composition	Mix No.							
	A	B	C	D	E	F	G	H
PS*	100	0	85	85	85	85	85	85
NR*	0	100	15	15	15	15	15	15
Dicumyl peroxide (phr)	0	0	0	2(2.8)**	0	0	0	0
Untreated N6 fibre [F(U)] (wt.%)	0	0	0	0	1	0	1	0
RFL-coated N6 fibre [F(R)] (wt.%)	0	0	0	0	0	1	0	0
Surface Treated N6 fibre[F(T)] (wt.%)	0	0	0	0	0	0	0	1
MA-g-PS wt.(%)	0	0	0	0	0	0	0.75	0.75

\*parts per hundred polymer

\*\* Concentration expressed in milliequivalents.

## 6.3 Results and Discussions

### 6.3.1 Effect of blend ratio & dynamic vulcanisation

The derivative TGA (DTG) of polystyrene (PS), natural rubber (NR) and 85/15 PS/NR blend are shown in Figure 6.1. The temperature of onset of decomposition ( $T_i$ ), maximum decomposition temperature ( $T_{max}$ ), peak rate of decomposition ( $R_{max}$ ), temperature at 50 % loss and residual weight at 600 °C are given in Table 6.2.

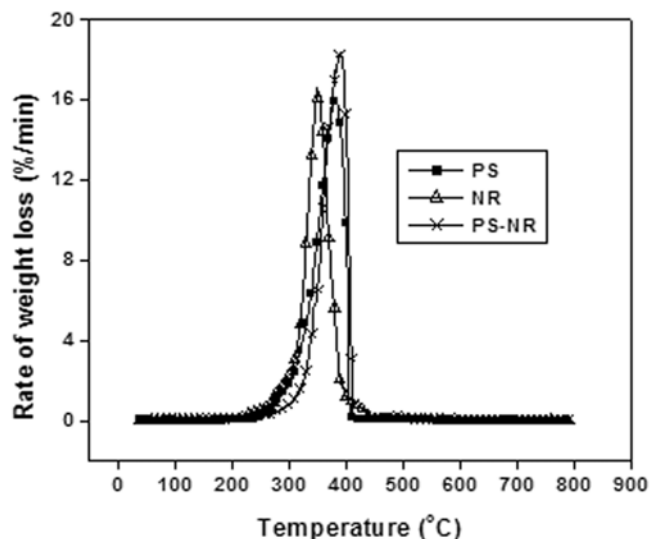


Figure 6.1: DTG curve of PS, NR and 85/15 PS/NR blend.

It is clear from the Figure 6.1 and Table 6.2 that PS starts to degrade at a temperature of 262 °C in a single step with a maximum decomposition rate of 16 %/min. While NR starts degradation at a lower temperature of 227 °C in a single step with maximum rate of decomposition of 16.6 %/min. The temperatures at which maximum degradation occurs are about 380 °C and 350 °C for PS and NR, respectively. The temperature at which 50 %



loss of material occurs is higher for PS (368 °C) in comparison to NR (350 °C). In the case of 85/15 PS/NR blend, the onset of decomposition is similar to that of PS as the amount of NR in the blend is low. However, the temperature of maximum decomposition increases to 389 °C. But the peak rate of decomposition increases from 16 to 18.4 %/min. The temperature at 50 % degradation of the blend increased from 368 to 377 °C.

With the dynamically vulcanised blends, the onset temperature of decomposition has increased to 270 °C when compared to the unvulcanised blend. However, there is no change in the temperature of maximum decomposition, the peak rate of decomposition and the temperature at 50 % degradation for the dynamically vulcanised blends. The DTG curve of the unvulcanised and vulcanised blend are shown in Figure 6.2. The residue remaining at 600 °C is higher for the dynamically vulcanised blends when compared to the unvulcanised blend. This may be attributed to the presence of extender such as calcium carbonate or clay present in 40 % active dicumyl peroxide (DCP). The dynamically vulcanised blends have improved thermal stability than the unvulcanised blends.

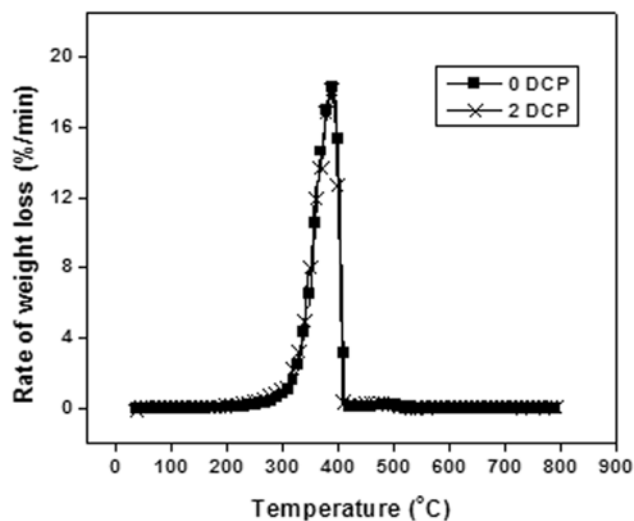


Figure 6.2: DTG curve of unvulcanised and dynamically vulcanised PS/NR blend.

Table 6.2 Thermal degradation characteristics of PS/NR blend.

Parameters	Mix No.			
	A	B	C	D
Onset of decomposition ( $T_i$ ), °C	262	227	260	270
Maximum decomposition Temp. ( $T_{max}$ ), °C	382	350	389	389
Peak rate of decomposition ( $R_{max}$ ) %/min	16	16.6	18.4	18.3
Temp. at 50 % loss ( $T_{50}$ ), °C	368	350	377	378
Residue at 600 °C (%)	0.06	0.3	0.07	0.17

The kinetics of the degradation reaction was studied by using the Freeman-Carroll method [28]. According to this method

$$\Delta \log (dW / dt) = n \cdot \Delta \log W_r - (\Delta E / 2.3 R) \Delta(1/T) \dots\dots\dots(6.1)$$

where  $dW/dt$  is the rate of reaction,

$n$  is the order of reaction,

$R$  is the gas constant,

E is the activation energy,

T is the absolute temperature, and

$W_r$  is proportional to the amount of reactant remaining.

The above equation can be rearranged to

$$\frac{(\Delta \log dW/dT)}{\Delta \log W_r} = n - \frac{(\Delta E/2.3R)\Delta(1/T)}{\Delta \log W_r} \dots\dots\dots(6.2)$$

The order of the reaction can be obtained from the intercept of the plot of the left hand side of equation (6.2) versus  $\Delta(1/T) / \Delta \log W_r$  and such a plot is given in Figure 6.3. A common line with an intercept of one can be drawn to represent all the data points showing that the degradation of the 85/15 PS/NR blend follow first order kinetics. Freeman-Carroll plot of the dynamically vulcanised is shown in Figure 6.4. The intercept shows that the degradation of the dynamically vulcanised blends also follow first order kinetics.

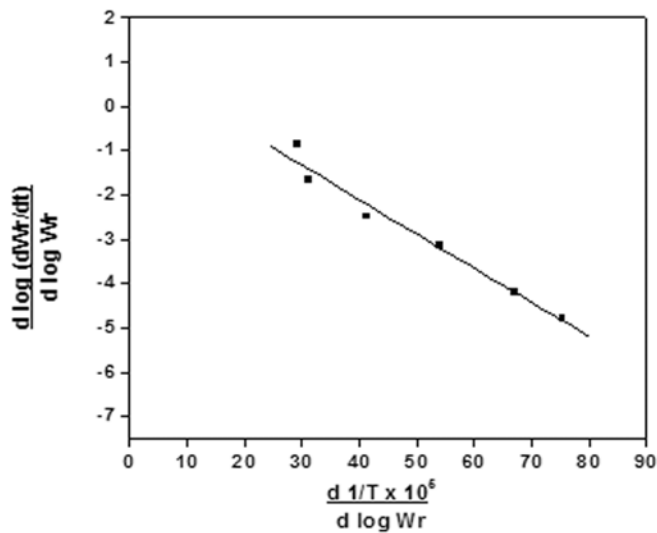


**Figure 6.3: Freeman-Carroll plot of 85/15 PS/NR blend.**

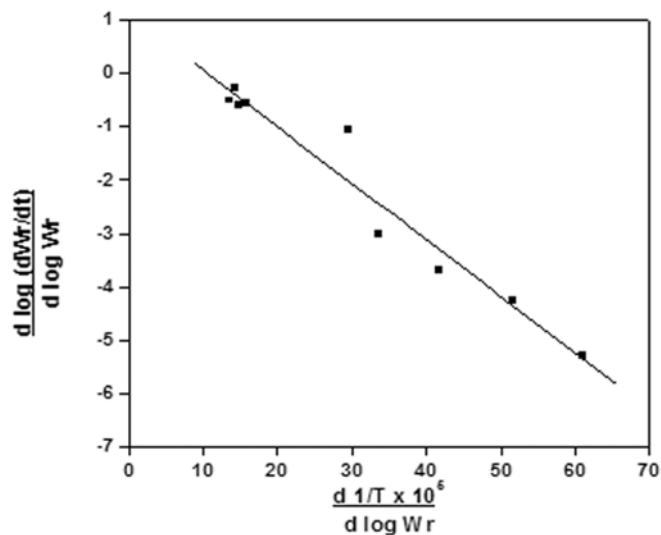


Figure 6.4: Freeman-Carroll plot of dynamically vulcanised 85/15 PS/NR blend.

### 6.3.2 Effect of short Nylon-6 fibres

The DTG curve of untreated and RFL-coated Nylon fibre composites are shown in Figure 6.5. The corresponding  $T_i$ ,  $T_{max}$ ,  $R_{max}$ , temperature at 50 % loss and residue are given in Table 6.3.

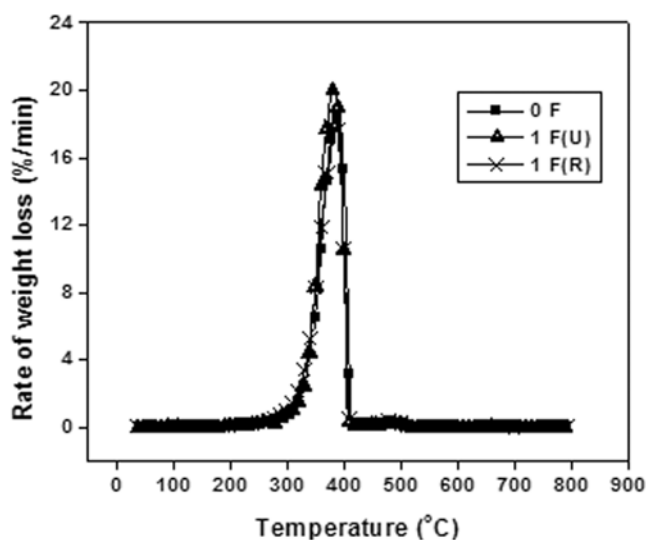


Figure 6.5: DTG curves of short Nylon-6 fibre PS/NR composites.

**Table 6.3 Thermal degradation characteristics of untreated and RFL-coated fibre composites.**

Parameters	Mix No.		
	C	E	F
<b>Onset of decomposition (<math>T_i</math>) °C</b>	260	270	272
<b>Maximum decomposition Temp. (<math>T_{max}</math>) °C</b>	389	380	383
<b>Peak rate of decomposition (<math>R_{max}</math>) %/min</b>	18.4	20.1	18.4
<b>Temp. at 50 % loss (<math>T_{50}</math>) °C</b>	377	373	374
<b>Residue at 600 °C (%)</b>	0.07	0.07	0.07

The onset temperature of decomposition of the composites is higher compared to that of the unreinforced blends. The temperature at which peak degradation occurs is increased slightly from 380 °C to 383 °C for RFL-coated fibre composites when compared to untreated fibre composites. The  $T_{max}$  is, however, slightly lower compared to the blends. The peak rate of decomposition is reduced for RFL-coated fibre composites (18.4 %/min) in comparison to untreated fibre composites (20.1 %/min). This may be due to the better interaction between the fibre and the matrix. The temperature at 50 % loss and the residue remaining at 600 °C remains identical for both the composites.

The Freeman-Carroll plots for the degradation of the composites with 1 wt.% untreated and RFL-coated Nylon fibre given in Figure 6.6 and 6.7 respectively. The intercepts at one indicates that the degradation follows first order kinetics. Similar results have been reported by Kutty *et al.* [16] and Seema *et al.* [20] in the case of short Kevlar fibre-thermoplastic polyurethane composite and Nylon-6 fibre SBR composites, respectively.

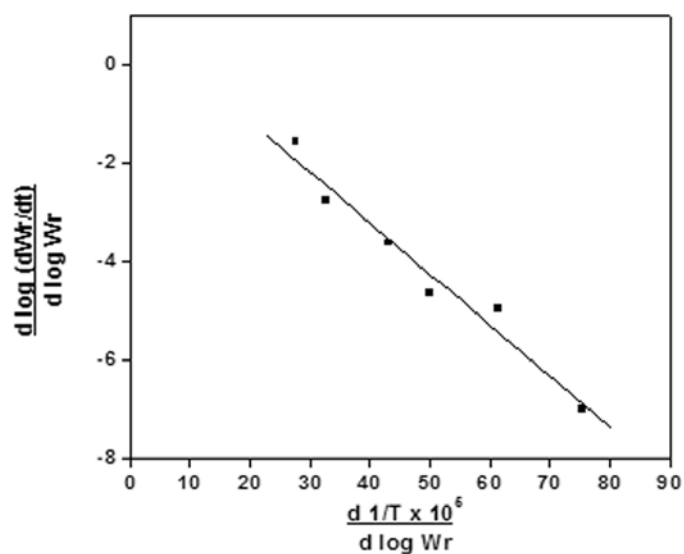


Figure 6.6: Freeman-Carroll plot of PS/NR composites with untreated fibre.

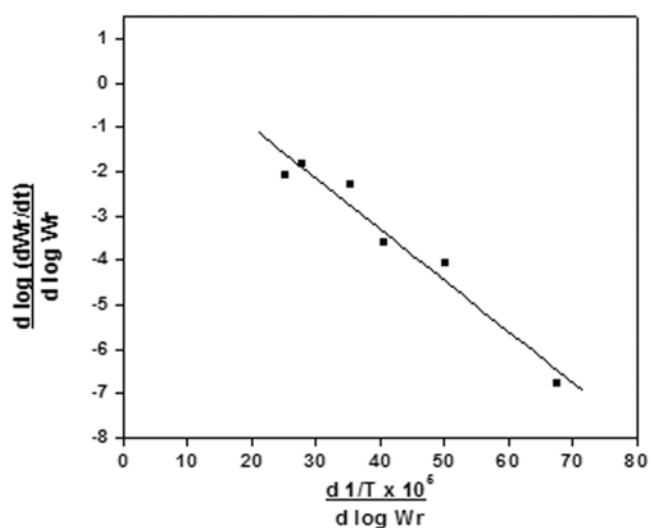


Figure 6.7: Freeman-Carroll plot of PS/NR composites with RFL-coated fibre.

### 6.3.3 Effect of surface treated fibre and the use of a compatibiliser

The DTG curve of untreated and surface treated fibre in conjunction with the compatibiliser and its degradation characteristics are given in Figure 6.8 and Table 6.4.

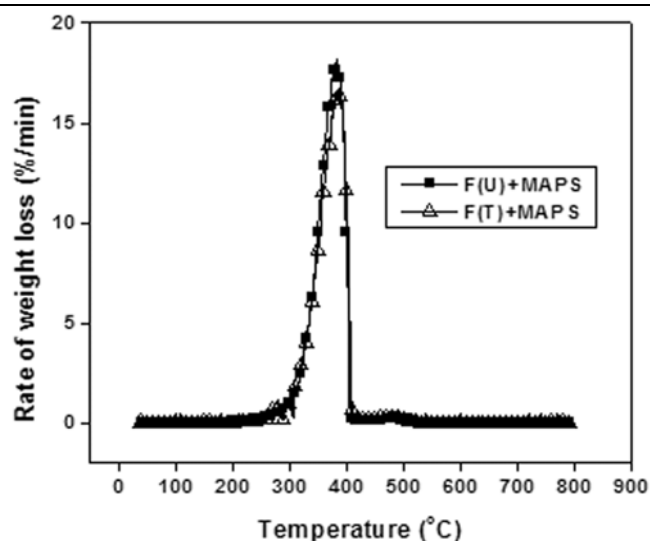
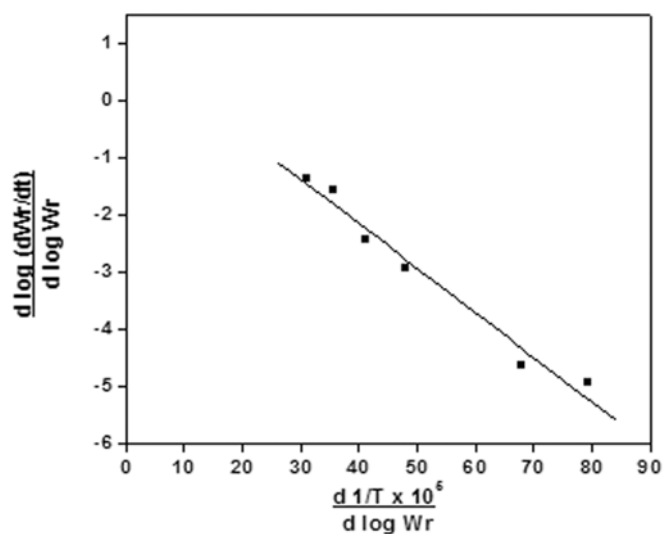


Figure 6.8: DTG curves of untreated and treated fibre composites containing compatibiliser.

Table 6.4 Thermal degradation characteristics of untreated and treated fibre composites with compatibiliser.

Parameters	Mix No.		
	E	G	H
Onset of decomposition ( $T_i$ ) °C	270	273	278
Maximum decomposition Temp. ( $T_{max}$ ) °C	380	382	385
Peak rate of decomposition ( $R_{max}$ ) %/min	20.1	18.2	16.3
Temp. at 50 % loss ( $T_{50}$ ) °C	373	372	372
Residue at 600 °C (%)	0.07	0.07	0.07

The degradation of untreated and treated Nylon fibre composites in conjunction with compatibiliser starts at a higher temperature in comparison to composites without compatibiliser. Similarly the maximum temperature of decomposition of composites in the presence of compatibiliser increases slightly when compared to the one without compatibiliser.



**Figure 6.9:** Freeman-Carroll plot of PS/NR composites with untreated fibre and compatibiliser.

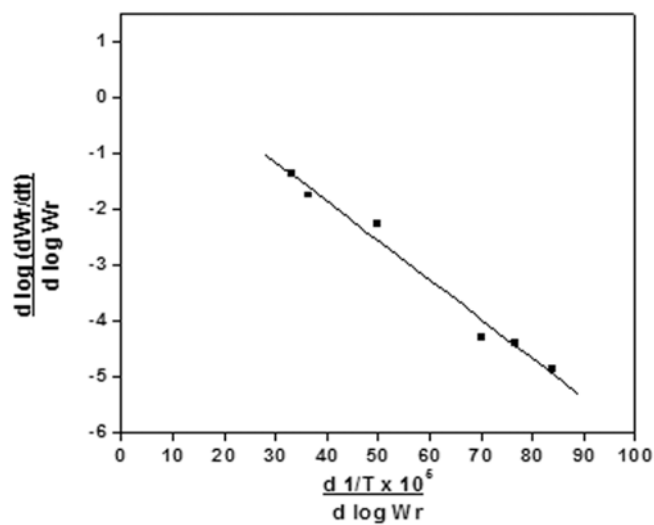


**Figure 6.10:** Freeman-Carroll plot of PS/NR composites with treated fibre and compatibiliser.

The peak rate of decomposition reduces significantly to 16.3 % for treated fibre composites along with compatibiliser. This implies an improved thermal stability of treated fibre composites containing compatibiliser when



compared to untreated one. This may be due to the strong interaction between fibre and matrix in the presence of compatibiliser.

The Freeman-Carroll plots for the degradation of the composites with untreated and surface treated Nylon fibre in conjunction with the compatibiliser are presented in Figures 6.9 and 6.10 respectively. The presence of compatibiliser does not alter the degradation kinetics and both the composites follow first order kinetics.

## **6.4 Conclusions**

The degradation of PS/NR blend, dynamically vulcanised blend and composites with short Nylon fibre, RFL-coated Nylon fibre, untreated and treated composites in conjunction with the compatibiliser follows single step degradation pattern. The dynamically vulcanised blends show improved thermal stability compared to the simple blend. Incorporation of short Nylon-6 fibre in the blend delays the onset of degradation but the maximum decomposition temperature decreases marginally. The peak rate of decomposition decreases in the presence of RFL-coated fibre in comparison to untreated fibre composites. The untreated and partially hydrolysed fibre composites enhances the thermal stability when compared to the one without compatibiliser.

## **6.5 References**

- [1] Torre L, Kenny JM, Maffezzoli AM. *J Mater Sci* 1998; 33:3137.
- [2] Flynn JH. *Aspects of Degradation and Stabilisation of Polymers*. Jellinel HHG, editor. New York: Elsevier; 1978.
- [3] Montaudo G, Puglisi C. *Development in Polymer Degradation-7*. Grassie N, editor. London: Elsevier; 1987.

- [4] Hawkins WL. Polymer Degradation and Stabilisation. New York: Springer-Verlag; 1983.
- [5] Schnabel W. Polymer Degradation. Hanser International; 1981.
- [6] Nam JD, Seferis JC. J Appl Polym Sci 1993; 50:1555.
- [7] Kissinger HA, Anal Chem 1957; 29:1702.
- [8] Flynn JH, Wall LA. Polym Lett 1966; 4:323.
- [9] Shneider HA. Polym Eng Sci 1992; 32:17.
- [10] Jimenez A, Berenguer V, Lopez J, Vilaplana J. J Appl Polym Sci 1996; 60: 2041.
- [11] Jimenez A, Lopez J, Vilaplana J, Dussel HJ. J Anal Appl Pyrolysis 1997; 40-41:201.
- [12] Ashaletha R, Kumaran MG, Thomas S. Polym Degrad Stab 1998; 61:431.
- [13] Rajesh C, Manoj KC, Unnikrishnan G, Purushothaman E. Polymers and Polymer Composites 2009; 17:133.
- [14] Reis PNB, Ferreira JAM, Antunes FV, Costa JDM. Polym Degrad Stab 2008; 93:1170.
- [15] Torre L, Kenny JM, Lopez-Manchado M. Rub Chem Tech 2000; 73:694.
- [16] Kutty SKN, Chaki TK, Nando GB. Polym Degrad Stab 1992; 38:187.
- [17] Younan AF, Ismail MN, Khalaf AI. Polym Degrad Stab 1995; 48:103.
- [18] Suhara F, Kutty SKN, Nando GB. Polym Degrad Stab 1998; 61:9.
- [19] Rajeev RS, De SK, Bhowmick AK, Baby John, Polym Degrad Stab 2003; 79:449.
- [20] Seema A, Kutty SKN, Int J Polym Mater 2006; 55:25.
- [21] Seema A, Kutty SKN, Int J Polym Anal Charact 2005; 10:169.
- [22] Navarro R, Torre L, Kenny JM, Jimenez A. Polym Degrad Stab 2003; 82:279.

- [23] Agung EH, Saupan SM, Hamdan MM, Zaman HMDK, Mustofa U. Int J Phy Sci 2011; 6:2100.
- [24] Rezaei F, Unus R, Ibrahim NA. Mat Des 2009; 30:260.
- [25] Smita M, Verma SK, Nayak SK. Comp Sci Technol 2006; 66:538.
- [26] Smita M, Verma SK, Nayak SK, Tripathy SS. J Appl Polym Sci 2004; 94:1336.
- [27] Weizhi W, Longxiang T, Qu B. Eur Polym J 2003; 39:2129.
- [28] Freeman ES, Carroll B. J Phy Chem 1958; 62:394.

.....❧.....

## **SUMMARY AND CONCLUSIONS**

---

In recent years thermoplastic-rubber blends and its composites are becoming increasingly important. Blends of polystyrene (PS) with rubbers have been prepared as a means to improve its toughness. However, introduction of elastomeric phase results in a decrease in mechanical properties such as modulus and strength. This puts a serious limitation on the potential of these blends. Dynamic vulcanisation of the blends can be resorted to as a technological compatibilisation method. Another method to improve the strength and stiffness of these blends is to use fillers such as short fibres. It is expected that the incorporation of short Nylon fibres will improve properties while reducing cost substantially. In the present study, systematic investigations on the various properties of rubber-toughened PS and its composites based on short Nylon-6 fibres have been carried out and the results are summarized below.

The mechanical properties, morphology and dynamic mechanical properties of Natural rubber (NR)-toughened PS were studied with reference to blend ratio. The mechanical properties of the blends are strongly influenced by blend ratio. The tensile strength, Young's modulus, flexural strength and flexural modulus of the blends decrease with increase in rubber content, whereas the impact strength increase significantly by 46 % at 85/15 PS/ NR. So the optimum blend ratio for maximum toughness of PS is

85/15 PS/NR blend. The morphology of the blends with rougher surface indicates a two phase structure. The effect of the blend ratio on the dynamic mechanical properties was investigated in the temperature range 40 to 120 °C. A linear relationship exists between the storage modulus at 60 °C and NR content as:  $E' \text{ (MPa)} = 2567 - 67 \text{ NR (wt.\%)}$  with a regression coefficient of 0.99. The peak loss modulus values and peak  $\tan \delta$  values decrease with increase in NR content.

Dynamic vulcanisation studies on 85/15 PS/NR blends using dicumyl peroxide shows that DCP dosage has a significant effect on the extent of crosslinking. The tensile strength and flexural properties slightly increase up to 2.8 meq of DCP whereas the Young's modulus and impact strength increase by 23 % and 50 %, respectively, at an optimum DCP concentration of 2.8 meq. The morphology changes drastically as a result of dynamic vulcanisation. Dynamical mechanical studies reveal that the storage modulus is at the maximum and the  $\tan \delta$  peak, the minimum at optimum DCP content. Dynamic vulcanisation brings about overall improvement in properties.

Investigations on the effect of short Nylon-6 fibres- unmodified and RFL-coated on the mechanical properties of 85/15 PS/NR blends show that the tensile strength, Young's modulus, flexural strength, flexural modulus and impact strength significantly improved for both the composites when the Nylon content is 1 wt. %. The improvement with RFL-coated fibre composites is 45 %, 14 % and 27 % for tensile strength, Young's modulus and impact strength, respectively. The maximum storage modulus for 85/15 blend is obtained with 1 wt% Nylon fibre (unmodified and RFL-coated). It shows that an optimal concentration of 1 wt.% Nylon fibres (unmodified and RFL-coated) can effectively reinforce the 85/15 PS/NR blend.

The properties of 85/15/1 PS/NR/Nylon-6 fibre composites can be improved by proper treatment of the fibre surface and also by using a proper compatibiliser. Alkaline hydrolysis of the Nylon fibre can make the fibre surface more reactive. Maleic anhydride-grafted-polystyrene (MA-g-PS) prepared by the melt mixing process using DCP at 170 °C, can function as a good compatibiliser. The use of 0.75 wt.% compatibiliser improves the tensile strength, Young's modulus, flexural strength, flexural modulus and impact strength of the composites. The improvement is more significant with treated fibre composites in the presence of compatibiliser with an increase of 23 %, 13 % and 39 % in tensile strength, Young's modulus and impact strength, respectively. Dynamic mechanical analysis measurements reveal that the storage modulus of the treated fibre composites in the presence of MA-g-PS is better compared to that of the untreated fibre composites- with and without compatibiliser.

An investigation on the effect of blend ratio on the mechanical properties, morphology and dynamic mechanical properties of the PS/SBR blend shows that as the SBR content of the blend increases, the tensile strength, Young's modulus, flexural strength and flexural modulus are reduced. The impact strength of 90/10 PS/SBR blend is improved markedly by 36 %. The dynamic mechanical analysis shows that the storage modulus decreases with increasing rubber content. The variation of storage modulus at 60 °C with SBR content could be predicted by the a polynomial of the second order as  $E' \text{ (MPa)} = 2331 - 41.92\text{SBR} + 0.317 \text{ SBR}^2 \text{ (wt.\%)}$  with a correlation fit coefficient of 0.96.

Dynamic vulcanisation of 90/10 PS/SBR blend using DCP improves the tensile properties, flexural properties and impact strength. The tensile

strength increases by 17 %, whereas the Young's modulus and impact strength improves by 11 % at 2.1 meq. The optimum DCP content is 2.1 meq. Dynamic mechanical studies reveal that the storage modulus is the highest for blends vulcanised dynamically with 2.1 meq of DCP.

Short Nylon-6 fibres- unmodified and RFL-coated- can improve the mechanical properties of 90/10 PS/SBR blend. The tensile modulus, flexural strength, flexural modulus and impact strength improve with 1 wt.% of unmodified and RFL-coated fibre loading. The tensile strength is only marginally reduced at 1wt.% fibre content. The enhancement was better for RFL-coated fibre composites with an increase of 13 %, 10 % and 29 % in Young's modulus, flexural strength and impact strength, respectively. The dynamic mechanical studies of unmodified Nylon fibre composites show that the storage modulus at room temperature remains unchanged for 1 wt.% fibre content. While with RFL-coated fibre composites, the storage modulus is marginally reduced compared to the unreinforced blend.

The effect of surface treatment of Nylon fibres and the use of a compatibiliser on the mechanical properties and dynamic mechanical properties of 90/10/1 PS/SBR/Nylon-6 fibre composites were investigated. The use of compatibiliser at 0.5 wt.% improves the tensile properties, flexural properties and impact strength of untreated and treated fibre PS/SBR composites. The treated fibre composites in the presence of compatibiliser improved by 12% in both tensile strength and Young's modulus, and about 7 % in impact strength. DMA reveals that the storage modulus at room temperature is higher for untreated composites with compatibiliser.

Investigations on the effect of blend ratio on the mechanical properties, morphology and dynamic mechanical properties of PS/WTR (Whole tyre reclaim) shows that the toughness of PS can be improved by blending with WTR. The optimum blend ratio is 90/22. The tensile properties and flexural properties decrease with increase in WTR content. The dynamic mechanical studies show that the storage modulus at 60 °C decreases with increase in WTR content which could be expressed by the regression equation as  $E' \text{ (MPa)} = 2535 - 130 \text{ WTR} + 3.33 \text{ WTR}^2 \text{ (wt.\%)}$  with a regression coefficient ( $R^2$ ) of 0.98.

Short Nylon-6 fibre- unmodified and RFL-coated fibres can be used to improve the properties of PS/WTR blends. The 90/22 PS/WTR composite containing 1 wt.% unmodified fibre and 0.5 wt.% RFL-coated fibres shows improved tensile modulus, flexural strength, flexural modulus and impact strength. The tensile strength is only marginally improved. The Young's modulus and flexural strength increased by 8 % whereas the flexural modulus and impact strength improved by 15 % for RFL-coated fibre composites. The dynamic mechanical study reveals that the storage modulus at room temperature is enhanced for 0.5 wt.% and 1 wt.% unmodified fibre composites. But the loss modulus peak is maximum and loss tangent peak, the lowest for 1 wt.% unmodified fibre composites.

Investigation on the dynamic mechanical properties of 90/22/1 PS/WTR/Nylon-6 fibre composites with emphasis on the effect of surface treatment and the use of a compatibiliser show that there is enhancement in the tensile properties, flexural properties and impact strength. The optimum loading of compatibilizer is 0.5 wt.%. The untreated fibre composite shows only limited improvement in mechanical properties with the addition of the



compatibiliser. The tensile strength, Young's modulus and impact strength improve by 15 %, 8 % and 19 %, respectively for treated fibre composites in the presence of compatibiliser. The dynamic mechanical analysis reveals that the storage modulus at low temperatures is better for untreated composites in conjunction with the compatibiliser, compared to treated composites with compatibiliser and untreated composites.

The thermal degradation of PS/NR blend, dynamically vulcanised blend, composites with short Nylon fibre, RFL-treated Nylon fibre; untreated and surface treated Nylon fibre composites in conjunction with the compatibiliser follows single step degradation pattern. The dynamically vulcanised blends show improved thermal stability compared to the uncrosslinked blend. Incorporation of short Nylon-6 fibre in the blend delays the onset of degradation but the maximum decomposition temperature decreases marginally. The peak rate of decomposition decreases in the presence of RFL-coated fibre in comparison to untreated fibre composites. The untreated and partially hydrolysed fibre composites, in conjunction with the compatibiliser, enhances the thermal stability. Kinetic studies show that the degradation of the blends and the composites follows first order kinetics.

The above studies show that short Nylon-6 fibres at optimal concentration can significantly reinforce PS/NR blends when compared to PS/SBR and PS/WTR blends. The mechanical and dynamic mechanical properties of PS/NR blends can be further enhanced with RFL-coated Nylon fibres. Properties of PS/NR/Nylon-6 composites can be significantly improved by surface treatment of the Nylon fibres in conjunction with a proper compatibiliser. Modified Nylon-6 fibre also enhances the thermal stability of the composite

### **Future Outlook**

- [1] Evaluation of other rubbers such as EPDM and NBR as toughening agent for PS.
- [2] The rheological characteristics of the blends and composites are to be studied.
- [3] The use of other fibres such as Kevlar, polyolefin etc. on rubber-toughened PS can be explored.
- [4] The effect of partially replacing NR with WTR in toughening PS and development of its composites with short fibres are to be investigated.
- [5] The effect of other chemical modifications of the fibre surface can be explored for improving the fibre-matrix adhesion.

....END....

## *Abbreviations and Symbols*

ABS	Acrylonitrile-butadiene-styrene terpolymer
ACM	Acrylate rubber
ACS	Thermoplastic blend of a copolymer from acrylonitrile and styrene with chlorinated polyethylene
ASTM	American Standard for testing and materials
BR	Butadiene rubber
cc	cubic centimeter
cm	centimeter
CPE	Chlorinated polyethylene
CR	Chloroprene rubber
DCP	Dicumyl peroxide
DMA	Dynamic mechanical analysis
DTG	Derivative thermogravimetry
E'	Storage modulus
E''	Loss modulus
ENR	Epoxidised natural rubber
EOC	Ethylene octene copolymer
EPDM	Ethylene-propylene-diene-terpolymer
EPR	Ethylene propylene rubber
EVAc	Ethylene-vinyl acetate copolymer
FTIR	Fourier Transform Infrared Spectroscopy
g	gram
GRT	Ground rubber tyre
h	hour
HDPE	High density polyethylene
HIPS	High impact polystyrene
HVTEM	High voltage transmission electron microscope
Hz	Hertz
ID <sub>crit</sub>	Critical interparticle distance
IIR	Butyl rubber

ISNR	Indian Standard Natural Rubber
J	Joule
kN	kilo Newton
KOH	Potassium hydroxide
$l_c$	Critical fibre length
LDPE	Low density polyethylene
MA	Maleic anhydride
MAPP	maleated PP
meq	milliequivalents
mg	milligram
$\mu\text{m}$	Micrometer
min	minutes
mm	millimeter
MPa	Mega Pascal
N	Newton
NaOH	Sodium hydroxide
NBR	Acrlonitrile-butadiene rubber
NR	Natural rubber
$P_0$	Initial plasticity number
PA	Polyamide
PB	Polybutadiene
PBT	Polybutylene terephthalate
PC	Polycarbonate
PE	Polyethylene
PET	Polyethylene terephthalate
php	parts per hundred polymer
PMMA	Polymethylmethacrylate
PP	Polypropylene
PRI	Plasticity retention index
PS	Polystyrene
PVC	Polyvinylchloride
RFL	Resorcinol formaldehyde latex

RHP	Rice husk powder
rpm	revolutions per minute
RVNR	Radiation vulcanized natural rubber
SAN	Styrene-acrylonitrile copolymer
SBR	Styrene-butadiene rubber
SBS	Styrene-butadiene-styrene block copolymer
SEBS	Styrene-ethylene-butylene-styrene block copolymer
SEM	Scanning electron microscopy
SEP	Styrene-ethylene-propylene copolymer
tpm	turns per metre
Tan $\delta$	Loss tangent
TEM	Transmission electron microscope
TG	Thermogravimetry
T <sub>g</sub>	Glass transition temperature
THF	Tetrahydrofuran
TPE	Thermoplastic elastomer
TPNR	Thermoplastic natural rubber
TPU	Thermoplastic polyurethane
TPV	Thermoplastic vulcanisate
UTM	Universal testing machine
WTR	Whole tyre reclaim

.....

## *List of Publications*

1. Effect of Short Nylon-6 Fibres on Natural Rubber-Toughened Polystyrene, G. Jayalatha and Sunil K.N. Kutty. *Materials & Design*. (In press)
2. Short Nylon-6 Fibre Reinforced Polystyrene/Natural Rubber blends: Effect of Maleated-Polystyrene compatibiliser, G. Jayalatha and Sunil K.N. Kutty. *Polymers and Polymer Composites*. (Communicated)
3. Composites of short Nylon-6 Fibre/SBR-toughened Polystyrene: Effect of Maleated-Polystyrene compatibiliser, G. Jayalatha and Sunil K.N. Kutty. *International Journal of Polymeric Materials*. (Communicated)
4. Short Nylon-6 Fibre/Reclaimed Rubber-toughened Polystyrene composites: Effect of compatibiliser, G. Jayalatha and Sunil K.N. Kutty. *Progress in Rubber, Plastics and Recycling Technology*. (Communicated)
5. Thermal degradation of short Nylon-6 fibre/Natural Rubber-toughened Polystyrene composites, G. Jayalatha and Sunil K.N. Kutty. *Polymer-Plastics Technology and Engineering*. (Communicated)

.....❧.....

## Curriculum Vitae



Name : Jayalatha Gopalakrishnan. G

Date of birth : 07-07-1975

Qualification : B.Tech (Polymer Science and Rubber Technology)  
M.Tech (Polymer Technology)

Official Address : Asst. Professor,  
Dept. of Polymer Science & Rubber Technology  
CUSAT, Kochi 682 022.

Teaching Experience : 8 years

### Publication

Effect of Short Nylon-6 Fibres on Natural Rubber-Toughened Polystyrene, G. Jayalatha and Sunil K.N. Kutty. *Materials & Design*.  
(In press)

.....✍.....